Use of the Mini-Cone Penetrometer for Evaluating the Liquefaction Potential of Sands Associated with Charleston, S.C. Seismic Events

by

Stephen Eugene Dickenson

Thesis submitted to the Faculty of the
Virginia Polytechnic Institute and State University
in partial fulfillment of the requirements for the degree of
Master of Science
in
Civil Engineering

APPROVED:

G.W. Clough, Chairman

T.L. Brandon

T. Kuppusamy

February, 1988

Blacksburg, Virginia

Use of the Mini-Cone Penetrometer for Evaluating the Liquefaction Potential of Sands Associated with Charleston, S.C. Seismic Events

by

Stephen Eugene Dickenson

G.W. Clough, Chairman

Civil Engineering

(ABSTRACT)

First-hand reports on the 1886 Charleston earthquake contain numerous accounts for the widespread occurrence of liquefaction related features in and near the meizoseismal zone. Recent geologic studies have found evidence for the repeated liquefaction of sandy soils in the Charleston area due to recurring large seismic events. In the course of this investigation 24 mini-cone penetration tests were performed at seven sites in or near the meizoseismal zone of the 1886 earthquake to determine the factors influencing ground failures due to liquefaction. These tests were supplemented with soil borings, sieve tests and a limited number of standard penetration tests to aid in characterization of the sandy soils. Additionally, soil boring records in Charleston were obtained which provided in-situ testing data in an area with documented historical damage. The range of sites at which testing was done, or information was available, represent locations experiencing various levels of liquefaction and distances from the zone of seismic energy release.

Penetration data were used to evaluate resistance of the sandy soil to cyclic loading and formed the basis for assessing the effects that the lateral extent and distribution of loose sand layers has on the surficial manifestation of liquefaction. With the absence of cementation and extensive soil development, soils as old as late Pleistocene age have been found to be very susceptible to liquefaction. At several sites these soils have undergone at least three episodes of liquefaction and presently exhibit low penetration resistances, indicating that the progressive densification of a liquefiable soil layer can be minor unless it is in very close proximity to a large venting feature. The size and density of occurrence of vents and sandblows has been found to be primarily dependent on the extent of both the liquefiable layer and any overlying resistant layers. Layered system relations utilized with field performance data, and historical and geologic evidence for the

occurrence of liquefaction features to suggest that the near surface peak horizontal accelerations induced by the 1886 earthquake were approximately 0.3g in the meizoseismal zone and 0.2g in the city of Charleston. This is in contrast with previous estimates of seismic shaking all of which point toward values in the range of 0.5 to 0.6g. The reason for the different acceleration estimates is not clear at this time, and will be further studied in future extension of this work.

This thesis is dedicated to my parents, Ronald and Lorna, whose guidance and loving support have instilled my desire to make this achievement possible.

Acknowledgements

I would like to thank Dr. G.W. Clough for giving me the opportunity to work on this particulary intriguing investigation. I have benefitted greatly from his assistance during the drafting of this report.

I would also like to thank committee members Dr. T.L. Brandon for development of the CPT data acquisition system and Dr. T. Kuppusamy for critical review of this report.

Sincere appreciation is extended to the following individuals whose efforts contributed greatly to the completion of this investigation:

- Fellow student and drilling partner Jimmy Martin, whose noxious budget cigars kept the bugs, and all other living things, at bay while testing in South Carolina. Thanks also for assistance in the endless data reduction.

- Mr. S. Obermeier of the U.S. Geological Survey for insights on the nature of liquefaction features at the test sites, assistance in the field work, and for providing me with numerous materials from his personal library.

- Dr. G. A. Bollinger for valuable discussions on seismicity in the Charleston region.

- Machinists Glenn Thomas and Brett Farmer, and electronics technician Clark Brown for completing jobs that were vital for the operation of the CPT system and always required immediate attention.

- Vickie Graham and Judy Dumin of the Civil Engineering department for providing necessary administrative assistance and handling ,unquestioningly, suspect expense accounts.

- Cathy Gorman whose extraordinary drafting and figure preparation made the data appear even more stunning.

- Mr. Hillyer Rudisill III, St. Michael's Church Historian, who provided descriptions and photographs of the 1886 eathquake damage and whose personalized tour of the church was one of the highlights of my stay in Charleston.

- And finally to my wonderful bride Julie, for sparing me the unbearable fate of manuscript typing, and whose patience and support during the last year and a half has made this experience much more enjoyable.

Table of Contents

List of Illustrations

List of Tables

Chapter I

Introduction

The largest historical earthquake ($m_b \simeq 6.6$ - 6.9, $M_s \simeq 7.1$) in the eastern United States occurred on the Atlantic coastal plane approximately 15 miles northwest of Charleston, South Carolina in 1886 (figure1). Modified Mercalli (MM) intensities of X in the meizoseismal zone and IX in the city of Charleston have been assigned on the basis of structural damage and widespread occurrance of liquefaction related features throughout the region (figure 2). In his comprehensive report of first-hand observations on the 1886 earthquake, Dutton (12) described areas exhibiting liquefaction phenomena ranging from spectacular sandblows ("craterlets" by Dutton) to ground fissuring and and minor sand venting. Structural damage caused by liquefaction related ground failures (i.e. loss of bearing capacity, differential ground settlement, and slope stability) contributed significantly to the over $5 million (1886 dollars) estimated damage from the earthquake.

Recent paleoseismological investigations involving the excavation and identification of relic liquefaction features have determined a recurrence of Holocene to late-Pleistocene moderate to large seismic events in the Charleston region. Long, open drainage ditches have allowed extensive exposure of the upper soil coditions in areas not associated with historical reported liquefaction phenomenon. Based on the geologic evidence, estimates of approximately 1700 years have been made

for the recurrence interval of MM≥X earthquakes. Superimposed sand blow features induced by successive earthquakes have been discovered in the region indicating that liquefaction can occur repeatedly at the same site. In light of the recurrence of moderate to large earthquakes, combined with the 300 year historical record of continuing weak seismicity near Charleston this observation is particulary important for the site evaluation and seismic design of critical structures in coastal South Carolina.

While recent geological work has revealed significant insights into the approximate recurrence and magnitude of seismicity in the Charleston area, it remains to study the engineering properties of the soils associated with the liquefaction features to characterize and determine the liquefaction susceptibility of these soils. Of primary interest are:

1. The engineering characteristics of the sands from the liquefaction sites. Are they all equally subject to liquefaction, and are they in any way different in their seismic response relative to other sands.

2. Property variation from site to site that would suggest that more damage may result in one area than other if an earthquake should occur. Also related to this is the identification of the liquefaction likelihood for future earthquakes.

3. The lateral extent and property distribution of the key soil layers around the liquefaction sites, and the relation of this to the type of liquefaction features.

4. The levels of near-surface accelerations needed to cause liquefaction, as determined at sites where major, minor, and no liquefaction occurred in the 1886 earthquake.

5. Relationships between the levels of acceleration determined as per item (4) to hypothesized seismic regimes in the Charleston area.

More general issues which can be addressed are:

1. Relationships between cone (CPT) and standard penetration (SPT) testing, and empirical relationships for cone and SPT in predicting liquefaction potential.

2. Evidence for progressive compaction of sediments in areas where liquefaction has repeatedly occurred.

3. Reasons for the different types of liquefaction features that have been observed, and their consistency with ideas existing in the literature. Note that the drainage ditches provide probably the most extensive exposure of liquefaction features that have ever been observed.

This study is the culmination of the first year's efforts on a continuing investigation to determine the engineering properties and response to seismic ground motions of near surface sandy soils in the Charleston area. Seven sites identified either in first hand accounts or by USGS researchers as areas exhibiting liquefaction features attributed to the 1886 earthquake have been tested with an electric mini-cone penetrometer recently developed at Virginia Tech by Dr. G.W. Clough and his students. Six of the test sites are located throughout the meizoseismal zone of the 1886 earthquake. One site is located outside of the zone of maximum intensity to evaluate the effects of epicentral distance and ground motion attenuation on the occurrance of liquefaction.

Two areas were judged particularly valuable for testing because of the nature of documented liquefaction features and data previously collected during recent geological investigations. An extensive testing program was completed at the Hollywood site located approximately 20 miles west of Charleston. In this area a suite of ten CPT's and six supplementary SPT's were performed to characterize the soil conditions along 9000 feet of a drainage ditch which exposes numerous relic sandblow features. Efforts were also concentrated at the Warren site, located five miles north of Hollywood. At this site three CPT's and five exploratory soil borings were conducted around the location of a liquefaction vent initiated during the 1886 earthquake. The remaining sites are also located in areas exhibiting liquefaction features attributed to the 1886 event. At these sites a preliminary assessment of the soil conditions was made with only one or two CPT's and borings for "grab" samples due to time constraints on the field testing program during this initial phase of the

investigation. Future field testing will be conducted at sites of particular interest. In all, 35 exploratory soil borings at ten sites and 24 CPT's at seven sites were performed during the 29 day field schedule.

The wealth of soil logs for downtown Charleston donated to this project by government agencies and local private soils firms alleviated the need for field testing in the area during this stage of the investigation. Compilation by small districts and analysis of the voluminous data will take considerable time and is, in part, being undertaken by students in the Civil Engineering department at The Citadel in Charleston. An example of the analytical procedure utilizing penetration resistances from this large data base is presented for a notable liquefaction site in downtown Charleston. An evaluation of the cyclic loading characteristics of soils located next to historic St. Michael's Church is made to estimate the near surface ground motions which occurred in downtown Charleston during the 1886 earthquake.

Penetration data is used to assess the nature of seismic load levels from past earthquakes, as well as, future cyclic stresses required to initiate liquefaction of the near surface sandy soils. It is realized that the soil properties of the loose noncohesive soils may not be the same as those which existed prior to the 1886 event. A substantial increase in the cyclic loading resistance following the earthquake would occur in areas where extensive liquefaction and venting of material has lead to an increase in the relative density of a deposit. In areas exhibiting the absence, or only minor liquefaction features it is believed that the soil may be only minimally disturbed. Testing at these sites may result in an upper bound for the ground motions required to initiate liquefaction and should aid in evaluating the possible densification effects that the 1886 earthquake had on the materials. Future work will involve continued field testing and laboratory testing to determine soil properties to be used for dynamic site response analyses.

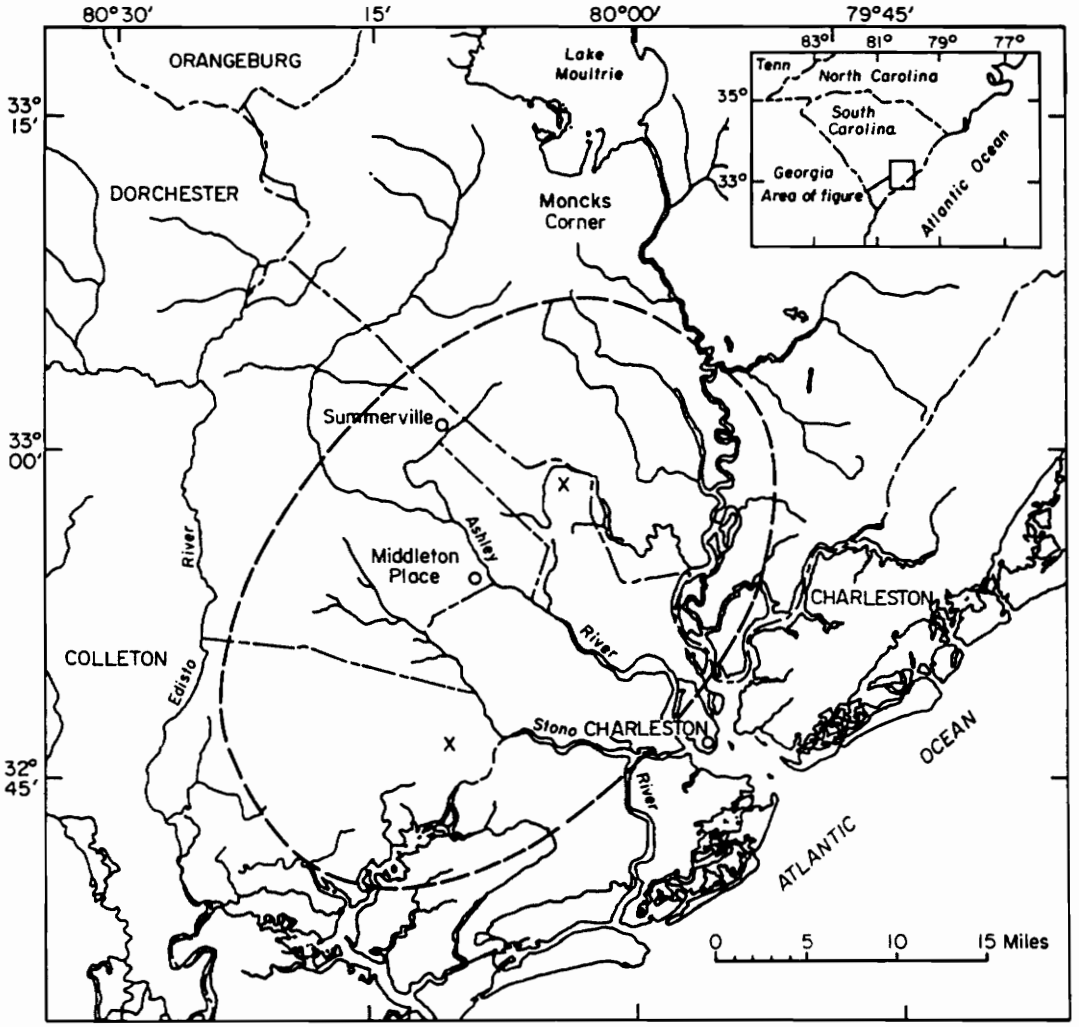

Figure 1. MAP OF THE AREA NEAR CHARLESTON, S.C., SHOWING THE MEIZOSEISMAL ZONE OF THE 1886 EARTHQUAKE

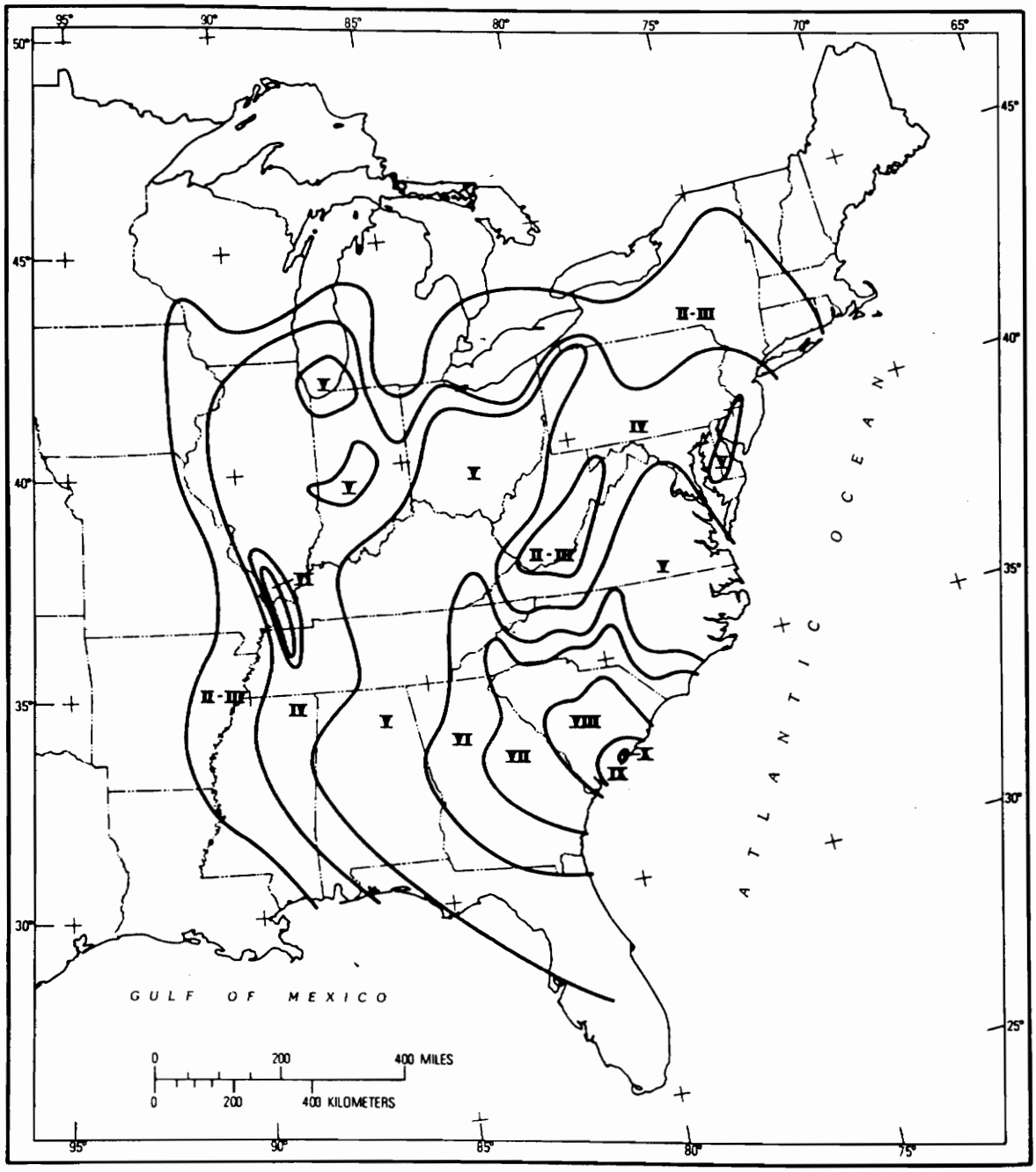

Figure 2. ISOSEISMAL MAP OF THE EASTERN U.S. SHOWING THE PATTERN OF REPORTED INTENSITIES FOR THE 1886 CHARLESTON EARTHQUAKE (4)

Chapter II

Background

2.1 The Charleston Earthquake of 1886

The "Great" Charleston earthquake of August 31, 1886 occurred at 9:51pm with the epicenter located between the towns of Summerville and Middleton Place approximately 15 miles northwest of Charleston. Following two days of several small tremors, the initial, main shock hit with a duration of approximately 35 to 70 seconds (12), and MM intensities were experienced of X in the meizoseismal zone and IX in the city of Charleston (4). The average radius of perceptibility as determined by newspaper accounts was about 840 miles (23). Using relationships regarding the attenuation of intensity with epicentral distance, Nuttli (in 4) has estimated the magnitudes of seismic shaking as $m_b \simeq 6.6$ - 6.9 and $M_s \simeq 7.1$, with peak horizontal accelerations of approximately 0.62g within the meizoseismal zone. Although no ground breakage associated with a causative fault was discovered during initial investigations (12,32) a zone of energy release was inferred from the distribution of widespread structural damage and liquefaction features initiated by the ground motion. Structural damage in Charleston was catastrophic, but the low population density and

predominance of single story, wood frame houses in the epicentral area, and the timing of the earthquake contributed to a reduction in the loss of life. While the cause of the 1886 earthquake is still speculative (5), recent geological evidence indicates that there has been a recurrence of moderate to large earthquakes in the Charleston region.

2.2 *First Hand Observations*

Of peculiar interest to inhabitants of the area was the venting of colorful sands and clays, and associated emmisions of sulphurous gases common throughout the epicenter region. At one location a citizen in Charleston observed a sandblow venting up through an old 25 foot deep fire well as, "spouting up a solid column of water over two feet in diameter, to a height of fully ten feet. When I examined the well, the next day, I found it nearly full of white sand." (44). Newspaper reports describing violent upheavals of sand and clay from orifices having shapes of inverted cones gave locals the impression that the earthquake was volcanically induced. A newspaper account (47) from Mt. Pleasant supported this popular notion;

> "Organic material was found scattered about in large quantities that a local scientist says of necessity must have come from a depth of 1,000 feet. Attempts were made to sound the cavities with sticks and poles, some of which were over twenty feet in length, but no bottom was found to any of them"

Immediately after the earthquake personnel from the U.S. Geologic Survey and the U.S. Ordnance Corps traveled to the area and ,with help from several Charlestonians, began documenting the structural damage and features of geologic interest caused by the ground motion. In his account of the 1886 earthquake, Dutton (12) reported that;

> "...water was extravasated in large quantity, some point in the line of the fissure would be often enlarged by the rapid flow or outrush of the water into a round hole of considerable size, with a crater-basin at the ground surface. These craterlets were of all dimensions, from the most diminutive up to 20 feet or more in diameter....As a general rule the water brought up great quantities of sand and silt....The quantity of water discharged during the earthquake was so great, that every stream-bed, even though ordinarily dry in summer, was awash. It was asserted by many of the residents in some parts of the epicentral tract that the waters were spouted upwards to great heights....That here and there it was thrown up in jets to a height of fifteen or twenty feet is rendered probable by finding the sand and mud smirching the limbs and foliage of trees overhanging the orifices."

An exceptional example of a craterlet located along the South Carolina Railroad line near Ten Mile Hill is presented in figure 3. This site is located adjacent to the present Charleston International Airport and Airforce Base.

Since most of the meizoseismal area was uninhabited forest and swampland the initial reconnaissance was limited to the several railroad lines emanating from Charleston and traversing the isoseismal zone. Seismically induced liquefaction features surficially expressed as fissures, vents, or sandblows that expelled sand and sometimes clay, were widespread in the loose sandy soils of the Charleston region (4,32,44). Much of the structural damage experienced throughout the Charleston area can be attributed to liquefaction related ground failures in both natural and fill, or "made" ground (37). Perhaps one of the most historically intriguing occurrence of liquefaction was the "formation of fissures in the tiling through which gushed water and strangely multicolored sand" in the center aisle of St. Michael's Church in downtown Charleston and the resulting 8 inch settlement of its steeple (51). While numerous occurrences of liquefaction related features were reported in Charleston the primary areas of documented liquefaction were located along the South Carolina railroad tracks at Ten Mile Hill and along the historic Charleston and Savannah railway near Ravenel. In these regions sandblow craters up to 20 feet in diameter and rifted vents up to 2000 feet long were found with surrounding land covered with expelled water and sand to depths of up to two feet (32). After an extensive reconnaissance Sloan (12) placed approximate boundaries on the areal extent of craterlets caused by the earthquake (figure 4).

2.3 Geologic Setting

The coastal plain region of South Carolina is locally referred to as "low country" due to its mimimal relief and low elevation (10 to 35 feet in the study area). The geology of the Charleston region is characterized as a series of interglacial, regressive backbarrier, beach and shelf sedimentary deposits which trend roughly parallel to the present shoreline and increase in age to the northwest

(inland). Most of the Carolina low country is covered by a 16 to 35 foot thick blanket of Quaternary marine and fluvial deposits which lies on semilithified Tertiary sediments (21). The sites evaluated for testing in this study are entirely late Pleistocene beach, shelf, and to a lesser extent backbarrier and fluvial deposits of the Pamlico, Talbot, and Princess Anne Formations (21). The groundwater table roughly mimics local topography and is found within 3 feet of the ground surface except at sites where lowered by drainage ditches. Soil studies conducted throughout the coastal region on the organic rich Bh horizon (the base of which closely demarks the maximum depth of the seasonal water table) indicate that the water table has been at a depth of roughly 2 to 3 feet throughout the Holocene (28).

The potential for liquefaction of a soil is dependent on both the characteristics of the seismic motion (intensity and duration) and the geologic setting and nature of the deposit (depth to ground water table, cementation, and relative density). The geologic setting most frequently associated with recognizable earthquake-induced liquefaction features in the Charleston area is the crest or flank of a Pleistocene beach ridge, where a thin cover of clay bearing sand or humate-rich-soil overlies uniform, clean sand (30). According to first hand accounts of effects of the 1886 earthquake, "these craterlets are found in greatest abundance in belts parallel with (beach) ridges and along their anticlines" (32). A schematic cross-section through a typical low country beach ridge, such as the ridges described by Sloan, is demonstrated in Figure 5.

2.4 Paleoseismological Investigations

The surface manifestation of seismically induced elevated pore pressures at depth ranges from minor sand boiling and venting to large, "explosive" sandblows. Both mechanisms of pore pressure release involve the extravasation of liquefied sand, and fracturing and displacement of overlying soil. The craters or vents are eventually obscurred by infilling and material collapse from their walls, but a distinctive morphology which cross cuts the surrounding undisturbed soil is preserved in the soil

column. Figures 6 and 7 are cross sections of representative explosive and non-explosive liquefaction features.

In recent years paleoseismological investigations involving the identification of relic sandblow features in the geologic column have been undertaken to date the events and establish the recurrence interval of the large ($m_b > 5.5$), prehistoric earthquakes that induce the formation of these features (28,43,48,42,46). Numerous examples of sandblows and non-explosive vents attributed to both the 1886 earthquake and several other episodes of Quaternary ground motion have been discovered in the walls of drainage ditches and small trenches in the low lying region around Charleston. Trenching and mineralogic investigations at two sites covered by this study were undertaken to : 1) determine the depth of the liquefied source beds and, 2) use mineralogic alteration of vented sands as an indicator of the age of the sandblow features. Radioisotope (^{14}C) age dating of wood fragments found in successive sandblow features located near the town of Hollywood, approximately 20 miles west of Charleston, has yielded a tentative, maximum recurrence interval for large earthquakes of approximately 1700 years (52). Age dating and size comparisons of sandblows located between North Carolina and Georgia, and initiated by successive earthquakes has lead to the conclusion that several moderate to large Quaternary earthquakes have occurred in the Charleston area and that Holocene shaking has been stronger near Charleston than elsewhere along the coast of South Carolina (30).

2.5 Mechanism of Liquefaction

The liquefaction of a loose, saturated granular soil occurs when cyclic shear stresses passing through the soil deposit induce a progressive increase in excess hydrostatic pore water pressure (39,16,22). During an earthquake the cyclic shear waves that propagate upward from the underlying rock formation induce the tendancy for a loose sand layer to decrease in volume. Cyclic shear straining and the volume contraction associated with collapse of the metastable structure of sand

can not occur simultaneously because the duration of shaking is much faster than the time necessary for drainage of pore water. This process is diagramatically represented in figure 8. If undrained conditions during the seismic disturbance are assumed, an increase in pore water pressure and resulting decrease of equal magnitude in the effective confining stress is required to keep the loose sand at a constant volume. The degree of excess pore water generation is a function of the initial density of the sand layer and the level and duration of seismic shaking. If the layer is initially loose enough pore pressures can be generated which exceed the confining stress. At this state no effective stress, or intergranular stress, exists between the sand grains and a complete loss of shear strength is experienced (figure 8b). This loss of strength is termed liquefaction, after which settling of the sand grains causes an expulsion of pore water towards the surface.

Even though a condition of zero effective stress develops in a sand during cyclic loading the sand may still exhibit considerable resistance to shear during a subsequent undrained loading. Castro and Poulos (7) have used the critical void ratio and steady-state strength concept to demonstrate for medium and dense sands that although initial liquefaction ($\sigma' \simeq 0$) can occur as a result of cyclic loading no large displacements are experienced. This has been termed *cyclic mobility* and corresponds to the limited shear strain potential of Seed (22). Cyclic mobility can lead to excessive ($\simeq 10\%$) permanent deformations but not instability due to the tendency for sands to the left of the critical state line (figure 9) to dilate under loading following initial liquefaction, thereby reducing the excess pore pressure. In this context undrained cyclic straing of very loose sands permits the particles to rearrange so that their cyclic resistance is less than the undrained steady state strength (similar to residual strength). This behavior is "true liquefaction" and results in a collapse of the sand structure and large deformations. An outstanding overview of liquefaction and cyclic mobility is contained in the National Research Council report on liquefaction (22). The formation of a sandblow or vent requires the generation of excess pore pressures and large strains which can only be realized during liquefaction of loose sands. This consequently greatly overshadows the contribution to increased pore pressures developed during cyclic mobility of dense sands which may be interlayered with the loose material.

2.5.1 Formation of Liquefaction Features

Sand boils, vents and blows are indicative of liquefaction at depth. Sand boils are formed by water venting to the ground surface from zones of high pore water pressure generated at shallow depth by the tendency for compaction of granular soils during seismic shaking, as previously described. The surface expression of liquefied material is primarily dependent on the intensity of seismic ground motions, as minor venting of mud and sand may be visible at a MM intensity of VIII, become notable at IX, and large and spectacular at X (Richter in 4). Based on field observations a correponding magnitude (m_b) of 5.0 has been presumed as the threshold value for liquefaction-induced ground failures (55). Magnitudes of 5.5 and 6.2 have also been postulated as values required for the initiation of liquefaction in specific regions (46,52). A value closer to the former would appear likely for the very loose sands in the Charleston area (26).

The surface manifestation of these features is also governed by both the extent of the liquefiable layer and any overlying liquefaction resistant layers. If a liquefiable layer is overlain by a thin mantle of liquefaction resistant material that can be easily fractured or heaved, the extrusion of fluidized sand will occur as mild sand boiling and fissuring. The presence of a thick overlying, cohesive layer will require large pore pressure generation to hydraulically fracture this overburden. Venting through non-cohesive soils may involve different mechanisms. Following the initiation of liquefaction a cavity of water can form at the base of the resistant non-cohesive material, which migrates toward the surface by continuous stoping from the roof of the cavity (22). If the cavity approaches the surface the pressurized, soil-laden water in the cavity can break through almost explosively to form a sandblow. This behavior can result in the formation of sandblows which reach the surface several minutes after the cessation of strong ground motions. In cases where thick overlying layers have been fractured the sandblows are found to be very large and fewer in number because the breakthrough of the first vents release pore pressures thereby inhibiting concurrently forming cavities. Based on field observations at sites in Japan and China where seismically induced liquefaction features were and were not apparent, Ishihara (16) has postulated relations between the

thicknesses of the liquefiable and overlying non-liquefiable layers and the surficial exposure of vented material. Figure 10 demonstrates the effects that the layered system and ground motion intensity have on the occurrence of observed ground failure. In the Charleston environment it appears that evidence of liquefaction at depth can be completely masked regardless of the thickness of the liquefiable layer if the surficial resistant layer is greater than about 10 feet (29). This observation is consistent with Ishihara's initial findings.

In the first hand accounts of the 1886 earthquake are descriptions of liquefaction features ranging from small vents issuing from fissures to spectacular 20 foot diameter sandblow craters formed during pore pressure releases. Strong venting of fluidized sand is favored when the liquefiable layer is capped by a thin layer of non-liquefiable, cohesive material. In this situation excess pore pressures in the liquefiable layer exceed the strength of the capping layer and a sand blow crater surrounded by an ejection sheet of liquefied sand an overlying material is formed. The development of a sand blow crater is shown in figure 11 (14). Numerous moderate to large relic sandblow features having similar morphology to those described in Dutton (12) have been discovered in the extensive network of drainage ditches in the Charleston region.

2.5.2 Recurrence of Liquefaction at the Same Site

Although the contraction of a saturated, loose sand during cyclic loading and resulting dissipation of pore water leads to a global increase in density of the layer, it is possible for a portion of the layer to be redeposited in a configuration that is as loose or looser than the initial arrangement. Laboratory triaxial and simple shear tests on Ottawa sands at relative densities between 37 and 70% have shown that for 15 loading cycles shear strains above a threshold value of approximately 0.5% create a structure in the the sand sample which is significantly more sensitive to liquefaction than the structure created by consolidation (13). These tests also indicated that for loadings of more than 15 cycles shear strains of $\pm$ 2.0% have a reducing effect on the resistance of sand to liquefaction in future cyclic loading tests. The range of single amplitude, cyclic shear strains where pore pressures

become equal to the initial confining stress under laboratory cyclic loading has been found to fall between 2.5 and 3.5% (16). An average value for cyclic shear strain of 3.0% is generally used as a criterion to specify the onset of liquefaction for loose sand, and is large enough to greatly reduce the liquefaction potential of a natural deposit in future earthquakes.

Laboratory reliquefaction studies are supported by field observations at numerous sites which have experienced repeated liquefaction (53). Paleoseismological investigations in the Charleston region have also located several sites where repeated liquefaction of loose sands has occurred during several episodes of seismic ground motion. Several mechanisms could account for the retained low resistance to cyclic shearing of a liquefied sand layer. Youd (53) has postulated that the liquefaction of a uniform layer begins at the upper portion where confining stresses are the lowest and propagates downward. The following compaction process begins at the base of the layer and proceeds to the top. If settling of the sand grains occurs after strong ground motions have ceased it is possible to create a loose zone at the top of the layer which is repeatedly liquefiable until the entire layer has been progressively compacted. Another condition may exist when liquefied layers are capped by impervious layers that inhibit the vertical release of pressure. In this situation excess pore pressures are either dissipated laterally throughout the layer or are reduced by a readjustment of void ratio in which the layer is globally undrained, but a portion becomes looser and more susceptible to reliquefaction. Field tests were performed during this investigation at sites where liquefaction has repeatedly occurred to find evidence for the progressive compaction of sands and to determine the liquefaction susceptibility of these sediments to future seismic loading.

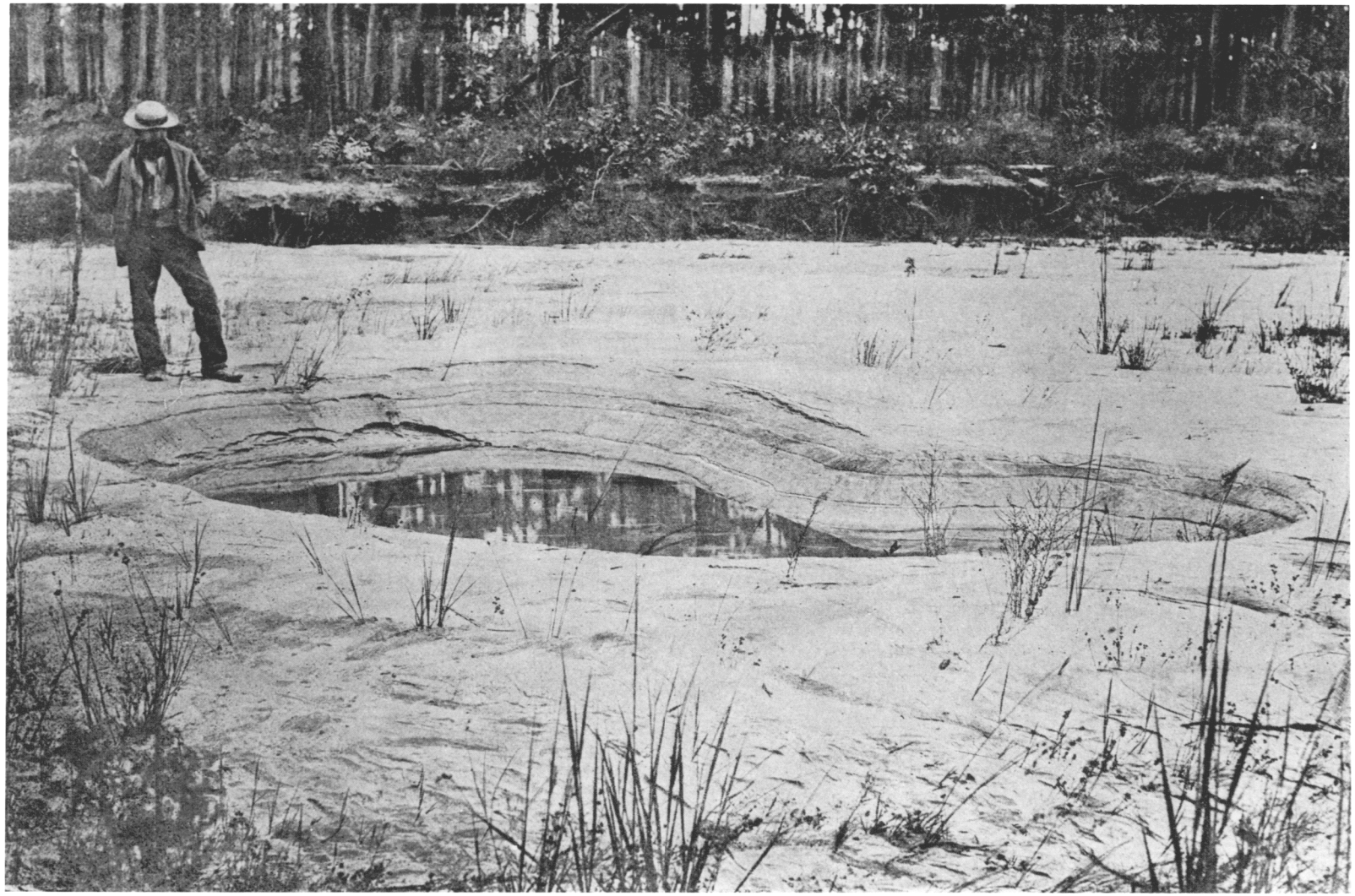

Figure 3. A large craterlet located near Ten Mile Hill.

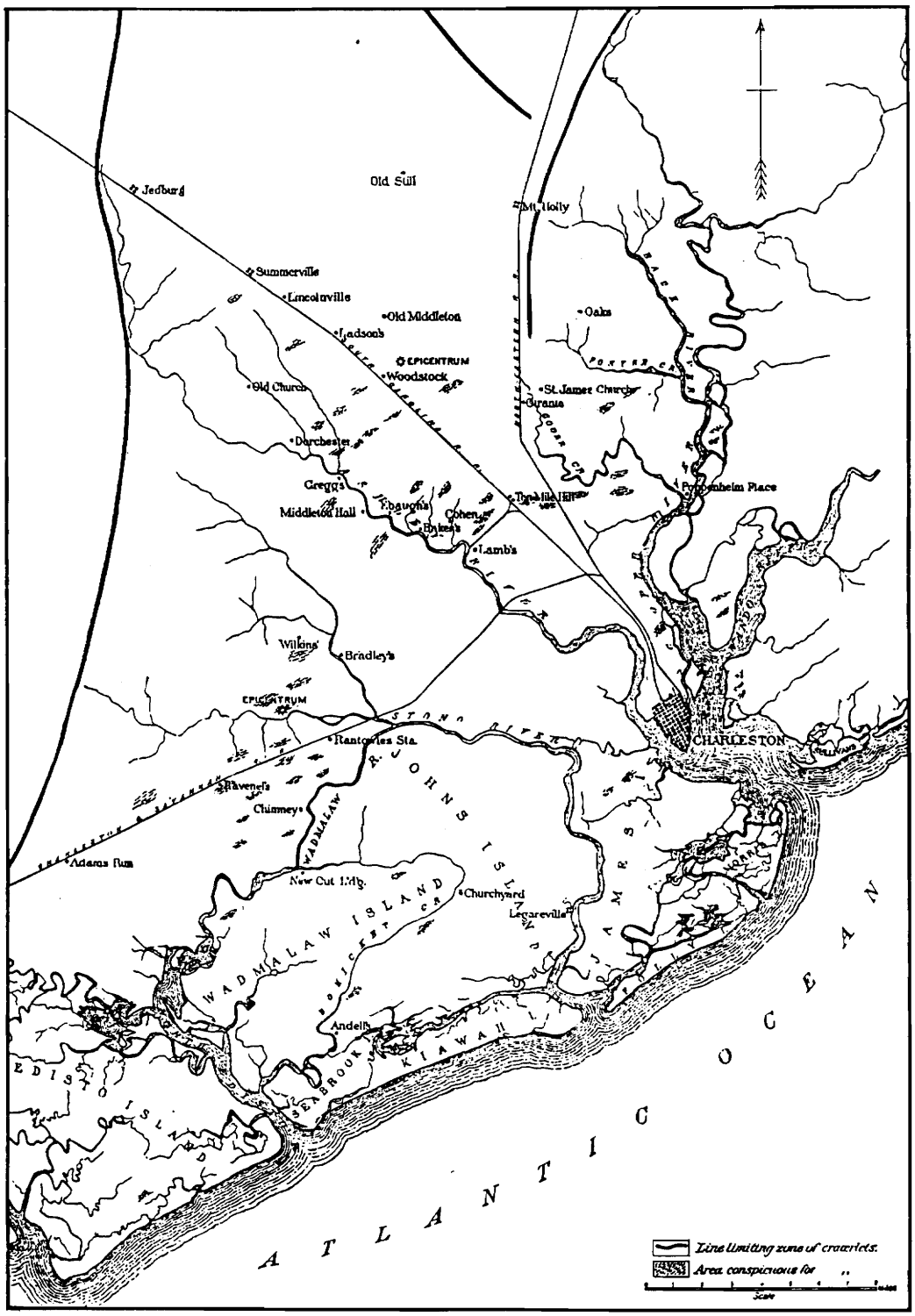

Figure 4. DISTRIBUTION OF CRATERLETS FORMED DURING THE 1886 CHARLESTON EARTHQUAKE (12)

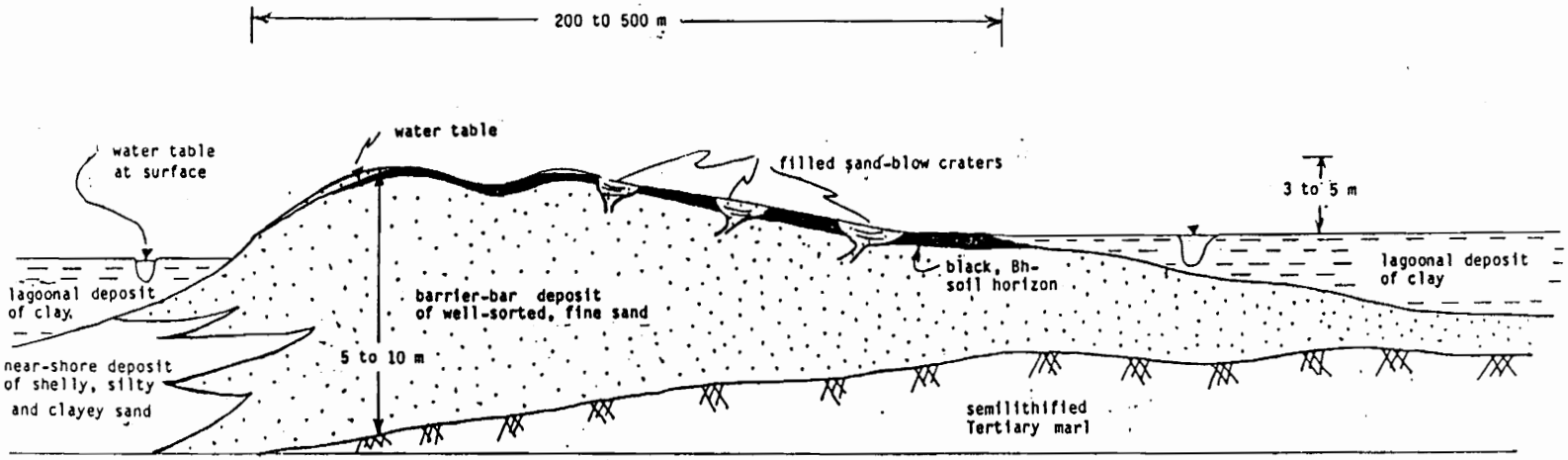

Figure 5. SCHEMATIC CROSS SECTION OF REPRESENTATIVE PLEISTOCENE BEACH BARRIER (30)

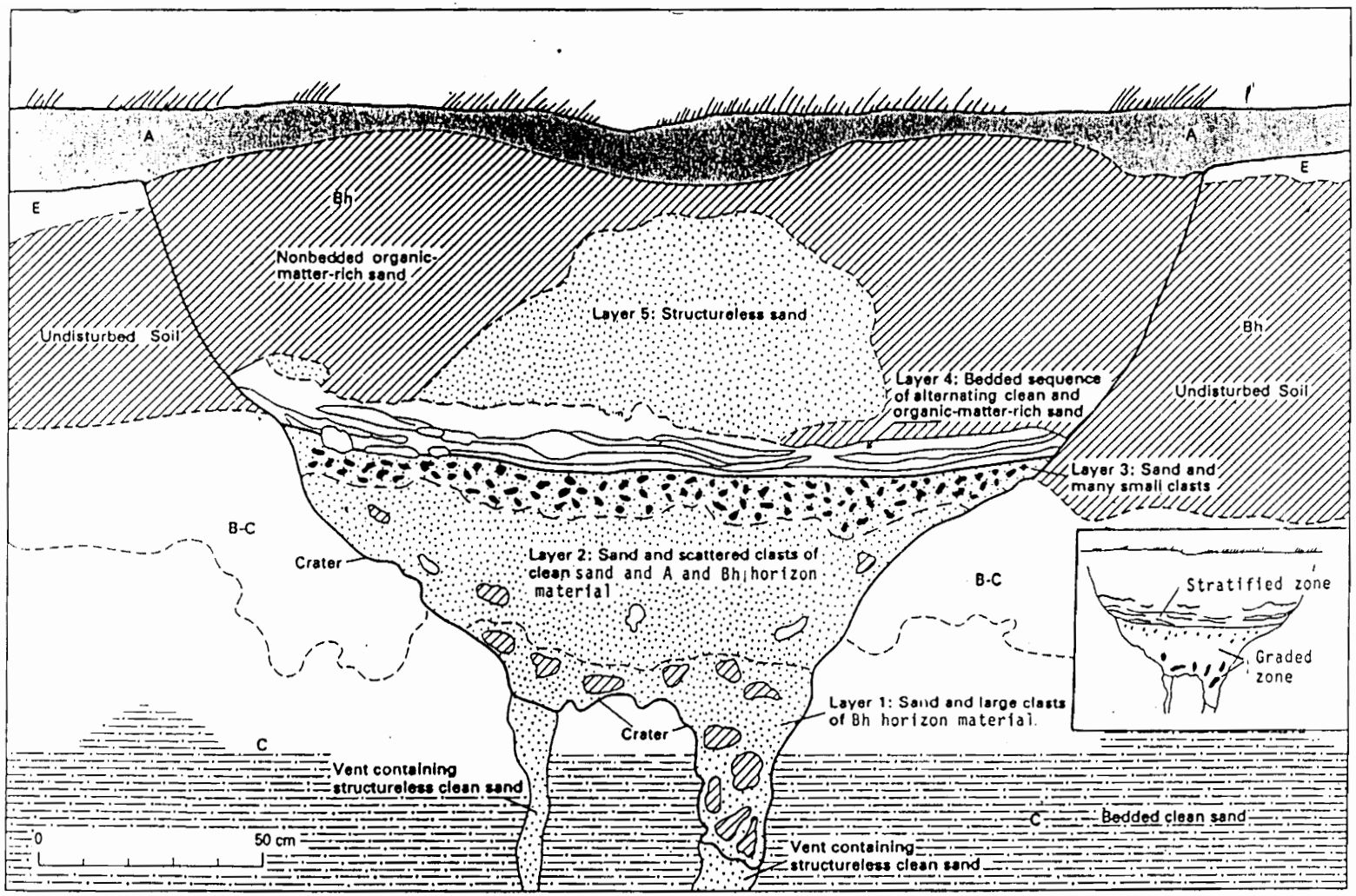

Figure 6. SCHEMATIC CROSS SECTION OF REPRESENTATIVE FILLED SANDBLOW CRATER. LETTERS CORRESPOND TO SOIL HORIZON DESIGNATIONS (30)

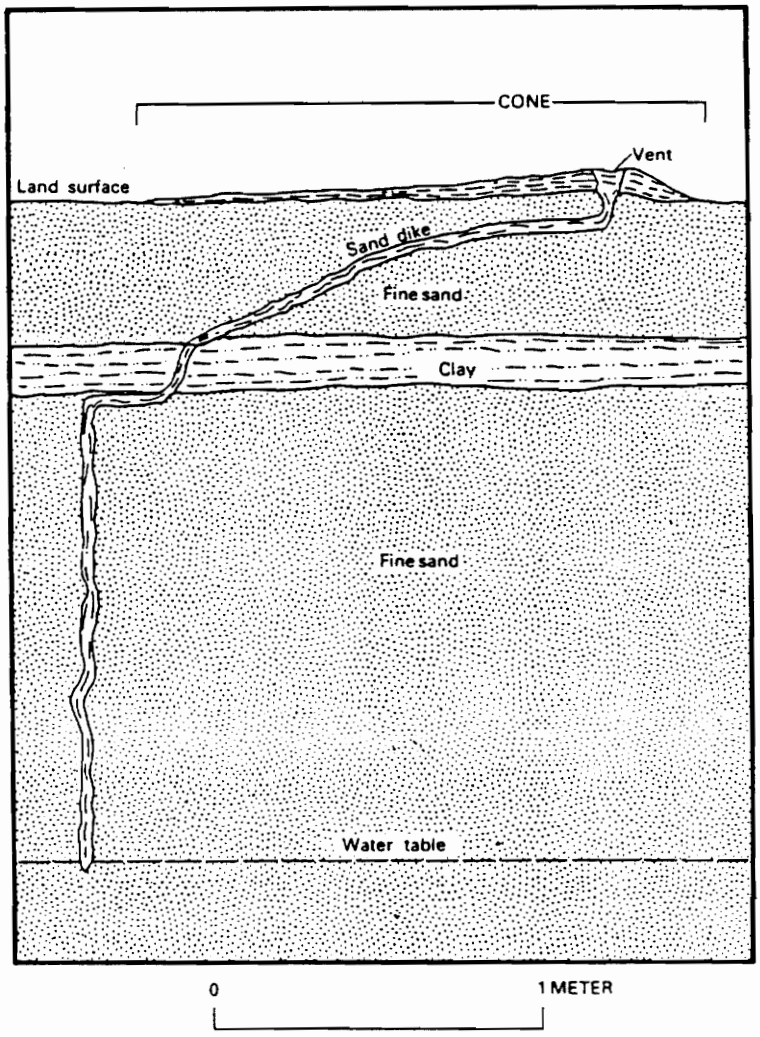

Figure 7. SCHEMATIC CROSS SECTION OF REPRESENTATIVE NON-EXPLOSIVE SANDBLOW

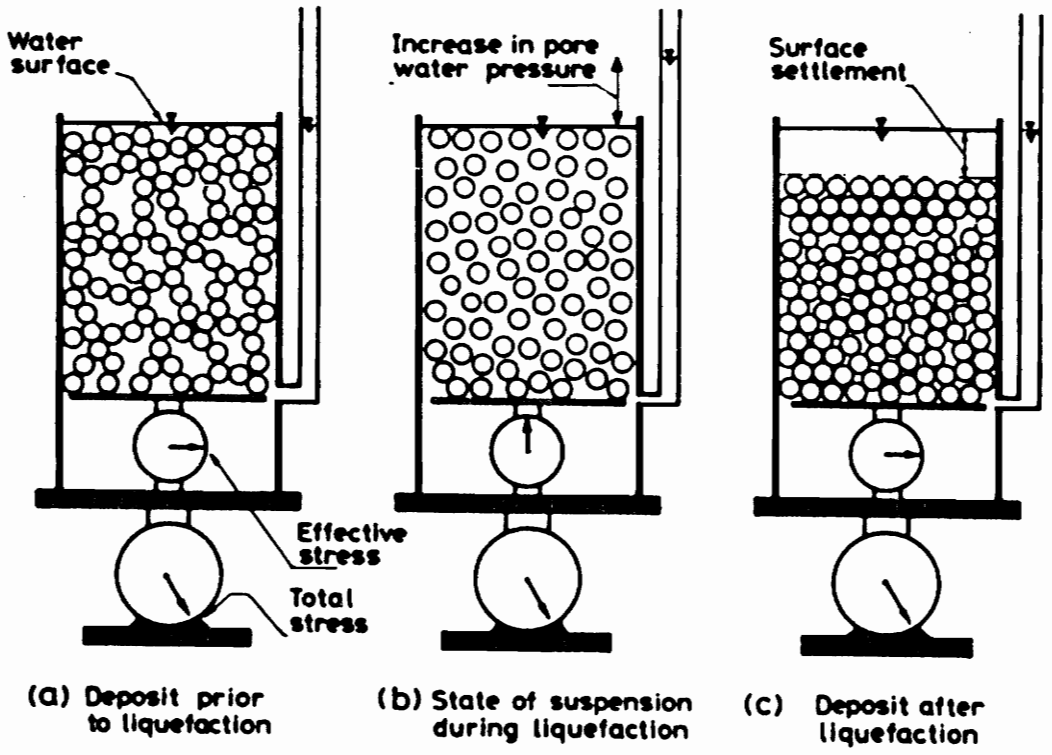

Figure 8. STRESS STATES DURING LIQUEFACTION OF A LOOSE SAND (16)

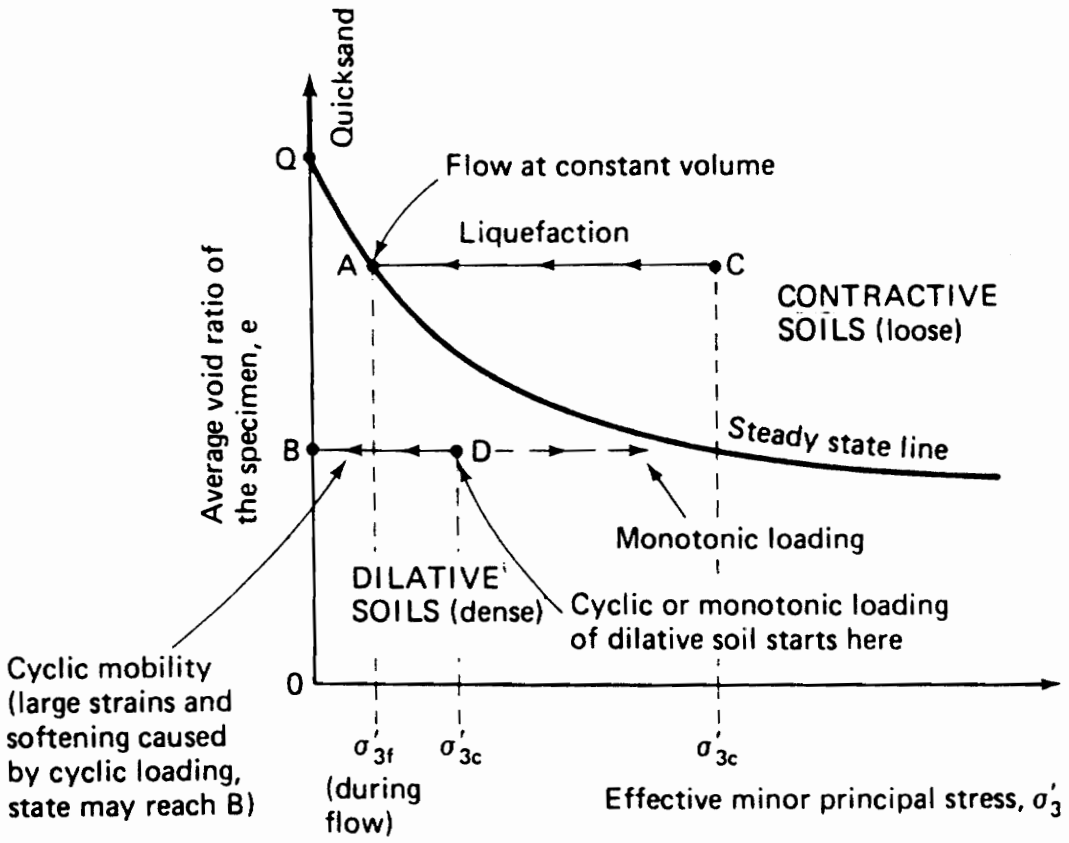

Figure 9. STATE DIAGRAM SHOWING LIQUEFACTION POTENTIAL BASED ON UNDRAINED TESTS OF SATURATED SANDS (7)

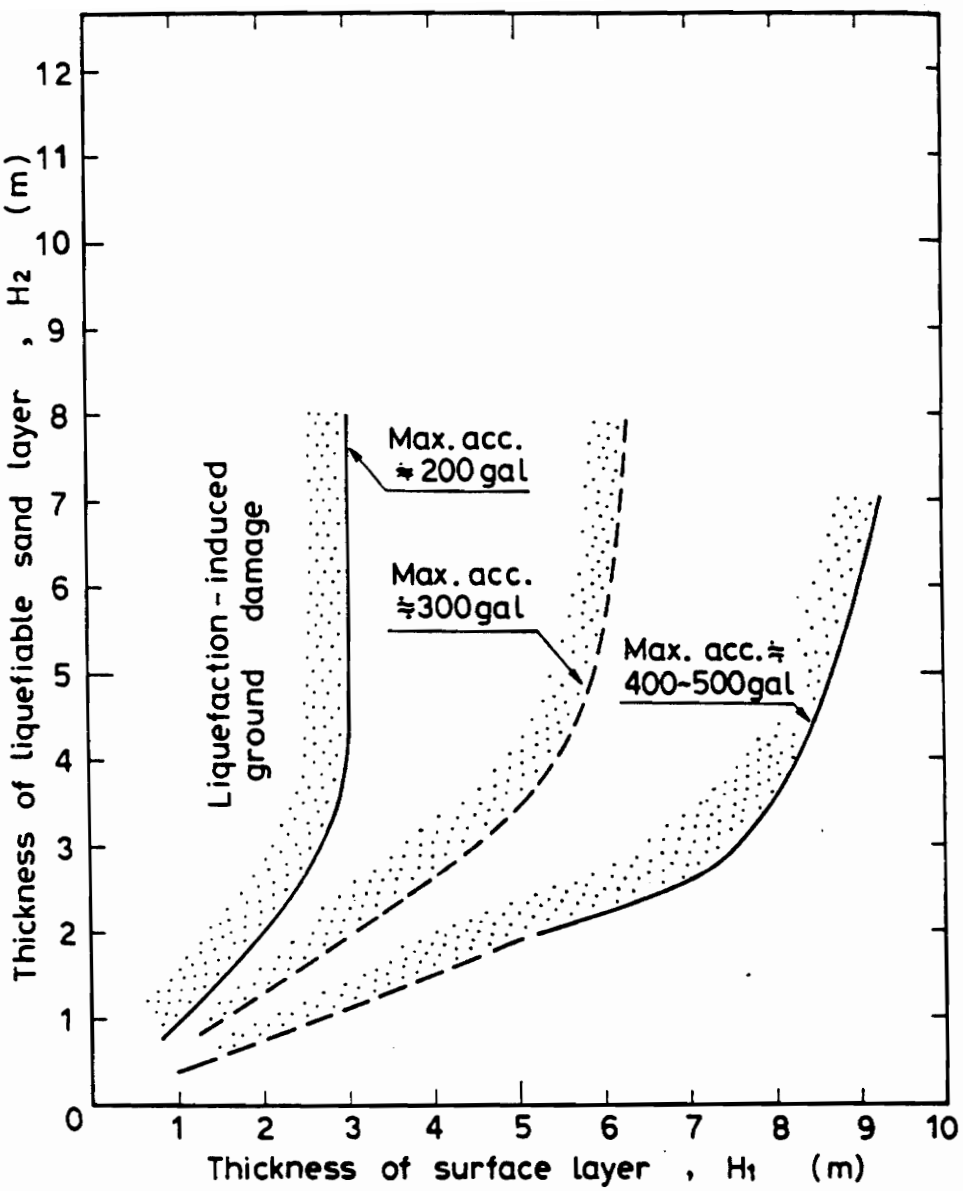

Figure 10. BOUNDARY CURVES FOR SITE IDENTIFICATION OF LIQUEFACTION INDUCED DAMAGE (16)

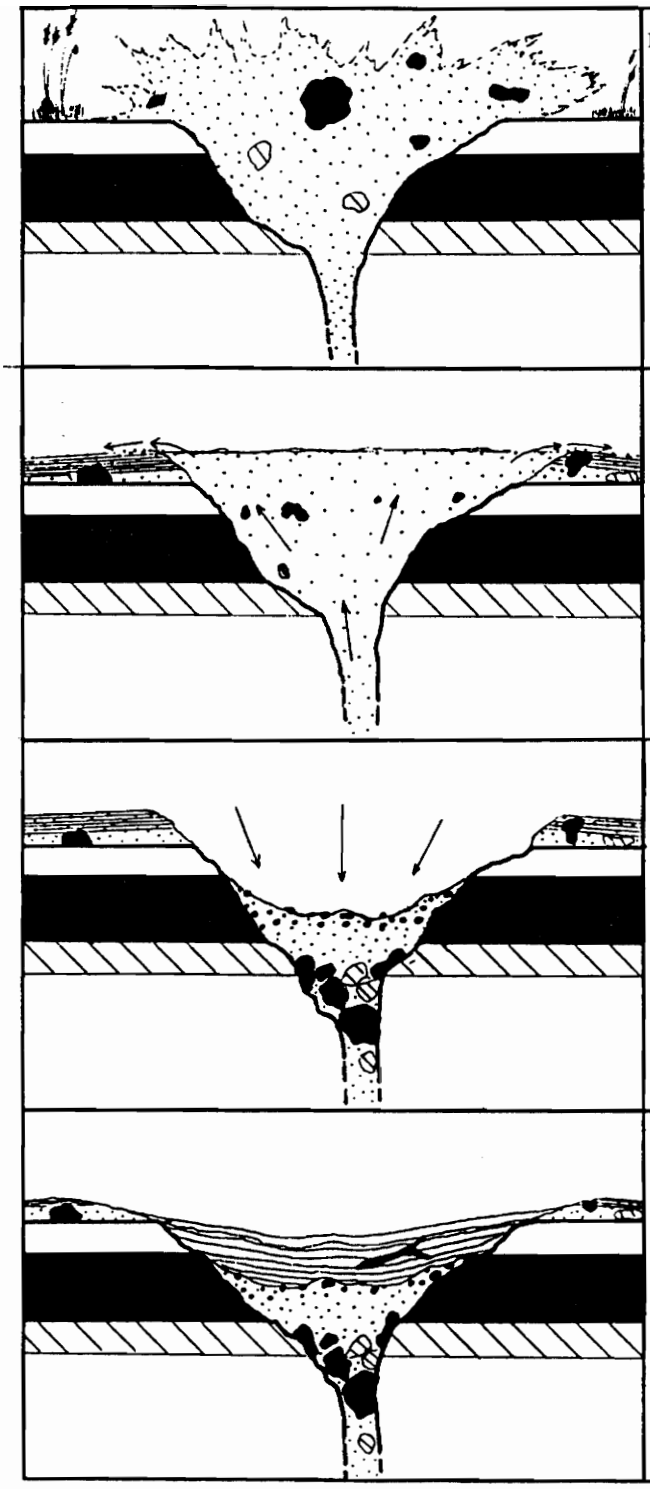

FIGURE A.-- Explosive phase. Excavation of a crater with an explosive discharge of sand, clasts, and water.

FIGURE B.-- Flowage phase. Continued expulsion of fluidized sand and clast materia Constructional feature forms with gently dipping laminations.

FIGURE C.-- Collapse phase. As upward flow of water diminishes churning of clasts, soil and water occurs followed by settling of larger clasts and finally collapse.

FIGURE D.-- Filling phase. Slow filling of the upper part of the crater from months to years after the event. Vegetative matter may be buried within the bedded sequence (which may be carbon dated).

Figure 11. SEQUENTIAL DEVELOPMENT OF A SANDBLOW CRATER (14)

Chapter III

Testing Program

3.1 Background

The liquefaction induced ground failures associated with the great earthquakes of 1964 in Niigata, Japan and Anchorage, Alaska prompted the need for an increased knowledge of the cyclic behavior of liquefiable soils. Over the past two decades the wealth of laboratory and field inverstigations has determined many of the factors which influence the liquefaction susceptibility of fine grained soils (13,7,41,22,16,19). Many of these reports acknowledge the difficulty encountered with the extraction of undisturbed samples of loose, non-cohesive soils and the deleterious effects that stress release, loss of in-situ sand structure and void ratio reduction can have on the results of laboratory cyclic shear tests. The difficulty in obtaining undisturbed, representative samples of loose sands has led to the acceptance and increasing use of in-situ testing methods for the direct measurement of soil properties influencing the liquefaction potential (31).

The basis for in-situ evaluations of liquefaction susceptibility has been the standard penetration test (SPT) due to its large data base compiled over years of world-wide use. More re-

cently the use of the cone penetration test (CPT) has gained favor due to its continuous record, which provides a better picture of the vertical variability of a deposit, and its standardized method of operation (1). The general success of these in-situ testing methods seems to indicate that the penetration resistance is sensitive to the same factors (i.e. relative density, lateral earth pressures, and over consolidation ratio) that effect resistance to liquefaction (22,11).

The objective of the field testing program was to utilize primarily the CPT and to a lesser extent the SPT in or near the meizoseismal zone of the 1886 earthquake to identify areas exhibiting different susceptibilities to liquefaction. During this phase of the investigation a testing schedule was performed that involved extensive coverage of the Hollywood and Warren sites and preliminary work at as many other sites as could be tested. Work scheduled for the next phase of the study will allow for more testing at each of these sites. While all of the test sites were located in areas exhibiting liquefaction features, attempts were made to locate a site where the absence of these features could be attributed to high relative densities of the sandy soil. These sites would have allowed for a lower bound to be placed on the peak ground motions experienced at the site during the 1886 earthquake. Although several large borrow pits located within the meizoseismal region were inspected and found to be free of relic venting features, in all cases the liquefaction resistance was attributed to high clay contents.

Approximately 200 hours of drill rig time were completed during the 29 day testing schedule. In this time the author and fellow student, James R. Martin II, augered approximately 35 exploratory 40 - 45 foot deep boreholes at ten sites and conducted 24 electric cone penetration tests at seven sites. The cone tests were conducted as close as possible to mapped or historically documented sandblows, and at several sites additional tests were carried out at selected distances from the liquefaction features to determine density and compositional variations of loose sand layers. Figure 12 shows the cone testing operation located at the Oakland Plantation near a thin seam of white, fine sand presumed to be a liquefaction vent of the 1886 earthquake. Penetration data were supplemented with auger borings adjacent to each testing site to allow for both visual classifications of the tested soil and grab bag samples for sieve analysis of sand in layers ex-

hibiting potentially liquefiable properties. The CPT data were reduced using guidelines presented by Robertson and Campanella (34).

3.2 Test Sites

Field sites were chosen to represent cases with varying degrees of liquefaction phenomena, and different positions relative to the earthquake epicenter. Several of the site locations and critical assessment of the relative degree of liquefaction which occurred at various sites were made by Mr. S. Obermeier of the U.S. Geological Survey. His assistance was important in view of his substantial experience in the area. Previously investigated drainage ditches affording continuous exposure of possible liquefaction features were primarily locales for CPT testing. Sites with historical documentation of extensive liquefaction and well constrained locations of sand blows were also considered valuable for testing. The sites studied in this investigation are shown in relation to the centers of highest intensity and approximate boundary of the meizoseismal zone of the 1886 earthquake (figure 13). The depositional ages determined by mineralogic, paleontologic and radiometric methods, and lithology of the soils at each test site are listed in Table 1. Of the sites, Hollywood and Warren have been areas of extensive paleoseismological investigation (28,30,52,14,9,46). The drainage ditches at Hollywood (HW) provide probably one of the most extensive exposures of relic liquefaction features that have ever been observed. Much of the cone and standard penetration testing was conducted along the Hollywood ditch at intervals which allowed for: 1) determination of the lateral extent of the liquefiable soil strata, and 2) possibly determine changes in soil properties that would account for the differences in number and size of liquefaction features found along the roughly 9000 feet of mapped ditch (25). The Hollywood ditch and CPT sites are shown in figure 14. It should be noted that State Route 162 is built on the crest of a beach barrier deposit and that the drainage ditch which trends subparallel to the crest, is cut through the flank of the deposit. Of

the seven sites, Hollywood ditch was the first tested and received the most extensive coverage. The wealth of information previously gathered at this site covers every facet of the investigation; first hand observations of wide spread craterlet formation in the area, numerous paleoseismological and mineralogic investigations, and work conducted at Virginia Tech on the dynamic properties and liquefaction susceptibility of sands excavated from areas exhibiting sandblow features (10).

Cone penetration testing along the Hollywood ditch was originally scheduled to be conducted at close spacings to determine any variations in the soil profile. Soil borings performed in this investigation along the ditch indicated that the profiles were compositionally very uniform to a depth of roughly 15 feet where the sands became increasingly clayey. After several CPT's carried out at spacings of 1000 feet indicated that the penetration resistances were not significantly different, this interval was chosen as optimum for representative coverage and expediency.

A local soils testing company was contracted to perform 6 SPT's in close proximity to CPT locations. The SPT's aided in characterizatin of the sandy soils at the site by providing samples and additional penetration resistance data. Penetration tests were perfomed with a track mounted drill rig equipped with a rope and pulley hammer release system. The donut hammer was raised and dropped on a cylindrical anvil rotating cathead. The borehole was stabilized using bentonite drilling mud. This system provided an estimated rod energy of 45% of the theoretical free-fall energy intended for the test. The SPT schedule started at the ground surface and involved testing at 2.5 foot intervals through the dense material that was generally found to a depth of 10 feet along the entire ditch, followed by continuous testing through the loose sand until material was encountered that was nonliquefiable due to high relative density or clay content. Split spoon samples were collected at every interval and at three stations borings were made to determine the depth to the rock-like (V_s > 1800 ft/sec) marl that underlies the site.

Cone penetration tests conducted at the Warren site (W) were located around an approximately 30 foot long vent that expelled a large quantity of sand during the 1886 earthquake (figure 15). This site had been trenched and analyzed by Cox (9) who investigated the morphology and stratigraphy, and inferred possible source beds of this relic liquefaction fissure. The testing coverage for this study included three CPT's and five exploratory borings to determine the soil variability

around the liquefaction feature. Field classifications of the soil were supplemented with 35 sieve analyses referenced from Cox's investigation.

The remaining sites are in areas where liquefaction features induced during the 1886 earthquake have either been described in the first hand observations or discovered during geologic investigations. The Sod Farm (SF), Montague (M), and Oakland Plantation (OP) sites (figures 16, 17, 18) are located in areas where relic liquefaction vents have been found. The Ten Mile Hill (TM) and Eleven Mile Post (EM) sites were historically well documented for the occurrence of craterlets. A literature review of reports by E. Sloan (32) and C.E. Dutton (12) revealed well constrained locations and photographs of liquefaction induced ground failures located in the Ten Mile Hill area. Contained in these reports are photographs from "George L. Cook's Earthquake Views" (32). Photos no. 53 and 54 of Cook's series were taken along the SCRR tracks at Ten Mile Hill and show in the background a switch post, side track, and whistle board signifying a nearby crossing. Although the photos are taken from different positions it is the author's opinion that Cook's photo no. 53 of a large, eroding craterlet is of the same feature as is shown in figure 3 (Dutton's plate XX, 12), only taken several days later. After a review of several maps at the South Carolina Historical Society determined the location of the crossing and side track along the SCRR line, the Ten Mile Hill site was chosen (figure 19). It is believed that the CPT was conducted within several hundred feet of the feature shown in figure 3. The Eleven Mile Post site (figure 20) was similarly chosen as Sloan reported the occurrence of localized craterlets in the area. At these sites one or two CPT's and borings were performed directly over or in the immediate vicinity of the observed liquefaction features. Time constraints on the testing program limited the initial site evaluation to a preliminary characterization of the soil conditions. Further testing will be completed during subsequent phases of this investigation.

Based on first-hand descriptions of the ground motions and intensity reports within the meizoseismal zone, it has been deduced that the energy release of the 1886 earthquake was initiated near Dutton's southwestern epicentrum and propagated toward the northeastern epicentrum (24). A line connecting the two centers of highest intensity can be interpreted to be the surface projection of the fault rupture plane and linear zone of seismic energy release. The distances from the test sites

to the rupture plane are taken as the closest point to the line connecting Dutton's epicentrum. Table 2 lists these distances and notes the nature of liquefaction which occurred at the sites during the 1886 event. The extent of liquefaction induced during the 1886 earthquake was inferred from the initial reports on the earthquake and in relation to the number and size of relic features discovered per unit area of exposure during geologic investigations. In the context of areas experiencing ground failures in 1886 the sites are graded as experiencing extensive, moderate, or minor liquefaction.

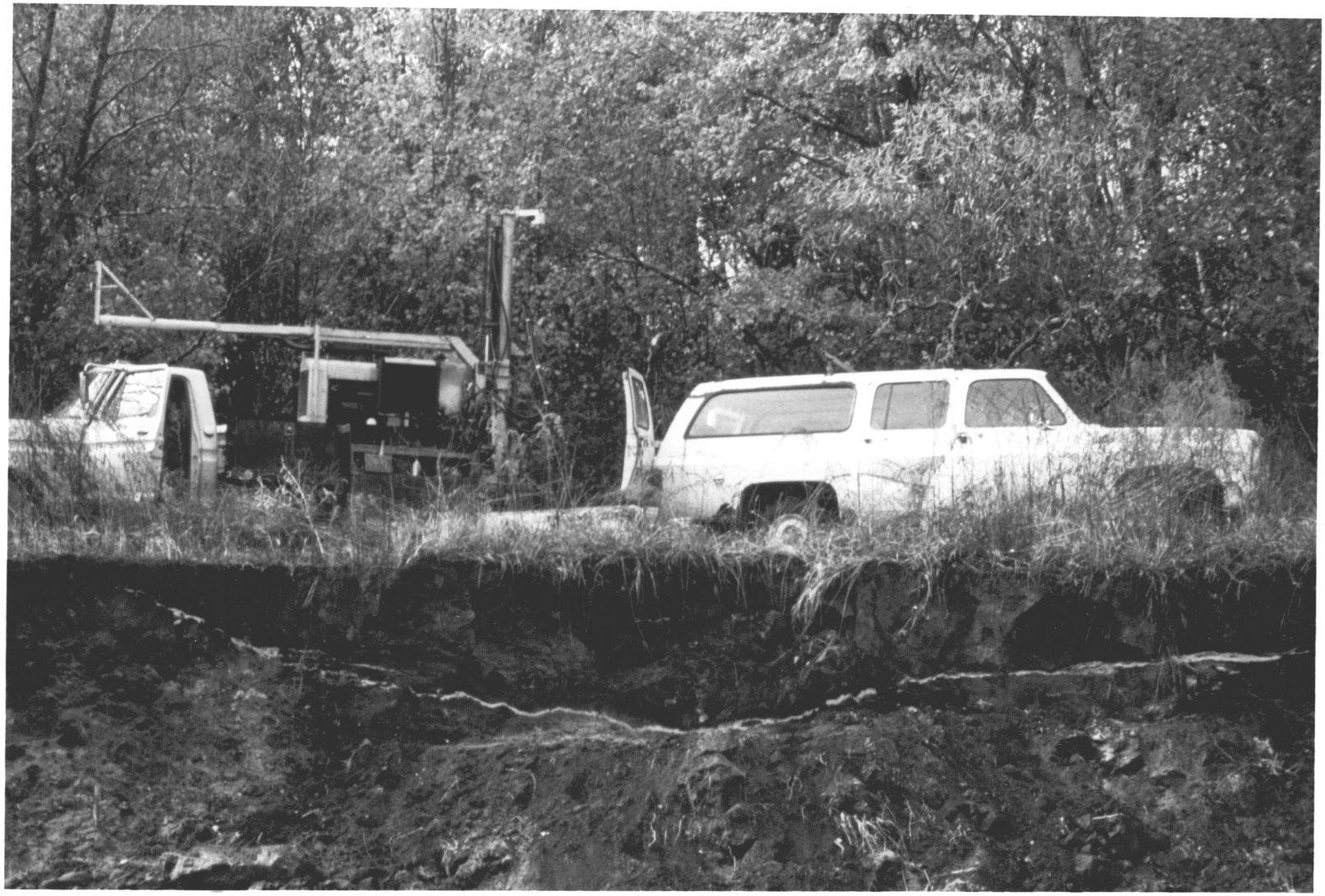

Figure 12. Cone Testing Operation at the Oakland Plantation Site. A thin white seam of vented sand can be seen in the wall of the sand pit.

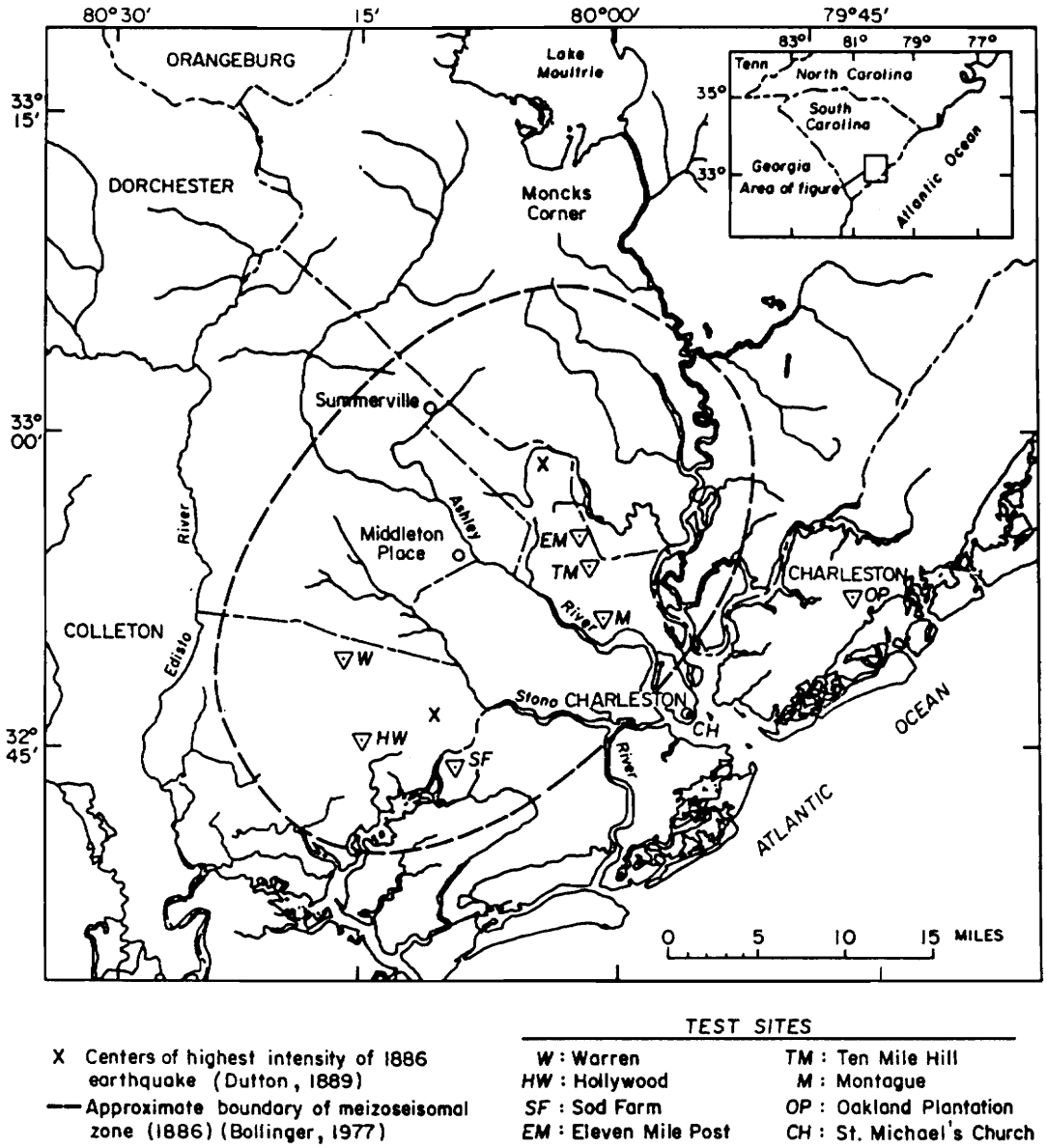

Figure 13. LOCATIONS OF THE STUDY SITES, SHOWING RELATION TO MEIZOSEISMAL ZONE OF THE 1886 CHARLESTON EARTHQUAKE

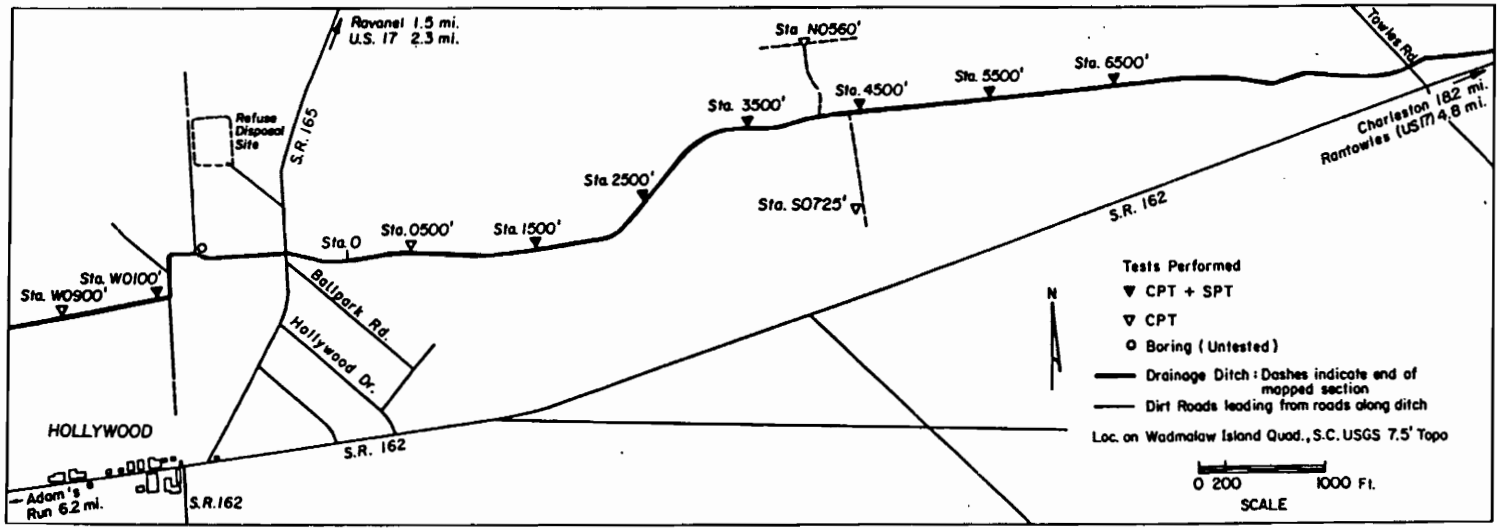

Figure 14. LOCATION OF PENETRATION TESTS PERFORMED AT THE HOLLYWOOD SITE

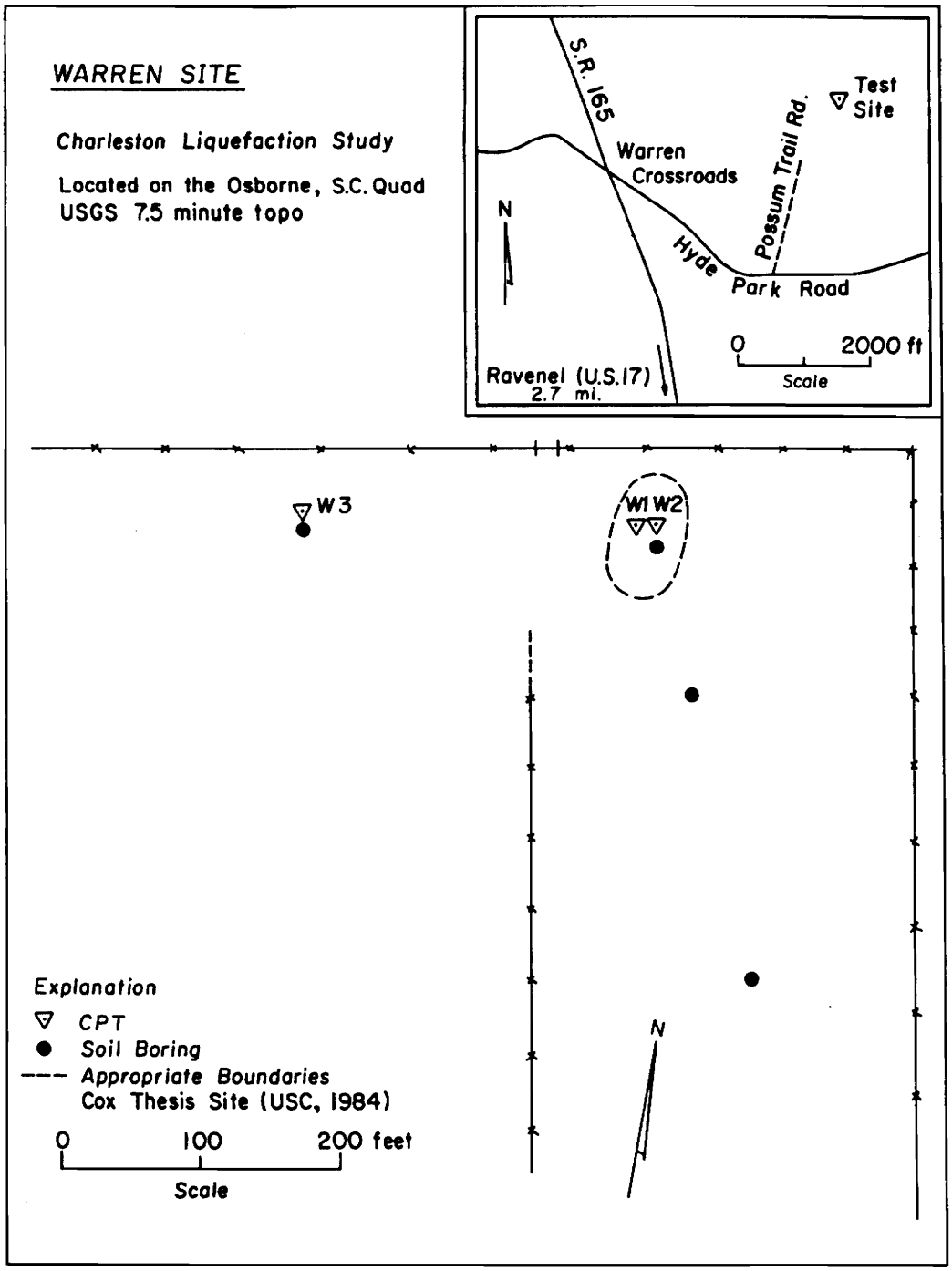

Figure 15. LOCATION MAP FOR THE WARREN SITE

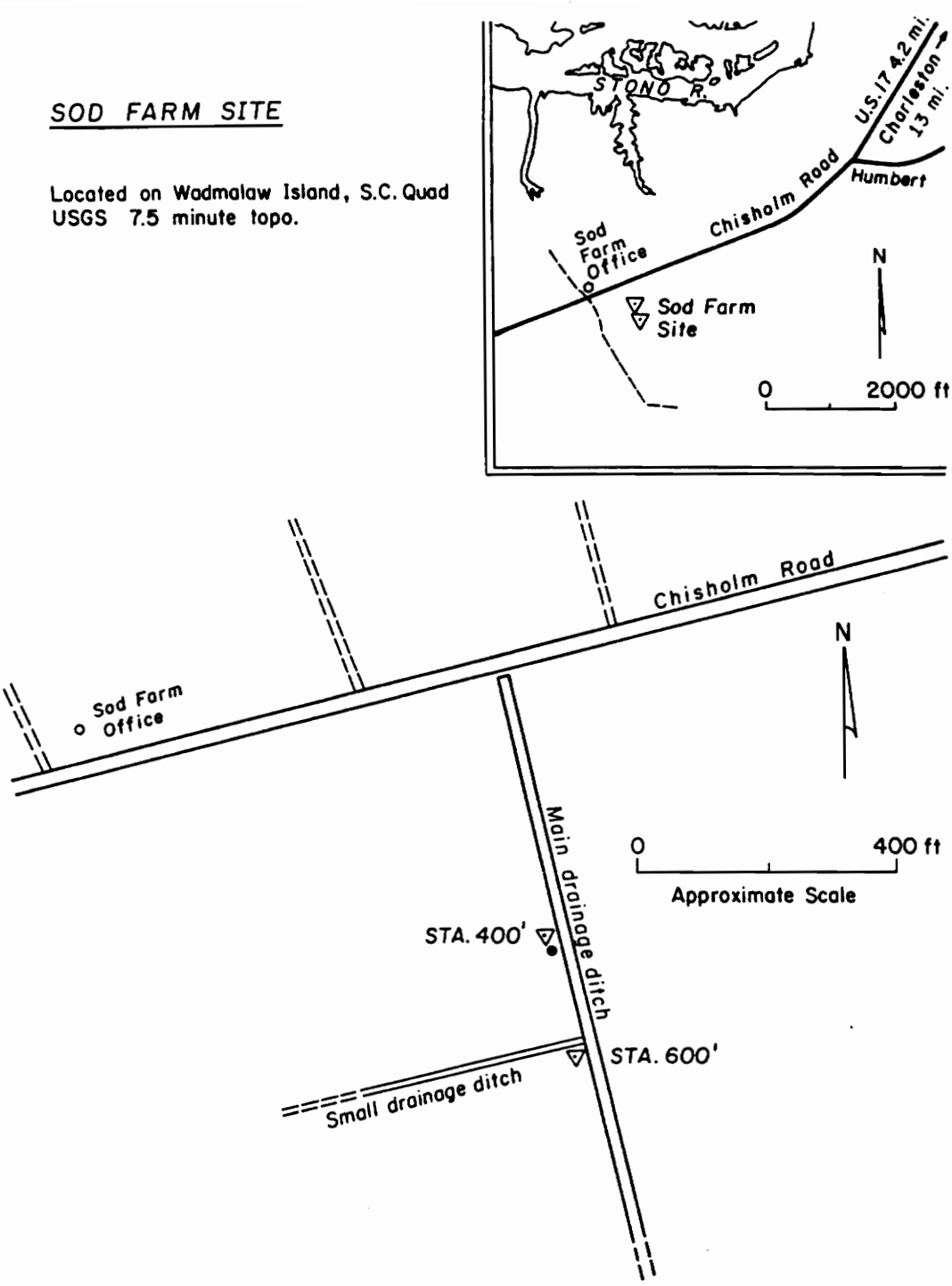

Figure 16. LOCATION MAP FOR THE SOD FARM SITE

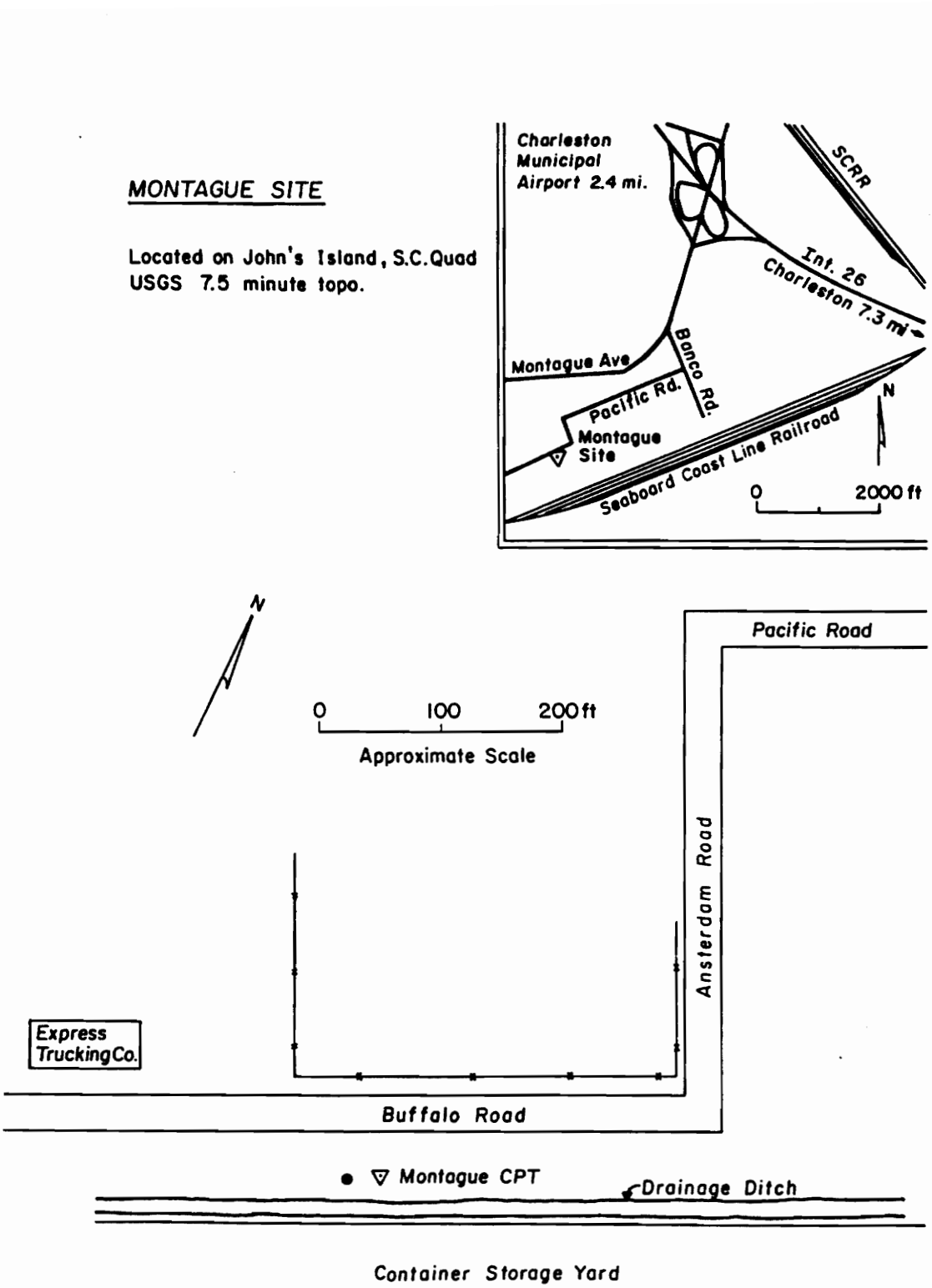

Figure 17. LOCATION MAP FOR THE MONTAGUE SITE

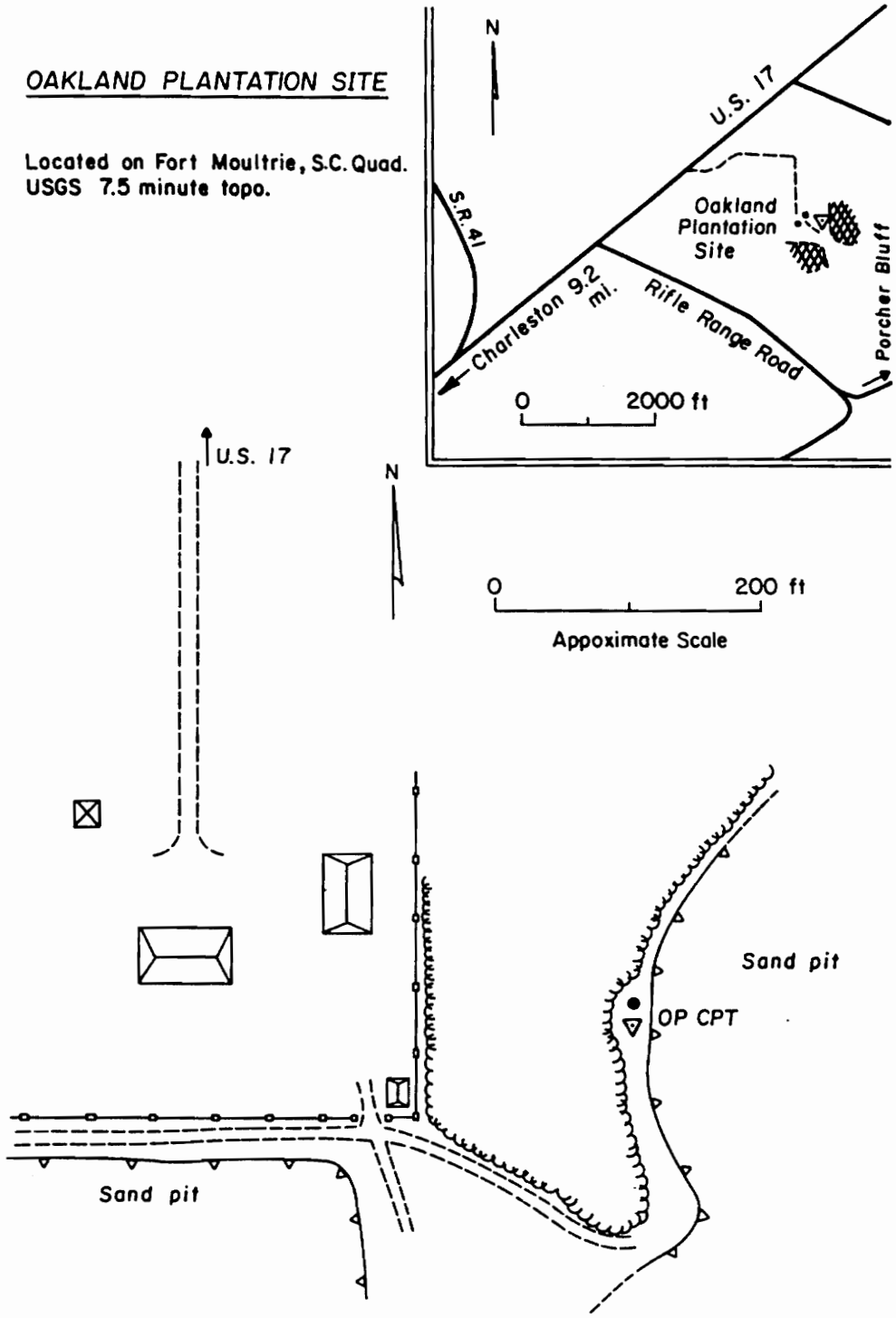

Figure 18. LOCATION MAP FOR THE OAKLAND PLANTATION SITE

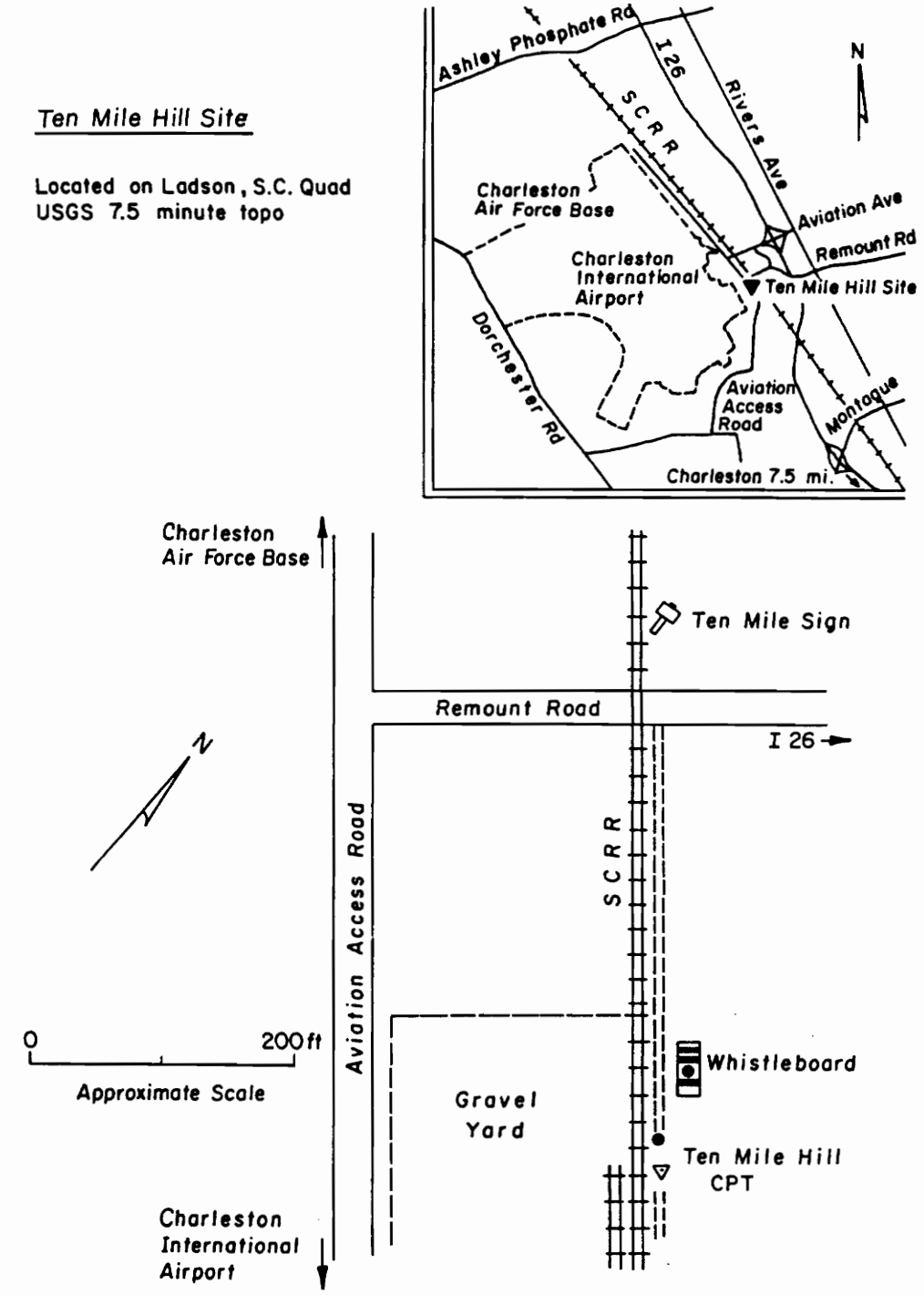

Figure 19. LOCATION MAP FOR THE TEN MILE HILL SITE

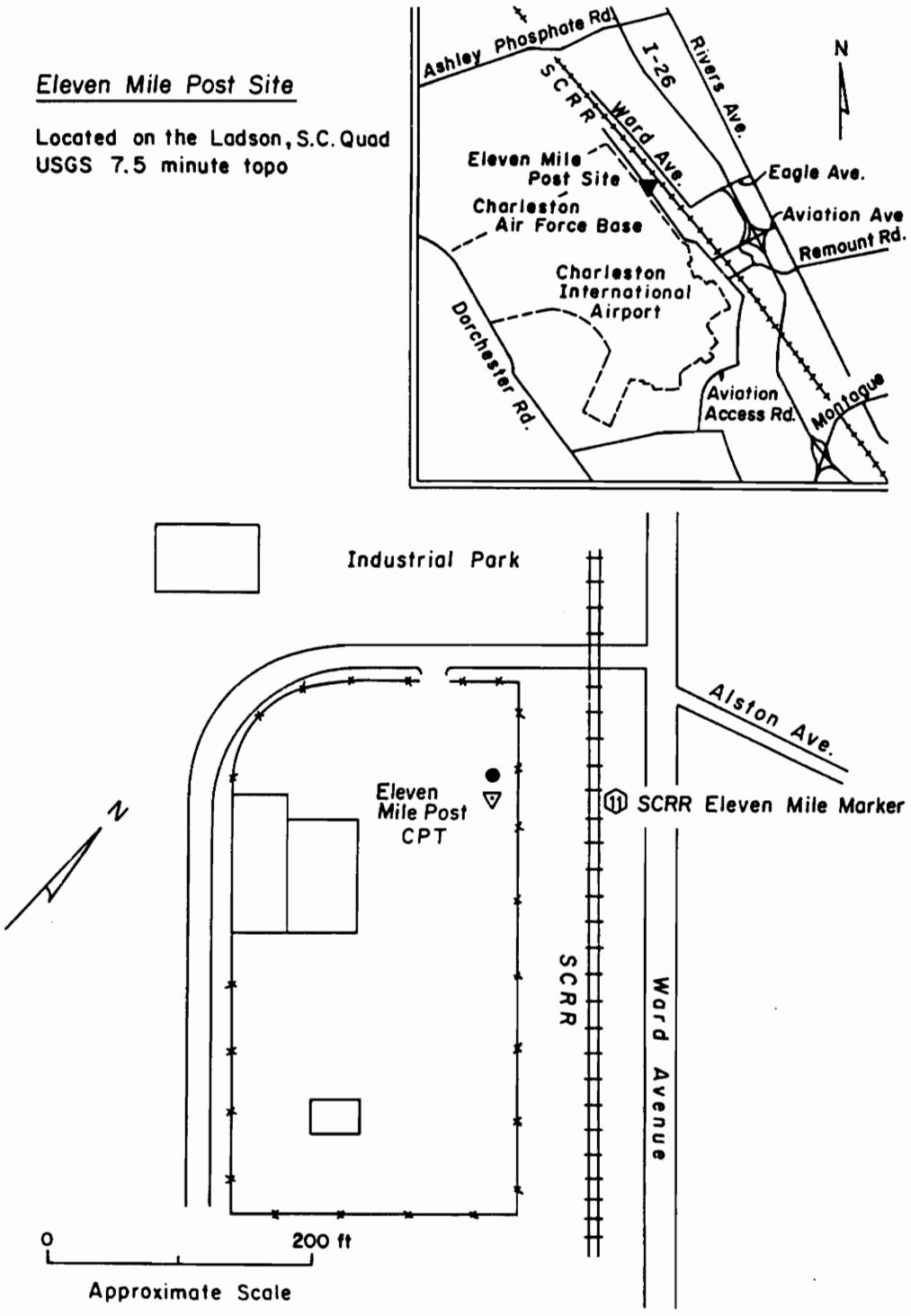

Figure 20. LOCATION MAP FOR THE ELEVEN MILE POST SITE

Table 1. DEPOSITIONAL AGES AND LITHOLOGY OF PLEISTOCENE SEDIMENTS FOUND AT THE TEST SITES

SITE	APPROXIMATE AGE OF DEPOSITION (years)	DEPOSITIONAL FACIES AND PREDOMINANT LITHOLOGY
Hollywood (HW)[1]	120,000-130,000	Barrier Island Complex: Shelf deposits of fine to silty sand with mud lenses overlying Beach shelly sands.
Warren (W)	200,000	Transitional environment of beach clean fine sands to backbarrier muddy fine sands.[2]
Sod Farm (SF)	100,000	Beach clean fine to medium sands overlying backbarrier muddy sand; clay, shell, and sand layers.
Montague (M)	200,000	Beach clean fine to medium sand overlying backbarrier muddy fine sands.
Ten Mile Hill (TM)	200,000	Beach clean fine to medium sand.
Eleven Mile Post (EM)	200,000	Backbarrier muddy fine sand.
Oakland Plantation (OP)	100,000	Beach clean fine to medium sand overlying backbarrier muddy sand; clay, shell, and sand layers.

All sites are underlain by rock-like calcareous silty clay (marl) at depths between 30 and 60 feet below the ground surface.

Data from McCartan and others, 1984, unless noted otherwise
[1]Weems and others, 1986
[2]Cox, 1984

Chapter IV

Equipment and Field Procedures

All of the cone penetration tests were conducted using a mini-cone system recently developed at Virginia Tech by Dr. G.W. Clough and his students. The impetus for development of the minicone was the need for a cone which could be pushed with less reaction force than necessary for the standard sized cone. The reduction in end bearing area fascilitates the use of a portable mini-cone system for investigations in remote areas where large rigs are not available. An introduction and field study utilizing the Virginia Tech mini-cone penetrometer has been presented by Sweeney and Clough (45).

4.1 The Mini-Cone Penetrometer

The mini-cone has a projected tip area of 0.65 in^2 (4.2 cm^2) with an apex angle of 60 degrees and a friction sleeve located behind the conical tip with an area of 10.0 in^2 (64.55 cm^2) These areas are compared to the standard cone which has tip and friction sleeve areas of 1.6 in^2 (10 cm^2) and

and 23.2 in^2 (150 cm^2). Bonded strain gauges are used as built-in load cells that record separately end bearing stress, q_c, and side friction stress, f_s. A schematic representation of the mini-cone is presented in figure 21. Each load cell consists of a wheatstone bridge with two active strain gages per arm of the bridge circuit. This arrangement compensates for bending strains and records only axial strains. The end bearing capacity of the mini-cone is one ton. This bearing correspondes to a q_c reading of 220 bars and is sufficient for liquefaction studies involving the penetration of shallow, loose to medium sand.

Scaling effects involved in using the mini-cone, as opposed to the standard cone, are related to the ratio of the cone diameter to 1) thickness of interbedded layers, and 2) grain size of the tested material. The thinnest layer the cone bearing can respond fully is about 10 to 20 tip diameters (34). This means that in interbedded deposits the tip bearing does not reach the true value for the material unless the layer thickness is at least 14 to 28 inches if using the standard cone and 9 to 18 inches thick for the mini-cone. In thinly, interbedded deposits the use of the mini-cone results in increased resolution and more pronounced peaks in the end bearing readings than the larger cone which would tend to "average" out the resistances. The tip also senses interfaces between 5 to 10 cone diameters ahead and behind. This contributes to the jagged nature of the mini-cone record in thinly interbedded soils.

Field and calibration chamber results indicate that scaling effects in uniform, clean sands are minimal between the mini and standard cones. In the absence of layering effects the cones have been found to give similar end bearing readings in fine grained material. Considerable scatter in the bearing is recorded in material larger than coarse sand where the large grain size to tip diameter ratio begins to influence the bearing resistance of the mini-cone. Particle effects are negligable in fine sands and clays. The mini-cone data recorded during preliminary field trials fit simplified soil classification charts derived for standard (10 cm^2) friction cones and closely matched SPT blow counts taken at the site after conversion with empirical q_c - N correlations, (36).

A Ford F350 truck modified with an engine on the flatbed to power an Acker drilling system was used for advancing the cone and performing soil borings. The cone testing system is shown in figure 22. The rig was equiped with solid-stem continuous-flight auger, donut hammer and

rods for performing SPT's. Utilization of the solid stem auger precluded the use of drilling mud or casing in boreholes, thereby rendering the system unuseable for conducting SPT's in the loose, saturated sands encountered in the Charleston area. The rig weighs approximately 7000 pounds and was found after preliminary cone testing to be too light for pushing the cone through dense or stiff material at depth. A system was subsequently developed whereby it was secured by a cable shackled to earth anchors consisting of two nine foot sections of screw auger placed on both sides and toward the rear of the rig. An approximate estimate of 3 tons was made for the pushing capacity of this penetration system. The existing hydraulic jacking system also was not designed for rate-regulated augering and had to be fitted with a rate control value that restricted fluid flow to the thrust generating hydraulic cylinders. This modification made it possible to advance the cone at a fairly constant rate of 2 cm/sec, (0.79 in/sec) which is specified in the ASTM standard (1).

While attempting to develop a light, portable cone penetration system it was felt that the test rod material used should be available near any test site and disposable if necessary. For this reason test rods of inexpensive, readily available 0.84 in. o.d. schedule 100 water pipe were used to push the cone. Use of the water pipe necessitated the fabrication of a thrust head device for pushing and pulling directly on the pipe couplings. The thrust head is slotted to prevent damage to the penetrometer wires during advance and had a sliding clamp arrangement for retreiving the test rod. The large loads transferred to the small diameter rods also required that the unsupported length of the rod be held at a length that would prevent buckling during cone advance. An optimum test rod length that was safe against buckling, yet not so short that excess time was spent on rod assembly was found to be 2.5 feet. A three foot long extension rod placed between the drilling head and thrust head lowered the thrust head closer to the ground and reduced the unsupported length of the test rod to 3.0-3.5 feet. Compressive loads of approximately 6,000 pounds were transmitted to the test rods during several tests with no buckling of the rods.

Pipe sections were threaded with standard sized tapered pipe threads and held together during cone advance with thin-walled steel gas line couplings. The outside diameter of the test rod was only 0.07 in. less than the cone, making it necessary to use thin-walled steel gas line couplings instead of thick standard water pipe couplings because the smaller protruding area required less re-

action force to push through the soil. An added benefit of the couplings is that they act as friction reducers which expand the diameter of the hole to reduce soil contact against the cone rods. This reduces rod friction behind the coupling at the expense of increased bearing and friction forces locally around the reducer. As a point of interest, the use of 1.05 in. O.D. couplings results in a close to 30% increase in the cross sectional area of the cone rod. It has been found that in uniform clean, angular fine sand that an increase in cone rod area of 25% is the most efficient in reducing rod friction, thus increasing penetration force at the tip (34).

4.2 Data Acquisition

The electric cone penetrometer produces a continuous signal of tip bearing and friction sleeve readings that must be recorded and processed. The 10 VDC excitation voltage for the strain gauges is transmitted through a seven-wire cable threaded through the test rods and passes across gauges wired in a wheatstone bridge configuration. The tip and sleeve gauges have a full-scale output (the maximum voltage change experienced over the allowable load range) of 5 mV and 1 mV, respectively. The tip and sleeve signals comprise the first two channels of data that were recorded, the third channel was supplied from an analogue to digital rotary depth trigger used to signal depth increments during cone advance. The return signals were collected by a portable PC and strip chart recorder both powered by a field generator.

The primary data collection tool was an IBM portable PC. The PC data acquisition system was driven by depth pulses from a depth trigger to record digital data at 1 inch increments during cone penetration. Real time plots of tip resistance and sleeve friction were generated and displayed on the PC screen while the test was in progress. The acquisition system has programmed software to alert rig operators when the cone loading limit is being approached. The three channel digital output was stored on floppy diskettes allowing test records to be easily prepared, copied for archival storage and plotted using available spread sheet editing soft-

ware. An analogue strip chart recorder was utilized as a secondary recording system. The strip chart recorder plotted only the tip and sleeve channels and was stopped during every test rod assembly and the test depth recorded. The strip chart plot was beneficial for recording operators' notes of starting depths and any peculiarities which may have occurred during testing. The entire data acquisition system was mounted in the back of a support vehicle that could be enclosed allowing for operation in dusty, rainy, or cold conditions.

4.3 Preliminary Field Testing

The several months prior to testing in the Charleston area were spent preparing the cone penetrometer and modifying a drill rig obtained from the Virginia Tech Agronomy department for penetration testing. The three mini-cones available for testing were tested extensively for accuracy and repeatability, calibration and linearity, output stability, temperature effects, and bridge shorting due to water intrusion. A detailed discussion of the factors affecting electric cone measurements is presented by Robertson and Campanella (34). After establishing a method that would allow for proper and repeatable cone performance a site was needed with soil conditions similar to those in Charleston. The Pepper's Ferry site located near Virginia Tech on a bank of the New River is an extensive fluvial terrace deposit, a portion of which is comprised of uniform silty sand overlying limestone at depth. This site was used to test and refine field procedures.

Only minor modifications were necessary to make the drill rig functional for penetration testing. The existing hydraulic jacking system was not designed for rate-regulated advance and was subsequently fitted with a passive rate control valve that restricted fluid flow to the thrusting hydraulic cylinders. This modification made it possible to advance the cone at a fairly constant 2 cm/sec. After completion of concurrent developments on the drill rig and data acquisition system, a series of 6 CPT's and 2 SPT's were conducted to determine the repeatibility and reliability of the cone in the field. A suite of sieve tests was run on the split spoon samples

so that established q_c to N conversions could be used to compare the CPT data to equivalent tip bearing values from the SPT blow counts. The cone provided repeatable field data (figure 23) which was judged to be reliable based on the soil classification chart for standard electric cones, visual soil classifications and relations to SPT's. The data plotted very favorable on the soil classification chart used to relate cone bearing, q_c, to friction ratio, $\frac{f_s}{q_c} \bullet 100$, (figure 24). The $\frac{q_c}{N}$ ratios obtained at Pepper's Ferry are in good agreement with established relations and are plotted in figure 25. Before traveling to Charleston, final tip and sleeve calibration factors were determined in the laboratory.

4.4 Testing Procedures

Prior to cone testing, soil borings were carried out for visual soil descriptions and grab-bag sampling. Particular attention was made while augering to the density of the sands at shallow depths. It was soon discovered that when CPT's started at the ground surface the thrust capacity of the rig typically was reached at depths between 20 and 25 feet. This is presumably due to the large bearing forces acting on the test rod couplings in the dense sand. After the soil log had been made two earth anchors each consisting of nine foot sections of solid-stem auger were placed at appropriate spacings, the rig positioned between them, and secured by a cable and load binder attached to the anchors. After several penetration tests at Hollywood demonstrated that the sands to a depth of roughly ten feet exhibited extremely low liquefaction potential due to high relative density, borings were made to the base of the dense sand. The boreholes were backfilled with sand at lower relative density to maintain lateral support for the test rods. CPT's began at the base of dense sand layers and ended when thrust capacity had been exceeded at depths generally ranging from 30 to 45 feet.

After preaugering, the two people working the system were free to prepare the rig and data acquisition system simultaneously. The universal-jointed augering head was removed and the ex-

tension rod and thrust head emplaced. The depth trigger was then bolted to the rig boom and the trigger wire attached behind the extension rod. The final step involved dialing the rate control value to the standard penetrometer advance rate. This was achieved using a stopwatch and tape measure to determine the advance rate over successive 1.0 ft. intervals.

Temperature equilibration of the penetrometer to subsurface conditions was achieved by placing the cone under the groundwater level in the backfilled borehole for not less than 15 minutes. With the data acquisition and drill rig ready for testing the penetrometer was then brought back to the surface and a zero-load reading of the tip bearing and sleeve friction was recorded. The cone was then pushed to the starting depth and the test begun. The cone was pushed in 2.5 foot increments, between which the data acquisition system stopped recording, the thrust head was backed off, and the next section of test rod was assembled and tightened with pipe wrenches. Data recording resumed with cone advance and this sequence was repeated until thrust capacity was reached.

At the end of the test, the rod was retrieved using the sliding collar on the thrust head which clamped around the test rod couplings. The cone was brought to the surface and a final zero load reading recorded. Test data was then saved and copied on floppy diskettes, the rig converted back to augering mode and the stout, hardworking crew enjoyed several beers kept ice cold in a portable refrigeration unit powered by the field generator.

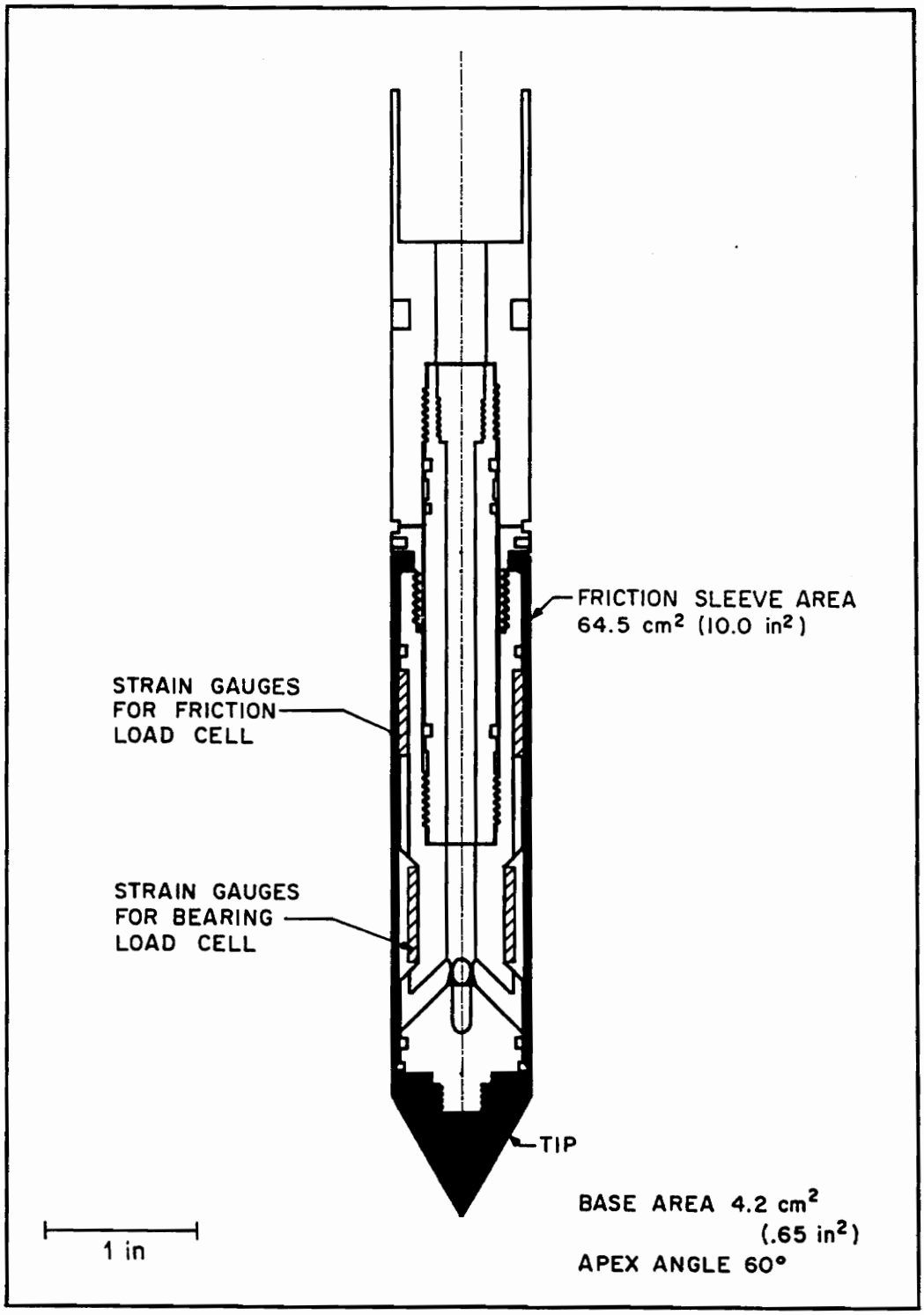

Figure 21. SCHEMATIC CROSS SECTION OF THE ELECTRIC MINI-CONE PENETROMETER

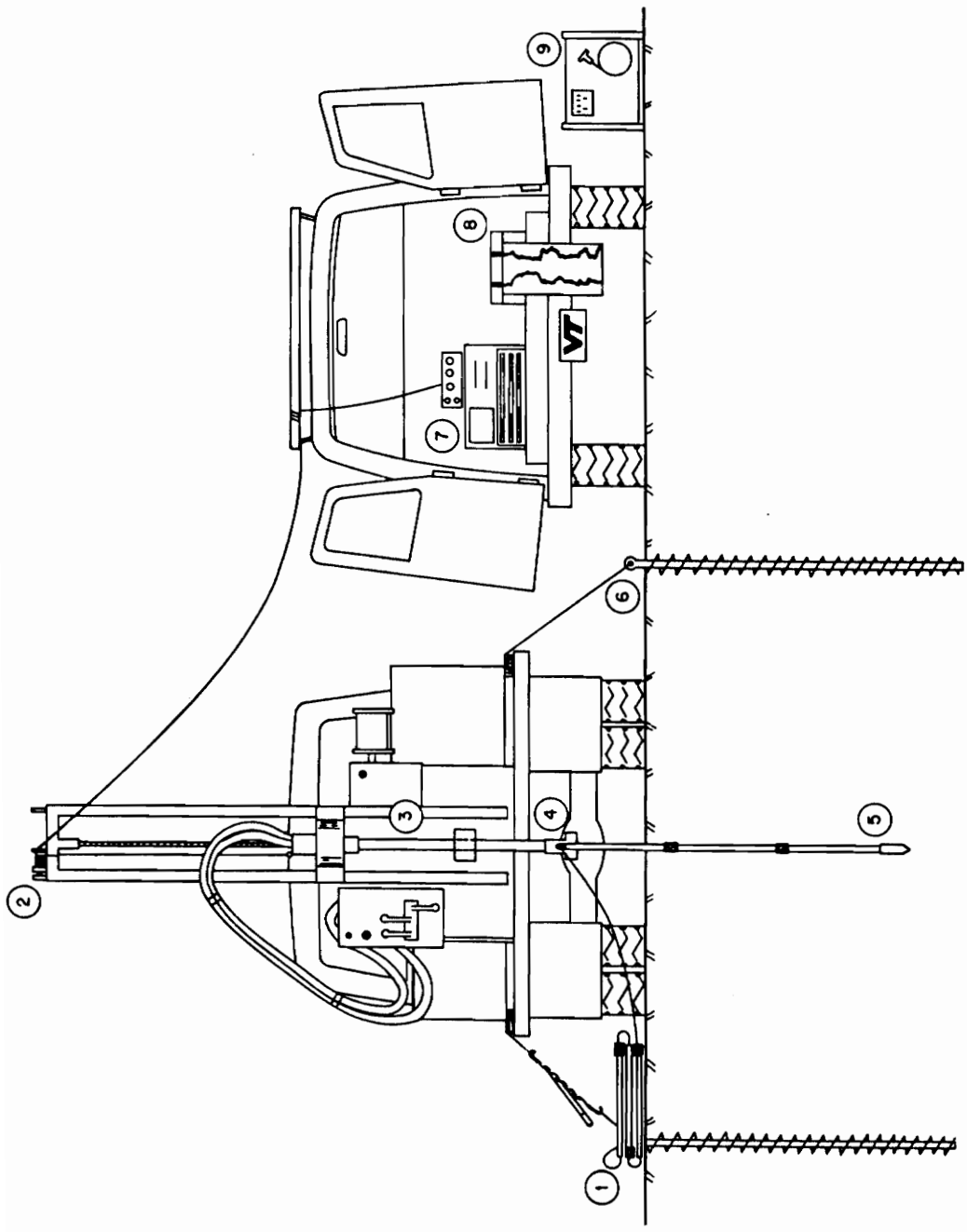

Figure 22. EQUIPMENT LAYOUT FOR THE CONE PENETRATION SYSTEM

Table 2. COMPONENTS OF CONE PENETRATION SYSTEM

1. Pre-wired test rod
2. A/D depth trigger
3. Extension rod
4. Thrust head
5. Mini-cone penetrometer
6. Earth anchoring system
7. Portable PC and instrumentation amplifier/ A/D trigger relay box.
8. Strip chart recorder
9. Gasoline-powered generator

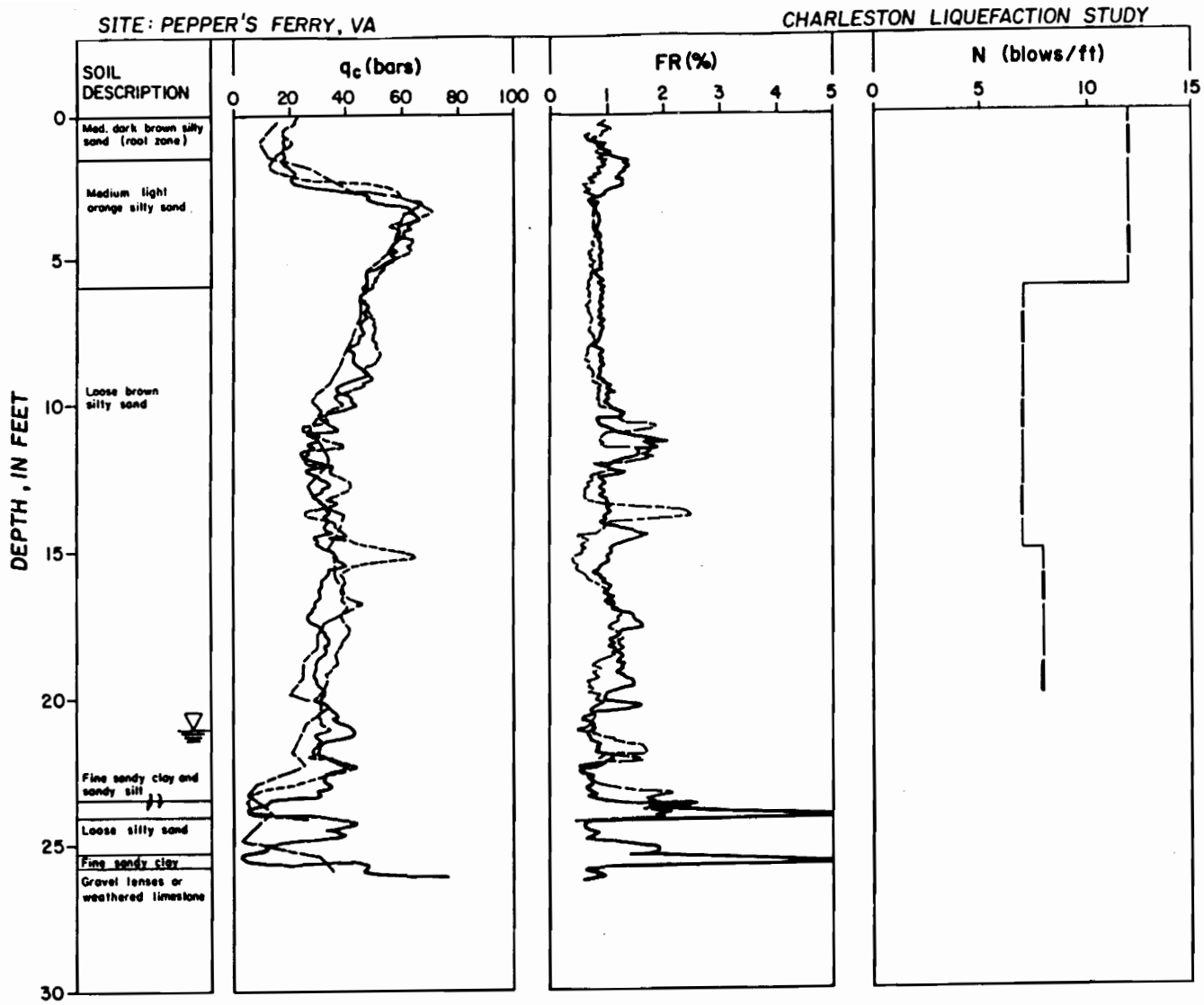

Figure 23. PENETRATION RECORDS FOR THE PEPPER'S FERRY, VA TEST SITE

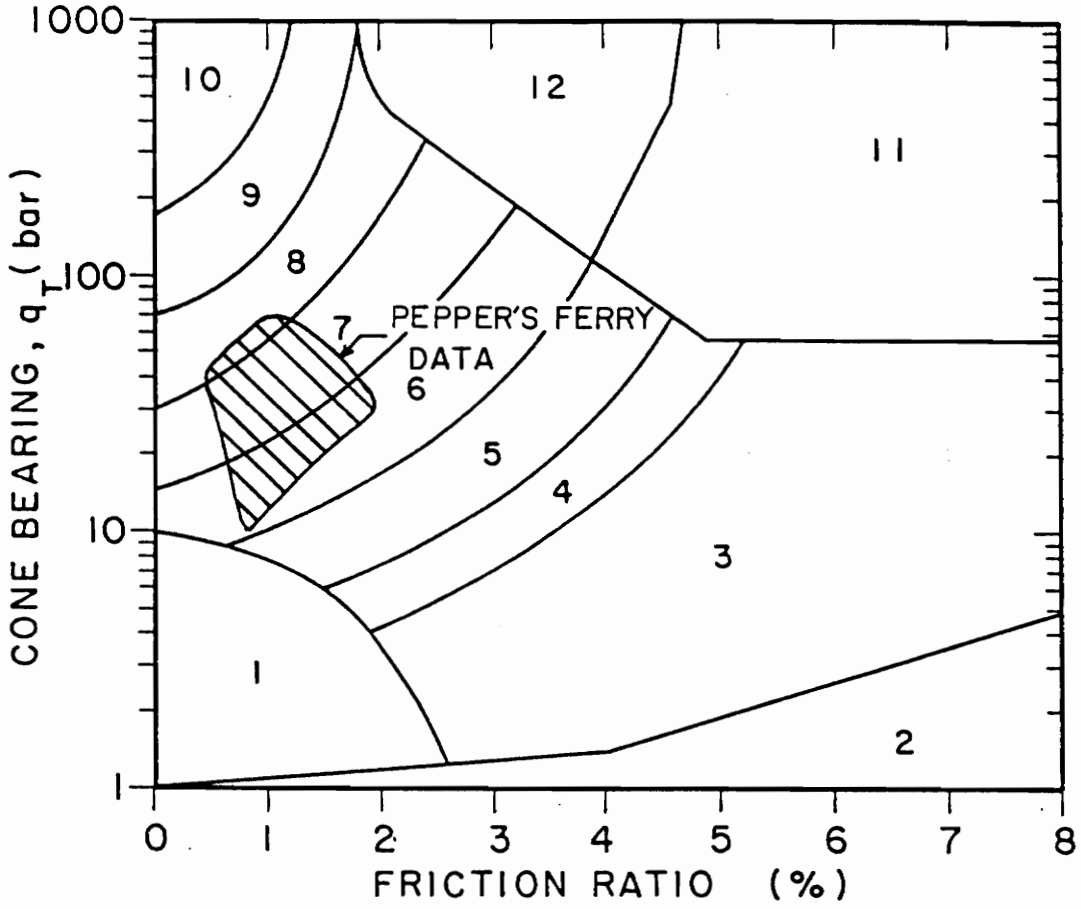

Zone	Qc/N	Soil Behaviour Type
1)	2	sensitive fine grained
2)	1	organic material
3)	1	clay
4)	1.5	silty clay to clay
5)	2	clayey silt to silty clay
6)	2.5	sandy silt to clayey silt
7)	3	silty sand to sandy silt
8)	4	sand to silty sand
9)	5	sand
10)	6	gravelly sand to sand
11)	1	very stiff fine grained (*)
12)	2	sand to clayey sand (*)

(*) overconsolidated or cemented

Figure 24. SIMPLIFIED SOIL CLASSIFICATION CHART FOR STANDARD ELECTRIC FRICTION CONE (34)

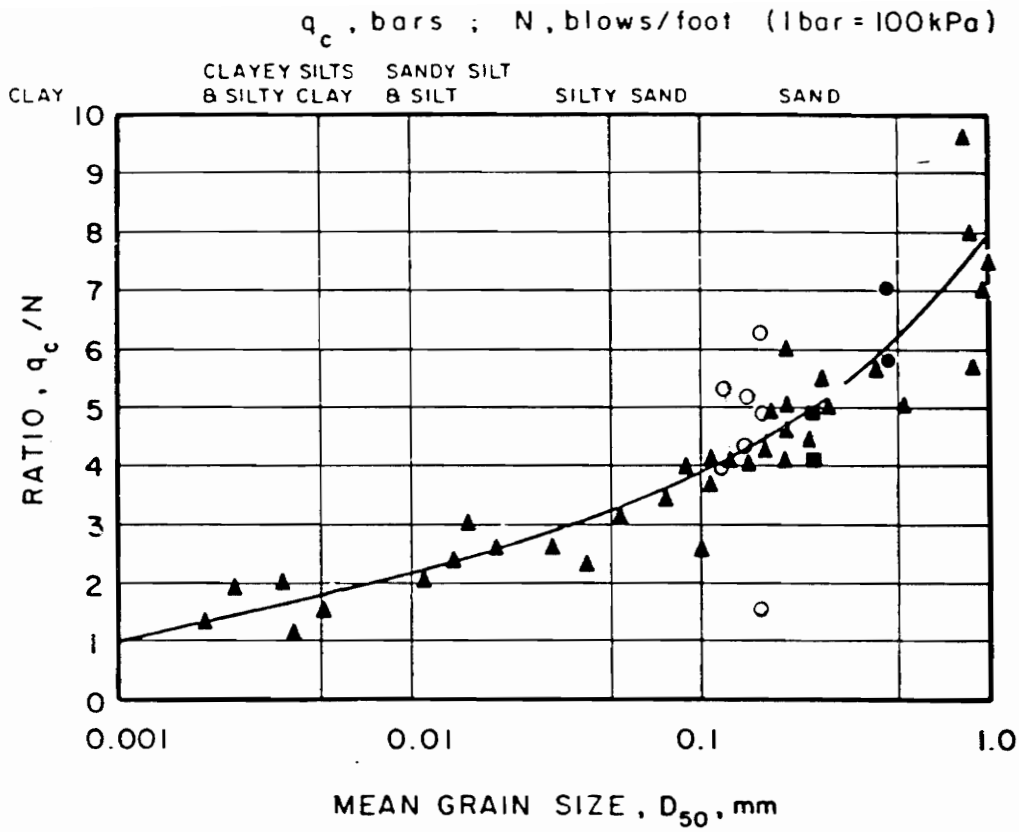

Figure 25. VARIATION OF THE q_c/N RATIO WITH MEAN GRAIN SIZE (36)

Chapter V

Soil Conditions

Coverage of soil conditions affecting the liquefaction potential of sediments at the test sites will focus primarily on the character of near surface layers of the loose to medium density fine sands. Although the complete soil column contributes to the nature of liquefaction by modifying the base ground motions propagating upward from the underlying rock, these factors are to be studied in subsequent phases of this research effort in dynamic response analyses. Apart from the location of the groundwater table and nature of seismic shaking the liquefaction susceptibility of a sand layer is dependent on its physical characteristics. Numerous investigations have demonstrated the effects that relative density, grain size gradation, grain angularity, fabric and strain history , and age of the deposit and cementation have on the cyclic behavior of sandy soils (7,16,50,13,49). While the ages of the deposits have been previously listed in Chapter 2, the remaining characteristics are covered here for the soils at each site.

5.1 *Hollywood Site*

The network of soil borings and penetration tests in proximity to the drainage ditches near Hollywood affords an extensive profile of the local soil conditions. Figure 26 presents a generalized soil profile along an approximately 9000 foot section of the east-west trending ditch. Of particular importance to the liquefaction analysis is the widespread deposit of clean, fine to silty sand located at depths generally between 3 and 14 feet. Similar soil conditions were encountered at stations N0560′ and S0725′ indicating that this sand layer is of large lateral extent as well (figure 27). The penetration resistances obtained from CPT's and SPT's are used as an indirect measure of the relative density and strength of the sands. The CPT records for the upper sand layer are presented in figure 28. The direct use of penetration resistance in empirically based liquefaction analyses are presented in the next chapter.

The relative density of sands can be estimated through correlations that relate penetration resistance (N or q_c) to overburden pressure and relative density. Charts by Gibbs, Holtz and Baldi (3) were used to correlate both SPT and CPT data to relative density. While these charts resulted in similar relative densities, the SPT data resulted in values that were slightly higher and showed wider variation than values determined from CPT resistance. The CPT and SPT data are presented for individual tests in appendix A. Tip bearing and friction sleeve valves have been normalized to an effective overburden pressure of one TSF using the C_q factor described in Seed and others (38) and Ishihara (16). Blow counts from standard penetration tests have been converted to a drill stem energy ratio of 60% the theoretical free fall energy delivered during penetration (38) and have also been normalized using C_N. The modified penetration resistances are designated as Q_c and $(N_1)_{60}$

The near surface fine sand layer at Hollywood exhibits a rather uniform relative density that increases from approximately 80% at the ground surface to values as high as 90 and 100% at depths of generally 5.0-7.5 feet. This dense material usually was augered through before cone tests were performed. A gradual loosening of the sand is observed below 7.5-10 feet. At depths be-

tween 12 and 17 feet along most of the ditch very loose to medium sands with very low penetration resistances (N = 2-3 blows/ft, q_c = 5 bars) have estimated relative densities in the range of 15 - 20%. The content of plastic fines of the soil increases markedly beneath the very loose fine sand. This condition precludes the rapid dissipation of pore water neccessary for the initiation of liquefaction in these materials.

A suite of sieve tests was performed on split spoon samples retrieved during standard penetration tests. The gradation curves for samples from every station that underwent standard penetration testing revealed that the soils are uniform (C_u: 1.24 - 2.10), fine to silty sands (D_{50}: 0.12 - 0.21 mm) and remain uniform with depth. A composite gradation curve for all Hollywood samples is shown in figure 29. The fines content (percentage of material which passes the no. 200 sieve) of the sands varied at all stations and depths and fell within a range of 1.8 to 9.2%, with an average of 4.5%. The fine grained material was predominantly non-plastic silt with negligible clay. While conducting work on the cyclic nature of reconstituted Hollywood sands Cullen (10) described the sand grains as angular to subangular. The sands retrieved during soil borings and inspected in the field exhibited negligible cementation.

The Hollywood site is located approximately four miles from Dutton's inferred southwestern "center of highest intensity" of the 1886 earthquake. Coupled with this fact, the large areal extent of the medium to loose fine sand found throughout the site indicates that the soils at this site should be susceptible to widespread liquefaction and easily capable of developing the moderately sized sandblow features that have recently been discovered. In relation to other areas experiencing liquefaction during the 1886 earthquake this site is considered to have undergone moderate to minor liquefaction based on exposures of relic sandblow features (27).

5.2 *Warren Site*

Soil borings and CPT's conducted over a 600 foot portion of the Warren site reveal uniform, layered conditions to a depth of roughly 20 feet (figure 30). Two continuous layers of silty to fine sand are present but represent widely differing densities (figure 31). Individual CPT records are contained in appendix A. As at Hollywood, the undisturbed surface portion of the sand to a depth of five feet is at relative densities of 90 - 100%. Below five feet there is a gradual reduction in density. At a depth of seven feet, a three foot thick layer is found comprised of loose to very loose sand with densities ranging from approximately 15 - 50%. Beneath this loose portion of the upper layer the relative density drastically increases again to roughly 90%. Underlying the loose clayey sand at depths between 12 and 14 feet is the second layer of clean fine sand. This layer extends to a depth of roughly 17 feet before grading into a clayey material. The relative density of this sand was estimated to be 80 to 90%.

The results of 35 sieve tests performed on samples from the sand blow vent and upper five feet of soil are referenced from Cox (9) and demonstrate that this material is also a very uniform (C_u = 1.35), very fine sand (D_{50} = 0.17 - 0.1 mm). All samples had less than 5% nonplastic fines. The range of gradation curves for all samples is shown in figure 32. The quartz grains in most of the sieve samples were described as sub-rounded to sub-angular, and no cementation of the soil particles was detected during soil logging. Tests conducted by Cox using dilute hydrochloric acid indicated that the samples were free of carbonate cement. While the vent at this site was rather large, the lack of first-hand reports or paleoseismological evidence of any other features in the area indicates than this was a site of minor liquefaction during the 1886 earthquake.

5.3 *Sod Farm Site*

One CPT, with a supplementary soil boring, was conducted in the clean, fine sands which constitute the upper 12.5 feet of the soil column next to a small liquefaction vent attributed to the 1886 earthquake. A second test was carried out approximately 200 feet away along the ditch where the vent was exposed (figures 33 and 34). The soil seemed during augering to be at least as dense toward the surface at this site as it is at Hollywood. The Tests were therefore started at 7.5 and 10 foot depths and indicated comparable results during the short advance through the medium to loose sands found between 9 and 13 feet. This layer was found to have estimated minimum and maximum relative densities of 20 and 65% ranging about an average of 30%. The clean fine sand grades into a clayey fine sand and sandy clay below 12.5 to 13 feet and remains clayey to a depth of 32 feet where it overlies a dense sand. The material to a depth of 13 feet was classified during field examinaitons as a fine to very fine sand. No notable cementation was observed during soil logging.

The Hollywood, Warren and Sod Farm sites are particularly valuable for assessing the role that variation of sand relative density and characteristics of the liquefiable and overlying layers (to be explained in the next chapter) have on the surface exposure of liquefaction features. The three sites are almost equidistant from the southwestern zone of maximum intensity of the 1886 earthquake and have very similar, potentially liquefiable sands, presumably of large lateral extent. The Hollywood site can be considered an area of minor to moderate venting and explosive liquefaction phenomena while the Warren and Sod Farm sites are locales of minor venting. Direct liquefaction analysis of penetration resistance presented in the next chapter should reveal characteristics of the loose sands and capping layers that account for this difference in modes of liquefaction.

It was felt that the Hollywood, Warren and Sod Farm sites warranted the most extensive site investigation during this first phase of the larger study, due to the nature of exposed liquefaction features, existing data base on the sites, and similar distances to inferred zones of seismic energy

release. The remaining sites were covered with a limited number of soil borings and CPT's leaving the lateral extent of liquefiable layers unknown at this time. Where necessary, additional studies will be performed in the future. At these sites, extensive areal coverage by the loose layers can be inferred by the documented occurance of widespread liquefaction following the 1886 earthquake, and in one case by large, dewatered sand borrow pits located next to the test site. It was anticipated that these sites would be particularly useful in evaluating the effects of distance from the zone of energy release both within and outside the meizoseismal zone on the surface manifestation of liquefaction.

5.4 Montague Site

The Montague site northwest of Charleston is composed of a surface layer of clean fine sand which extends to a depth of 18 feet, the upper ten feet of which was estimated during soil boring to be very dense. The tested portion of the layer exhibits relative densities decreasing from approximately 90% at a depth of ten feet to 50-55% at 17 feet (figure 35). The loosest section of fine sand is the basal 4 feet which has relative densities between 50 and 65%. It is inferred from the locally uniform nature of soil deposits in the Charleston area that this thick layer of fine sand should be extensive, but what can not be determined at this time is the nature of density variations in the immediate area. At 18 feet the clean fine sand becomes clayey and grades into a sandy clay. The sand to this depth is a uniform uncemented, fine to very fine sand. A small relic vent attributed to the 1886 earthquake has been uncovered in the walls of a drainage ditch at the site indicating the generation of excess pore pressures in the medium dense sands. Additional in-situ testing may be required to determine if an isolated loose, sandy layer exists in the vicinity of the vent. This site is considered to be a location which experienced minimal liqufaction during previous seismic events.

5.5 *Ten Mile Hill and Eleven Mile Post Sites*

Located along the South Carolina Rail Road line from Charleston, the Ten Mile Hill and Eleven Mile Post sites are located in areas well documented for extensive craterlet formation during the 1886 earthquake. The Ten Mile Hill site is located in an area described by Sloan as being;

> "honeycombed with craterlets affording abundant quicksand...composed of sandy subsoil extending 8 to 12 feet below the surface and overlying bed of quicksand defying efforts (immediately after the earthquake) to sink artesian well pipe".

The soil profile at this site consists of a surface layer of clean, fine to silty sand which is essentially uniform to a weathered contact with the underlying Cooper Marl at a depth of 40 feet (figure 36). Beneath the first five feet of medium to dense material is a 2.5 foot thick layer of loose sand exhibiting a relative density of approximately 45%. The fine sand between 7.5 and 16 feet demonstrates two distinct layers of relatively uniform penetration resistance. The upper portion occurs between 7.5 and 11 feet and has an average relative density of 55%. The latter extends from 11 to 16 feet with D_r of 65%. At a depth of 16 feet the sand becomes very dense. The gradation curves for samples from 12.5 and 15 feet are shown in figure 37 and indicate that the material is uniform (C_u: 2.14 - 2.19), fine sand (D_{50}: 14mm). The fines content of 11%, with trace (< 1%) clay is slightly higher than either the Hollywood or Warren site sands. Based on visual classifications the soil remains a fine to silty sand to depth. The sands are sub-angular and non-cemented. Of the seven test sites, this is located in an area reported as exhibiting the most extensive liquefaction features during the 1886 earthquake.

Approximately 1.5 miles northwest of Ten Mile Hill along the SC RR tracks, the area in the vicinity of the eleven mile marker was conspicuous for craterlets "in belts conforming to the ridges" (32) which trend perpendicular to the tracks. A boring and CPT conducted near the eleven mile post revealed a soil profile that includes a layer of fine sand to 4.5 feet overlying a slightly clayey fine sand which extends to a depth of seven feet (figure 38). Below seven feet the fine sand contains trace clay and grades into a clean, fine sand at 13 feet. The fine sand remains clean to 18

feet at the contact with a sandy clay. Although the minor to trace clay content may have contributed minute cohesion to the fine sand, no cementation of grains was observed.

As with other sites, dense, fine sands occur to depths of roughly ten feet. Beneath the dense material is a three foot layer of loose fine sand at a relative density of approximately 40%. Most of the clean, loose to medium sand found between 13 and 18 feet has a relative density of 45%, but contains a thin section of silty sand with density as low as 15 - 20%. This site has been considered an area of minor liquefaction occurrence during the 1886 earthquake based on historical observations.

5.6 *Oakland Plantation Site*

A long, thin liquefaction vent attributed to the 1886 earthquake was discovered, by S. Obermeier, in the walls of a roughly nine foot deep, dewatered sand borrow pit located 11 miles northeast of Charleston and 7 miles from Bollinger's approximate meizoseismal zone boundary. For this investigation, a soil boring and CPT was performed over the projected plane of the feature. The CPT revealed a five foot thick layer of well to poorly graded, loose silty sand ($D_r = 40\%$) underlying the surficial seven feet of medium to dense material (figure 39). Beneath the loose sand, at a depth of 11.5 feet, is a five foot layer of interbedded loose, slightly clayey sand. Another layer of loose to medium silty sand occurs at depths between 16.5 and 34 feet. As with the other sites there did not appear to be any grain cementation. The sand pits in the immediate area cover several acres and afford widespread exposures of the surficial sand layers. No other relic liquefaction features were discovered here indicating that this was a site of minimal liquefaction.

5.7 *Discussion of Soil Conditions*

The soil profiles at all sites demonstrate a medium to dense surficial sand that becomes gradually looser at depths between 5 and 10 feet. A suite of sieve analyses on material from the Hollywood, Warren, and Ten Mile Hill sites was performed to determine possible variations in grain size that could result in differing liquefaction susceptibilities. The gradation curves revealed that the soils are uniform (C_u: 1.24-2.29), fine to silty sands (D_{50}: 0.12 - 0.20 mm) and remain uniform with depth. Figure 40 shows the composite grain size curve for all Hollywood, Warren, and Ten Mile Hill samples. The composite curve is bounded by Tsuchida's (16) empirical limits for the "most liquefiable soils", determined by gradation curves plotted for soils which did or did not liquefy during recent earthquakes. Laboratory data (7,39) support this proposed boundary by demonstrating that sands with D_{50} in the range of 0.1 mm and constant coefficient of uniformity have a low resistance to cyclic loading. While sieve tests were not conducted on material from other sites it is felt, based on visual field classifications, that the fine sands at these sites fall on or very close to the composite curve. Relations between the CPT q_c and f_s values were used to supplement the sieve tests utilizing a simplified soil classification chart. The cone data for surficial sands at all sites plots almost entirely in the shaded zone of figure 41, well within the stippled zone A proposed by Robertson and Campanella (35) to be liquefiable soils.

The cyclic behavior of a sand can be affected by its angularity, degree of cementation, and prior strain history. The effects of grain angularity on the liquefaction potential of medium sands has been investigated by Vaid and others (50). Their results indicate that at low confining stress the resistance to liquefaction increases with increasing grain angularity. Grain angularity determinations made during previous studies and field observations with a 20x hand lens found most of the quartz sand grains to be sub-angular to angular. The sandy soils retrieved during soil borings exhibited negligable cohesion due to grain cementation. The effects of strain history on the liquefaction susceptibility of sands are dependent on the magnitude of strain emparted to the soil during seismic loading. While the OCR and past straining influence the cyclic resistance

of cohesionless soils, calibration chamber tests indicate that response of both the CPT and SPT are minimal to OCR and independent of past straining along the K_o -line (3). It will be assumed that since all test sites are located in approximately the same seismic regime that the strain histories of these deposits are similar. It appears that with regard to grain size and angularity, cementation, and strain history, the soils of interest at all seven test sites are very similar in character. All other factors being equal, the uniform, fine-grained character of the near surface sands increases the likelihood of liquefaction during seismic loading. The fine-grained, non-cemented nature of these sands also contributes to liquefaction susceptibility.

In order to evaluate the property variations that may suggest that the initiation and surface manifestation of liquefaction would be different from site to site the relative densities (a measure of cyclic strength) and areal extent of the potentially liquefiable sand layers have been estimated based on penetation resistances and soil borings. While soil borings at all sites revealed that the near surface sands were similar in composition, the penetration resistances exhibited varying profiles of relative density with depth. The penetration data at all sites indicated a layered system consisting of a dense surficial layer overlying loose to medium dense sands. The high groundwater table and characteristics of the loose sand contribute to a high liquefaction potential. With the intensity of ground motions that can be inferred for an earthquake the size of the 1886 event it seems likely that significant excess pore pressures were generated in the loose sandy layers. The observed differences in the types and extent of liquefaction features are probably due to the relationship between the thicknesses of the liquefiable and overlying liquefaction resistant layers. In the Charleston region it appears that an overlying layer greater than 6.5 - 10 feet can impede the venting of induced pore pressures at depth, and thicknesses of 13 - 16 feet are sufficient to prevent sandblow formation (29).

The liquefaction susceptibility of a sand is dependent on the intensity and duration of the ground motions. With the exceptions of St. Michael's Church and Oakland Plantation, all of the sites lie between 3 and 6.5 miles to the inferred zone of energy release of the 1886 earthquake. Based on the relatively low rate of seismic energy attenuation for eastern United States earthquakes it is assumed that each of the sites in close proximity to the epicentral tract were subjected to approximately the same levels of ground shaking. Although all of the sites exhibited loose to medium dense

sandy soil layers, the differences in the exposure of liquefaction features, again appear to be attributable to the layering effects encountered at each site. Table 3 lists a summary of the near surface soil properties that influence the liquefaction susceptibility and inferred performance of these soils during the 1886 earthquake.

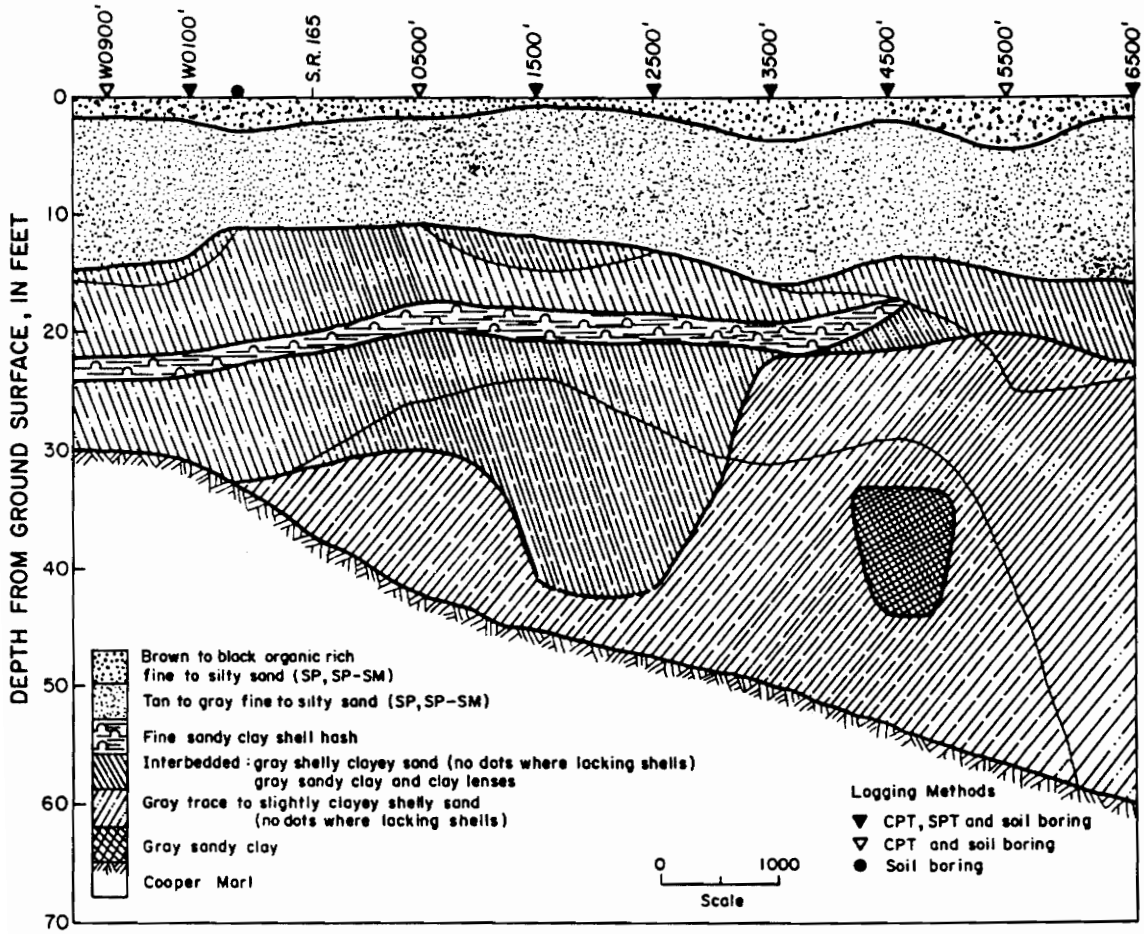

Figure 26. GENERALIZED SOIL PROFILE ALONG THE DRAINAGE DITCH AT THE HOLLYWOOD SITE

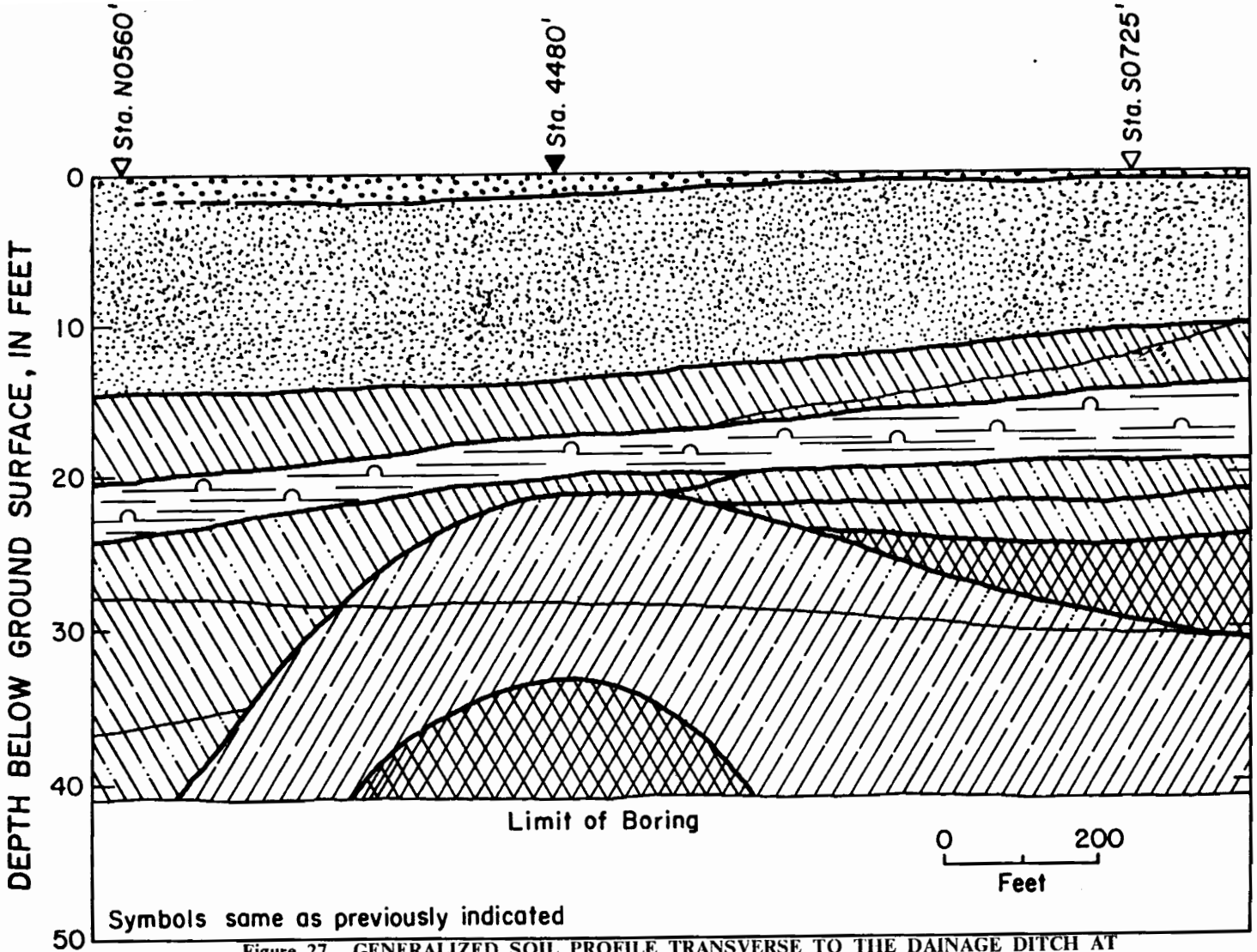

Figure 27. GENERALIZED SOIL PROFILE TRANSVERSE TO THE DAINAGE DITCH AT THE HOLLYWOOD SITE

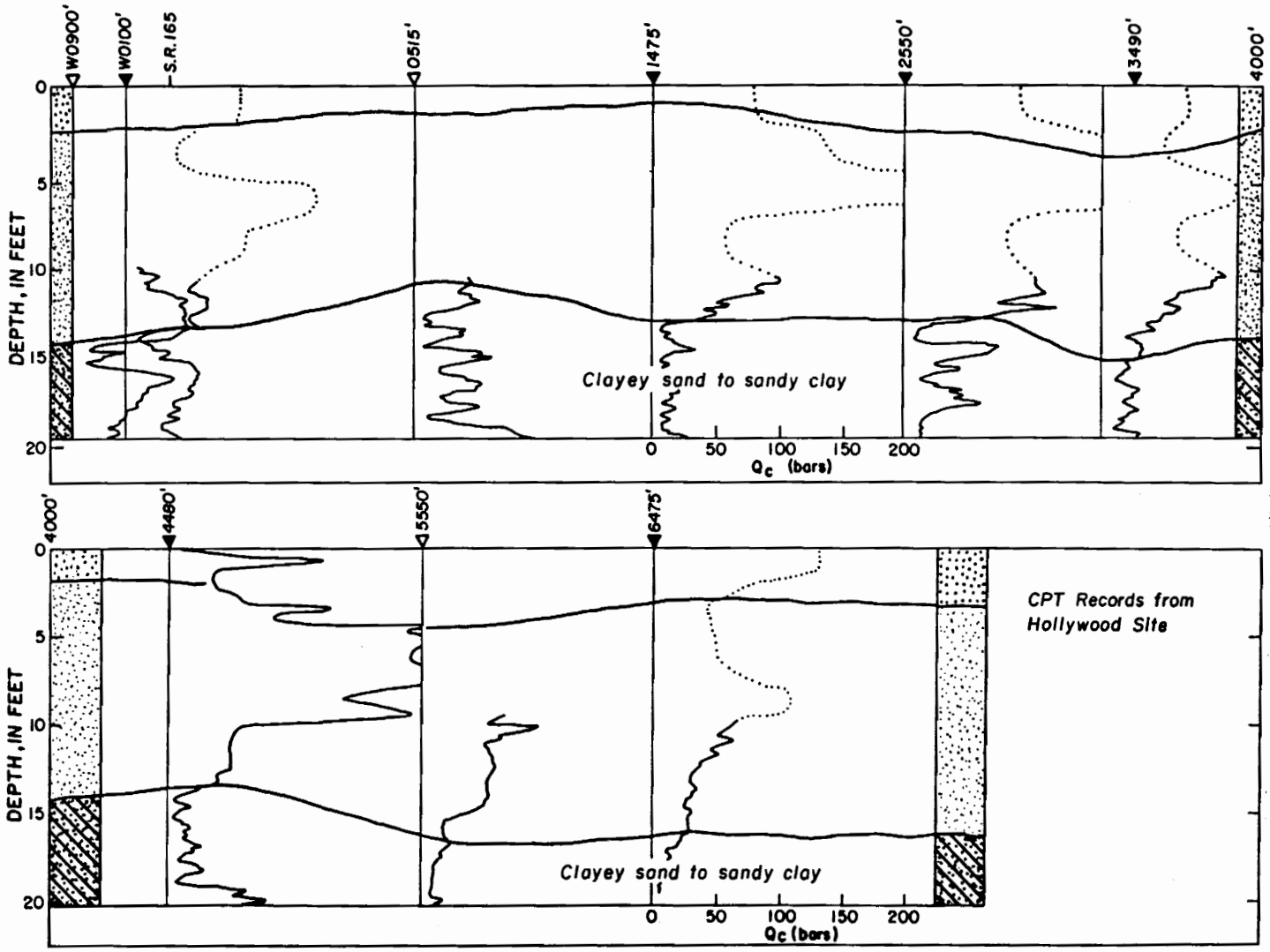

Figure 28. CPT RECORDS FOR STATIONS ALONG THE HOLLYWOOD DRAINAGE DITCH

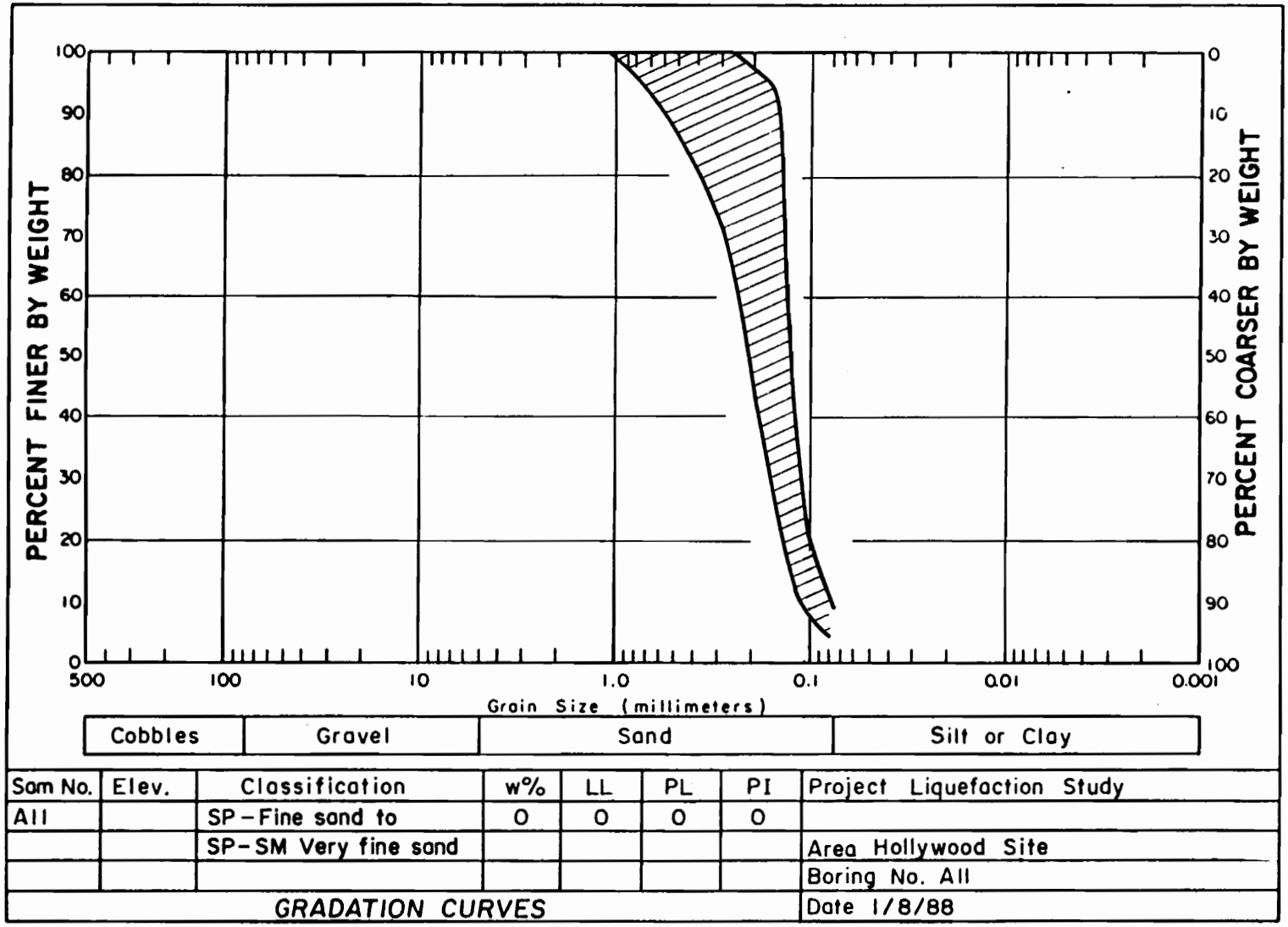

Sam No.	Elev.	Classification	w%	LL	PL	PI	Project Liquefaction Study
All		SP – Fine sand to	0	0	0	0	
		SP-SM Very fine sand					Area Hollywood Site
							Boring No. All
GRADATION CURVES							Date 1/8/88

Figure 29. RANGE OF GRADATION FOR HOLLYWOOD SAMPLES TAKEN FROM DEPTHS BETWEEN 5.0 AND 16.0 FEET

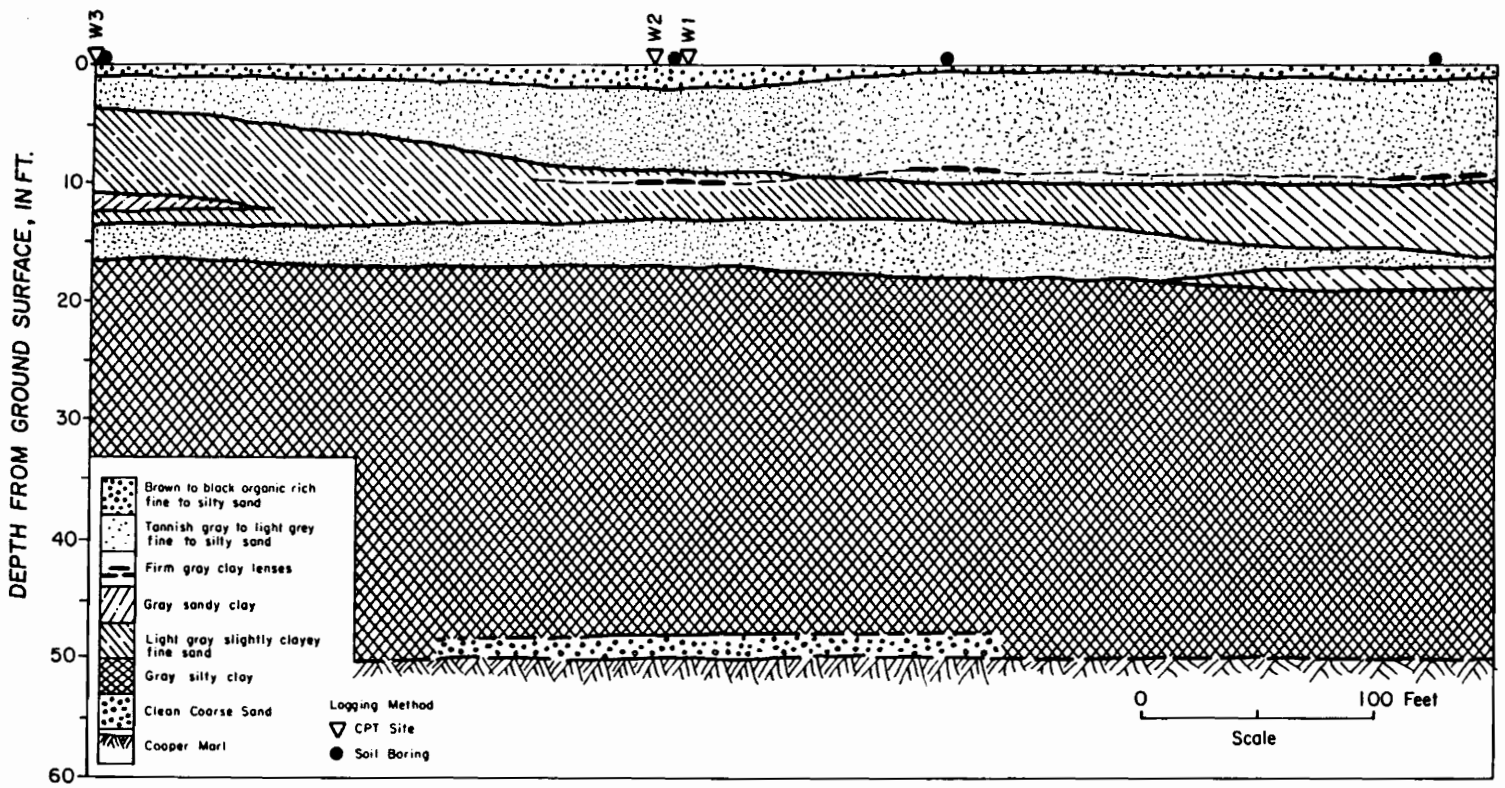

Figure 30. GENERALIZED SOIL PROFILE FOR THE WARREN SITE

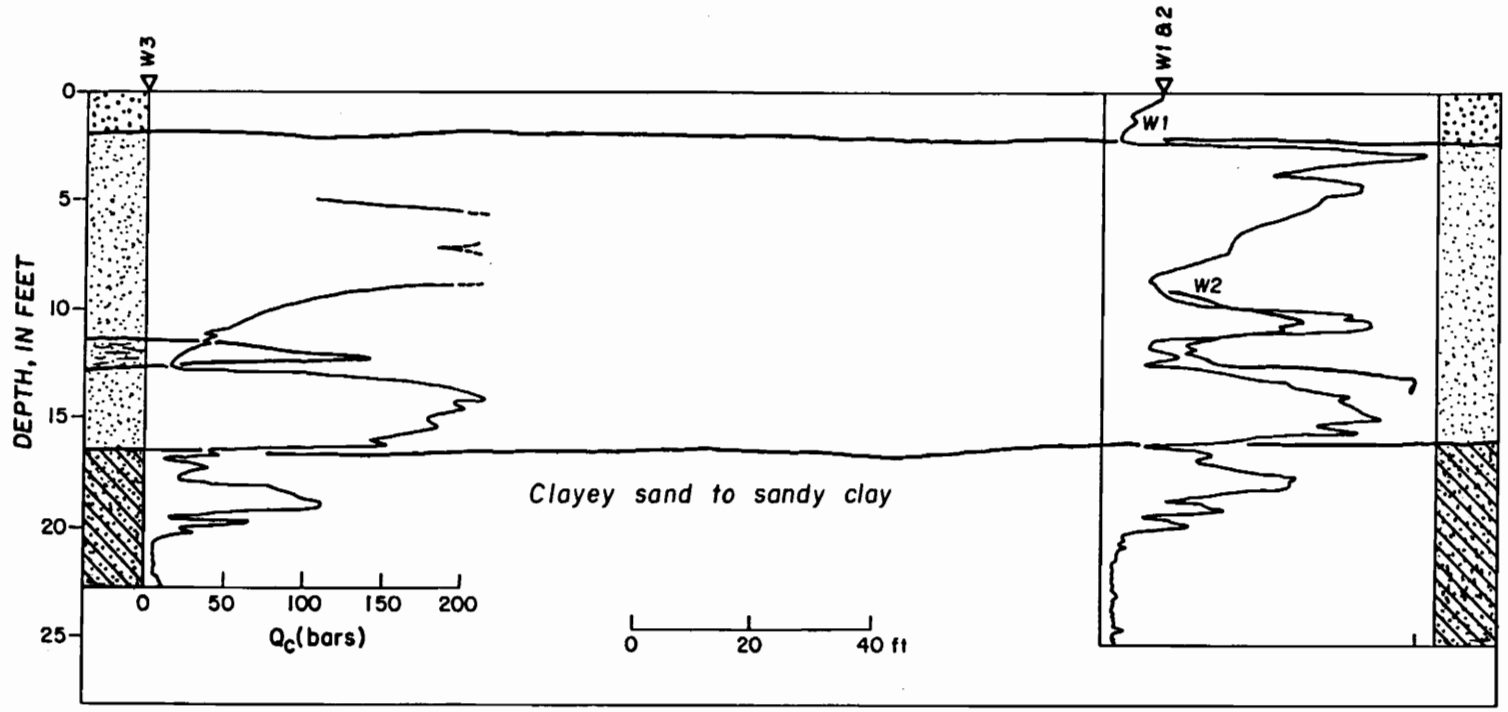

Figure 31. CPT RECORDS FOR STATIONS AT THE WARREN SITE

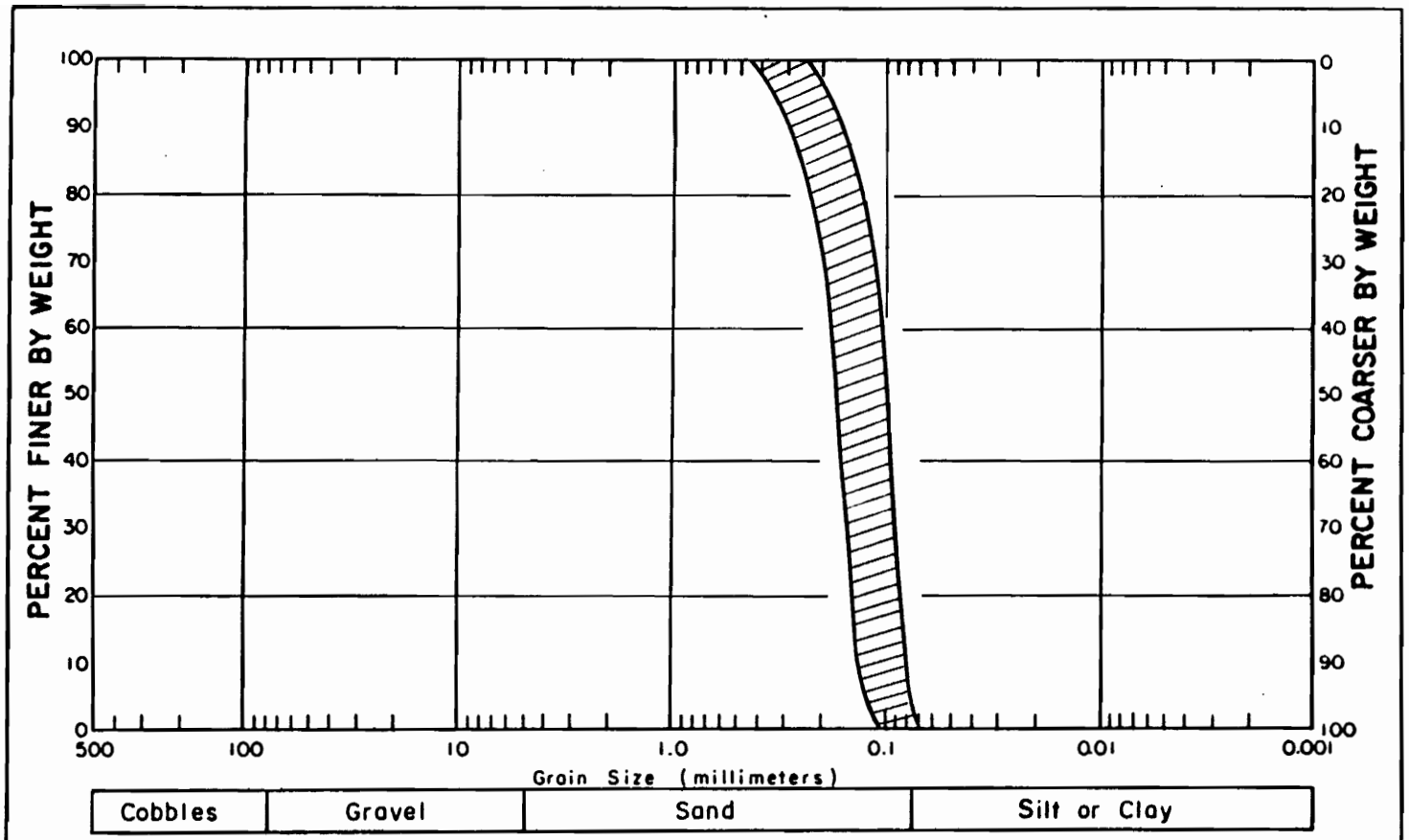

Sam No.	Elev.	Classification	w%	LL	PL	PI	Project Liquefaction Study
All		SP Fine sand	0	0	0	0	
							Area Warren Site
							Boring No. All
GRADATION CURVES							Date 1/19/88

Figure 32. RANGE OF GRADATION FOR WARREN SAMPLES (9)

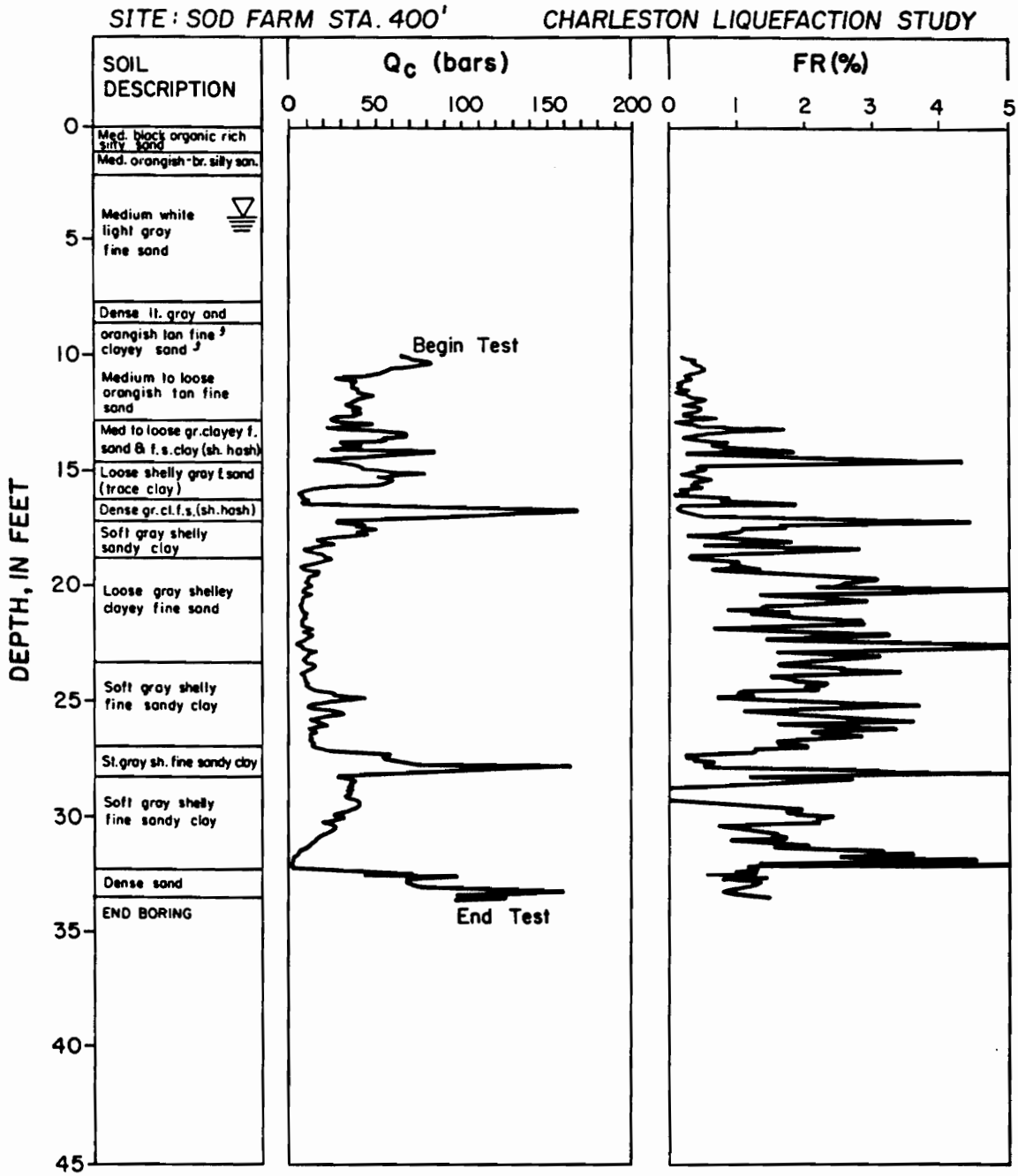

Figure 33. CPT RECORD FOR SOD FARM STATION 400'

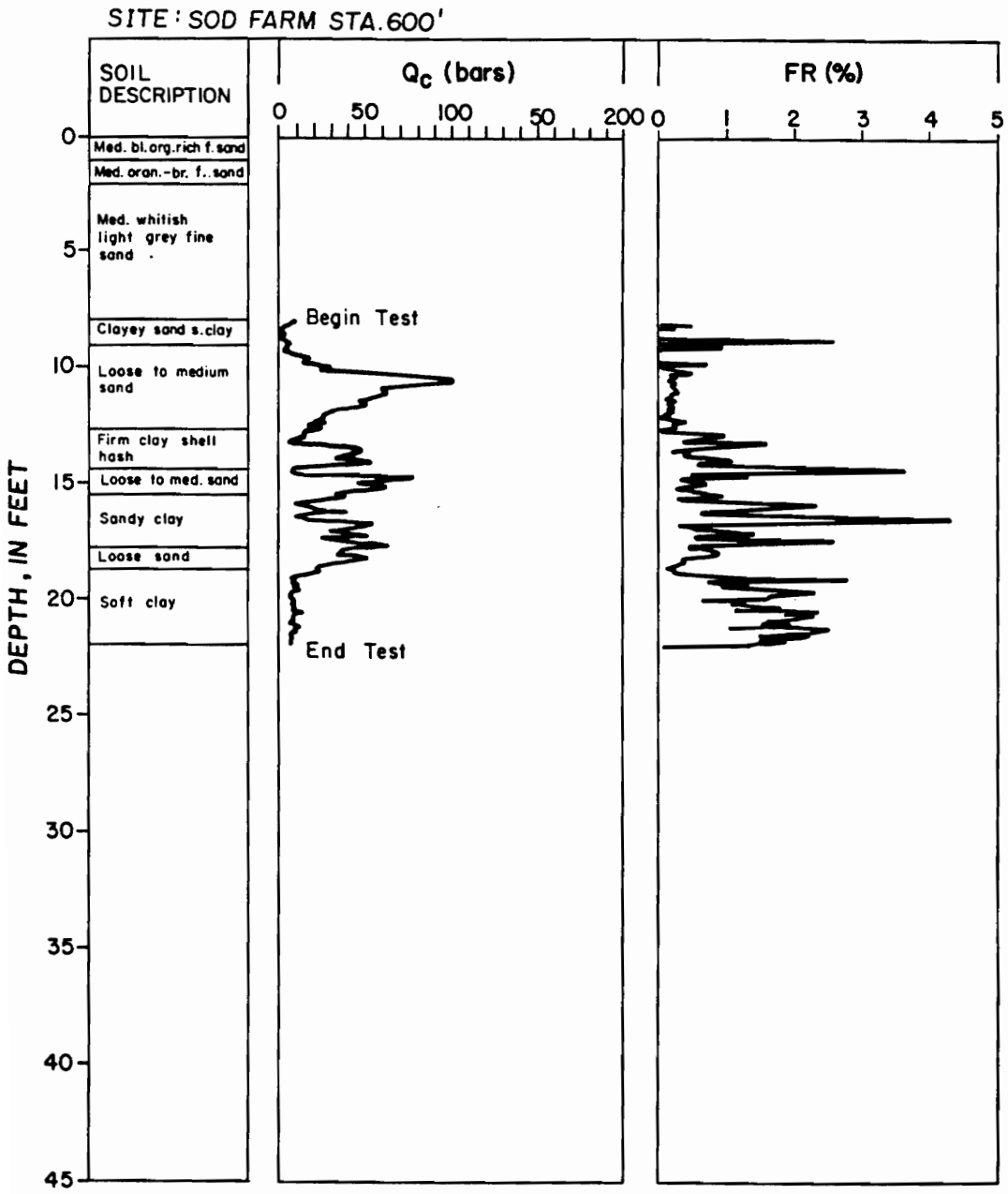

Figure 34. CPT RECORD FOR SOD FARM STATION 600'

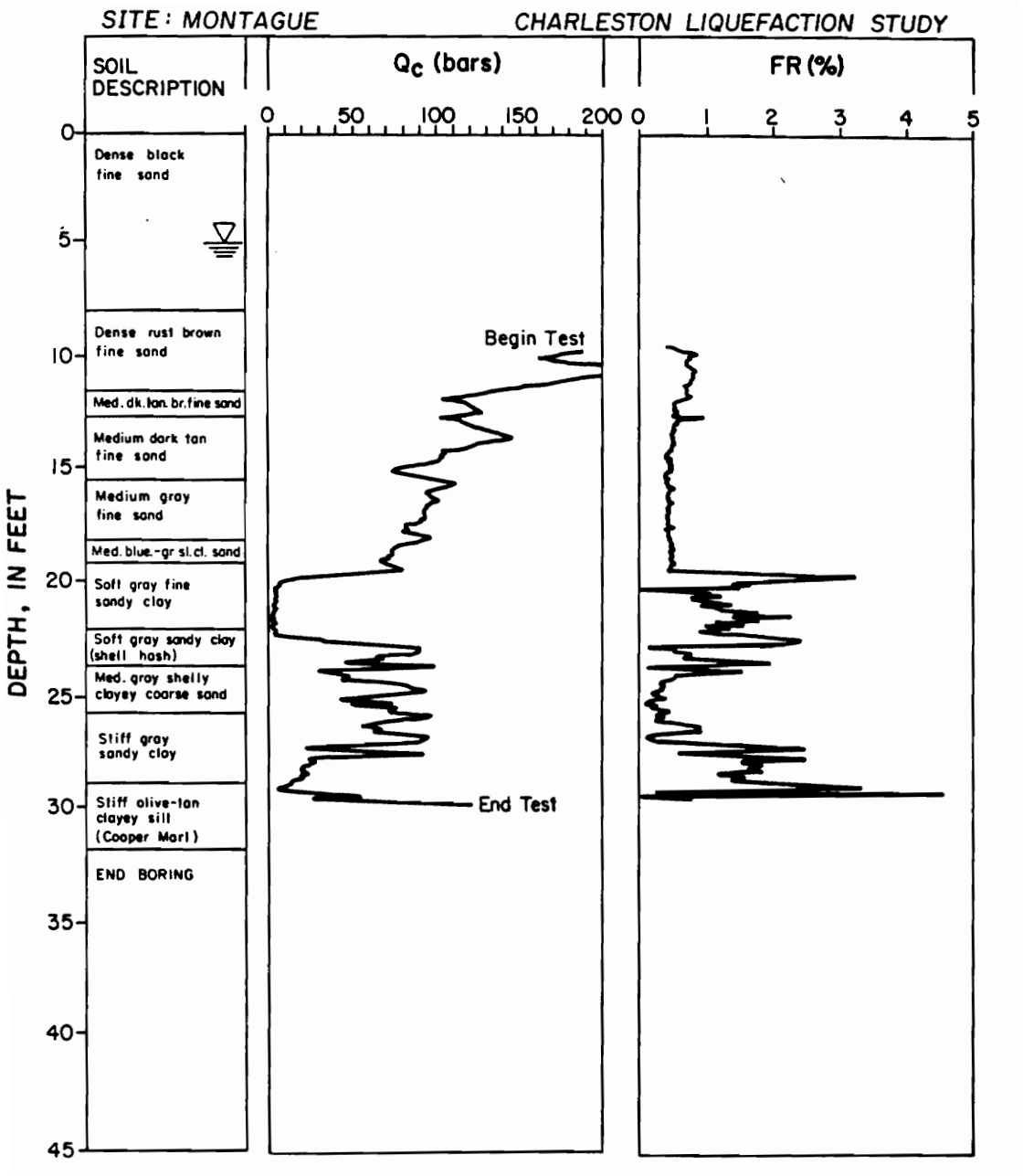

Figure 35. CPT RECORD FOR THE MONTAGUE SITE

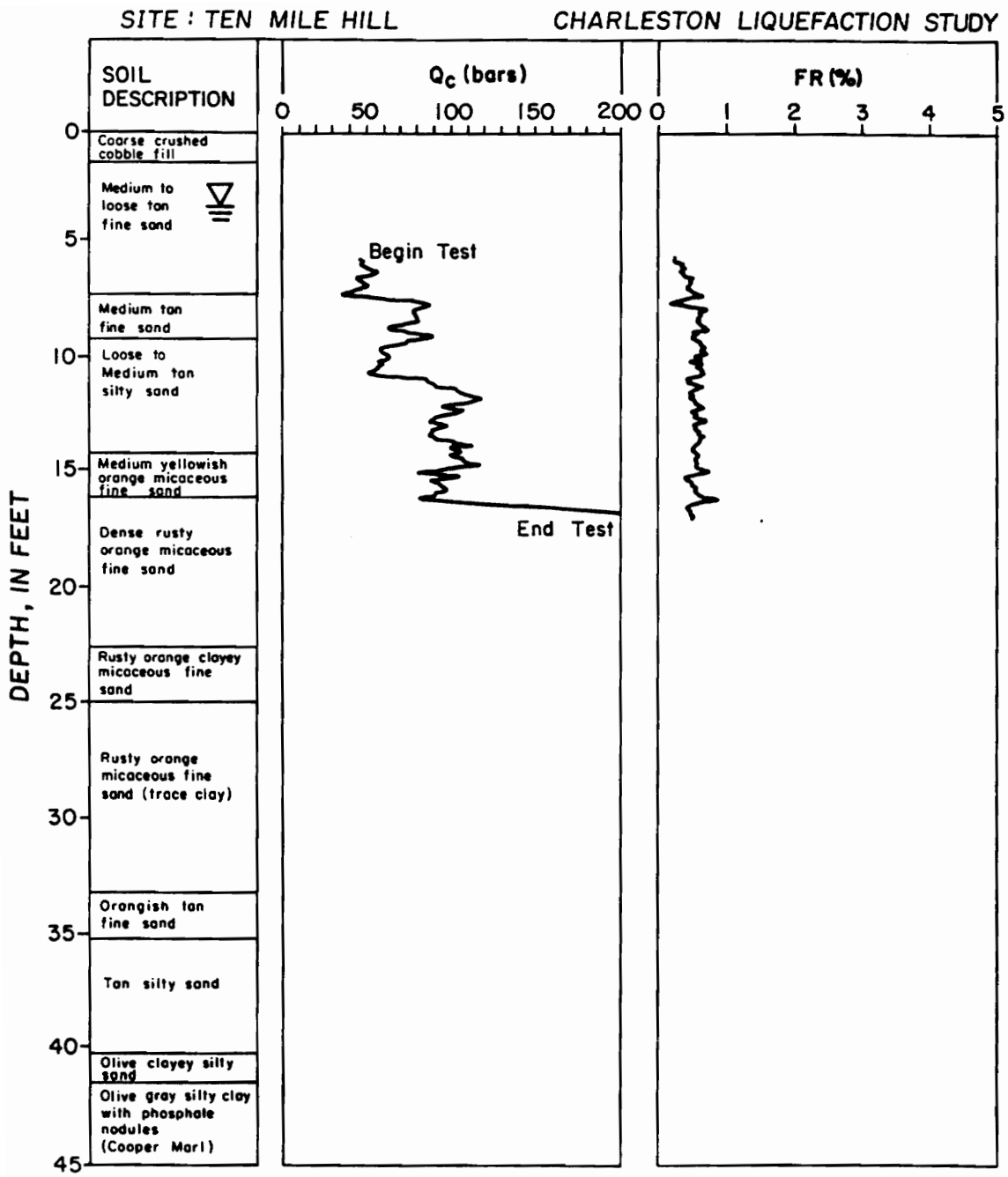

Figure 36. CPT RECORD FOR THE TEN MILE HILL SITE

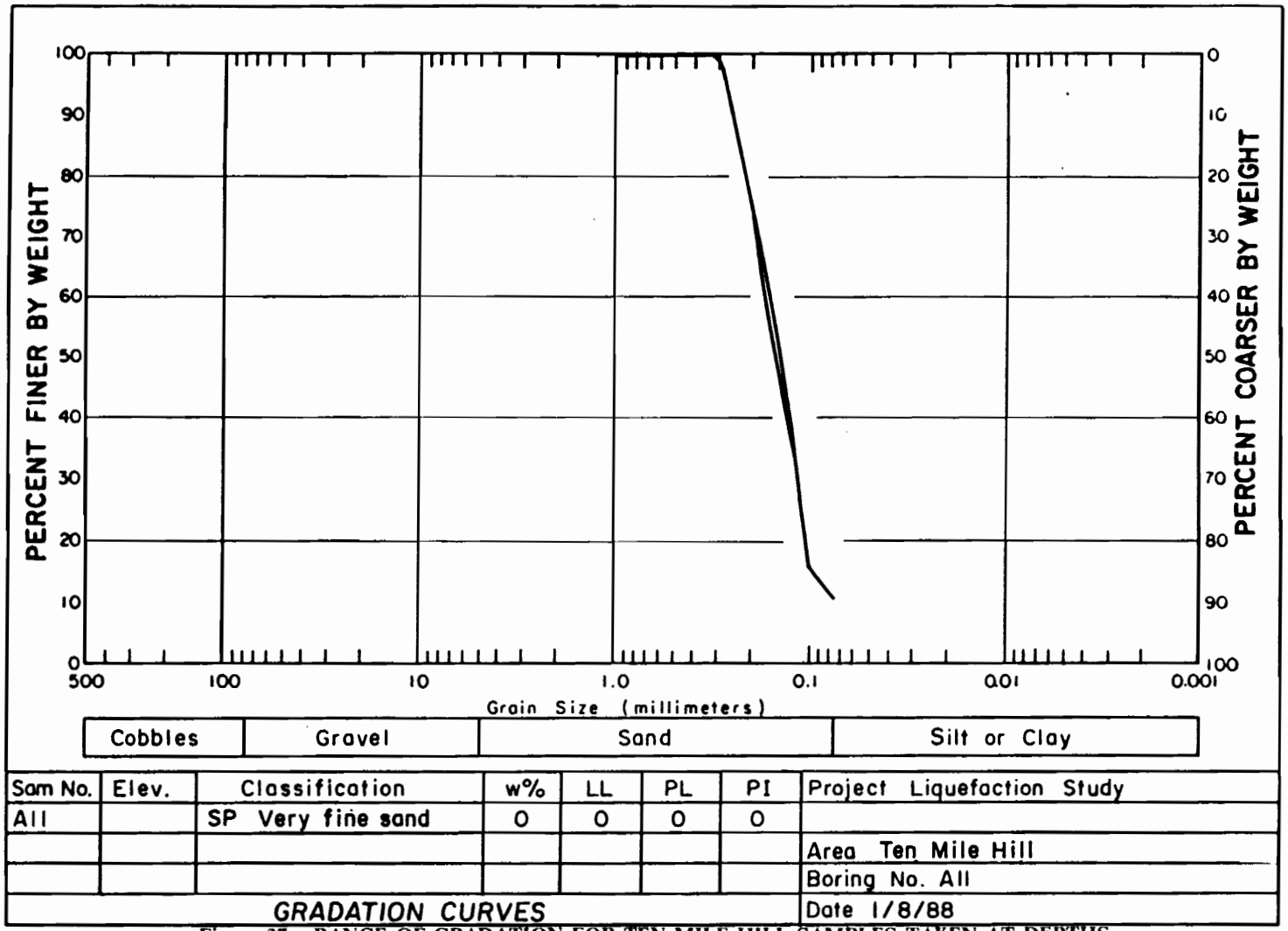

Figure 37. RANGE OF GRADATION FOR TEN MILE HILL SAMPLES TAKEN AT DEPTHS BETWEEN 12.5 AND 15.0 FEET

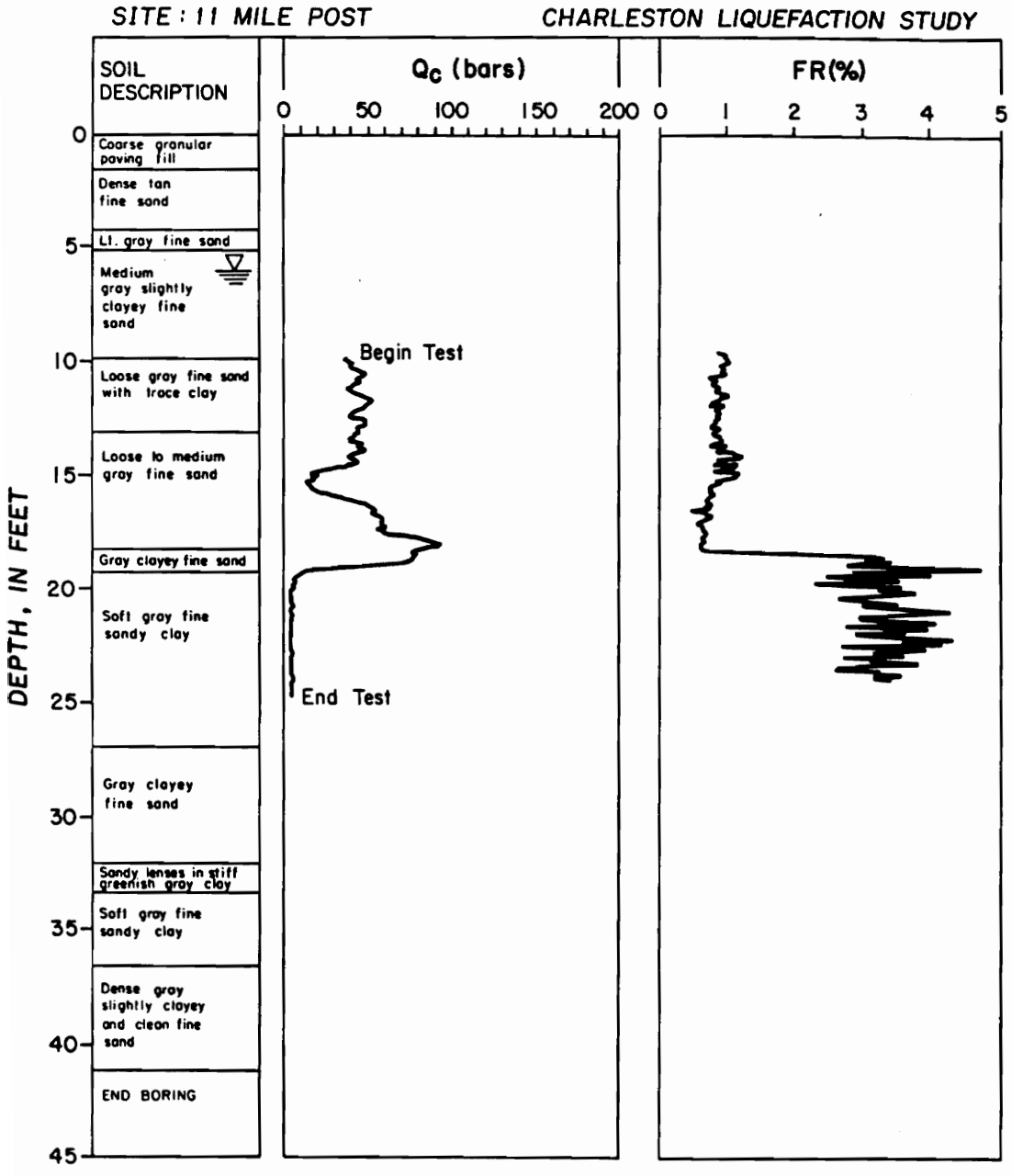

Figure 38. CPT RECORD FOR ELEVEN MILE POST SITE

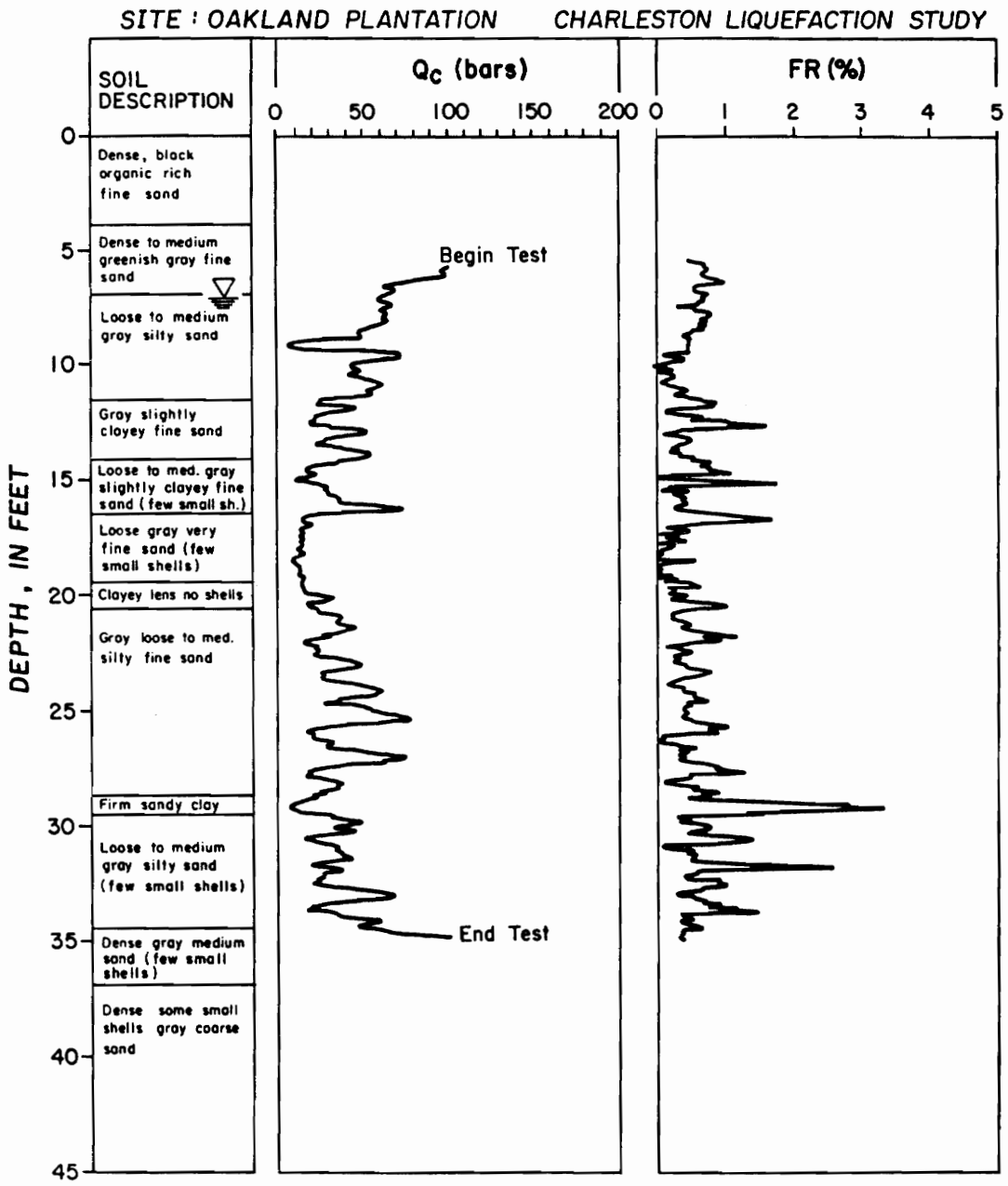

Figure 39. CPT RECORD FOR THE OAKLAND PLANTATION SITE

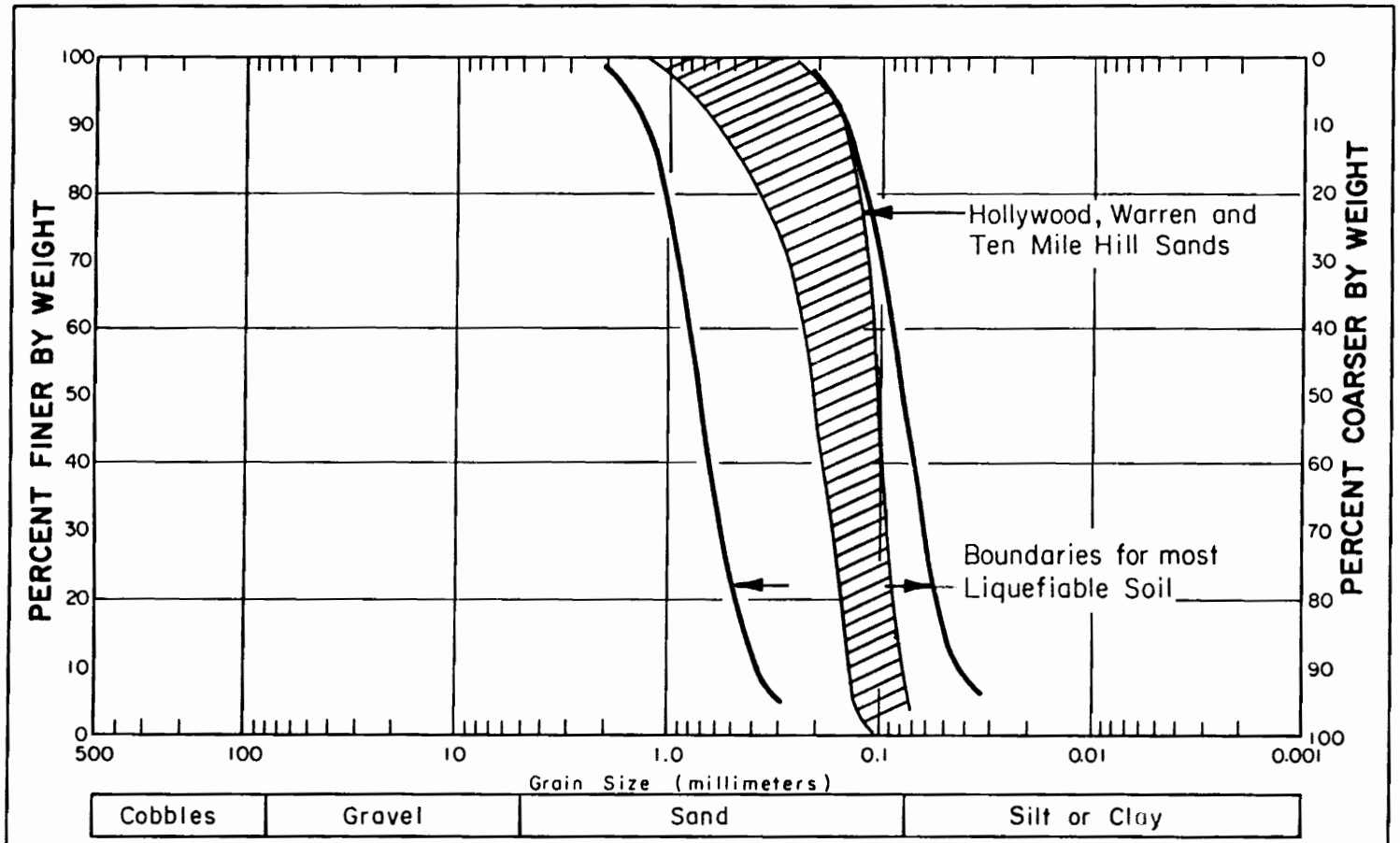

Sam No.	Elev.	Classification	w%	LL	PL	PI	Project Liquefaction Study
All		SP Fine sand to	0	0	0	0	
		SP-SM Very fine sand					Area HW, Warren, and TM Hill Sites
							Boring No. All
GRADATION CURVES							Date 1/8/88

Figure 40. COMPOSITE RANGE OF GRADATION FOR HOLLYWOOD, WARREN AND TEN MILE HILL SOILS AND BOUNDARIES FOR "MOST LIQUEFIABLE SOILS"

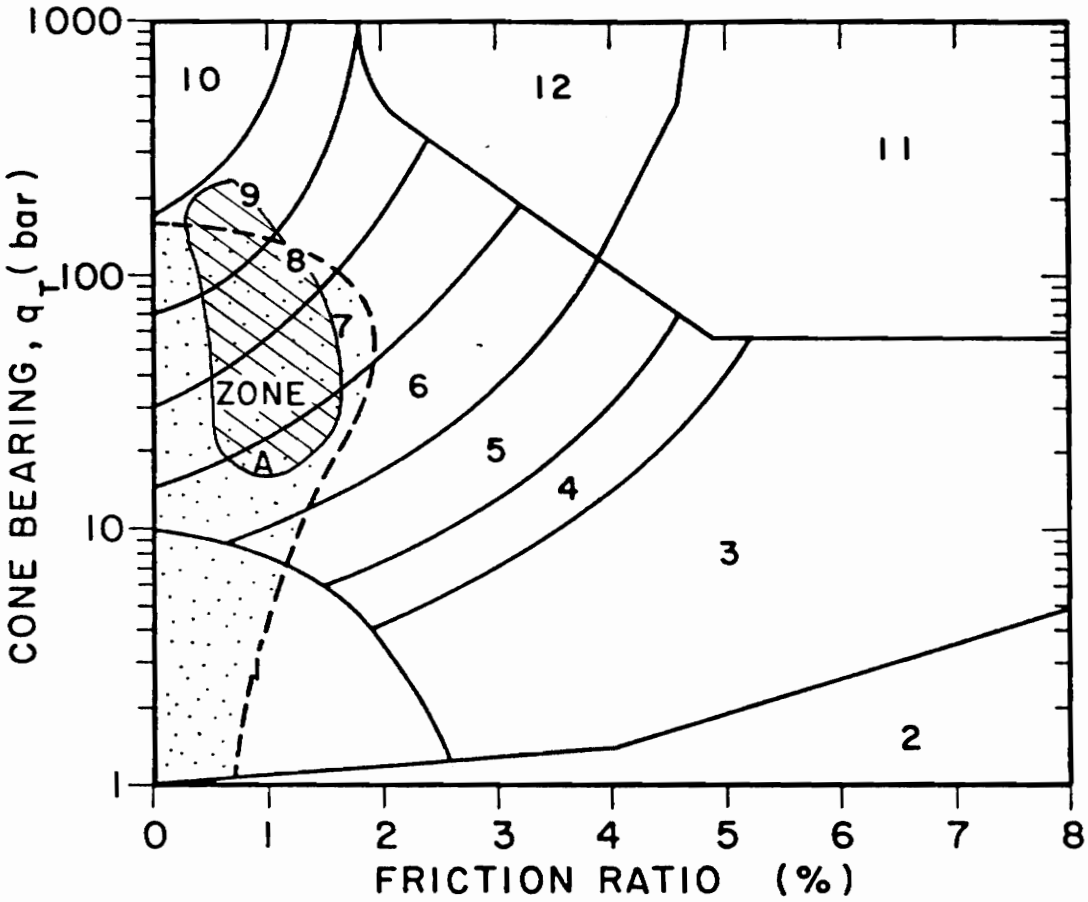

Zone	Soil Behaviour Type
1	sensitive fine grained
2	organic material
3	clay
4	silty clay to clay
5	clayey silt to silty clay
6	sandy silt to clayey silt
7	silty sand to sandy silt
8	sand to silty sand
9	sand
10	gravelly sand to sand
11	very stiff fine grained*
12	sand to clayey sand*

* overconsolidated or cemented.

Figure 41. SOIL CLASSIFICATION CHART FOR ELECTRIC CONE: SHOWING PROPOSED ZONE OF LIQUEFIABLE SOILS AND RANGE OF CPT DATA FOR THE NEAR SURFACE SANDS AT ALL TEST SITES.

Table 3. PROPERTIES OF THE NEAR SURFACE SANDY SOILS AND INFERRED PERFORMANCE DURING THE 1886 EARTHQUAKE

Test Sites	USCS Classification	D_{50} (mm)	C_u	% passing no.200 sieve	Lowest Penetration Resistance Q_c (bars)	Lowest Penetration Resistance $(N_1)_{60}$ (blows/ft)	D_r (%)	Distance to Zone of Energy Release	Extent of Liquefaction During 1886 Earthquake
Hollywood	fine sand	0.12-0.21	1.24-2.10	1.8-9.2	17	2	15-20	4.4	moderate
Warren	fine sand	0.17-0.10	1.35	< 1	25	-	15	6.0	minor
Sod Farm	fine sand	_	_	≃5 (est.)	20	-	20	3.2	minor
Montague	fine sand	-	-	≃10 (est.)	85	-	50	6.5	minor
Ten Mile Hill	fine to silty sand	0.14	2.14-2.19	11	40	-	45	4.7	extensive
Eleven Mile Post	fine to silty sand	-	_	≃10 (est.)	40	-	15-20	3.5	minor
St.Michael's Church	fine to silty sand	-	-	≃10 (est.)	-	3	15-20	13.2	minor
Oakland Plantation	fine sand	-	-	≃10 (est.)	40	-	40	19.0	minor

Chapter VI

Analysis

One of the objectives of this research is to use the findings of the field and laboratory work to help understand the levels of seismic shaking which occurred during the 1886 Charleston earthquake. At this stage of the research (the end of the first year of the larger study), the data base is only partially complete, and it is not appropriate to attempt to draw definitive conclusions. However, it is possible to propose the methods that can be used for definition of seismic shaking levels, and apply them to the existing data base. This approach is used in this chapter.

In the absence of seismic records for the 1886 earthquake, previous strong motion estimates have been postulated based on what is known of attenuation of intensity with distance from the epicenter and scaling relationships for simulated eastern United States earthquakes (4,5,6,33). Based on the historical evidence for damage, the duration of the earthquake, and the first hand accounts of the earthquake effects, it has generally been accepted that the MM intensities in the meizoseismal zone and just outside the meizoseismal zone in Charleston were X and IX respectively. In their work, Bollinger and Nuttli (4) postulated that the Charleston earthquake magnitudes were $M_s = 7.1$ and $m_b = 6.6 - 6.9$. Using this information, and a variety of procedures, different estimates have been obtained for the peak horizontal accelerations that might have oc-

curred in the 1886 Charleston event. Based on scaling relationships for eastern United States earthquakes of $M_s = 7.5$, $m_b = 6.6$, recent studies have estimated that peak horizontal accelerations of 0.6g were experienced within the meizoseismal zone of the 1886 earthquake. This estimate was made for the near surface peak acceleration at a "soft" site composed of unlithified sediments (33). Campbell (6) has used three empirical seismological techniques to estimate ground motion intensities for a seismic event on the east coast of the United States similar to that inferred for the 1886 Charleston earthquake. The use of magnitudes M = 7, $m_b = 6.8$ resulted in median acceleration values of 0.55g for soft sites located along the surface projection of the fault rupture and 0.30g for sites 9.3 miles from this fault projection.

The estimates for near field accelerations would approximately agree with a new study by Krinitzsky an Chang (18) who compiled data from world-wide earthquakes for soft sites. As shown in figure 42, for a MM intensity = X, these data suggest that in the near field (< 25 miles), the peak horizontal acceleration would be about 0.5g. Thus, the seismological evidence would appear to place the peak horizontal acceleration in the meizoseismal zone in the range of 0.5 to 0.6g. However, it is important to note that there are still open questions about these conclusions because of our lack of hard knowledge about some of the assumptions upon which the estimates are based.

6.1 Fundamentals Important to the Methods Used to Determine Seismic Shaking Levels

The information that is available to this investigation which relates to the determination of seismic shaking levels includes:

1. Sand densities - The SPT and CPT data can be directly related to the in-situ density of the sands.

2. Sand grain sizes and grain size distribution - sieve tests on samples from the SPT spoons and from the auger cuttings have been performed in large numbers. Additional SPT and sieve data for sites in Charleston have been made available to this investigation by local soils engineering firms and government agencies.

3. Site stratigraphy - Soil layering profiles are determined from the visual classification logs of the augers and SPT holes, as well as from the friction ratio and cone tip resistance correlations of the CPT tests.

4. Historical and/or paleoseismological records of liquefaction occurrences at each site. In some cases this is important in demonstrating a large extent of liquefaction, while in others it is important that few features exist.

To translate this type of information into likely earthquake shaking levels requires interpretation and back calculation. In this process ground rules need to be established. First, it is pertinent to state the parameters that are considered as constant among the sites: (1) The available information would suggest that for practical purposes all of the sands have had an equal stress history; (2) None of the sand samples showed signs of cementation, thus it is assumed that no differences in site behavior are caused by this factor; and, (3) The historical record and the coincidence of the surficial organic horizon with the present water levels suggests that the ground water table has been at the same depth since the 1886 earthquake, except in local situations where drainage trenches were dug in the recent past. In these areas, the water table was lowered near the trench, but it is apparent from nearby swampy areas where the water table was previously. It is therefore assumed that the water table for the 1886 earthquake is the same as its present position unless there are obvious recent local drainages.

Second, we need to recognize the possible reasons for the presence of or lack of liquefaction features. Liquefaction features are likely to occur where cyclic loading of sufficient strength and duration is applied to shallow saturated sands and silts. They will be most prevalent in areas with a high ground water table and loose sands. In addition, the occurrence of liquefaction features is

enhanced if the liquefiable sands are present in thick layers and the overlying thicknesses of non-liquefiable soils are small. The presence of liquefaction features is suppressed if the situation is reversed from that just described.

Third, there is the question of the present density of the sands versus that of the sands before the 1886 earthquake. This relates to two issues: (1) Can the densities today be used to infer the response of the sands in 1886?; and, (2) If today's densities are thought to be different thant those in 1886, what is the implication relative to progressive densification as a result of prior liquefaction? In regard to the first of these points, it would appear reasonable to assume that if the site is out of the meizoseismal zone, and little evidence exisits that liquefaction of any significance developed at a site, then the sand densities today should be reasonable representative of the densities prior to 1886. At the same time, it seems that even if the paleoseismological evidence showing that few liquefaction phenomena developed during the earthquake, then the density today does not greatly differ from that at the time of the earthquake. These two assumptions will be used in this preliminary interpretation. The credibility of the assumptions is assessed as a matter of course in examining the consistency of the findings of the analyses. Conversly, if the site were subject to liquefaction, and liquefaction features wee prominent, it will be assumed that the sand densities may have been significantly modified as a result of the earthquake.

6.2 Analysis of Liquefaction in Sandy Soils with Level Ground Conditions

The analysis of liquefaction to allow estimation of levels of ground shaking consists of two parts. First, the possibility that liquefaction can occur in the sandy soils at at site must be evaluated. Second, the possibility of development of liquefaction features as a result of the liquefaction needs to be determined. The first of these tasks involves testing the site conditions against the effects of

different possible levels of shaking following the procedures of Seed and others (36,39,41). The second is done using the layer effects chart of Ishihara (16), which relates the presence of liquefaction features to the size of the liquefiable layer and the overlying non-liquefiable soil layers.

6.3 *Introduction*

The process of liquefaction is induced by shear stresses that are transmitted to the saturated sand layers during seismic shaking, as described in chapter 2. The shear stresses developed in the soil layer during an earthquake are due primarily to the upward propagation of shear waves in the deposit. If the soil column above the layer of interest at depth h behaves as a rigid body, and the maximum ground surface acceleration is a_{max}, the maximum shear stress on the soil element is:

$$(\tau_{max}) = \frac{\gamma h}{g} a_{max} \qquad [eq.\ 1]$$

in which γ = unit weight of the soil (39). This equation indicates that the magnitude of the shear stresses and potential for liquefaction are directly related to the maximum horizontal acceleration induced by the earthquake. For this reason it is more meaningful to relate the initiation of excess pore pressures to acceleration than to indirectly related factors such as earthquake magnitude or seismic intensity. Although various levels of observable liquefaction phenomena have been related to MM intensity values, this relation makes no account for the nature of the soil conditions in the epicentral region.

Existing geotechnical methods for the evaluation of liquefaction potential using data obtained from in-situ penetration tests are based largely on the work of Seed and others (39,40,41). The procedure for assessing the liquefaction potential of a soil deposit subjected to seismic loading involves two steps; 1. estimation of the cyclic stress or strain condition developed in the field due to the design earthquake, and 2. estimation of the cyclic resistance of the soil. For soil under level

ground conditions, the cyclic behavior is represented by the average cyclic stress ratio, i.e., the ratio of the average cyclic shear stress, τ_{av}, developed on horizontal planes in the soil as a result of ground motions to the initial vertical effective stress, σ'_{ov}. This parameter has the advantage of taking into account the depth of the soil layer involved, the depth of the water table, and intensity of earthquake shaking (40). The cyclic stress ratio experienced in the field due to a design earthquake can be computed from the equation:

$$\frac{\tau_{av}}{\sigma'_{ov}} \simeq 0.65 \bullet \frac{a_{\max}}{g} \bullet \frac{\sigma_{ov}}{\sigma'_{ov}} \bullet r_d \qquad [eq.2]$$

in which $a_{\max}$ = maximum acceleration at the ground surface; g = gravitational acceleration; σ'_{ov} = initial effective stress in the sand layer under consideration ; σ_{ov} = the total stress at the same point; and r_d = stress reduction factor varying from a value of 1.0 at the ground surface to 0.9 at a depth of 30 feet (39). Values of the cyclic shear stress ratio have been determined for areas which have or have not exhibited surface evidence of seismically induced liquefaction. These values are then correlated with soil properties indicative of cyclic shear resistance.

Estimation of the field liquefaction potential is made using either laboratory testing methods on representative undisturbed samples or various in-situ testing methods. The inherent difficulties in obtaining undisturbed samples of loose, saturated cohesionless soils has led to the prominence of in-situ testing methods for this evaluation of liquefaction potential, with the SPT and CPT most commonly used. The first evaluation method was first developed for use with the SPT due to its predominant usage. Seed developed $\frac{\tau_{av}}{\sigma'_{ov}}$ vs N charts based on field data obtained in areas which did or did not liquefy following large earthquakes and boundaries are presented which separate conditions favorable for liquefaction from non-liquefaction. The lack of a significant data base for CPT's in areas experiencing seismic liquefaction necessitates the conversion of SPT based charts to equivalent cone bearing using empirical correlations described in chapter 4.

The cyclic stress ratio required to cause liquefaction is influenced by the nature of seismic shaking, i.e. magnitude and duration, and the grain size of the material under consideration. The field performance data is based on sites that either have or have not experienced liquefaction during

recent earthquakes and inherently accounts for the duration of seismic ground motions. Although most of Seed's field data is for M = 7.5 earthquakes, corrections can be made to account for the duration of earthquakes of different magnitude by the use of scaling factors which relate the number of stress cycles required for liquefaction and the number of representative stress cycles for earthquakes of different magnitude (40). Loose, silty sands and silts tend to have a higher resistance to liquefaction than coarser sands at the same penetration resistance due to the decrease in penetration resistance associated with reduced mean grain size (16,35,38). Corrections for the mean grain size and fines content of the soil can be made by shifting the liquefaction boundary on the cyclic stress ratio versus cone resistance chart as described by Seed and Alba (38).

Several recent field investigations have applied the methods based on the CPT to areas which did or did not exhibit liquefaction during seismic events (8,54,45). In all cases peak horizontal accelerations due to the seismic ground motions were either locally recorded or deduced from other near site earthquakes allowing for a direct evaluation of the penetration data. Although magnitudes have been inferred from intensity data for the 1886 Charleston earthquake, no recorded base or near surface acceleration is available for this event. Peak horizontal accelerations in the near surface sediments will be estimated from field performance and layer thickness relations, and nature of the liquefaction features attributed to the 1886 earthquake. This analysis allows for comparison with vlaues currently postulated in the seismology literature and derived by entirely different methods.

Consistent with magnitude estimates for the 1886 Charleston earthquake, a cyclic stress ratio versus modified cone resistance chart has been constructed for a M = 7 event and corrected for the mean grain size and fines content of the material of interest at the test sites. Based on recent probabilistic studies (2,17) indicating that the recurrence of MM = VIII earthquakes in the Charleston region is roughly 225 years, a separate boundary has also been constructed for M = 6 earthquake. Figure 43 shows the curves for the magnitudes corresponding to the 1886 earthquake and the initiation of liquefaction due to a probable near future seismic event. The range of fines content exhibited at the test sites is also included.

6.4 *Sites within the Meizoseismal Zone*

6.4.1 Hollywood Site

Of the sites within the meizoseismal zone, the Hollywood site was the most thoroughly investigated. This site is also unique because of the extensive exposure of the soils in the 9000 ft mapped portion of the drainage ditch, and the thorough work of Obermeier who documented that the 1886 event did not produce extensive liquefaciton features at the site. Since the ditch cuts through the flank of an ancient beach ridge, which is an area most likely to have exhibited sand boils, this is reasonably conclusive evidence that liquefaction features were not prominent in this locale. The number and size of venting features found by Obermeier within 200 feet of the CPT holes are listed in Table 5. This shows that small vents of liquefied sand layers developed in the 1886 event at four of the CPT sites, while no features were exposed at five of the sites. These circumstances suggest that while the sands may have liquefied, they were not strongly disturbed by the earthquake, and that the present day densities are probably not greatly different than those at the time of the 1886 event. It also suggests that the shaking at this site was not strong enough to cause significant liquefaction features, given the relative thicknesses of the liquefiable and non-liquefiable layers.

In most cases the cone penetration tests at the Hollywood site were begun at depths of approximately 10 feet following the results of the initial test at STA 4480′ and extent of the dense surficial material encountered during augering at other stations. In some cases, however, standard penetration test data demonstrate that potentially liquefiable sand layers exist between the ground surface and a depth of 10 feet. At stations where supplementary SPT's were performed, the CPT logs were extended to the surface using modified SPT data for the hole. A $Q_c/(N_1)_{60}$ factor of 4.5 was used to relate the penetration data. The STA 3490′ CPT log with curves for the peak horizontal acceleration (a_{max}) needed to initiate liquefaction superimposed is shown in figure 44 (the

curves for the remaining stations are contained in appendix B). This CPT record demonstrates that as a_{max} increases the thickness of the potentially liquefiable material also increases, with a resulting decrease in the extent of the overlying resistant layer. It is assumed that the water table was at 3.0 feet during the 1886 earthquake, and that at stations where CPT's began at 10 feet and data are not substantiated with SPT data to the surface, overlying layers are resistant to the generation of excess pore pressures. Points corresponding to the layer relations for the four a_{max} values were plotted on the Ishihara chart for every station. The peak horizontal acceleration that corresponded most closely to both, 1. Ishihara's boundary curves, and 2. historical and pleoseismological evidence for the extent of surficially manifested liquefaction was chosen to be representative of the seismic loading levels experienced at the site during the 1886 earthquake.

Inspection of the a_{max} curves for all of the Hollywood CPT records reveals that potentially liquefiable layers exist along the entire ditch. These curves indicate that surficially exhibited liquefaction features should occur at every station if the maximum 1886 acceleration approached 0.5g. However, this level of seismic ground motion is not reasonable given the minor to moderate venting which occurred in the area. Figure 45 shows for each station the layer thickness relations that give the best agreement between the a_{max} curves and Ishihara's boundary curves. These points indicate that ground failures should occur at every station, except 4480', if subjected to horizontal accelerations exceeding 0.4 to 0.5g. Of particular interest is the relation for each site between its position on the layer thickness chart and the extent of exposed liquefaction vents listed in table 5. Three of the four stations that exhibit relic venting features plot at or above the 300 gal (0.3g) boundary while the stations which appear to be devoid of 1886 vents plot at or below the 0.3g line. Although it appears to be the most prone to liquefaction, the conditions at STA 6475' are a major exception to the trend with no evidence found for liquefaction of the near surface sand layers during the 1886 earthquake. The data for each of the stations indicates that a peak horizontal acceleration of approximately 0.3g would account for the liquefaction which occurred at this site.

The locations of source beds for the liquefaction vents can be inferred from the CPT logs as occurring in the zones of lowest penetration resistance. Material susceptible to liquefaction at peak ground motion accelerations of 0.3g is shown in figures 46 and 47. Possible source beds for seven

liquefaction features located along the ditch have been tentatively determined on the basis of sedimentary mineralogy to exist at depths between 5.0 and 15.0 feet (14). From this data source beds of 5 - 10 feet and 10.5 - 15.0 feet have been estimated for pre-1886 features located at stations 0′ and 4125′, respectively. Before the location of the liquefied beds can be determined using CPT data the effects of progressive densification need to be evaluated. This effect is difficult to assess at the Hollywood site as the penetration resistance of the upper sandy soil decreases with depth and does not appear to follow the progressive upward densification model of Youd (53). What has been determined is that the materials which contributed to previous occurrences of liquefaction have remained very susceptible to seismically induced increases in excess pore pressure.

6.4.2 Warren Site

Documentation of conditions at the Warren site is not as complete as that at the Hollywood site, neither in terms of the knowledge of the past liquefaction at the site nor in terms of the amount of exploration performed. Documented liquefaction features at this site consisted only of one significant sand blow. The soil conditions in the upper 15 feet as determined from three CPT's and five auger holes at the site are similar to Hollywood. From the available evidence it would appear that the density of the sands in close proximity to the vent should have been changed significantly by the 1886 event, while sands located away the isolated vent should be approximately the same as that which existed in 1886.

The CPT logs and superimposed a_{max} curves, contained in appendix B, favor source layers for liquefaction located at depths of between 5.0 and 10.0 feet. The soil conditions determined at the three Warren CPT's are plotted on figure 48 and indicate that peak horizontal accelerations of approximately 0.3g were experienced at the site during the 1886 earthquake. The locations of the three Warren tests on the layer thickness boundary curves and proposed intensity of ground motion support the evidence that liquefaction at this site was localized and probably confined to the area around the large vent examined by Cox (9).

Paleoseismological evidence on the mineralogy of the sandblow material implies that ejected material came form depths of 14 to 17 feet (9,14). This is supported by the presence of angular clay fragments from the layer at approximately 10 feet in the sandblow material. The CPT logs demonstrate that if the silty sand at depths below 13 feet liquefied during the 1886 earthquake then extensive densification of this layer has occurred. This may be possible in light of the proximity of Warren 1 and 2 penetration tests to the location of the large liquefaction vent. Evaluation of the conditions presently existing leads to the layered system shown in figure 49. Densification of the sand layers would tend to increase the acceleration required to initiate observable liquefaction and results in an upper bound of roughly 0.3g for the ground motions induced by the 1886 earthquake.

6.4.3 Remaining Sites in the 1886 Meizoseismal Zone

As mentioned previously the remaining sites were tested with one or two CPT's in order to obtain a preliminary assessment of the soil conditions at various sites during this initial portion of the larger investigation. The limited test coverage allows for a tentative evaluation of several sites, but does not allow for the extent of the loose sand layers to be determined. In this case it may be possible for very loose layers or pockets in the vicinity of the relic liquefaction features to go undetected. The points of best agreement between the a_{max} curves and the ground failure boundary curves for the Sod Farm, Montague, Ten Mile Hill, and Eleven Mile Post sites are also shown in figure 48.

Geologic investigations of preserved liquefaction features at the Sod Farm and Montague sites indicate that liquefaction induced by the 1886 earthquake was very minor. Both of these sites exhibit penetration resistance profiles that decrease with depth through the surficial sand layers. The positions of these two sites on the layer thickness chart imply that peak accelerations exceeding 0.4 to 0.5g would be necessary to result in venting of liquefied material at the ground surface. Again, the existence of loose pockets in the immediate area could have been responsible for the features discovered in the drainage ditches at these sites.

The near surface soils at the Ten Mile Hill and Eleven Mile Post sites appear to be susceptible to liquefaction induced ground failures at seismic loadings of less than 0.3g. This relation would account for the extensive nature of liquefaction which was reported at the sites following the 1886 earthquake. The Eleven Mile site exhibits a medium dense layer to a depth of approximately 10 feet which becomes very loose to 18 feet and does not appear to have undergone substantial densification during the 1886 event. Conversly the Ten Mile Hill site demonstrates a stair stepped penetration resistance profile that may be due to reliquefaction and a progressive upward densification. This assumption is supported by first-hand reports of soundings made to depths of 12 feet in several sandblow craters located at Ten Mile Hill. This would indicate that the densified layer existed below 12 feet and may correspond with the dense sand found at a depth of 16 feet. Several of the first hand acounts note an abundance of mica (muscovite) in the vented sands at Ten Mile Hill. A dramatic increase in the mica content of the sand was located during soil borings at depths of 12 to 14 feet indicating that liquefaction of the presently dense sand below 16 feet may have been necessary for the formation of the spectacular sandblows which occurred in the area. The present soil profiles at these two sites support the assumptions that, 1. the magnitude of relative density increase is dependant on the extent of surficially vented material and can be minimal in areas where the venting of excess pore pressures is minor, and 2. even areas exhibiting large liquefaction features can remain reliquefiable.

Relations between the a_{max} and layer thickness boundary curves for sites located within the meizoseismal zone of the 1886 earthquake favor a peak horizontal acceleration throughout this area of approximately 0.3g. The geotechnical evidence based on in-situ soil properties and behavior to cyclic loading results in a considerably lower estimated peak horizontal acceleration in the meiszoseismal zone of the 1886 earthquake than estimates based on earthquake scaling and intensity reports. It would appear from the CPT records that if the sites tested had been subjected to ground motions on the order of 0.5 to 0.6g, liquefaction and the formation of craterlets would have been more widespread than indicated in the historic accounts or by geologic investigations.

6.5 *Sites Outside the Meizoseismal Zone*

6.5.1 St. Michael's Church

The St. Michael's Church and Oakland Plantation sites provide evidence for the effects of seismic energy attenuation on initiation of liquefaction. Historical and geologic observations indicate that liquefaction was of minor extent, being exhibited only in small, isolated vents. The extensive, first-hand reports on damage induced by the 1886 earthquake in downtown Charleston do not mention the formation of craterlets in the vicinity of St. Michael's Church. The sand pits, which cover several acres, near the Oakland Plantation afford widespread exposure of the near surface sands. At this site only one small vent was discovered indicating that liquefaction was minimal in this area. It can be assumed that with the localized, minor venting which occurred that densifiction due to seismic loading and liquefaction seems to be minimal at the St. Michael's Church and Oakland Plantation Sites.

St. Michael's Church, located in downtown Charleston, was the site of documented liquefaction during the 1886 earthquake. Built between 1751-1761 on one of the highest available natural sites in Charleston, no piles were driven for the foundation of its steeple. The colonial builders were apparently satisfied with the bearing characteristics of the clay stratum found eight to ten feet below grade. Liquefaction in the near surface silty sand was manifested by the venting of colorful sands inside the church, and resulted in an eight inch settlement of its steeple. The wrenching of the large front portico into the steeple and pattern of cracks in the exterior mortar demonstrated that settlement of the church was confined to its steeple.

Soil profiles and SPT data for this site are presented in figure 50 and can be considered representative of the conditions beneath St. Michael's Church. The shallow soils are sands with about 10% fines. The SPT data for the sandy material was normalized to 1 TSF and converted to equivalent CPT tip resistance using a multiplying factor of 4.5, an approximate value for soil

classified as silty, fine to medium sand (Table 4). The field performance charts used throughout this analysis are based on SPT data and adapted for CPT data using the same factor of 4.5. Use of the same factor for the chart and SPT data at St. Michael's Church results in an analysis that is equivalent to a direct evaluation of the SPT data. The CPT format is used at this site to allow for comparisons with data at the other test sites. The cyclic stress ratio can not be calculated using equation 2, without a peak horizontal acceleration. Assumptions regarding, 1. the extent of liquefaction in the area of close proximity to St. Michael's Church, and 2. the thickness of the non-liquefiable surface layer and underlying liquefiable layer are required before an estimation of the liquefaction inducing acceleration can be made.

It appears after reviewing several first-hand reports on the effects of the 1886 earthquake that the occurrence of minor liquefaction at St. Michael's Church was a singular event in that small portion of Charleston. It is inferred that the cyclic shear stresses at this site slightly exceeded the threshold level required for the surface manifestation of liquefaction. The ground water table is assumed to be at the same elevation now as during the 1886 earthquake, thereby precluding the development of excess pore pressures in the four feet of free draining sand above this level. The data shows that the maximum modified penetration resistance in the silty sand occurs at 6.5 feet, then decreases with depth. The field data are presented on the cyclic stress chart in a histogram format so that it may be viewed statistically (figure 51). The histogram allows for the data from several tests to be viewed in one plot. The penetration data for the silty, fine sand layer represent the depth range of 4 to 14 feet. The equivalent Q_c values were grouped into 15 bar increments and plotted versus the average cyclic stress ratio over the depth of interest. The boundary curve delineating liquefaction in this figure is defined for M = 7 and 10 percent fines content which closely reflect the conditions at this site during the 1886 earthquake.

The estimation of a near surface acceleration involved maneuvering the histogram, with abcissa fixed, parallel to the ordinate axis to a stress level that would account for the observed levels of liquefaction resulting from the 1886 event. The range of cyclic stress ratio between 0.295 and 0.115 and corresponding maximum horizontal accelerations of 0.32g and 0.13g represent extremes in the response of the soil at this site. The former values result in complete liquefaction of the entire 10

foot thick layer while the lack of surficial expression of generated pore pressures at depth would be probable under the latter.

It was assumed for the first refinement of the cyclic stress level that the sands exhibiting the highest penetration resistance were not liquefiable. In all borings except B-4 this led to a non-liquefiable surface layer close to 7.0 feet (2.1 m) thick overlying a 5.5 to 9.5 foot (1.7 to 2.9 m) liquefiable layer. Utilization of Ishihara's layer relations for these conditions results in required maximum horizontal accelerations of approximately 0.2g at B-1 and 0.3g at B-2 and B-3 for the surface manifestation of liquefaction. For the localized, minor amount of surface venting that was reported for this area of Charleston the former acceleration value would seem to be valid. This assumption also implies that portions of the sandy layer with equivalent Q_c values greater than 46 bars are not prone to liquefaction under the design earthquake. Locating the histogram so that the tip resistance of 46 bars lies on the liquefaction boundary results in a computed peak horizontal acceleration of 0.18g.

If liquefaction of the entire sandy layer is precluded by the lack of historical evidence of widespread craterlets, then the Q_c value that can be assumed to be at the threshold of excess pore pressure generation can be inferred from boring B-4 as approximately 43 bars. This corresponds to maximum horizontal accelerations of 0.18g by *eq.* 2 and alters the layer relations resulting in necessary accelerations in the range of 0.2g for observable liquefaction limited to the sands near boring B-4. It is recognized that soil structure and density are most likely not exactly the same as that which existed prior to the 1886 earthquake. However, with the absence of widespread surface venting it can be assumed that the relative density is approximately equal or slightly higher than during the earthquake. This would lead to an acceleration estimate that is very close or slightly higher than that necessary to have induced liquefaction in 1886. Although some subjectivity has been emparted to the analysis, data from the historical record and recent in-situ tests indicate that the peak near surface horizontal acceleration at this site was approximately 0.2g during the 1886 earthquake.

Of considerable importance in the site evaluation for future structures is the assessment of liquefaction potential for postulated near future earthquakes. The recurrence interval for

MM = VIII (M≃6) events generating peak accelerations of 0.2 - 0.25g has been estimated at 225 years. While this acceleration is greater than that proposed for this site during the 1886 event it is not unreasonable due to the floating nature of epicenters of current seismicity. A smaller earthquake located closer to Charleston could result in the proposed accelerations. Utilization of the field performance and layer thickness charts for a M = 6, a = 0.25g earthquake indicate that under the induced cyclic shear stress of 0.24 liquefaction of the loose sandy soil would be at least as prominent as during the 1886 earthquake.

6.5.2 Oakland Plantation

The St. Michael's Church and Oakland Plantation sites have both been described as experiencing limited, minor liquefaction during the 1886 earthquake. As previously demonstrated the soil profiles and extent of 1886 venting in the St. Michael's Church area indicate that a peak horizontal acceleration of approximately 0.2g was experienced at that time. The a_{max} curves on the CPT record for the Oakland Plantation site in figure 52 demonstrate that the extensive deposit of loose silty to fine sand is susceptible to liquefaction at acceleration levels of approximately 0.2g. A fines content of 10% and ground water table at 2 feet was assumed for construction of the a_{max} curves at this site. Although an overall site characterization of the soil profile is only tentative due to limited, preliminary testing, the CPT record shows the sandy material in close proximity to the lone liquefaction vent has remained very susceptible to reliquefaction. A peak horizontal acceleration induced by the 1886 earthquake of 0.2g has been assigned to this site. The material in the vent was free of shells indicating that the source bed of the generated excess pore pressures was located above the slightly shelly sand at a depth range of 14.5 to 19.5 feet.

6.6 *Discussion*

The estimated horizontal accelerations of 0.2g at the St. Michael's Church and Oakland Plantation sites provide evidence for the attenuation of strong motions in the Charleston environment. The diminution of a peak acceleration from approximately 0.3g near the zone of energy release to 0.2g at sites located 13 and 19 miles away is supported by the Hermann and Nuttli curve (figure 53) scaled down to an a_{max} of 0.3g. While there is evidence for greater attenuation of smaller ground motions this effect is assumed to be minor.

The estimation of peak horizontal accelerations that are lower than those often attributed to the 1886 earthquake does not necessarily contrast the widespread structural damage experienced in the Charleston region. It seems probable that if accelerations in the range of 0.3g were sustained for a large number of cycles during the 30 to 70 second duration of observed strong ground motions, soil-structure interactions could have resulted in magnified accelerations in the structures. The prevalence of masonary structures in Charleston would also account for vast damage as these structures are particularly vunerable to damage by cyclic loading and differential settlement. Failures of structures such as single story wood frame houses, bridges and railroad tracks were prevalent due possibly to both large elastic straining and ground failures induced by ground motions in the exceptionally soft and loose foundation soils. It has been demonstrated that sandy layers of low cyclic resistance occur at various depths at all of the test sites. These layers may have liquefied resulting in severe ground oscillations or loss of bearing capacity, but were prevented from venting at the surface due to thick layers of overlying resistant material.

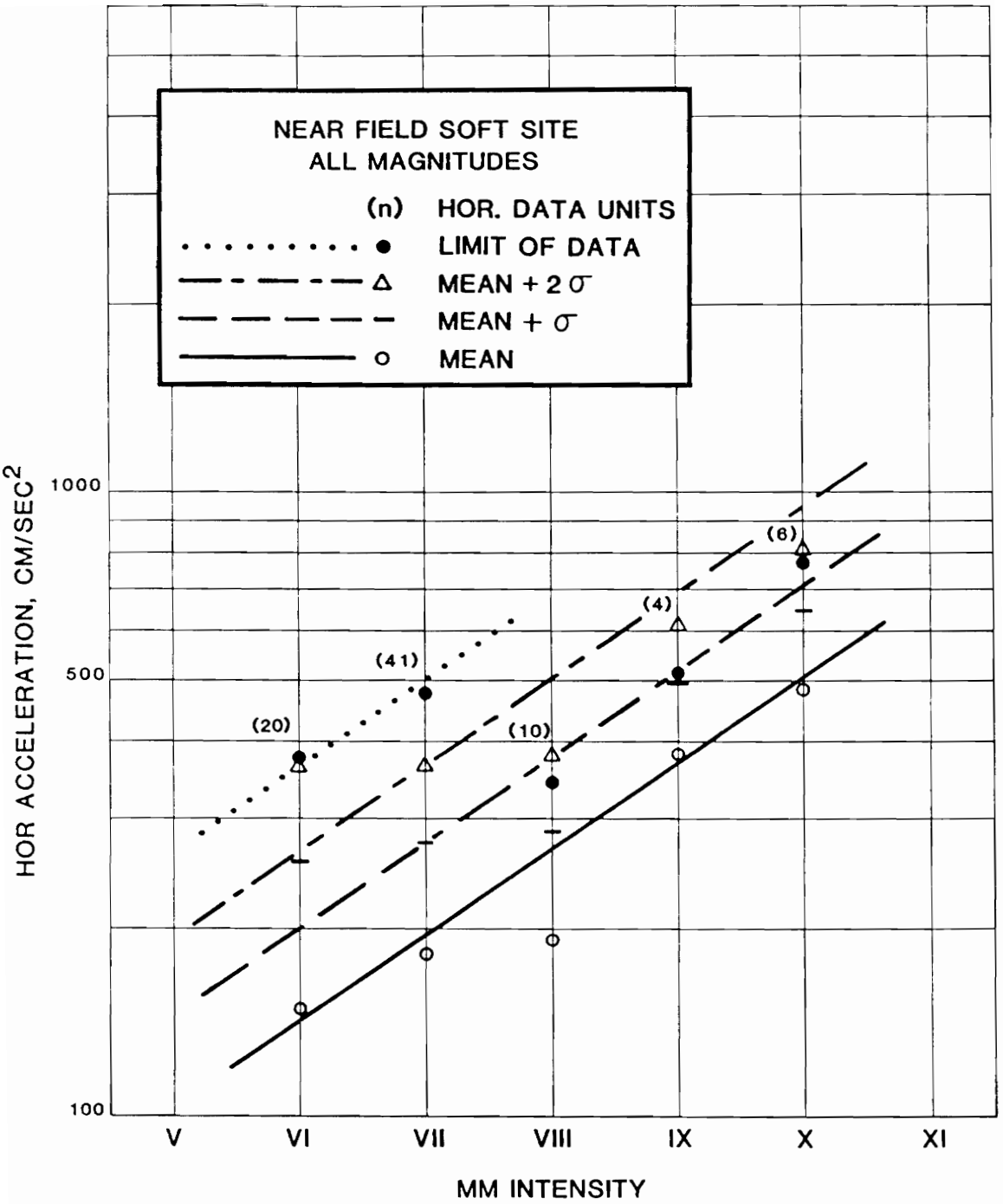

Figure 42. PEAK HORIZONTAL ACCELERATION VERSUS MODIFIED MERCALLI INTENSITY

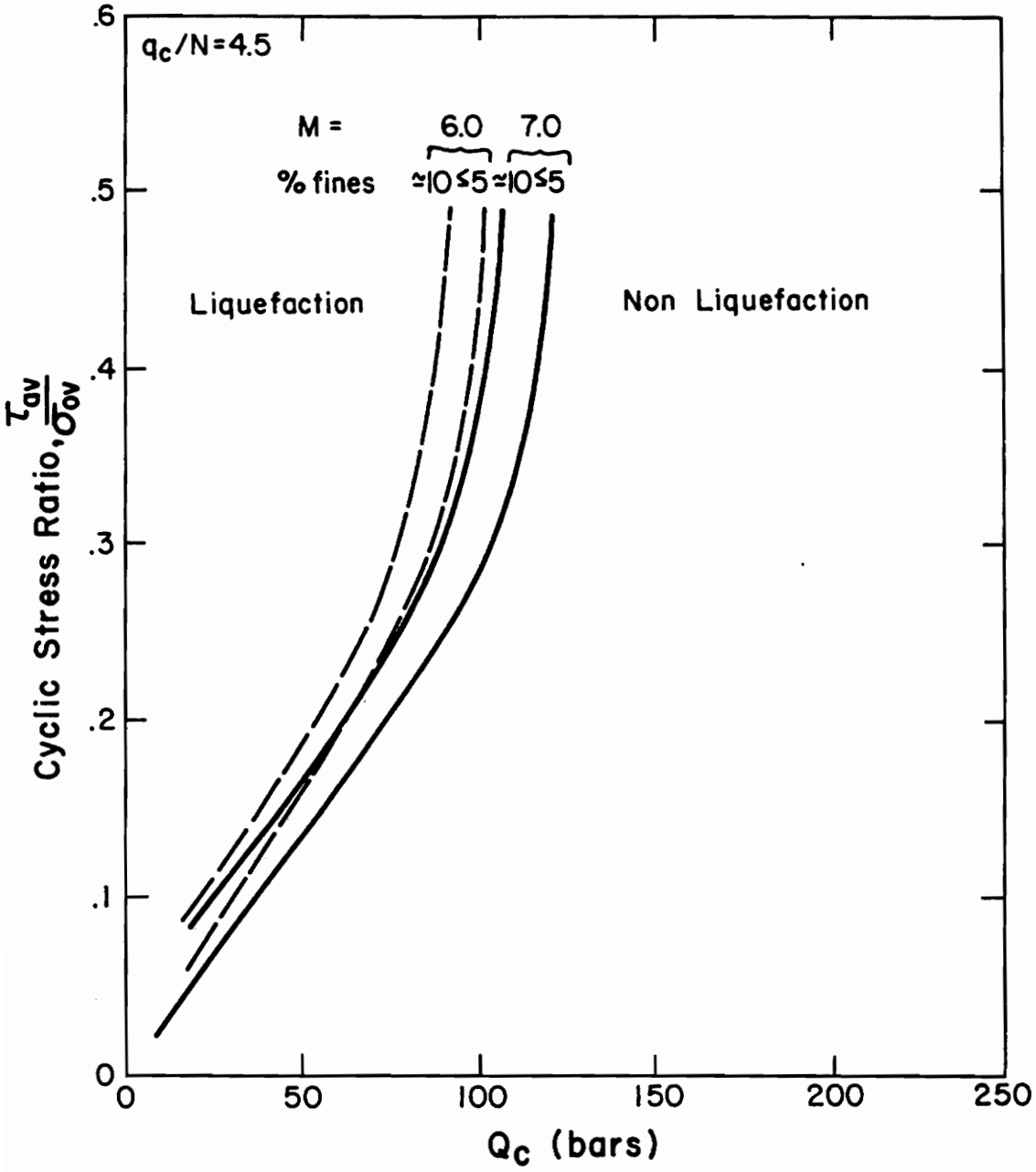

Figure 43. CORRELATION BETWEEN FIELD LIQUEFACTION BEHAVIOR OF SILTY SANDS AND CONE PENETRATION RESISTANCE

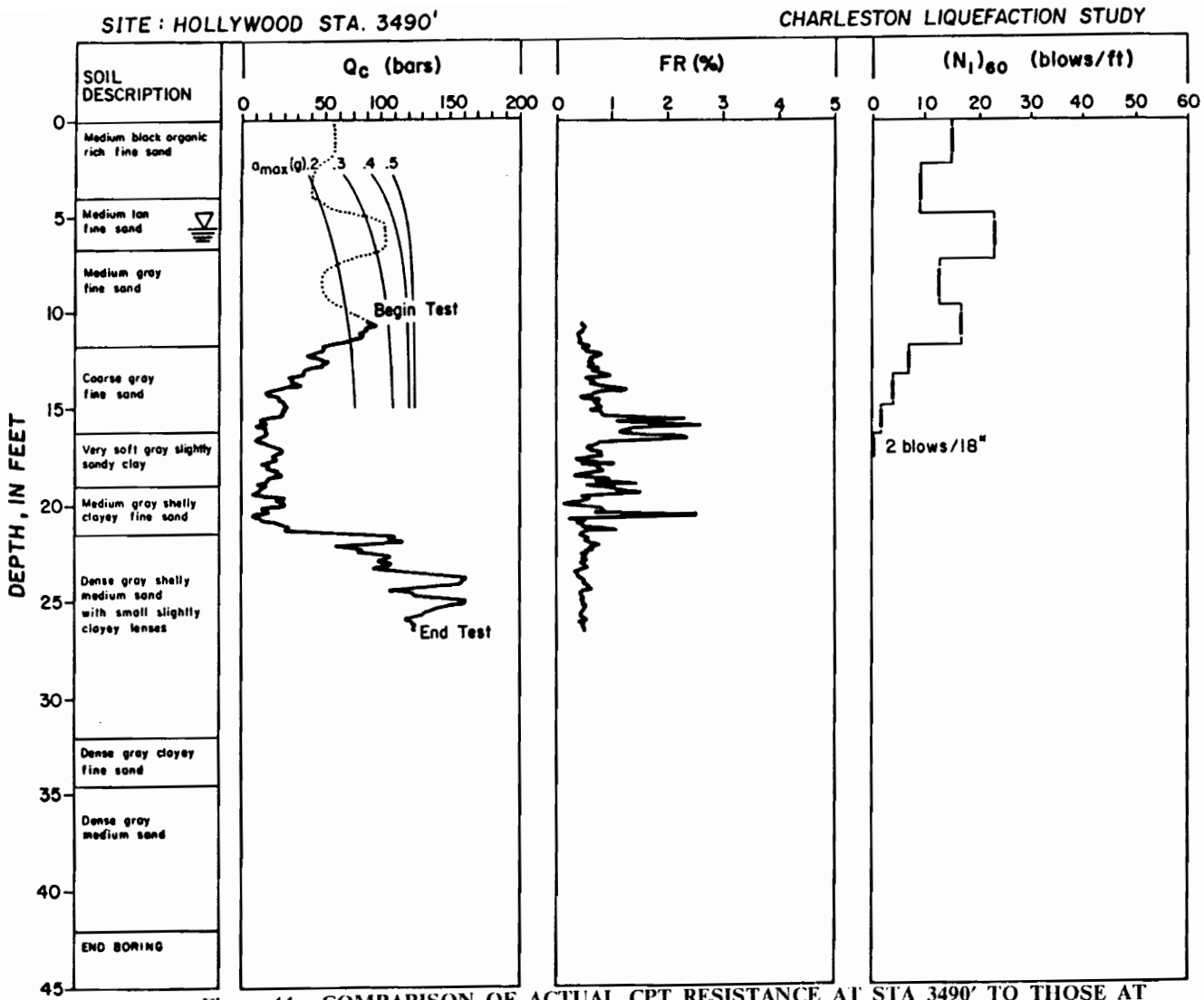

Figure 44. COMPARISON OF ACTUAL CPT RESISTANCE AT STA 3490' TO THOSE AT WHICH LIQUEFACTION IS PREDICTED: FOR AN EARTHQUAKE OF MAGNITUDE = 7.0 AND VARIOUS PEAK HORIZONTAL ACCELERATIONS

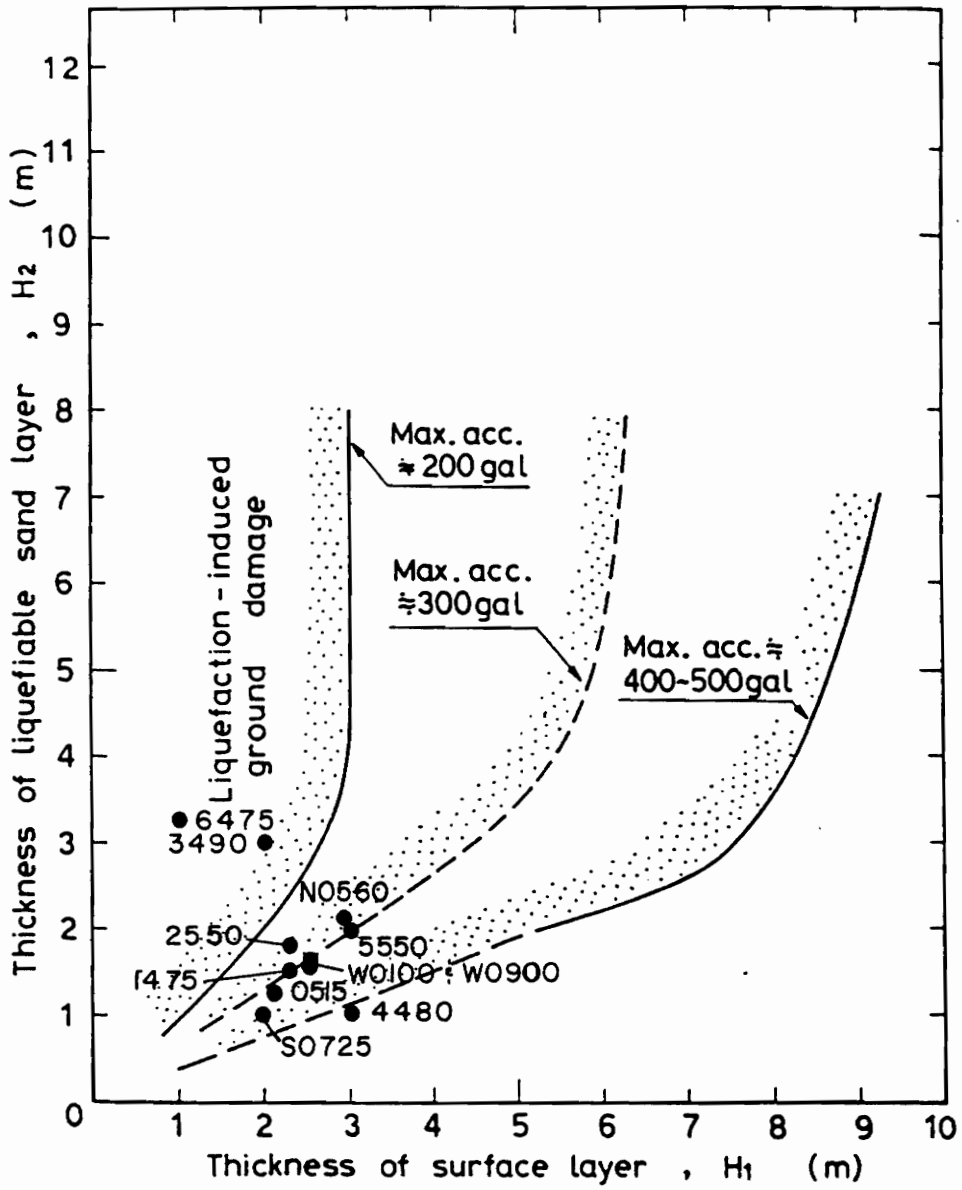

Figure 45. ESTIMATED LAYER THICKNESS RELATIONS FOR EACH HOLLYWOOD CPT STATION DURING THE 1886 EARTHQUAKE

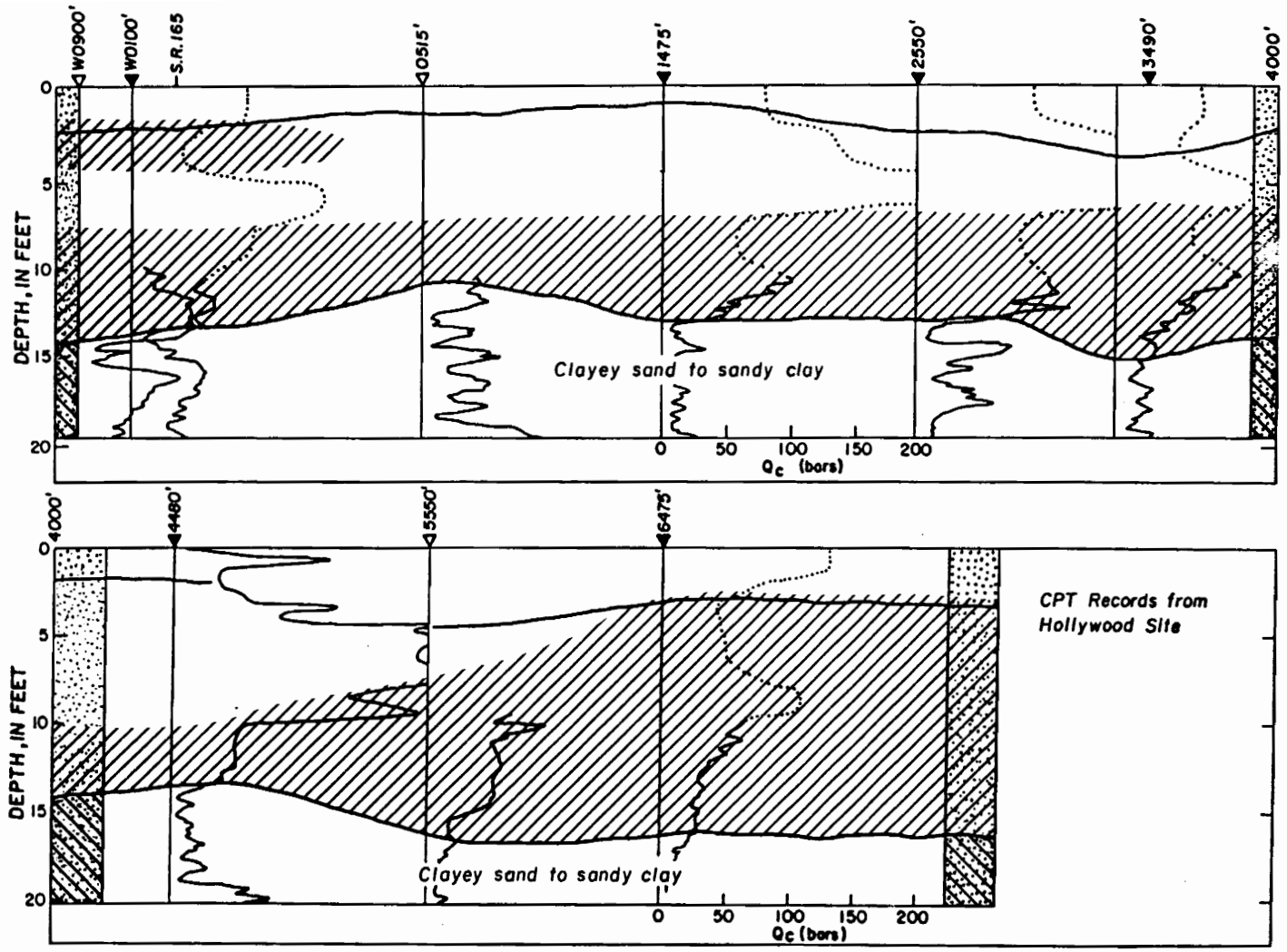

Figure 46. LOCATION OF SAND LAYERS SUSCEPTIBLE TO LIQUEFACTION UNDER SEISMIC LOADINGS ESTIMATED FOR THE 1886 EARTHQUAKE

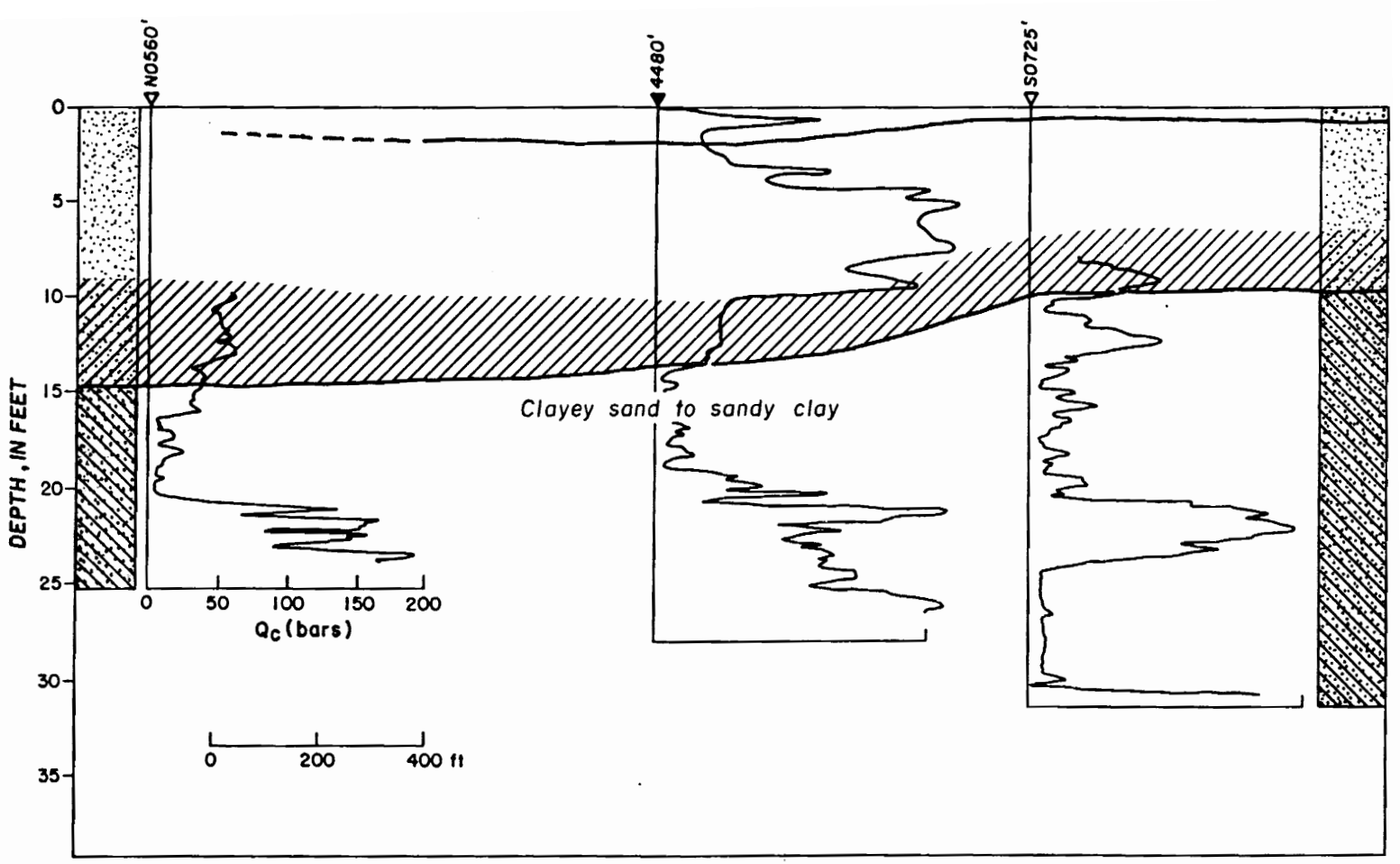

Figure 47. LOCATION OF SAND LAYERS SUSCEPTIBLE TO LIQUEFACTION UNDER SEISMIC LOADINGS ESTIMATED FOR THE 1886 EARTHQUAKE

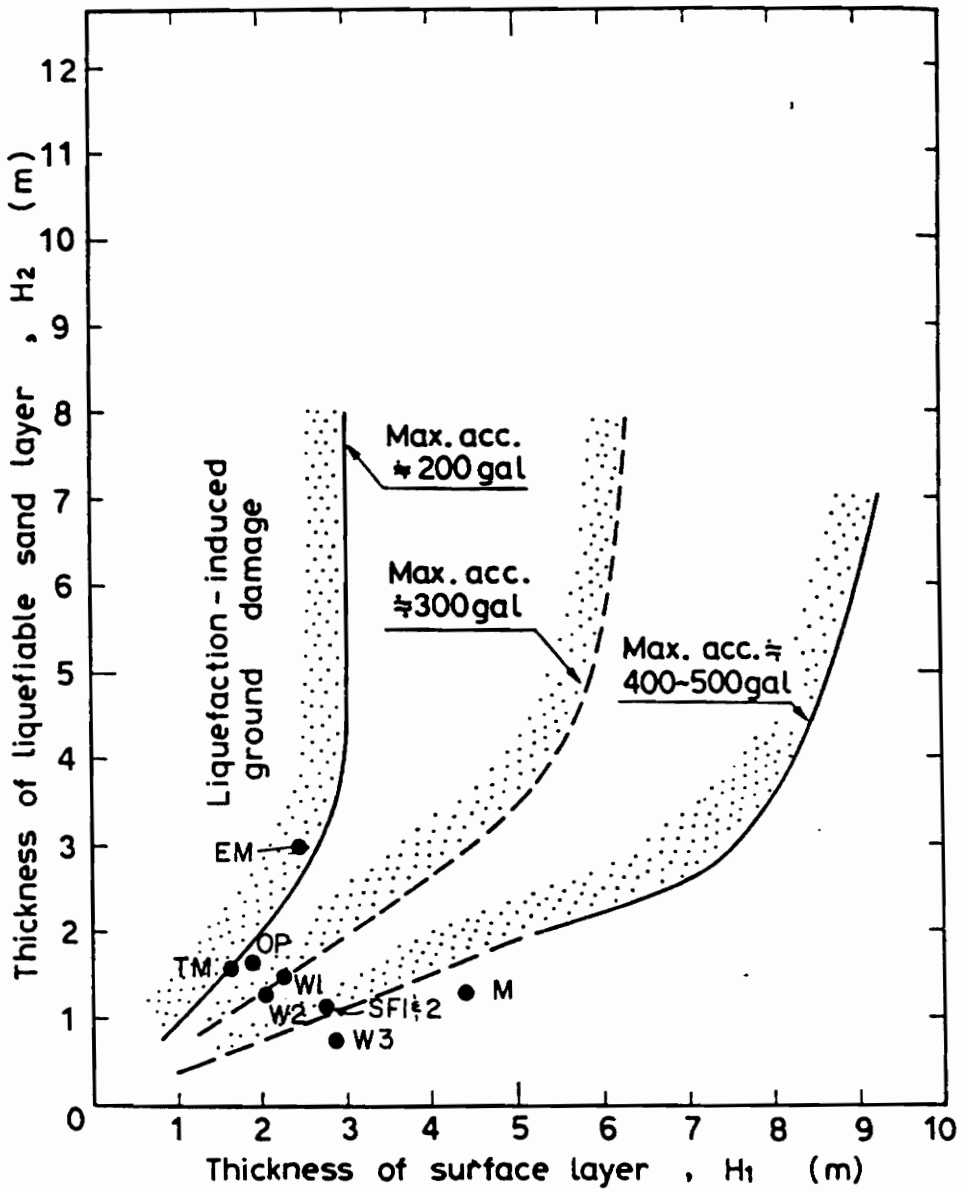

Figure 48. ESTIMATED LAYER THICKNESS RELATIONS FOR ALL SITES, EXCEPT HOLLYWOOD, DURING THE 1886 EARTHQUAKE

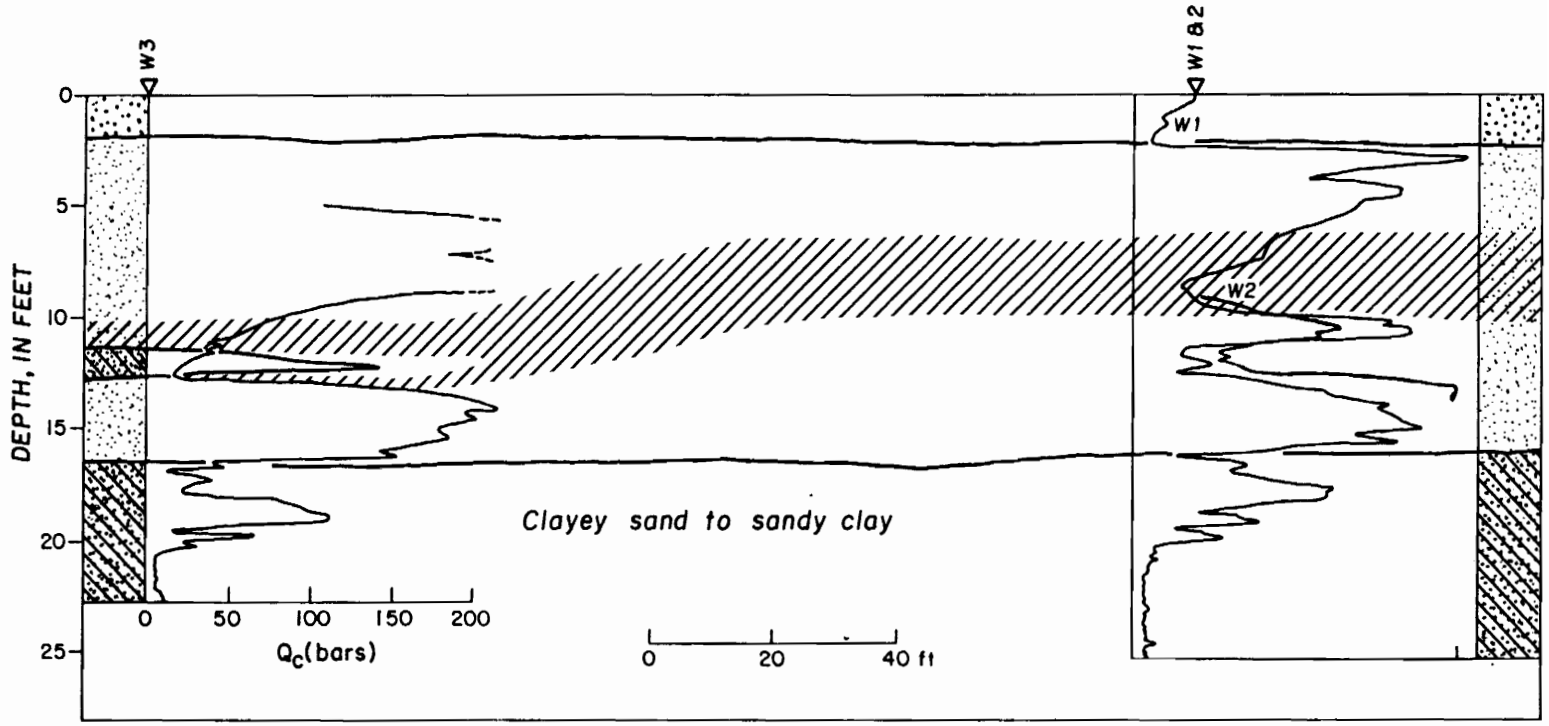

Figure 49. LOCATION OF SAND LAYERS SUSCEPTIBLE TO LIQUEFACTION UNDER SEISMIC LOADINGS ESTIMATED FOR THE 1886 EARTHQUAKE

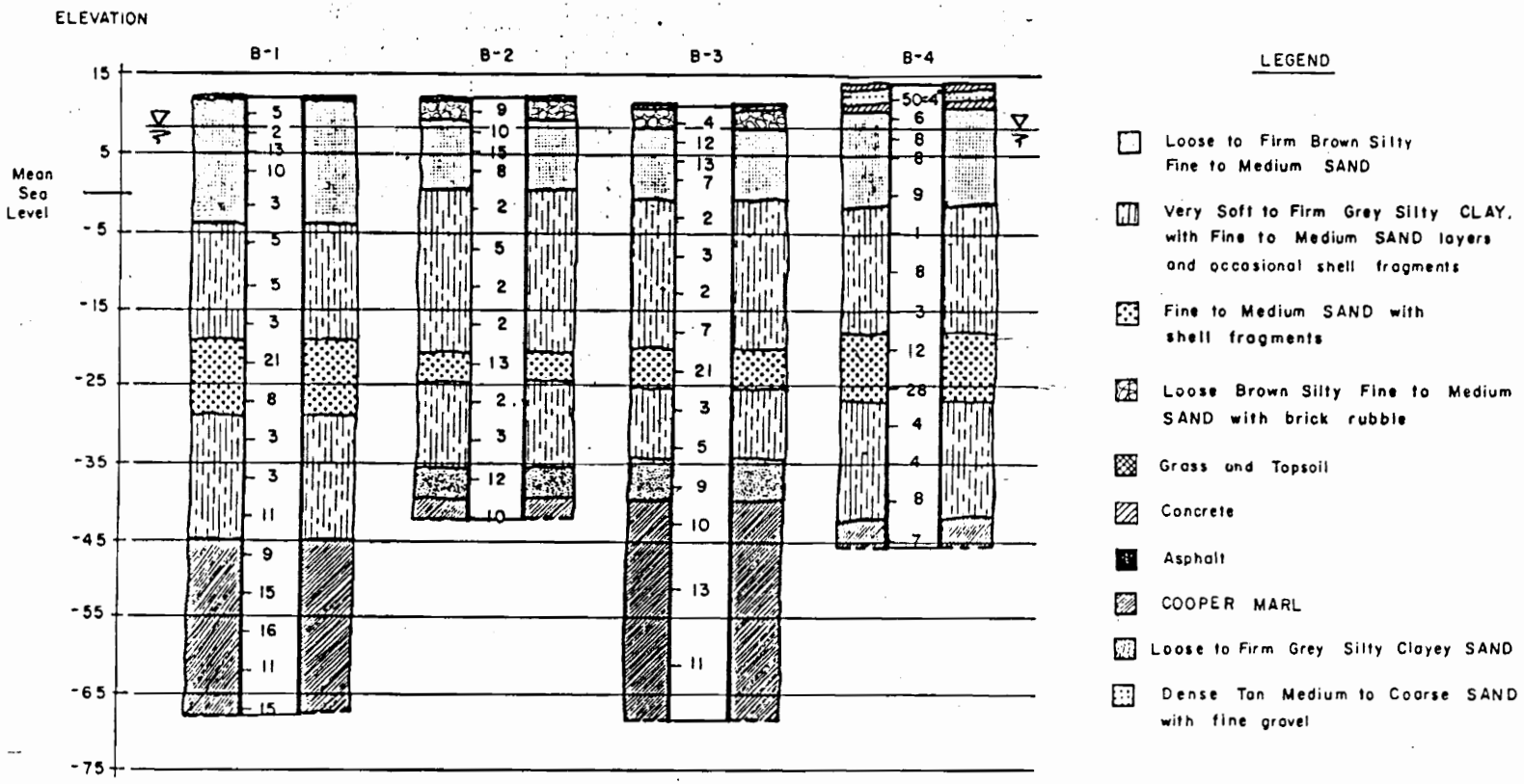

Figure 50. SPT LOGS FOR THE ST. MICHAEL'S CHURCH AREA

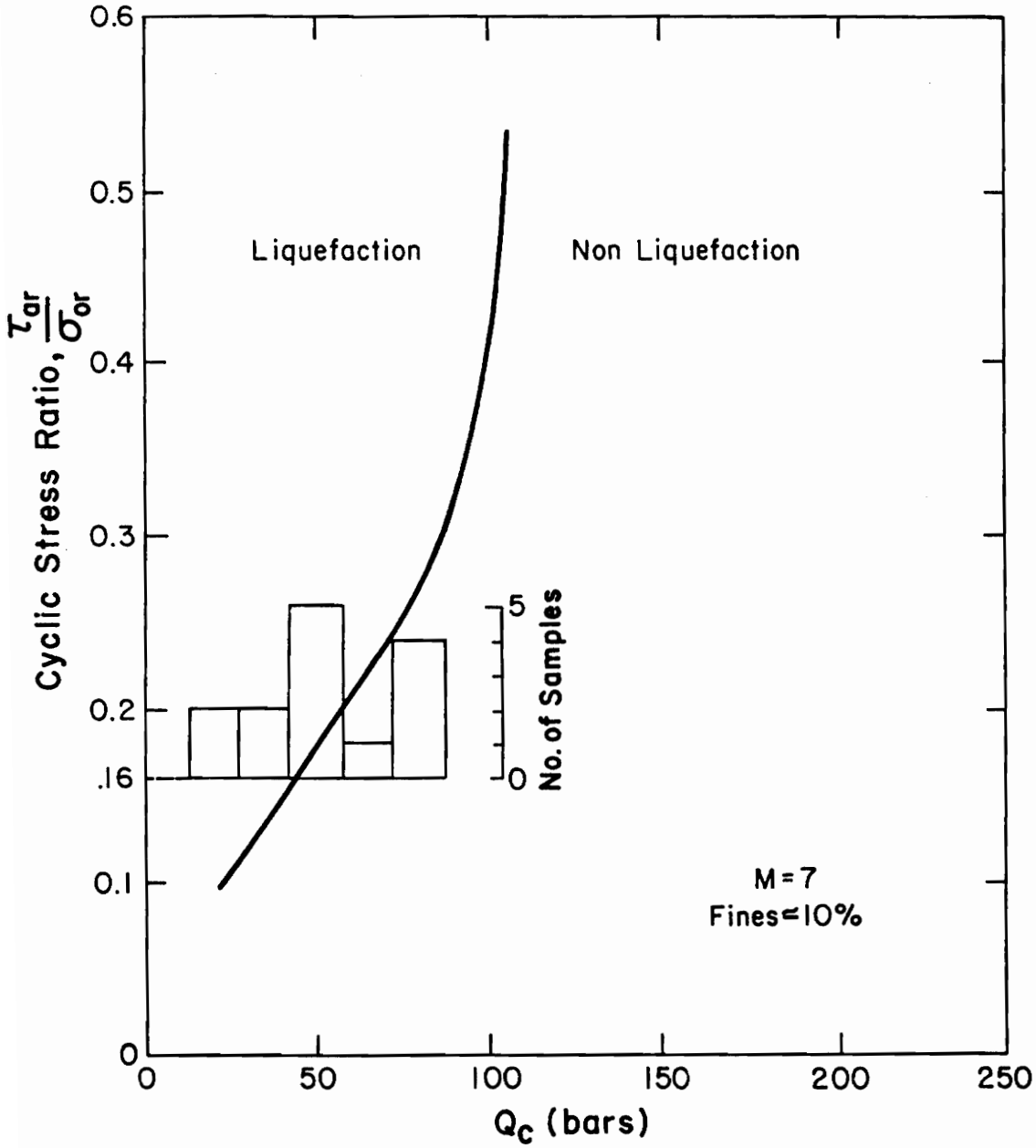

Figure 51. RELATIONSHIP BETWEEN FIELD LIQUEFACTION BEHAVIOR AND CONE PENETRATION RESISTANCE FOR THE ST. MICHAEL'S CHURCH SITE

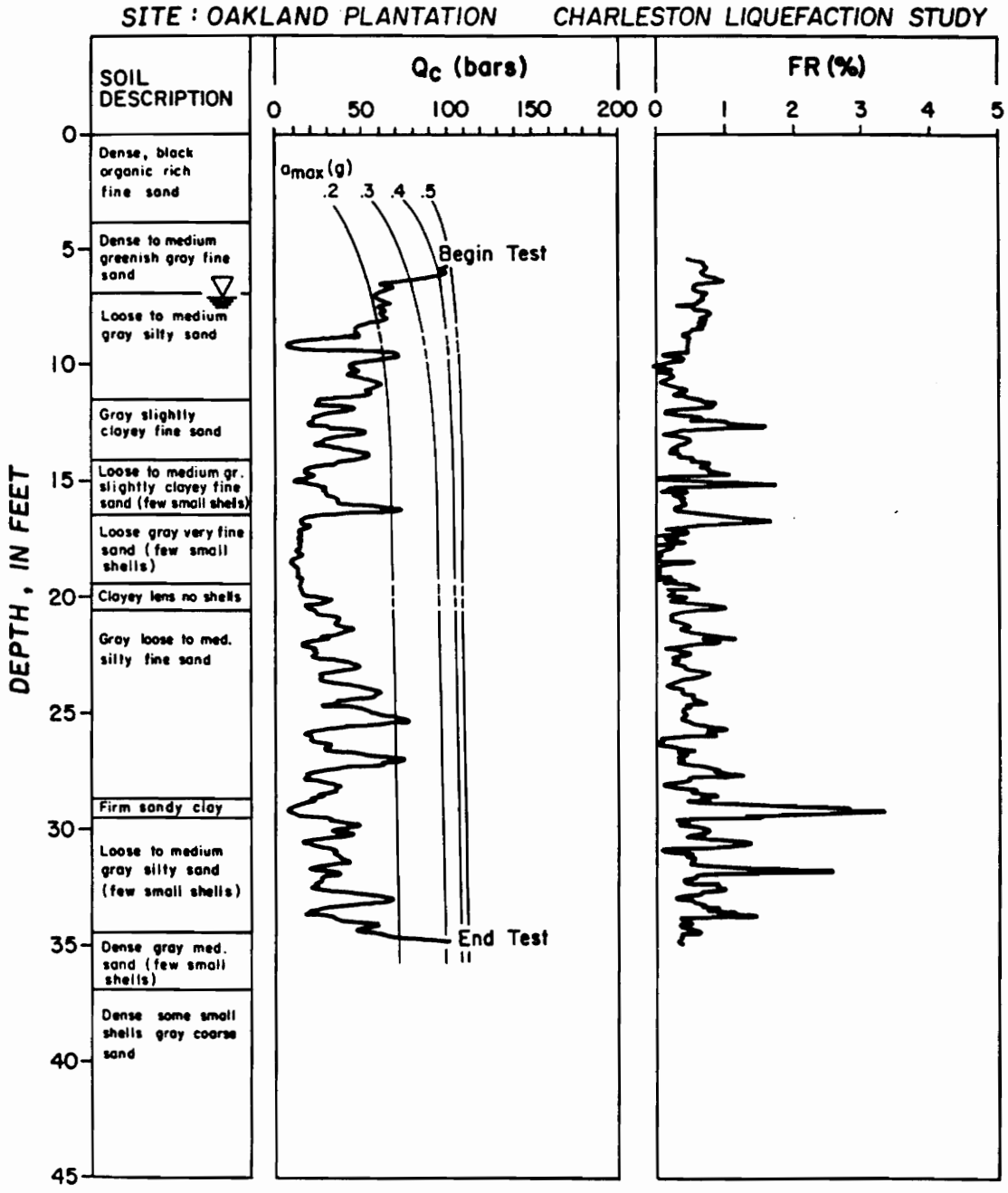

Figure 52. COMPARISON OF ACTUAL CPT RESISTANCE AT OAKLAND PLANTATION TO THOSE AT WHICH LIQUEFACTION IS PREDICTED: FOR AN EARTHQUAKE OF MAGNITUDE = 7.0 AND VARIOUS PEAK HORIZONTAL ACCELERATIONS

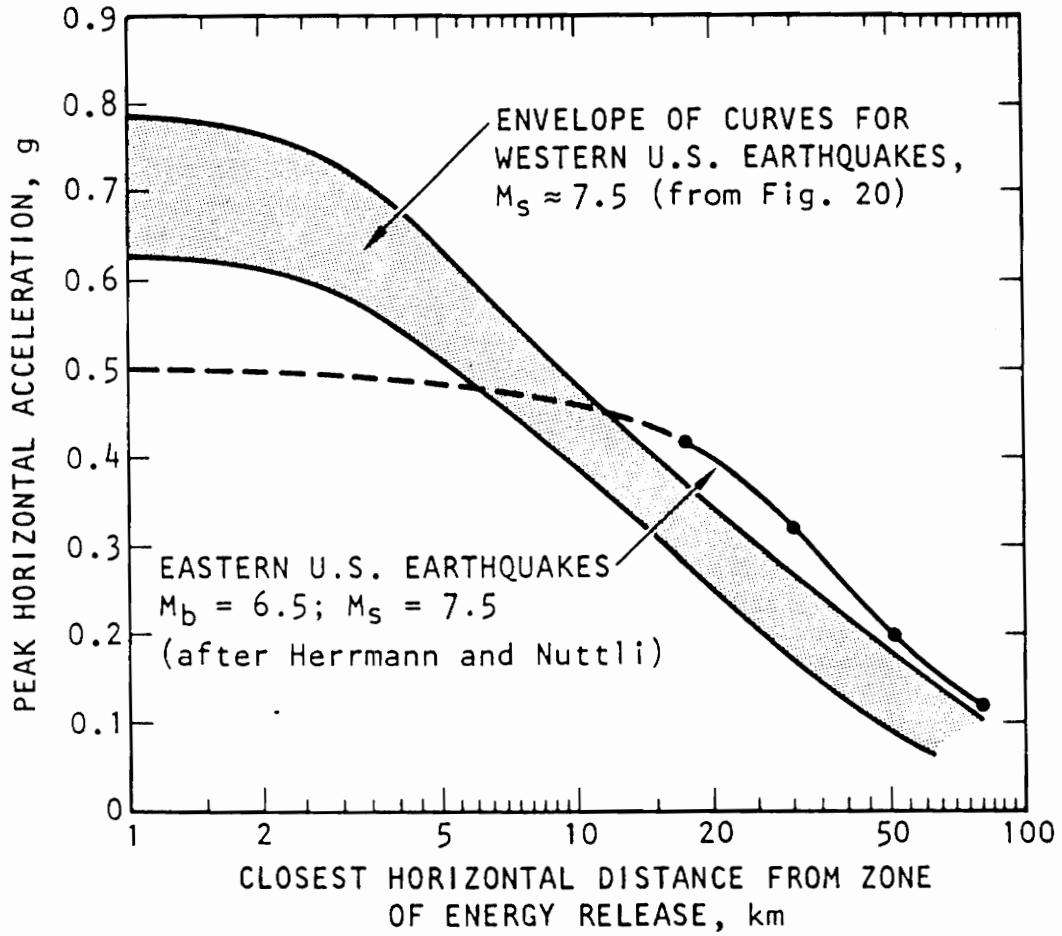

Figure 53. ATTENUATION CURVES FOR WESTERN AND EASTERN U.S. EARTHQUAKES (40)

Table 4. DETERMINATION OF EQUIVALENT CPT TIP RESISTANCE FROM SPT BLOW COUNTS

BORING	SAMPLE DEPTH (ft)	N (blows/ft)	C_N	$(N_1)_{60}$ (blows/ft)	Q_C (bars)
B1	4.0	2	1.83	3	12
	6.5	13	1.71	17	75
	9.0	10	1.60	12	54
	14.0	3	1.42	3	14
B2	4.5	10	1.80	14	61
	6.5	15	1.70	19	86
	8.0	8	1.64	10	44
B3	4.5	12	1.80	16	73
	6.5	13	1.70	17	75
	9.5	7	1.58	8	37
B4	6.5	8	1.61	10	43
	9.5	8	1.49	9	40
	14.0	9	1.35	9	41

$$C_N = \left(\frac{1.7}{0.7 + \sigma'_{ov}}\right)$$

σ'_{ov} ; Effective overburden pressure in TSF.

$\gamma_T \simeq 115 \text{lb/ft.}^3$

$$(N_1)_{60} = N \bullet C_N \bullet \frac{ER_m}{60}$$

$$= 0.75\, C_N \bullet N$$

C_N ; Normalizing factor.

$\frac{ER_m}{60}$; Energy ratio for donut type SPT hammers.

$$Q_c = 4.5 \bullet (N_1)_{60}$$

4.5 ; Approximate conversion factor dependent on mean grain size of material (34).

Table 5. GEOLOGIC EVIDENCE FOR LIQUEFACTION NEAR THE HOLLYWOOD CPT STATIONS

	CAUSITIVE SEISMIC EVENT:				
	Possibly Attributed to 1886 Earthquake	Probably Induced by 1886 Event	Size	Earthquake Prior to 1886	Size
W0900	0	0	-	3	l-h
W0100	0	0	-	3	m-l
0515	3	1	s	7	m-h
1475	0	3	s-m	8	m-h
2550	3	1	s-l	9	m-l
3490	1	2	s	7	m-l
4480	0	0	-	9	s-l
5550	0	0	-	3	m-l
6475	0	0	-	6	m-h

Sandblow Crater Diameter

s	0- 3 ft
m	3- 6 ft
l	6-10 ft
h	> 10 ft

Chapter VII

Summary and Conclusions

Recent research in the Charleston , S.C. area has led to the discovery of important sites which exhibit relic liquefaction features from the 1886 earthquake and other seismic events much older than the 1886 event. This information has revealed significant insights into the seismic history of the Charleston region. The studies to date have focused on the geologic aspects of Charleston seismicity, and little opportunity has existed to perform engineering based investigations of the liquefaction sites. This study represents the first phase of an effort to obtain engineeering parameters at the sites, and to draw conclusions from this data regarding the liquefaction phenomena themselves, and the levels of causative seismic shaking.

The primary field study method in this investigation is a cone penetration system which utilized a specially adapted light drill rig to perform tests with a unique small-scale electric cone. This system was used at seven sites to conduct 24 Cone Penetration Tests. With each CPT, an auger boring was make to allow for visual and sieve classifications of the soils. In addition to these tests, six Standard Penetration Tests were performed at one particularly well documented site. The SPT's gave yet another means to independently check the CPT data. As a means of supplementing the

field exploration, boring logs from previous geotechnical investigations in Charleston are also being collected and integrated with the information obtained during this investigation.

Field sites were chosen to represent cases with different degrees of liquefaction phenomenon and different positions relative to the inferred zone of energy release of the 1886 event. Standard penetration test data was used for an additional site in the city of Charleston and also supplemented CPT's at the Hollywood site. The Hollywood site warrented expanded test coverage for the following reasons; the drainage ditch affords extensive exposure of numerous, relic liquefaction features formed during several episodes of seismic shaking, the geologic setting around the ditch contributes to conditions favorable for the formation of sand boils, the limited extent of liquefaction and present day properties of the near surface sands indicate that no significant density changes occurred due to the 1886 earthquake, and numerous geologic investigations have been conducted at the site to determine the nature of liquefaction which has been experienced in the sandy soils. The penetration resistances were used in conjunction with historical observations and geologic evidence for the occurrence of liquefaction to estimate levels of the near-surface accelerations induced by the 1886 earthquake.

Field tests conducted with the mini-cone penetrometer during both preliminary work near Virginia Tech and at site evaluations in the Charleston area concluded that the cone gives reproducible data that compares favorably to empirical correlations with the SPT and plots well within boundaries for individual soils on simplified classification charts constructed for standard sized cones. The compositional uniformity of the silty to fine sands and constant depth to the ground water table in the Charleston area reduced two test variables and made the study sites optimal for assessing the effects that relative density variations have on the surficial manifestion of liquefaction. It appears that the engineering characteristics of the sands from test sites are very similar in their properties and cyclic loading response. Sand layers susceptible to liquefaction under cyclic loading inferred to be similar for the meizoseismal zone of the 1886 earthquake ($M = 7$, $a_{max} \simeq 0.3g$) were discovered at every site. At least three episodes of liquefaction demonstrated by relic sand vents and sandblows at the Hollywood site indicate that: 1. sediments as old as late Pleistocene age can be susceptible to liquefaction, and 2. sandy layers can remain reliquefiable after several occurrences

of liquefaction. Penetration data at several 1886 liquefaction sites support these findings and appear to show that the progressive compaction of liquefied sediments is minimal unless the sands are in proximity to large sandblows or vents. In areas close to liquefaction features the extensive relief of excess pore pressure and venting of soil-laden water results in densification of the liquefied layers. Of importance for the evaluation for critical structures in the Charleston region is that even after liquefaction in 1886 soil conditions at most of the sites in this investigation remain susceptible to liquefaction.

With the fairly uniform ground water table observed to occur naturally at 2 to 3 feet in the Charleston area, the CPT records demonstrate that the distribution and extent of liquefiable soil layers are primarily responsible for the observed nature of the liquefaction features. Ground failures and structural damage would be more widespread where extensive layers of liquefiable material are overlain by thin resistant layers. Small vents can be assumed where either thin liquefiable layers at shallow depths are overlain by thin resistant material or where thicker, liquefiable layers at depth hydraulically fracture the overburden through small conduits i.e. fissures, root or animal holes. Large sandblows or craterlets are favored when an extensive layer of loose sand is capped by a thick layer of semi-brittle dense noncohesive or soft slightly cohesive material. Use of the Seed field performance charts combined with estimates for the effect that a layered system of soils can have on the surface venting of liquefied material appears to be a viable method for the back analysis of ground motions induced by seismic events.

Near surface, peak horizontal accelerations have been estimated for the 1886 earthquake by compiling data from historical reports, geologic investigations, and results of in-situ geotechnical tests performed during this study on areas which exhibited various levels of liquefaction. Based on this data for sites located in the meizoseismal zone at distances of between 3.5 and 6.5 miles from the inferred linear zone of energy release, an estimate of 0.3g has been made for the area of maximum intensity. That such a low acceleration cold liquefy the soil reflects the fact that the densities of the soils are very low. Preliminary results for two sites, one in Charleston and one northeast of Charleston, located at distances of 13 and 19 miles from this zone indicate that a peak horizontal acceleration of approximately 0.2g was experienced near, yet outside the meizoseismal zone. These

estimates are lower than range of postulated in recent seismologic studies. At the present the reasons for the differences in shaking levels obtained by the different investigations are not clear. This issue will by studied further in subsequent extentions of this investigation.

Appendix A

Individual CPT Records for the Hollywood and Warren Sites

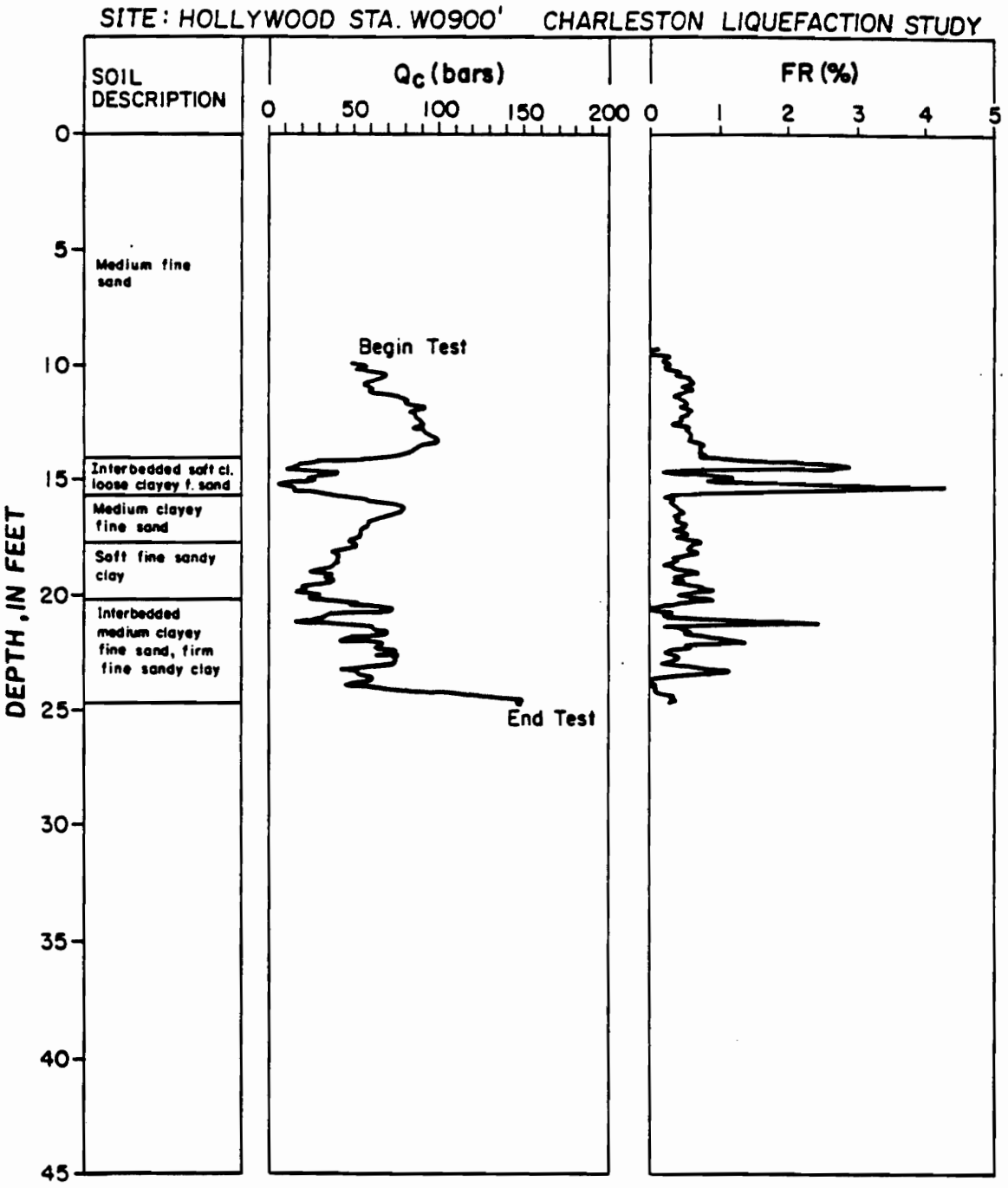
SITE: HOLLYWOOD STA. W0900' CHARLESTON LIQUEFACTION STUDY
SOIL DESCRIPTION
Qc (bars)
0 50 100 150 200
FR (%)
0 1 2 3 4 5
DEPTH, IN FEET
0
5
10
15
20
25
30
35
40
45
Medium fine sand
Interbedded soft cl. loose clayey f. sand
Medium clayey fine sand
Soft fine sandy clay
Interbedded medium clayey fine sand, firm fine sandy clay
Begin Test
End Test

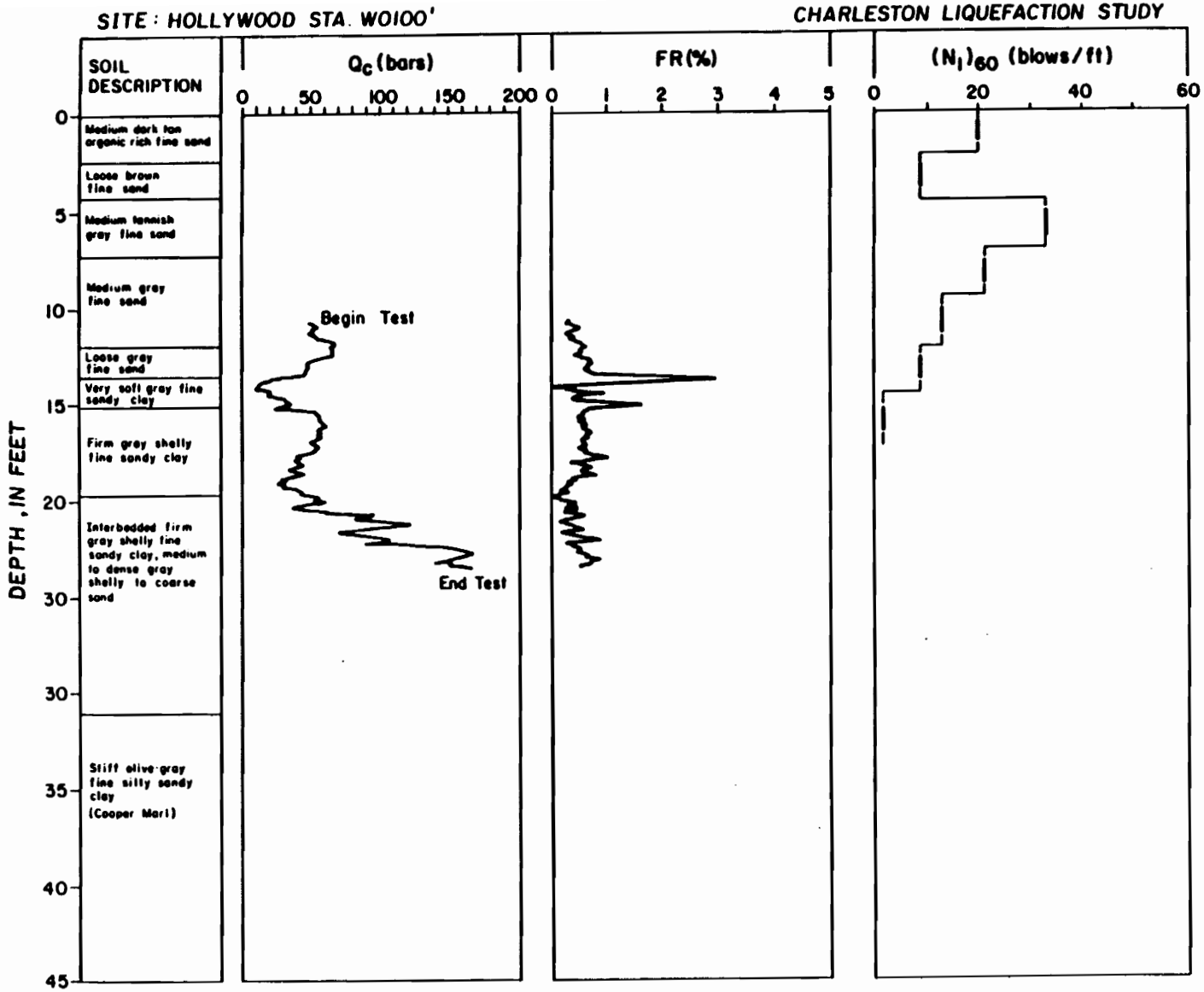
SITE : HOLLYWOOD STA. WOIOO'
CHARLESTON LIQUEFACTION STUDY
SOIL DESCRIPTION
Medium dark tan organic rich fine sand
Loose brown fine sand
Medium tannish gray fine sand
Medium gray fine sand
Loose gray fine sand
Very soft gray fine sandy clay
Firm gray shelly fine sandy clay
Interbedded firm gray shelly fine sandy clay, medium to dense gray shelly to coarse sand
Stiff olive-gray fine silty sandy clay (Cooper Marl)
DEPTH , IN FEET
0
5
10
15
20
30
35
40
45
Q_c (bars)
0 50 100 150 200
Begin Test
End Test
FR(%)
0 1 2 3 4 5
$(N_1)_{60}$ (blows/ft)
0 20 40 60

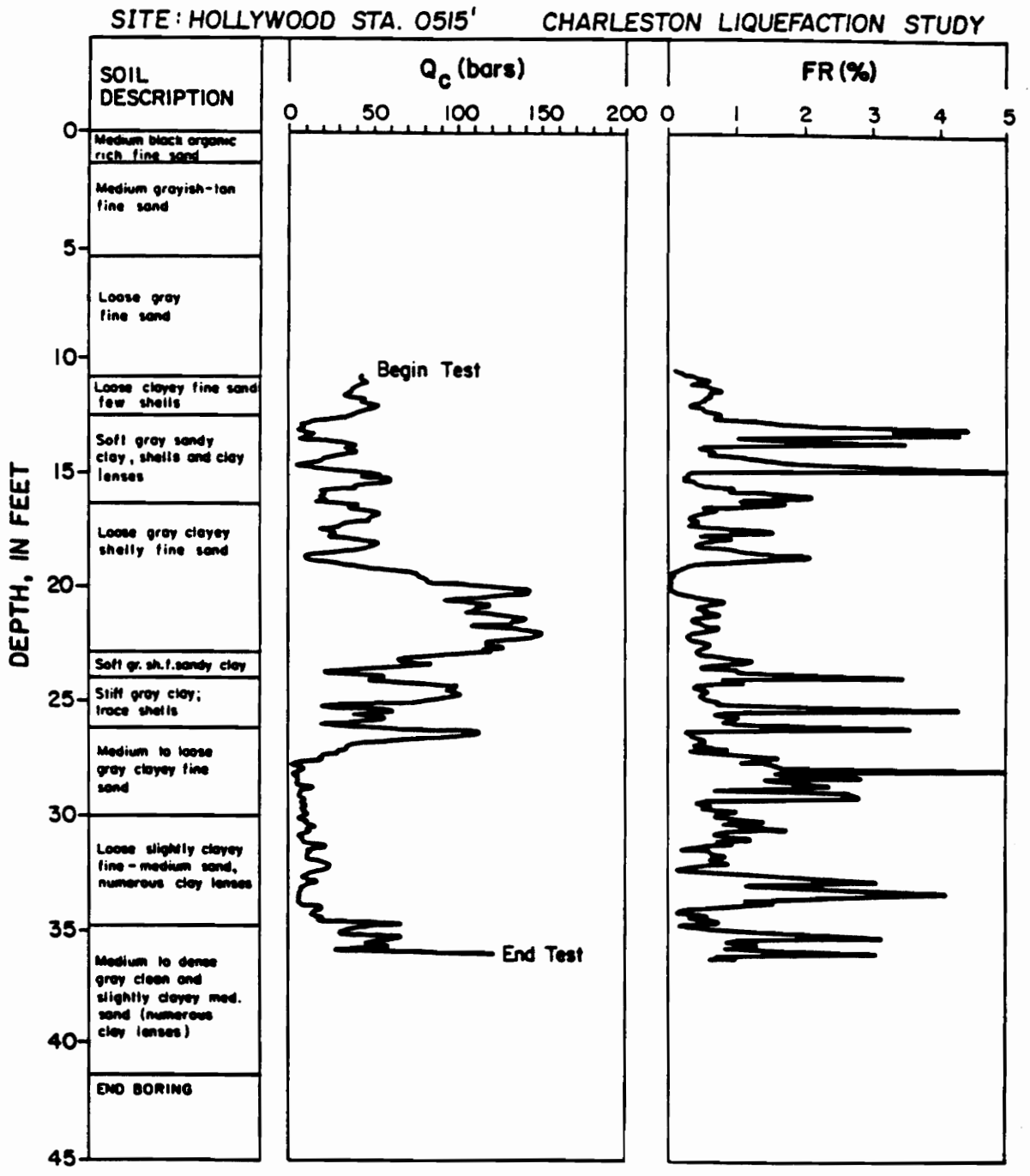
SITE: HOLLYWOOD STA. 0515'
CHARLESTON LIQUEFACTION STUDY
SOIL DESCRIPTION
Medium black organic rich fine sand
Medium grayish-tan fine sand
Loose gray fine sand
Loose clayey fine sand few shells
Soft gray sandy clay, shells and clay lenses
Loose gray clayey shelly fine sand
Soft gr. sh. f. sandy clay
Stiff gray clay; trace shells
Medium to loose gray clayey fine sand
Loose slightly clayey fine - medium sand, numerous clay lenses
Medium to dense gray clean and slightly clayey med. sand (numerous clay lenses)
END BORING
DEPTH, IN FEET
0
5
10
15
20
25
30
35
40
45
Q_c (bars)
0 50 100 150 200
FR (%)
0 1 2 3 4 5
Begin Test
End Test

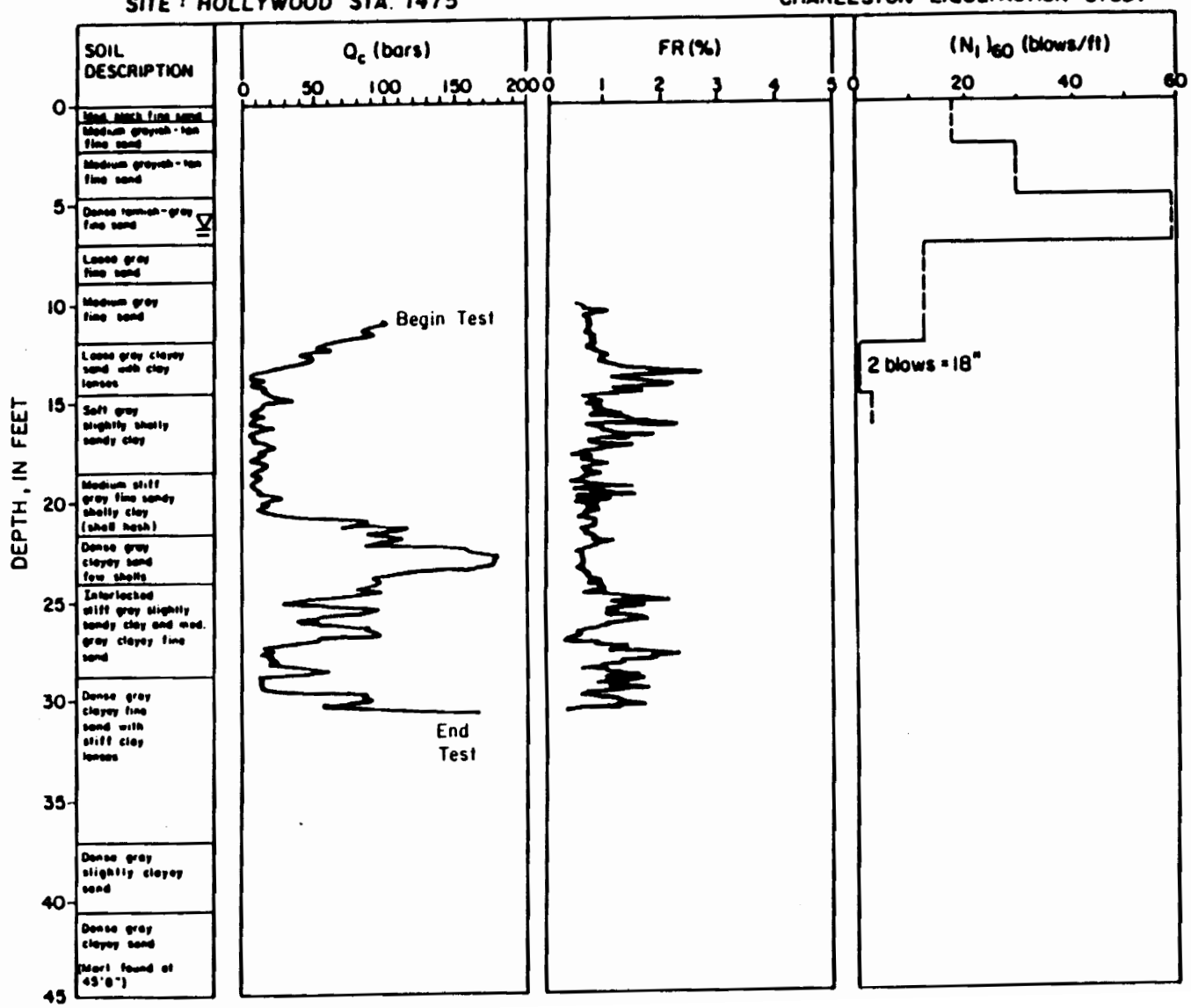
SITE : HOLLYWOOD STA. 1475'
CHARLESTON LIQUEFACTION STUDY
SOIL DESCRIPTION
Q_c (bars)
0 50 100 150 200
FR (%)
0 1 2 3 4 5
$(N_1)_{60}$ (blows/ft)
0 20 40 60
DEPTH, IN FEET
0
5
10
15
20
25
30
35
40
45
Med. black fine sand
Medium grayish - tan fine sand
Medium grayish - tan fine sand
Dense tannish - gray fine sand
Loose gray fine sand
Medium gray fine sand
Loose gray clayey sand with clay lenses
Soft gray slightly shelly sandy clay
Medium stiff gray fine sandy shelly clay (shell hash)
Dense gray clayey sand few shells
Interlocked stiff gray slightly sandy clay and med. gray clayey fine sand
Dense gray clayey fine sand with stiff clay lenses
Dense gray slightly clayey sand
Dense gray clayey sand
[Marl found at 45'0"]
Begin Test
End Test
2 blows = 18"

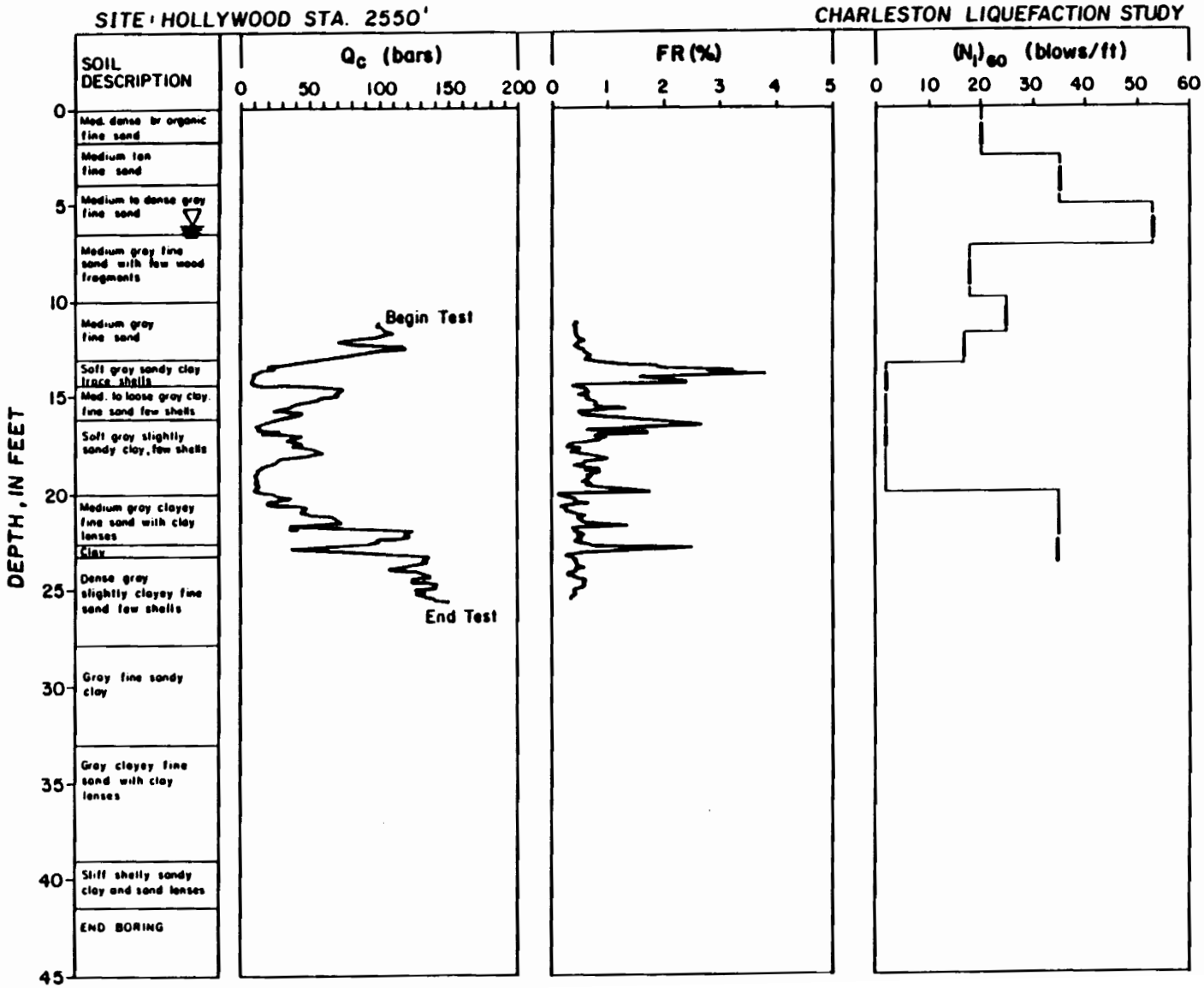
SITE: HOLLYWOOD STA. 2550'
CHARLESTON LIQUEFACTION STUDY
SOIL DESCRIPTION
Qc (bars)
FR (%)
(N1)60 (blows/ft)
DEPTH, IN FEET
Med. dense to organic fine sand
Medium tan fine sand
Medium to dense gray fine sand
Medium gray fine sand with few wood fragments
Medium gray fine sand
Soft gray sandy clay trace shells
Med. to loose gray clay, fine sand few shells
Soft gray slightly sandy clay, few shells
Medium gray clayey fine sand with clay lenses
Clay
Dense gray slightly clayey fine sand few shells
Gray fine sandy clay
Gray clayey fine sand with clay lenses
Stiff shelly sandy clay and sand lenses
END BORING
Begin Test
End Test

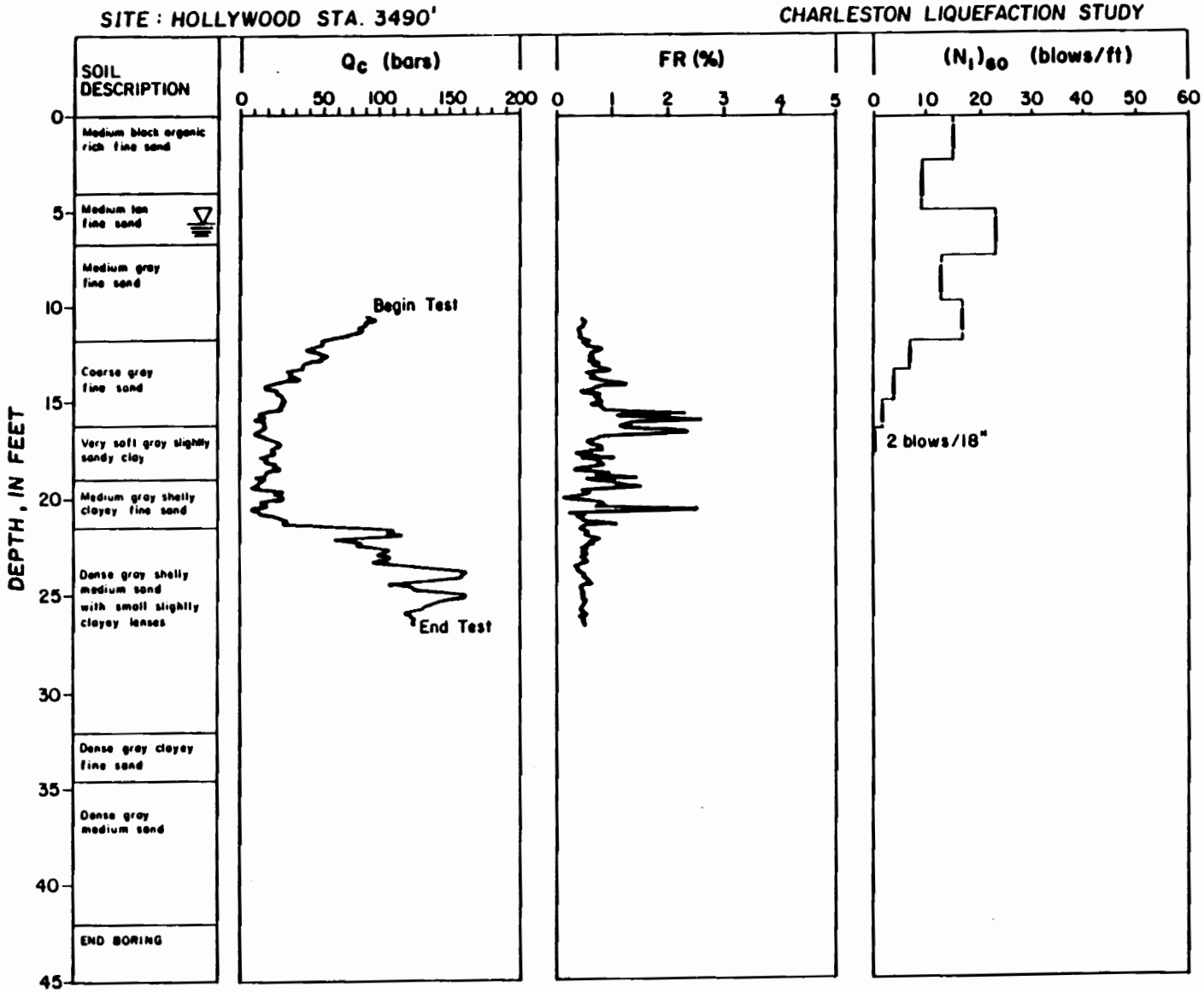
SITE : HOLLYWOOD STA. 3490'
CHARLESTON LIQUEFACTION STUDY
SOIL DESCRIPTION
Medium black organic rich fine sand
Medium tan fine sand
Medium gray fine sand
Coarse gray fine sand
Very soft gray slightly sandy clay
Medium gray shelly clayey fine sand
Dense gray shelly medium sand with small slightly clayey lenses
Dense gray clayey fine sand
Dense gray medium sand
END BORING
DEPTH, IN FEET
0
5
10
15
20
25
30
35
40
45
Q_c (bars)
0 50 100 150 200
Begin Test
End Test
FR (%)
0 2 3 4 5
$(N_1)_{60}$ (blows/ft)
0 10 20 30 40 50 60
2 blows/18"

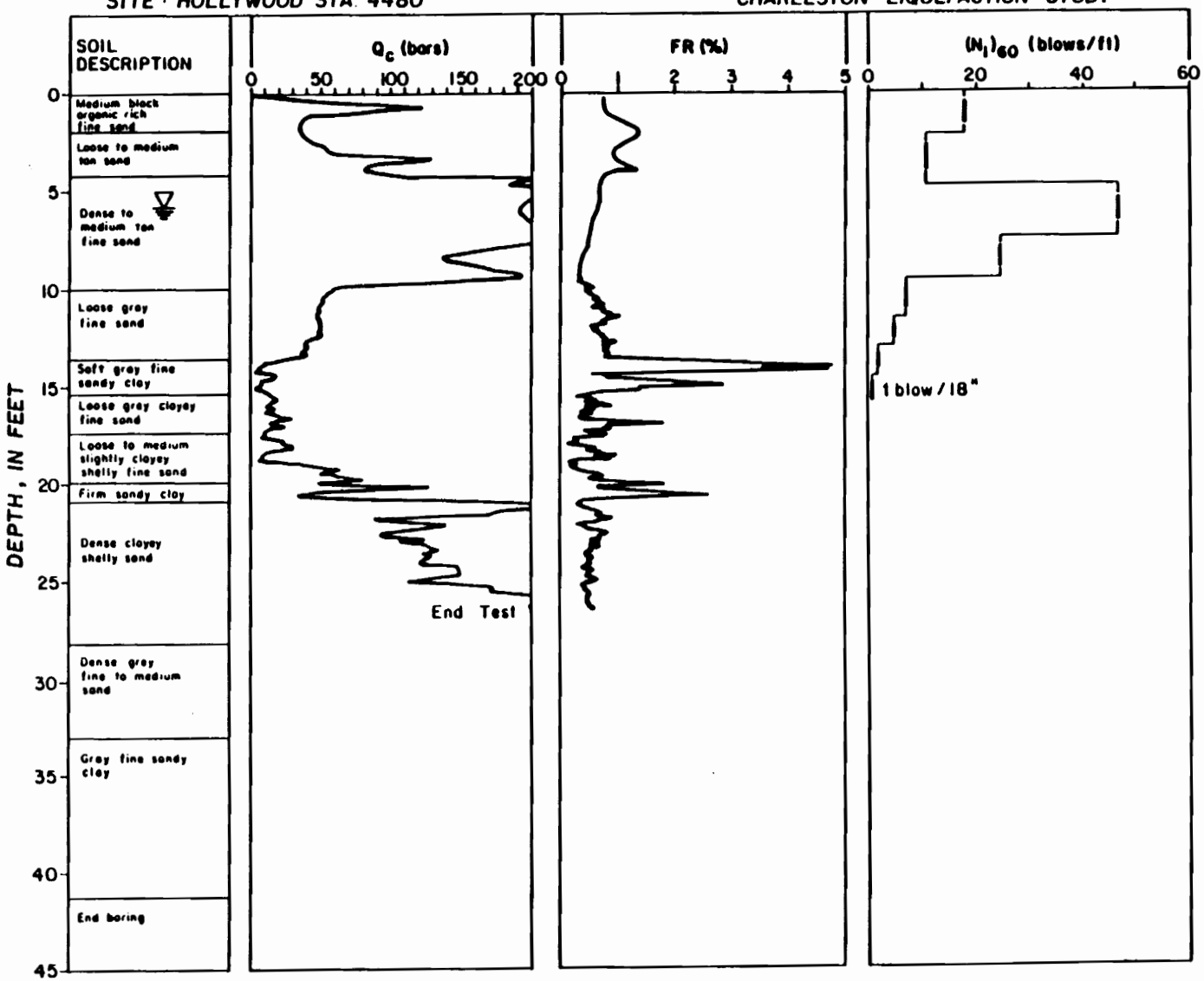
SITE : HOLLYWOOD STA. 4480'
CHARLESTON LIQUEFACTION STUDY
SOIL DESCRIPTION
Medium black organic rich fine sand
Loose to medium tan sand
Dense to medium tan fine sand
Loose gray fine sand
Soft gray fine sandy clay
Loose gray clayey fine sand
Loose to medium slightly clayey shelly fine sand
Firm sandy clay
Dense clayey shelly sand
Dense gray fine to medium sand
Gray fine sandy clay
End boring
DEPTH, IN FEET
0
5
10
15
20
25
30
35
40
45
Q_c (bars)
0 50 100 150 200
End Test
FR (%)
0 2 3 4 5
$(N_1)_{60}$ (blows/ft)
0 20 40 60
1 blow / 18"

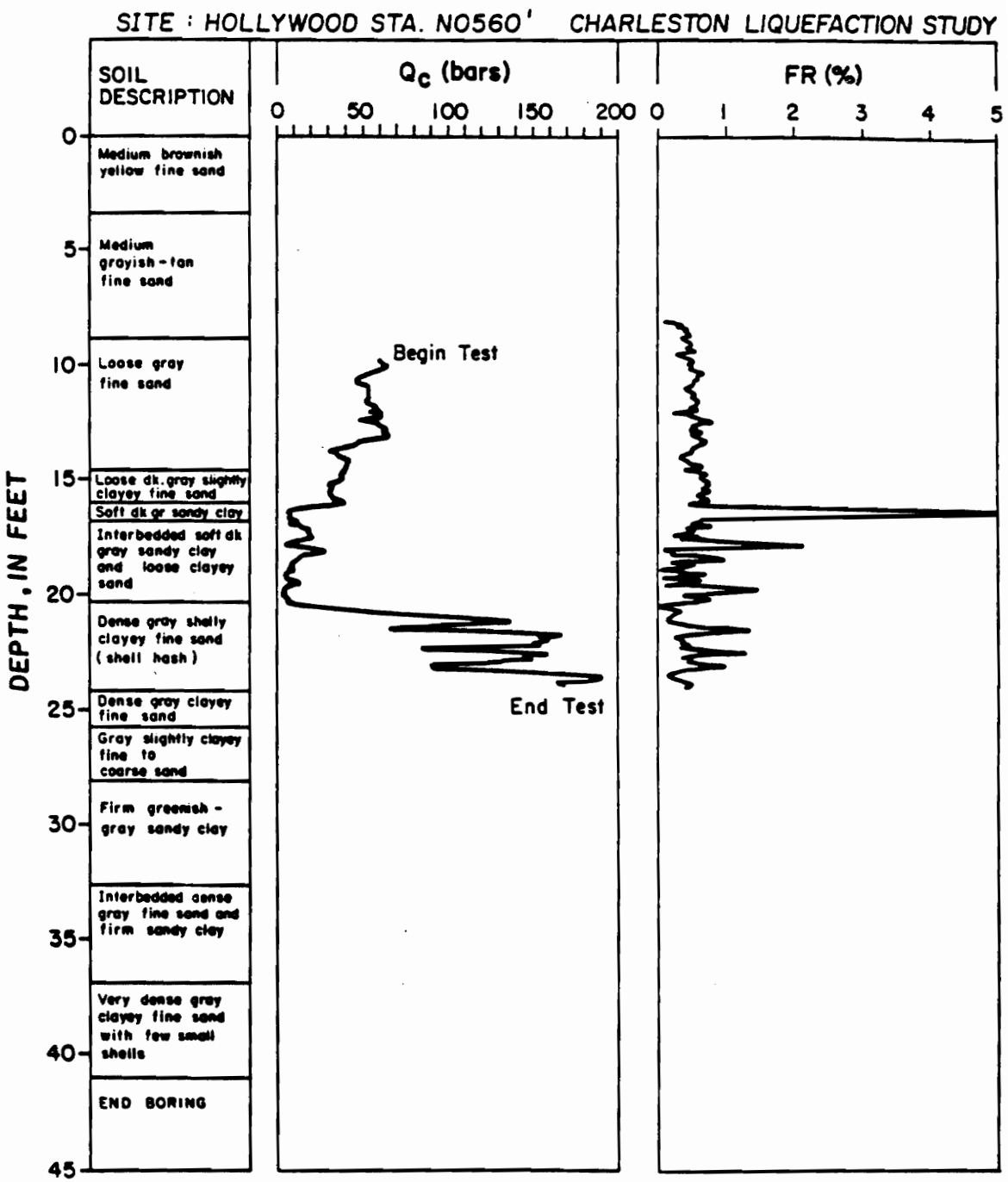
SITE : HOLLYWOOD STA. NO560' CHARLESTON LIQUEFACTION STUDY
SOIL DESCRIPTION
Medium brownish yellow fine sand
Medium grayish-tan fine sand
Loose gray fine sand
Loose dk. gray slightly clayey fine sand
Soft dk gr sandy clay
Interbedded soft dk gray sandy clay and loose clayey sand
Dense gray shelly clayey fine sand (shell hash)
Dense gray clayey fine sand
Gray slightly clayey fine to coarse sand
Firm greenish-gray sandy clay
Interbedded dense gray fine sand and firm sandy clay
Very dense gray clayey fine sand with few small shells
END BORING
DEPTH, IN FEET
0
5
10
15
20
25
30
35
40
45
Q_c (bars)
0 50 100 150 200
FR (%)
0 1 2 3 4 5
Begin Test
End Test

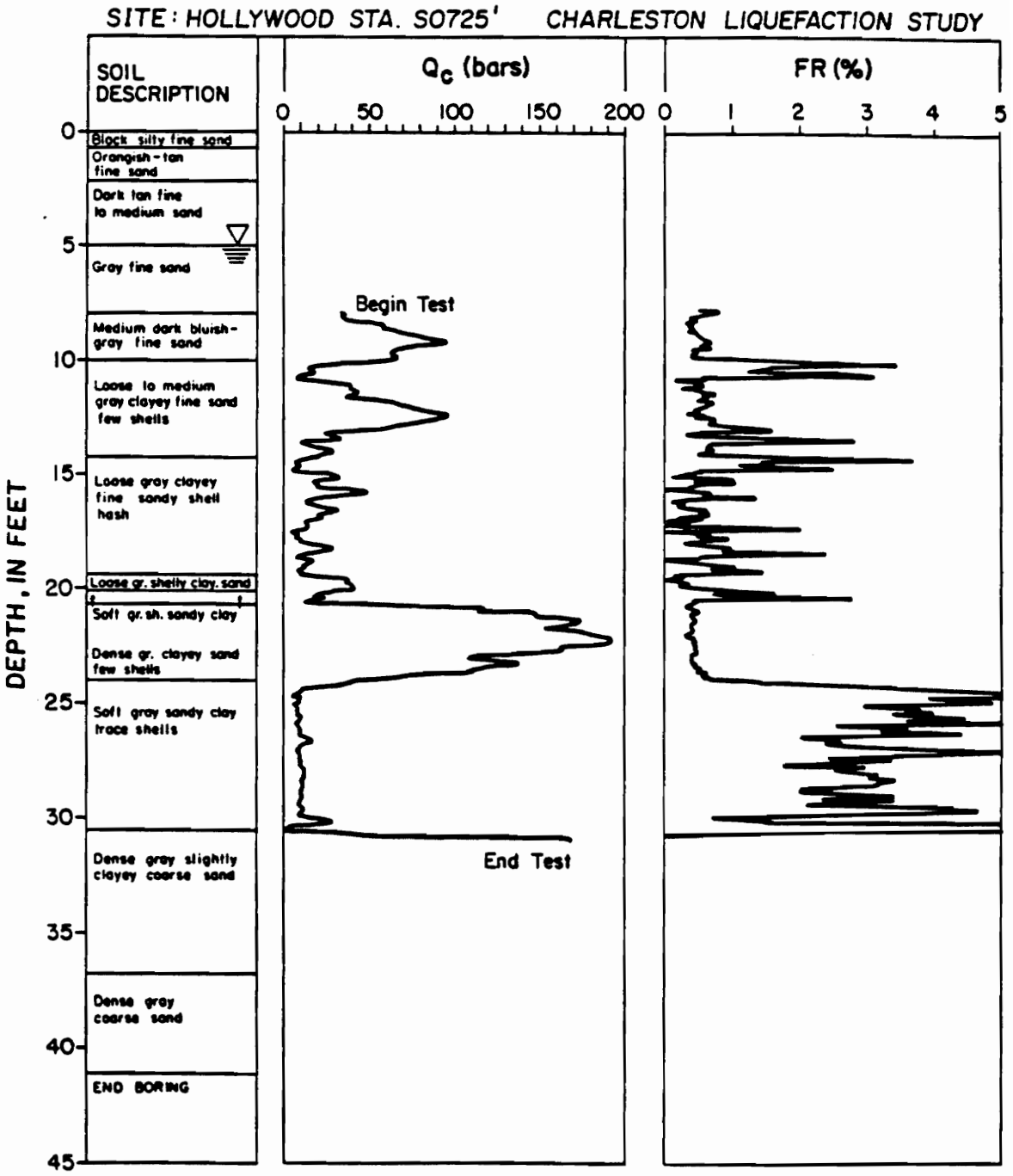
SITE: HOLLYWOOD STA. S0725'
CHARLESTON LIQUEFACTION STUDY
SOIL DESCRIPTION
Qc (bars)
FR (%)
0
50
100
150
200
0
1
2
3
4
5
Black silty fine sand
Orangish-tan fine sand
Dark tan fine to medium sand
Gray fine sand
Medium dark bluish-gray fine sand
Loose to medium gray clayey fine sand few shells
Loose gray clayey fine sandy shell hash
Loose gr. shelly clay. sand
Soft gr. sh. sandy clay
Dense gr. clayey sand few shells
Soft gray sandy clay trace shells
Dense gray slightly clayey coarse sand
Dense gray coarse sand
END BORING
Begin Test
End Test
DEPTH, IN FEET
0
5
10
15
20
25
30
35
40
45

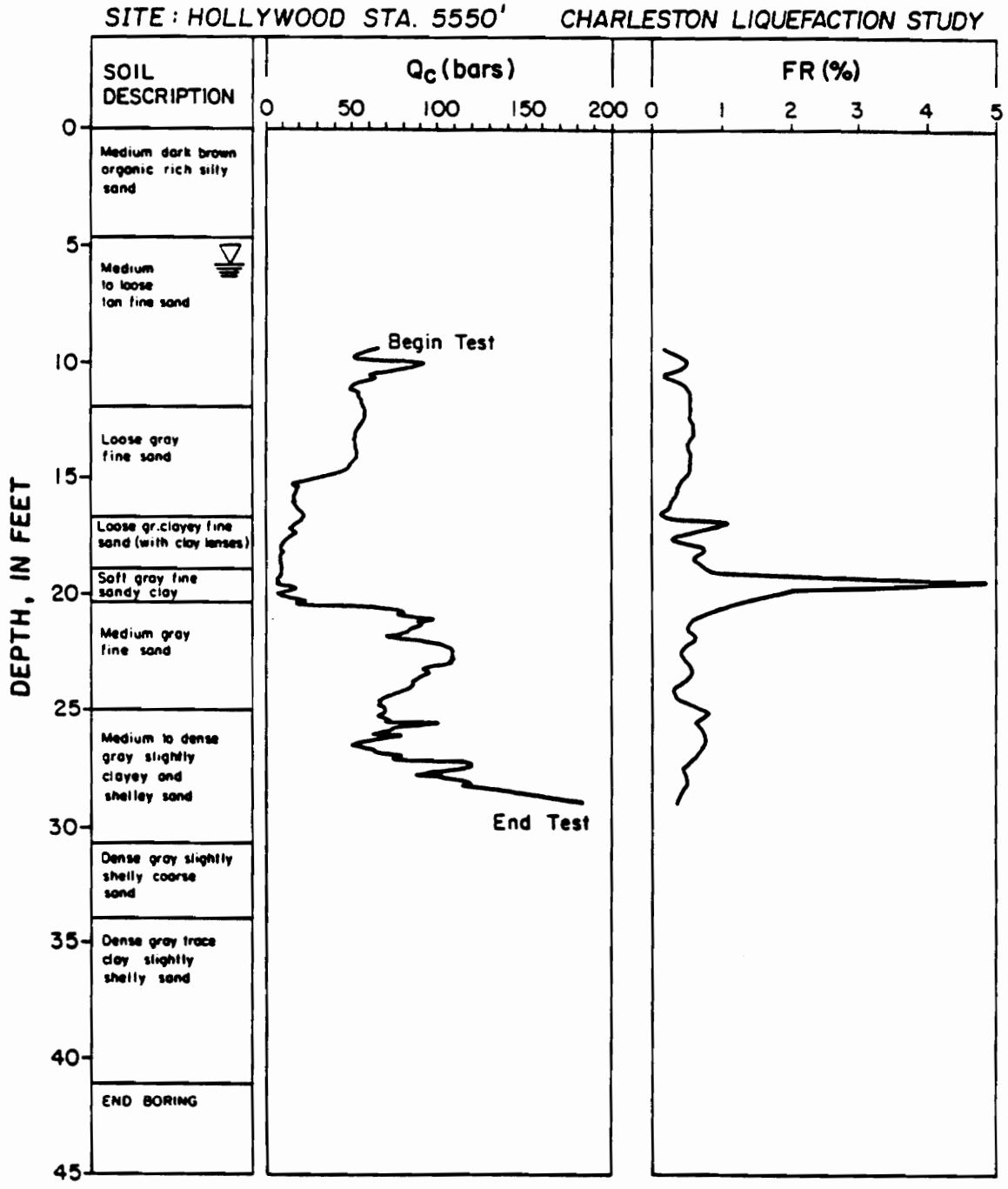
SITE : HOLLYWOOD STA. 5550'
CHARLESTON LIQUEFACTION STUDY
SOIL DESCRIPTION
Qc (bars)
FR (%)
0
50
100
150
200
0
1
2
3
4
5
Medium dark brown organic rich silty sand
Medium to loose tan fine sand
Loose gray fine sand
Loose gr.clayey fine sand (with clay lenses)
Soft gray fine sandy clay
Medium gray fine sand
Medium to dense gray slightly clayey and shelley sand
Dense gray slightly shelly coarse sand
Dense gray trace clay slightly shelly sand
END BORING
Begin Test
End Test
DEPTH, IN FEET
0
5
10
15
20
25
30
35
40
45

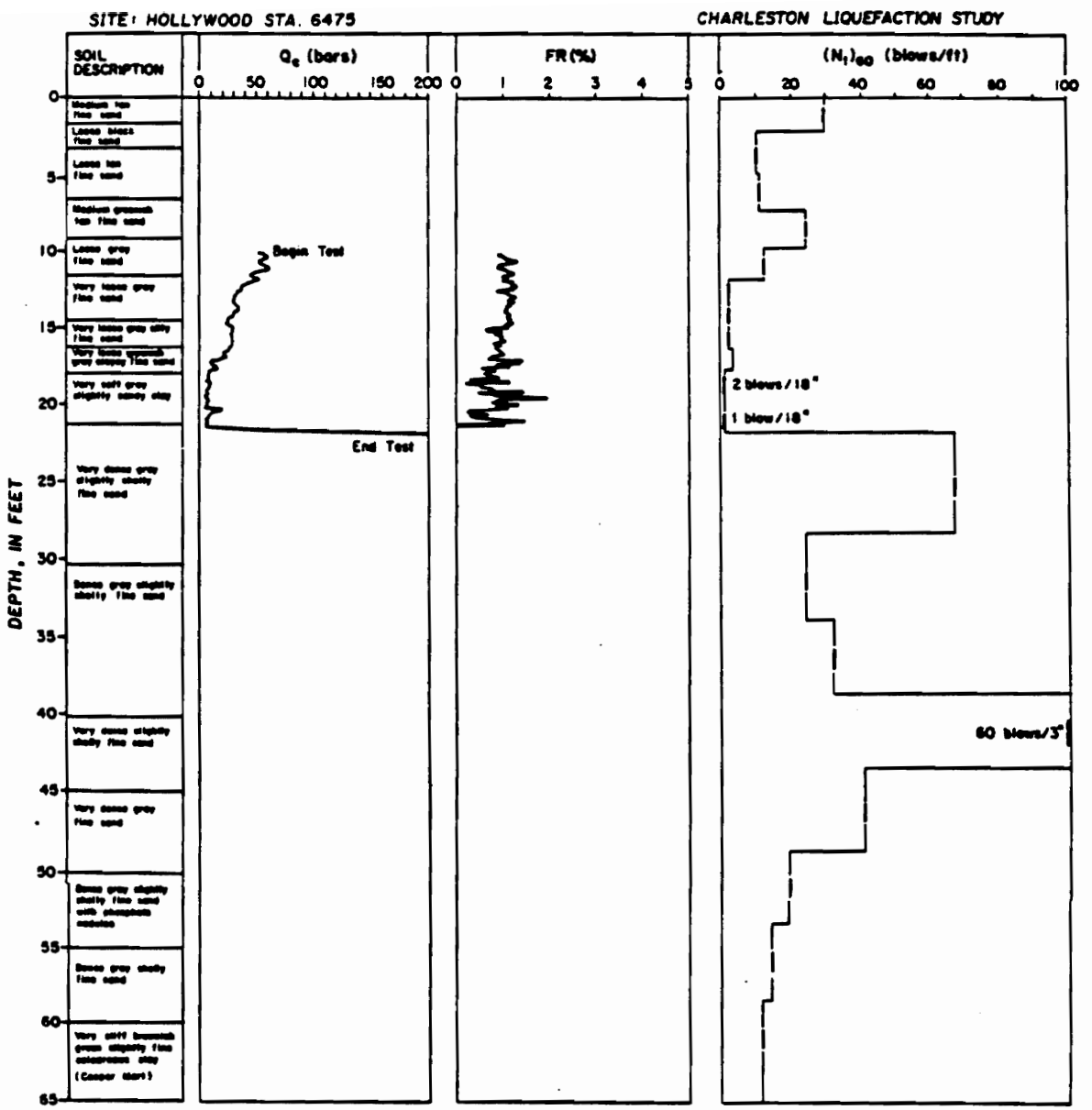
SITE: HOLLYWOOD STA. 6475
CHARLESTON LIQUEFACTION STUDY
SOIL DESCRIPTION
Q_c (bars)
0 50 100 150 200
FR (%)
0 1 2 3 4 5
$(N_1)_{60}$ (blows/ft)
0 20 40 60 80 100
DEPTH, IN FEET
0 5 10 15 20 25 30 35 40 45 50 55 60 65
Begin Test
End Test
2 blows / 18"
1 blow / 18"
60 blows/3"

S0725'
4480'
N0560'
Clayey sand to sandy clay
0
50
100
150
200
Q_c (bars)
0
200
400 ft
0
5
10
15
20
25
30
35
DEPTH, IN FEET

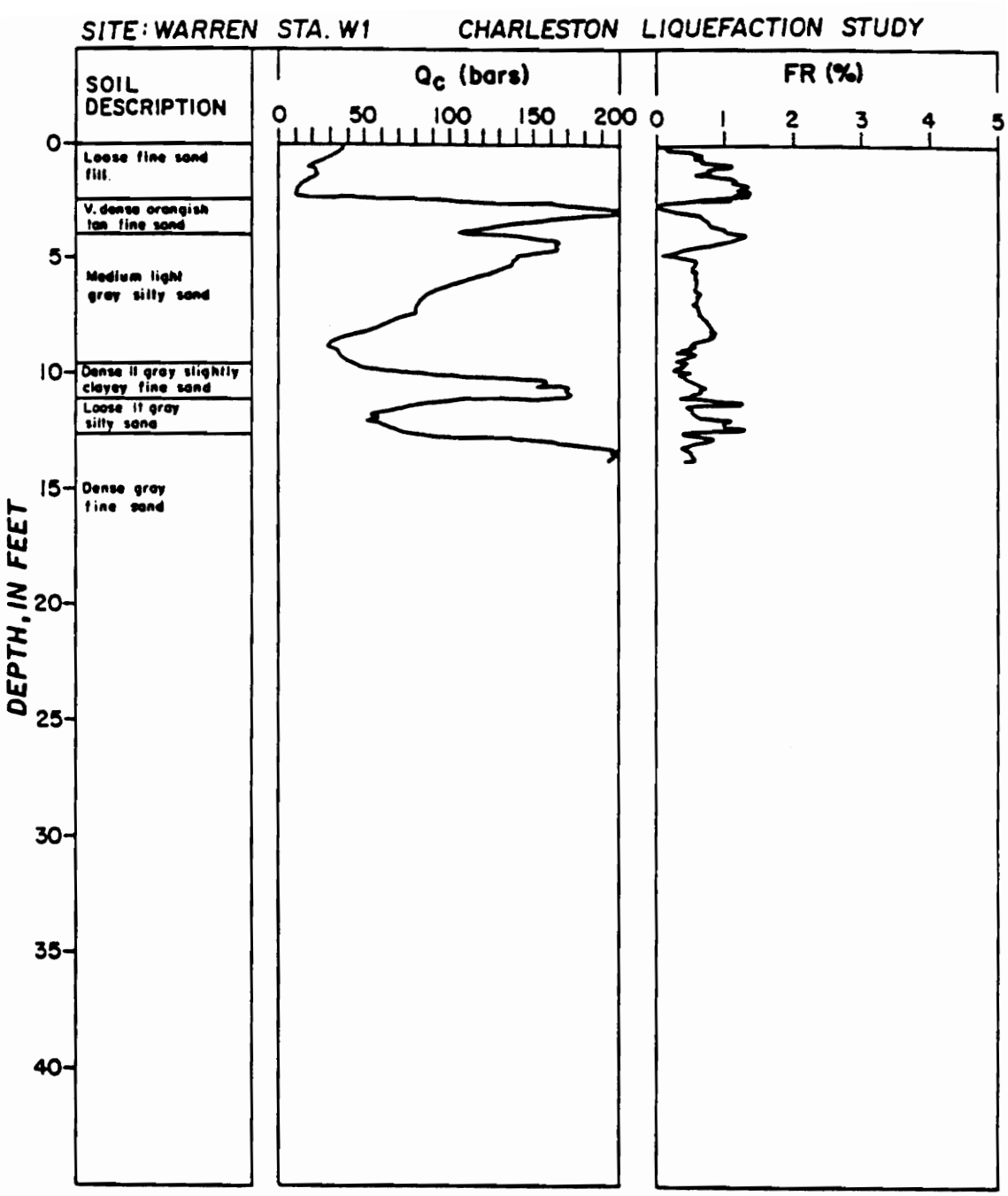
SITE: WARREN STA. W1
CHARLESTON LIQUEFACTION STUDY
SOIL DESCRIPTION
Qc (bars)
FR (%)
0
50
100
150
200
0
1
2
3
4
5
Loose fine sand fill.
V. dense orangish tan fine sand
Medium light gray silty sand
Dense ll gray slightly clayey fine sand
Loose lt gray silty sand
Dense gray fine sand
DEPTH, IN FEET
0
5
10
15
20
25
30
35
40

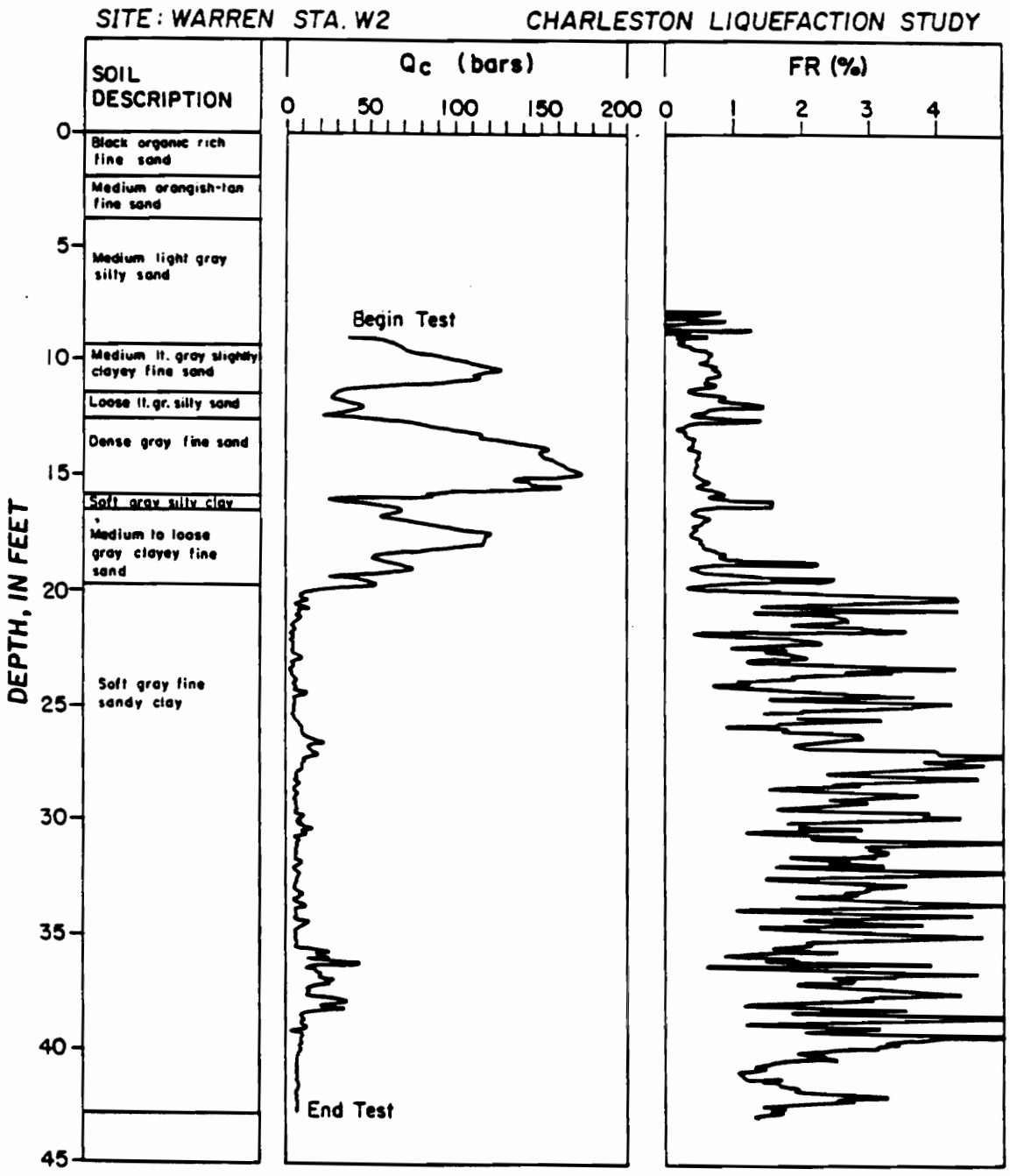
SITE: WARREN STA. W2
CHARLESTON LIQUEFACTION STUDY
SOIL DESCRIPTION
Qc (bars)
FR (%)
0
50
100
150
200
0
1
2
3
4
DEPTH, IN FEET
0
5
10
15
20
25
30
35
40
45
Black organic rich fine sand
Medium orangish-tan fine sand
Medium light gray silty sand
Medium lt. gray slightly clayey fine sand
Loose lt. gr. silty sand
Dense gray fine sand
Soft gray silty clay
Medium to loose gray clayey fine sand
Soft gray fine sandy clay
Begin Test
End Test

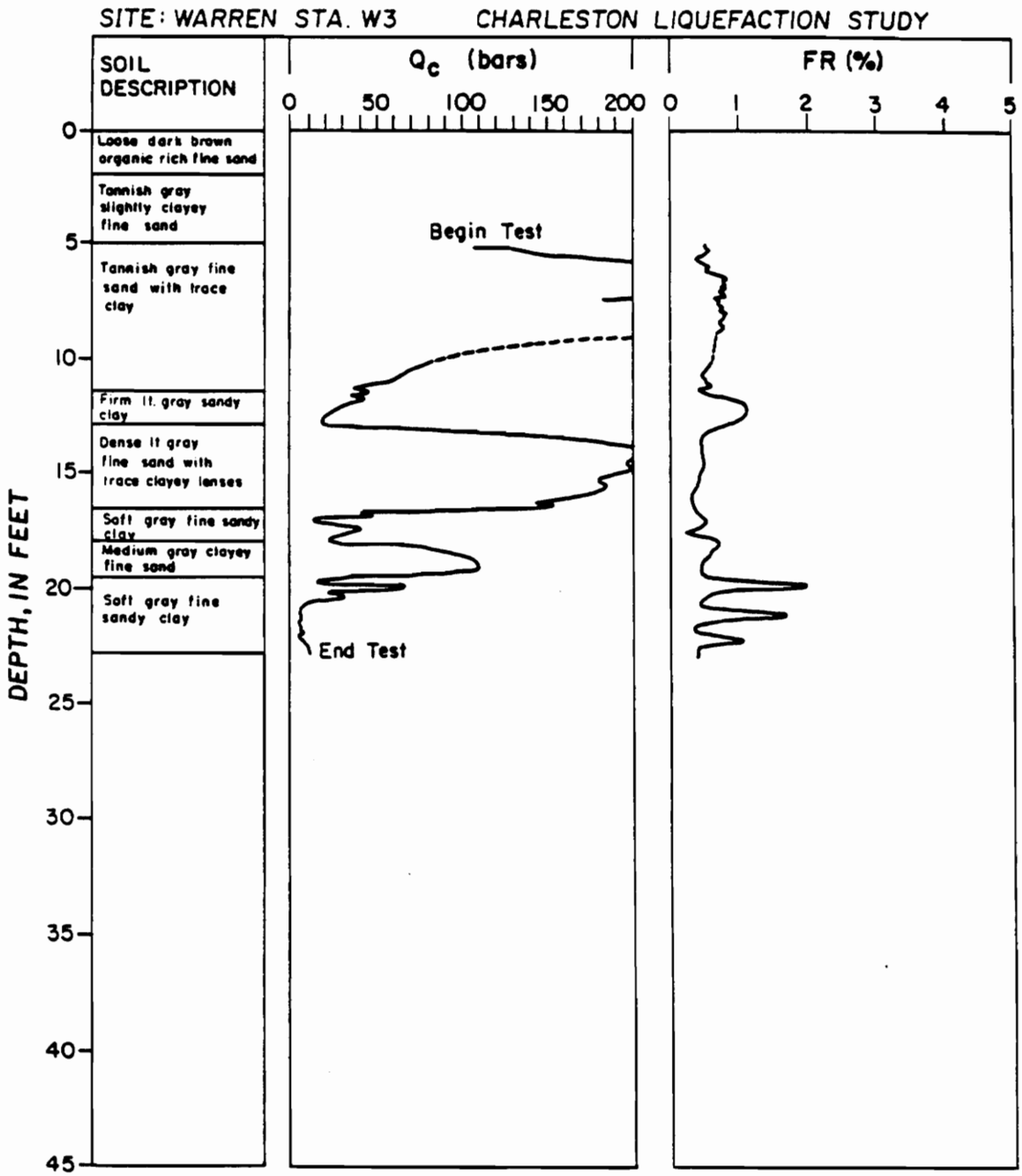
SITE: WARREN STA. W3
CHARLESTON LIQUEFACTION STUDY
SOIL DESCRIPTION
Loose dark brown organic rich fine sand
Tannish gray slightly clayey fine sand
Tannish gray fine sand with trace clay
Firm lt. gray sandy clay
Dense lt gray fine sand with trace clayey lenses
Soft gray fine sandy clay
Medium gray clayey fine sand
Soft gray fine sandy clay
Q_c (bars)
0 50 100 150 200
FR (%)
0 1 2 3 4 5
Begin Test
End Test
DEPTH, IN FEET
0 5 10 15 20 25 30 35 40 45

Appendix B

Individual Records Showing Comparisons Between CPT Penetration

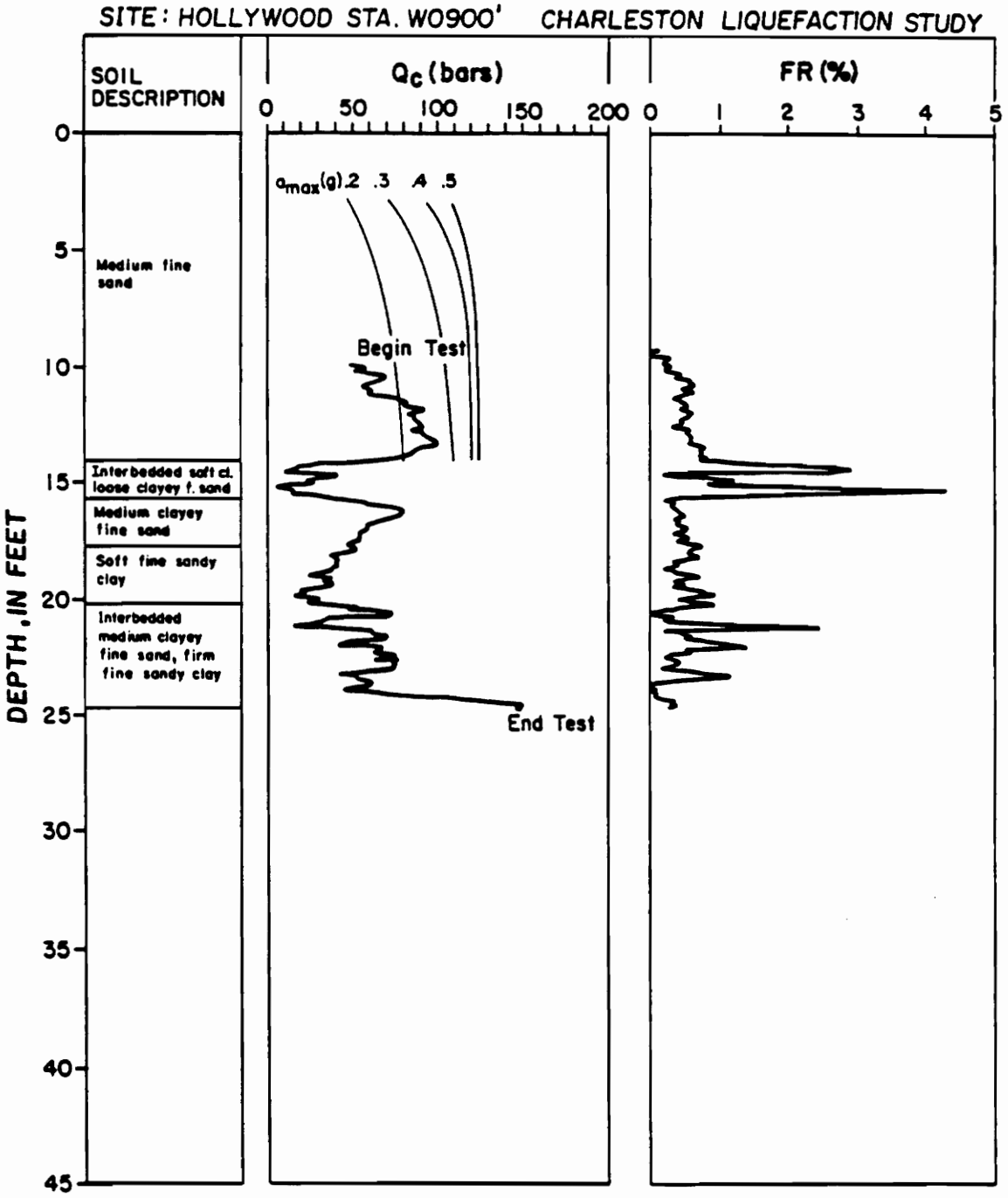
SITE: HOLLYWOOD STA. W0900'
CHARLESTON LIQUEFACTION STUDY
SOIL DESCRIPTION
Qc (bars)
0
50
100
150
200
FR (%)
0
1
2
3
4
5
amax(g) .2 .3 .4 .5
Begin Test
End Test
Medium fine sand
Interbedded soft cl. loose clayey f. sand
Medium clayey fine sand
Soft fine sandy clay
Interbedded medium clayey fine sand, firm fine sandy clay
DEPTH, IN FEET
0
5
10
15
20
25
30
35
40
45

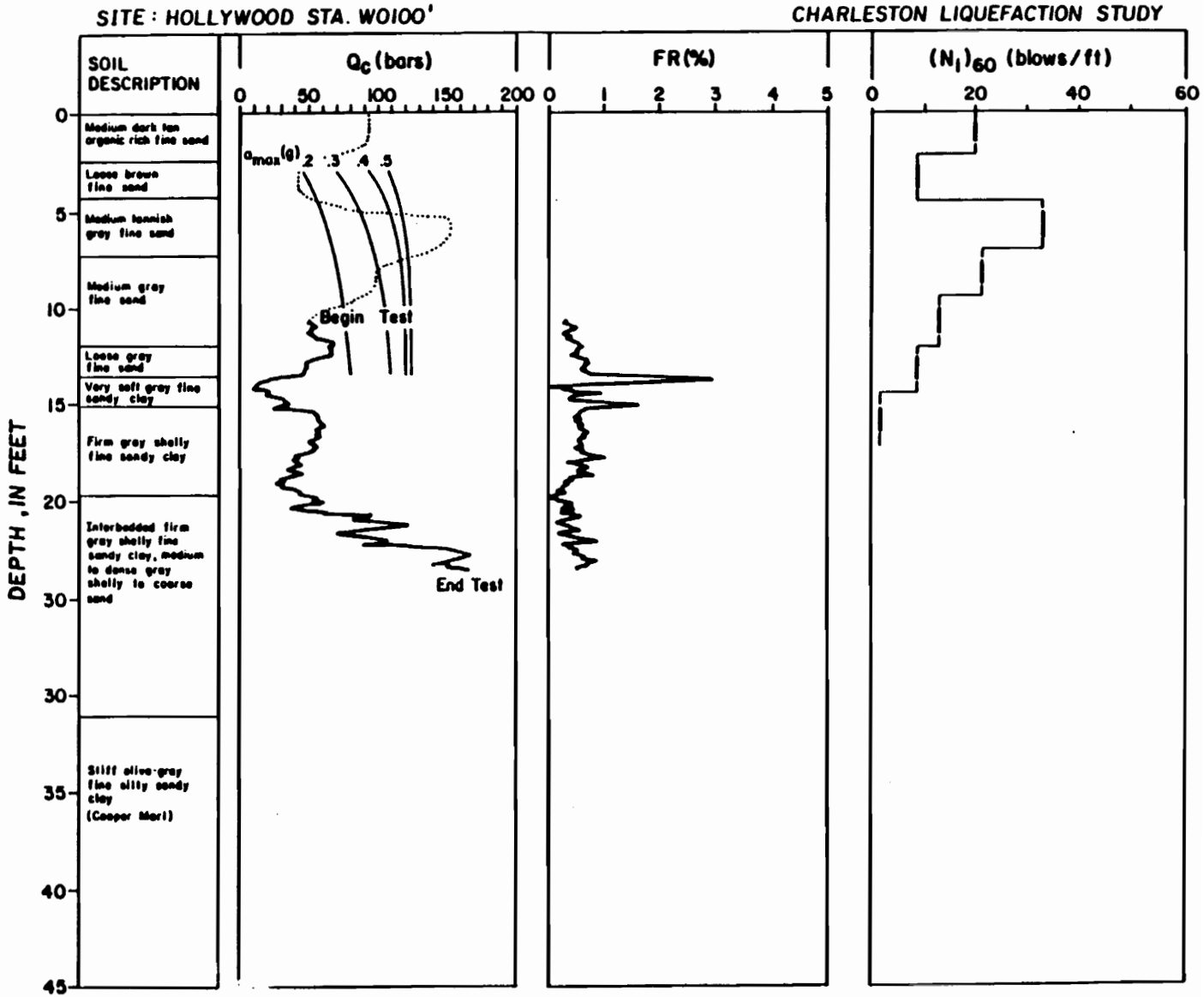
SITE : HOLLYWOOD STA. WOIOO'
CHARLESTON LIQUEFACTION STUDY
SOIL DESCRIPTION
Medium dark tan organic rich fine sand
Loose brown fine sand
Medium tannish grey fine sand
Medium grey fine sand
Loose grey fine sand
Very soft grey fine sandy clay
Firm grey shelly fine sandy clay
Interbedded firm grey shelly fine sandy clay, medium to dense grey shelly to coarse sand
Stiff olive-grey fine silty sandy clay (Cooper Marl)
DEPTH , IN FEET
Qc (bars)
0 50 100 150 200
amax(g) .2 .3 .4 .5
Begin Test
End Test
FR(%)
0 1 2 3 4 5
(N1)60 (blows/ft)
0 20 40 60
0 5 10 15 20 30 35 40 45

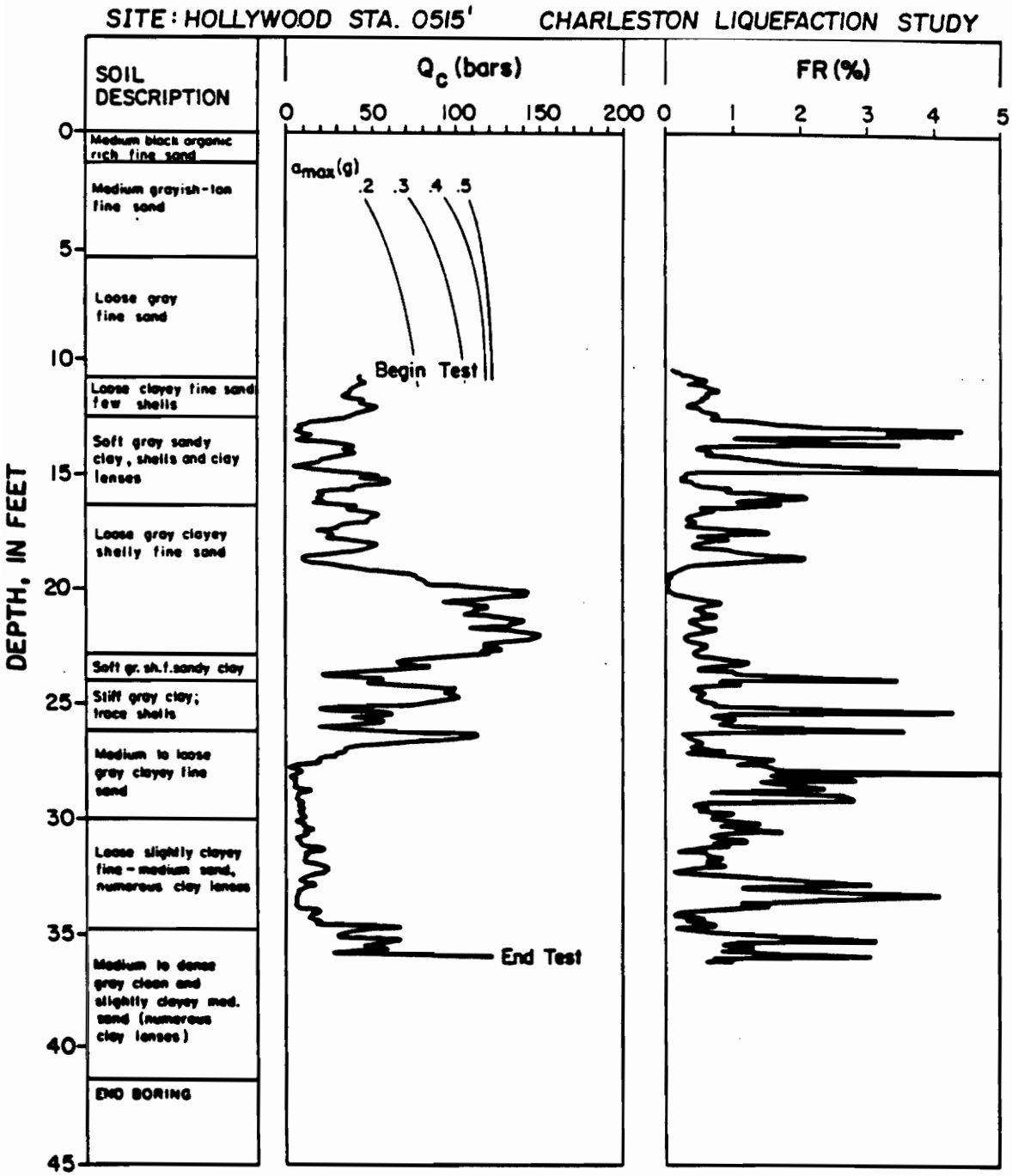
SITE: HOLLYWOOD STA. 0515'
CHARLESTON LIQUEFACTION STUDY
SOIL DESCRIPTION
Medium black organic rich fine sand
Medium grayish-tan fine sand
Loose gray fine sand
Loose clayey fine sand few shells
Soft gray sandy clay, shells and clay lenses
Loose gray clayey shelly fine sand
Soft gr. sh. f. sandy clay
Stiff gray clay; trace shells
Medium to loose gray clayey fine sand
Loose slightly clayey fine - medium sand, numerous clay lenses
Medium to dense gray clean and slightly clayey med. sand (numerous clay lenses)
END BORING
DEPTH, IN FEET
0
5
10
15
20
25
30
35
40
45
Q_c (bars)
0 50 100 150 200
a_{max}(g)
.2 .3 .4 .5
Begin Test
End Test
FR (%)
0 1 2 3 4 5

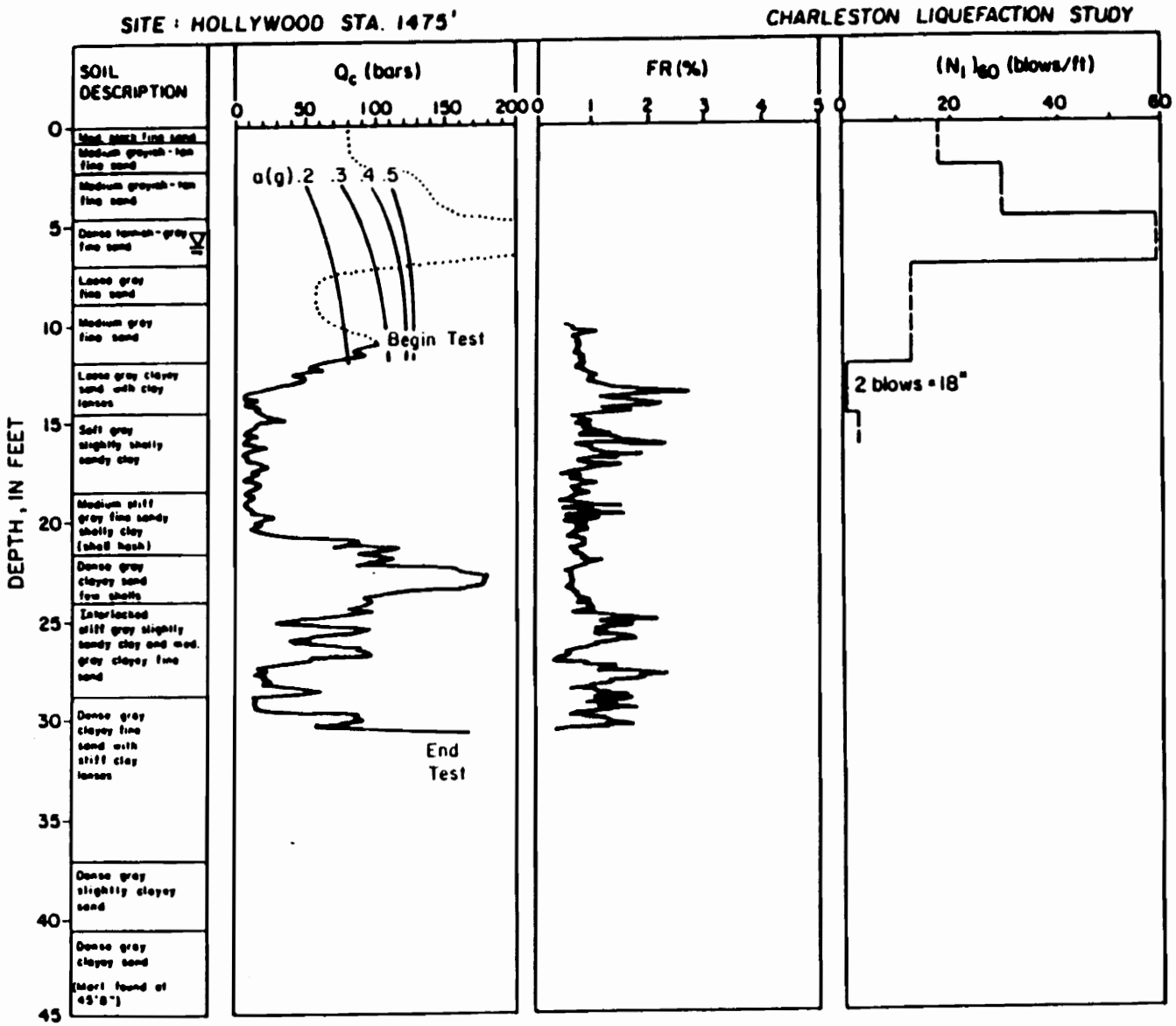
SITE : HOLLYWOOD STA. 1475'
CHARLESTON LIQUEFACTION STUDY
SOIL DESCRIPTION
Q_c (bars)
FR (%)
$(N_1)_{60}$ (blows/ft)
DEPTH, IN FEET
a(g) .2 .3 .4 .5
Begin Test
End Test
2 blows = 18"
Medium gray fine sand
Loose gray fine sand
Medium gray fine sand
Soft gray slightly shelly sandy clay
Dense gray clayey sand few shells
Dense gray slightly clayey sand
Dense gray clayey sand

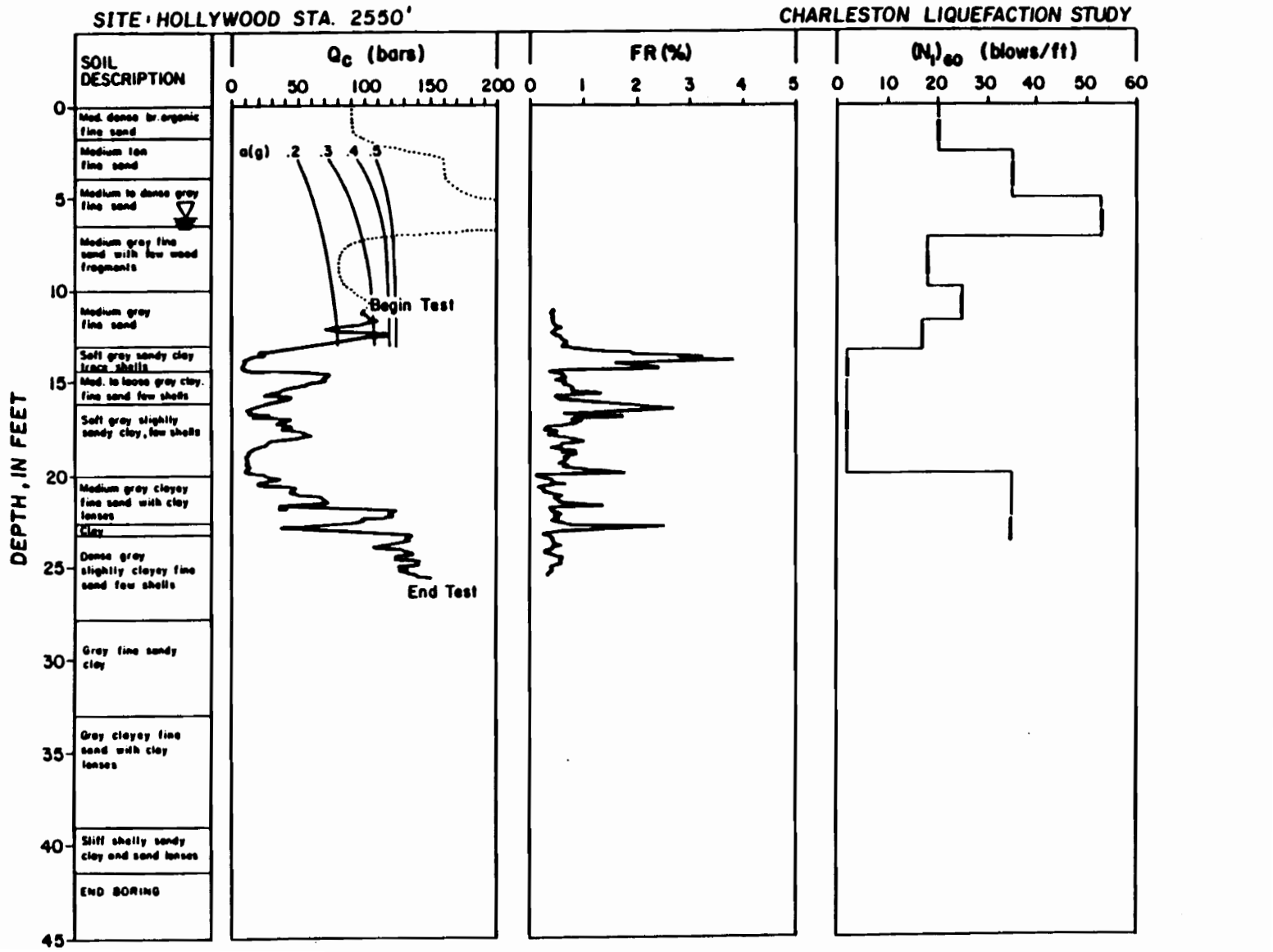
SITE : HOLLYWOOD STA. 2550'
CHARLESTON LIQUEFACTION STUDY
SOIL DESCRIPTION
Qc (bars)
FR (%)
(N1)60 (blows/ft)
DEPTH, IN FEET
Mod. dense br. organic fine sand
Medium loo fine sand
Medium to dense gray fine sand
Medium gray fine sand with few wood fragments
Medium gray fine sand
Soft gray sandy clay trace shells
Med. to loose gray clay. fine sand few shells
Soft gray slightly sandy clay, few shells
Medium gray clayey fine sand with clay lenses
Clay
Dense gray slightly clayey fine sand few shells
Gray fine sandy clay
Gray clayey fine sand with clay lenses
Stiff shelly sandy clay and sand lenses
END BORING
a(g) .2 .3 .4 .5
Begin Test
End Test

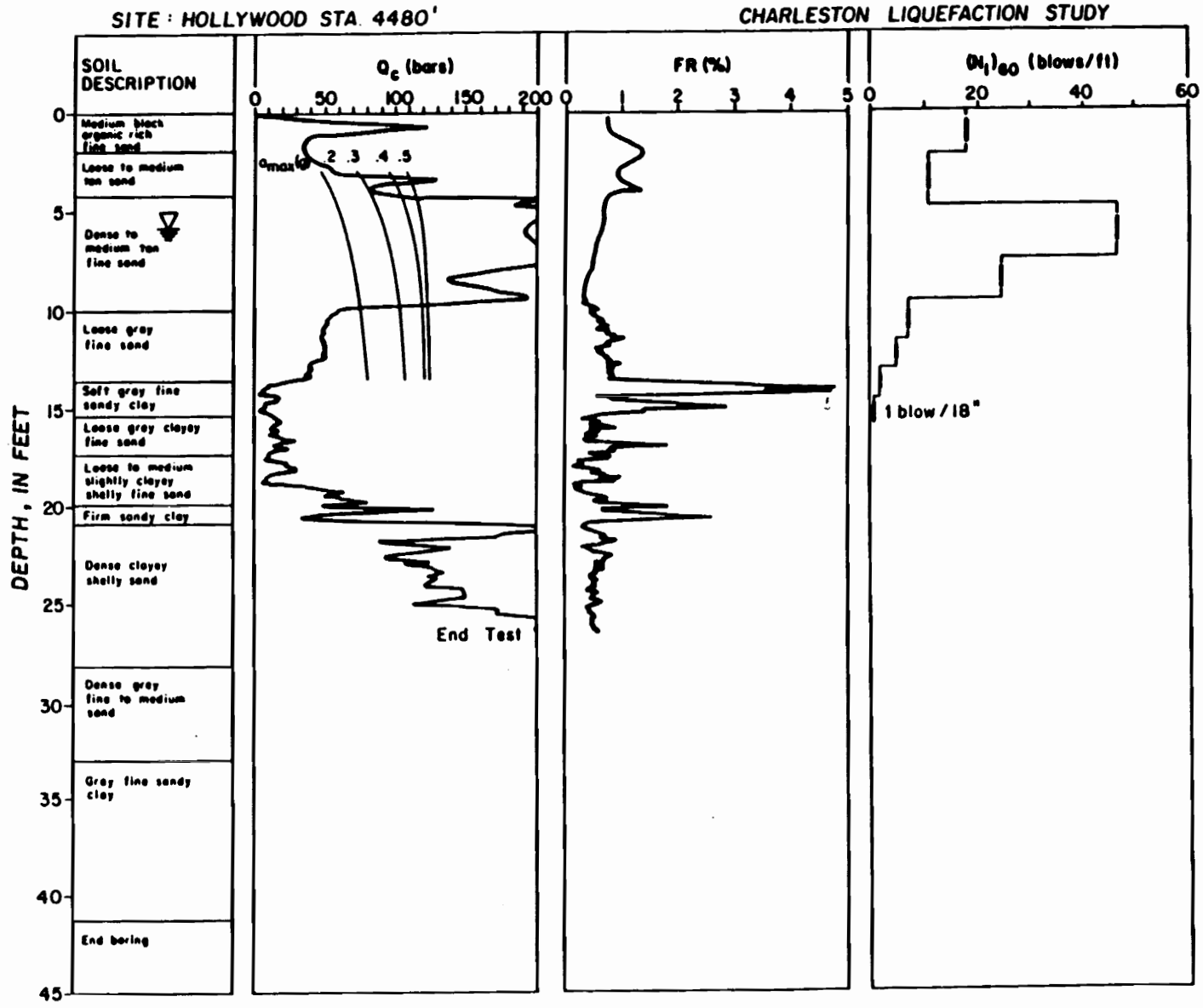
SITE : HOLLYWOOD STA. 4480'
CHARLESTON LIQUEFACTION STUDY
SOIL DESCRIPTION
Medium black organic rich fine sand
Loose to medium tan sand
Dense to medium tan fine sand
Loose gray fine sand
Soft gray fine sandy clay
Loose gray clayey fine sand
Loose to medium slightly clayey shelly fine sand
Firm sandy clay
Dense clayey shelly sand
Dense gray fine to medium sand
Gray fine sandy clay
End boring
DEPTH, IN FEET
0
5
10
15
20
25
30
35
40
45
Q_c (bars)
0
50
100
150
200
q_{max} @
2 .3 .4 .5
End Test
FR (%)
0
2
3
4
5
$(N_1)_{60}$ (blows/ft)
0
20
40
60
1 blow / 18"

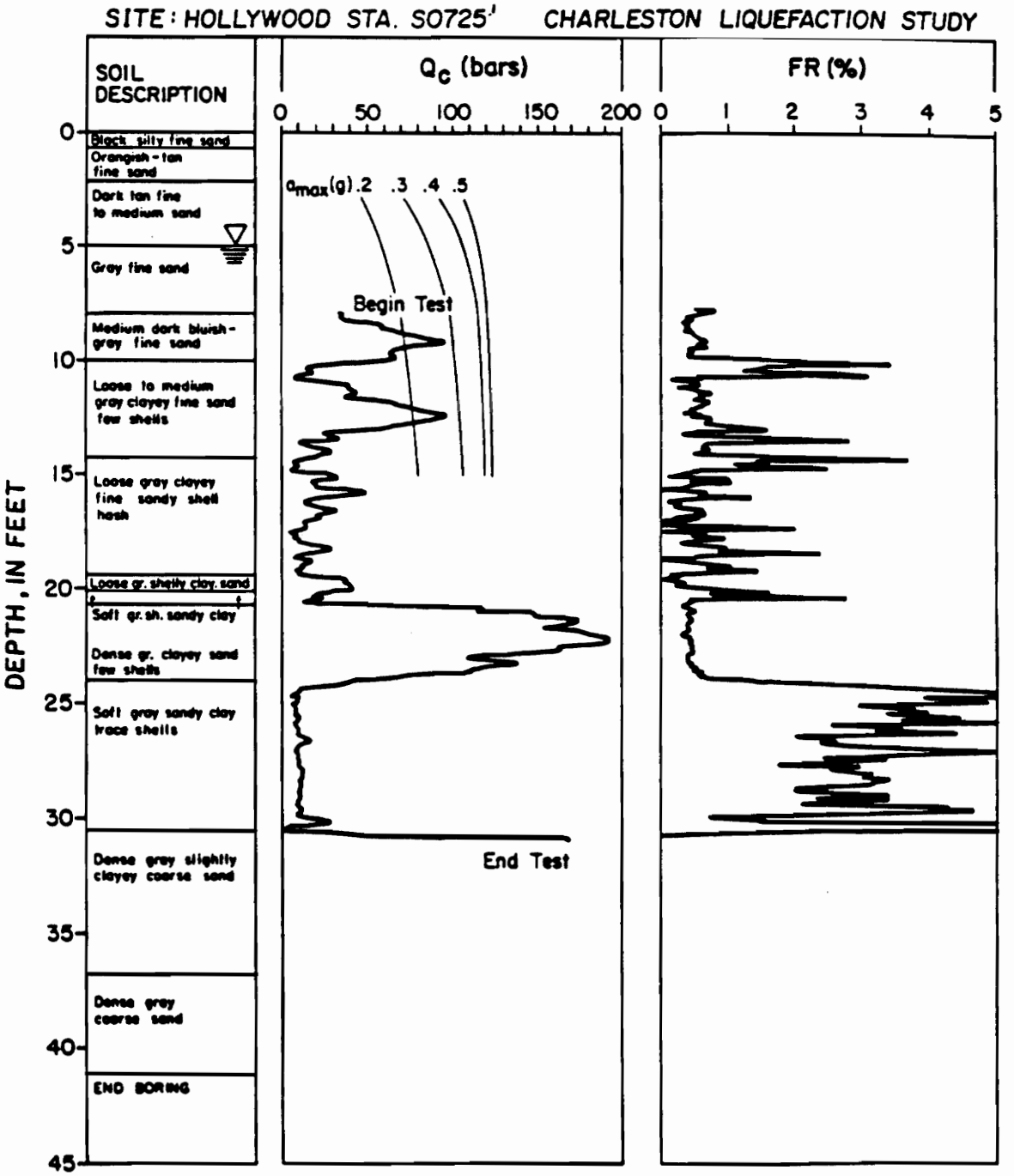
SITE: HOLLYWOOD STA. SO725'
CHARLESTON LIQUEFACTION STUDY
SOIL DESCRIPTION
Qc (bars)
FR (%)
DEPTH, IN FEET
Black silty fine sand
Orangish-tan fine sand
Dark tan fine to medium sand
Grey fine sand
Medium dark bluish-grey fine sand
Loose to medium gray clayey fine sand few shells
Loose grey clayey fine sandy shell hash
Loose gr. shelly clay. sand
Soft gr. sh. sandy clay
Dense gr. clayey sand few shells
Soft gray sandy clay trace shells
Dense grey slightly clayey coarse sand
Dense grey coarse sand
END BORING
amax(g) .2 .3 .4 .5
Begin Test
End Test

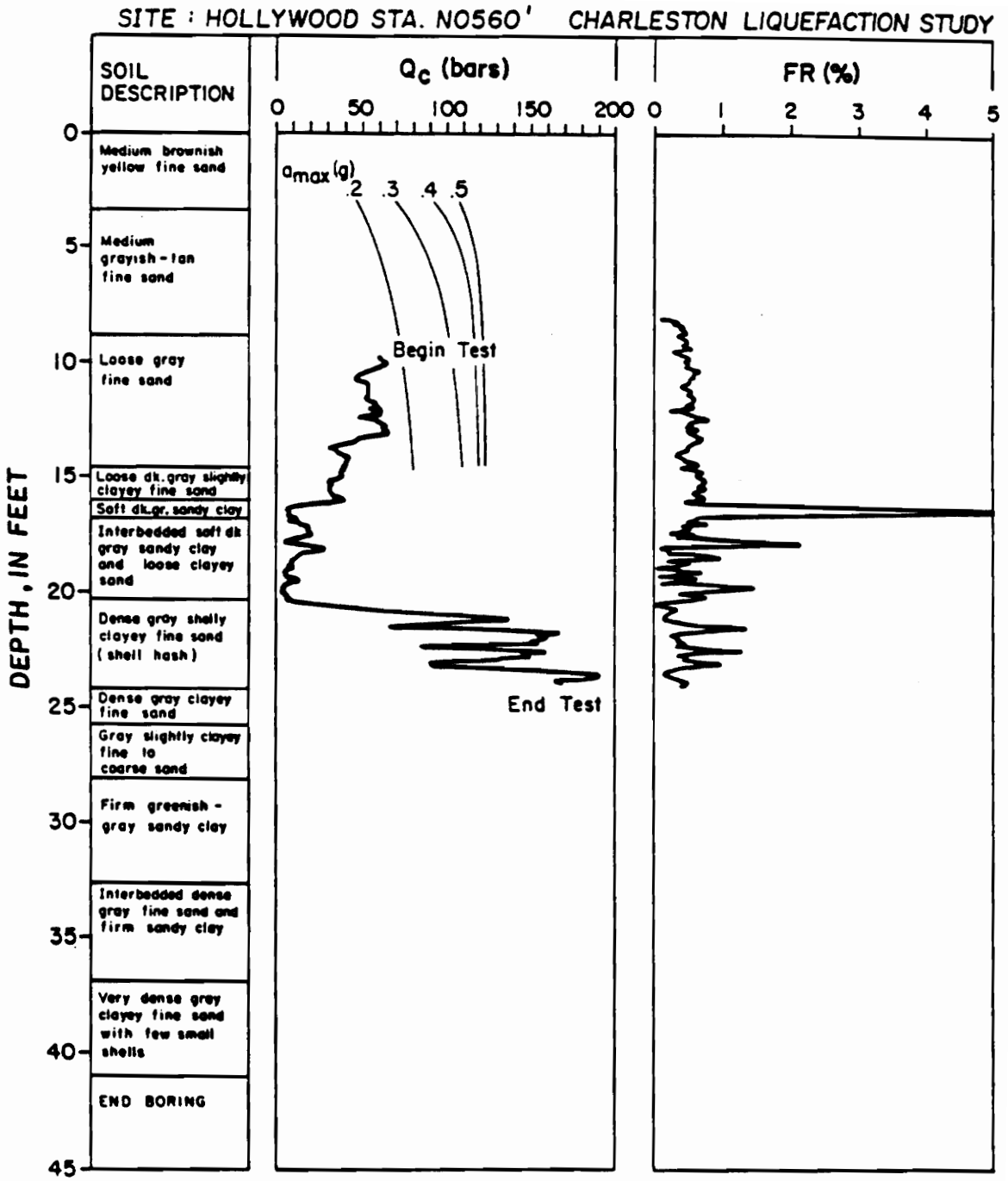
SITE : HOLLYWOOD STA. NO560'
CHARLESTON LIQUEFACTION STUDY
SOIL DESCRIPTION
Medium brownish yellow fine sand
Medium grayish - tan fine sand
Loose gray fine sand
Loose dk. gray slightly clayey fine sand
Soft dk.gr. sandy clay
Interbedded soft dk gray sandy clay and loose clayey sand
Dense gray shelly clayey fine sand (shell hash)
Dense gray clayey fine sand
Gray slightly clayey fine to coarse sand
Firm greenish - gray sandy clay
Interbedded dense gray fine sand and firm sandy clay
Very dense gray clayey fine sand with few small shells
END BORING
DEPTH, IN FEET
0
5
10
15
20
25
30
35
40
45
Q_c (bars)
0 50 100 150 200
a_{max} (g)
.2 .3 .4 .5
Begin Test
End Test
FR (%)
0 1 2 3 4 5

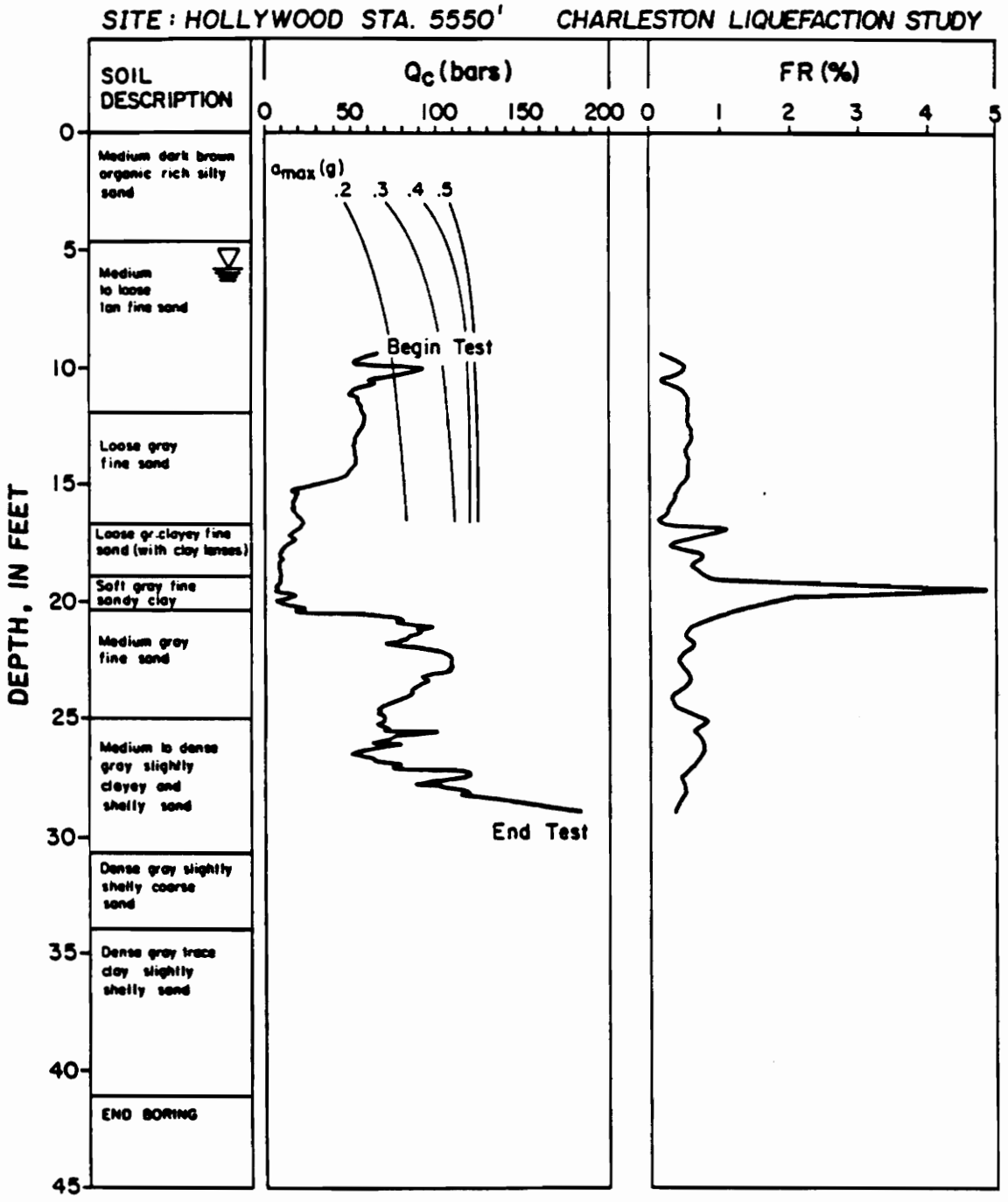
SITE : HOLLYWOOD STA. 5550'
CHARLESTON LIQUEFACTION STUDY
SOIL DESCRIPTION
Qc (bars)
FR (%)
0
50
100
150
200
0
1
2
3
4
5
amax (g)
.2
.3
.4
.5
Begin Test
End Test
DEPTH, IN FEET
0
5
10
15
20
25
30
35
40
45
Medium dark brown organic rich silty sand
Medium to loose tan fine sand
Loose gray fine sand
Loose gr.clayey fine sand (with clay lenses)
Soft gray fine sandy clay
Medium gray fine sand
Medium to dense gray slightly clayey and shelly sand
Dense gray slightly shelly coarse sand
Dense gray trace clay slightly shelly sand
END BORING

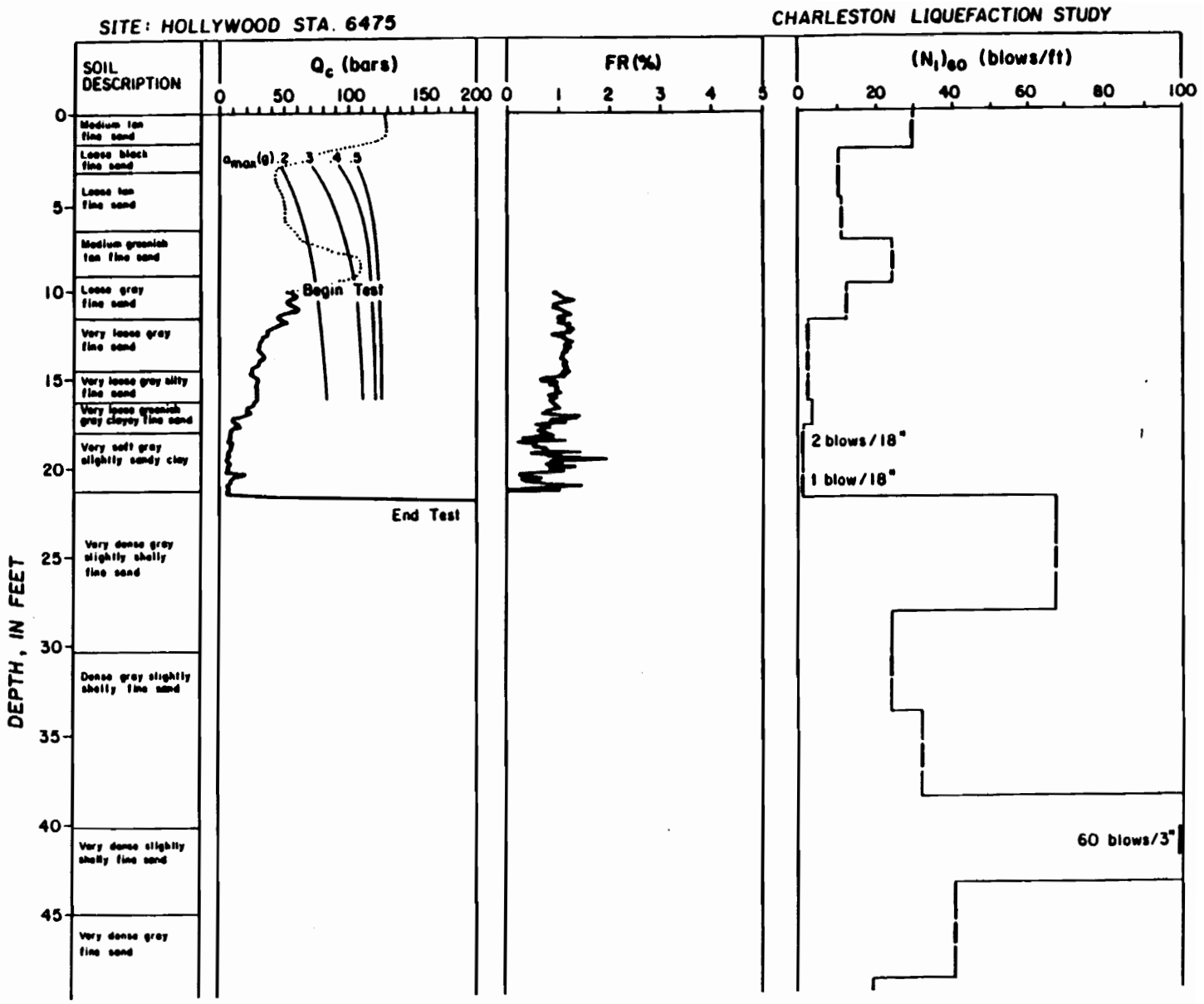
SITE: HOLLYWOOD STA. 6475
CHARLESTON LIQUEFACTION STUDY
SOIL DESCRIPTION
Q_c (bars)
FR(%)
$(N_1)_{60}$ (blows/ft)
DEPTH, IN FEET
Medium tan fine sand
Loose black fine sand
Loose tan fine sand
Medium greenish tan fine sand
Loose gray fine sand
Very loose gray fine sand
Very loose gray silty fine sand
Very loose greenish gray clayey fine sand
Very soft gray slightly sandy clay
Very dense gray slightly shelly fine sand
Dense gray slightly shelly fine sand
Very dense slightly shelly fine sand
Very dense gray fine sand
a_{max}(g) .2 .3 .4 .5
Begin Test
End Test
2 blows/18"
1 blow/18"
60 blows/3"

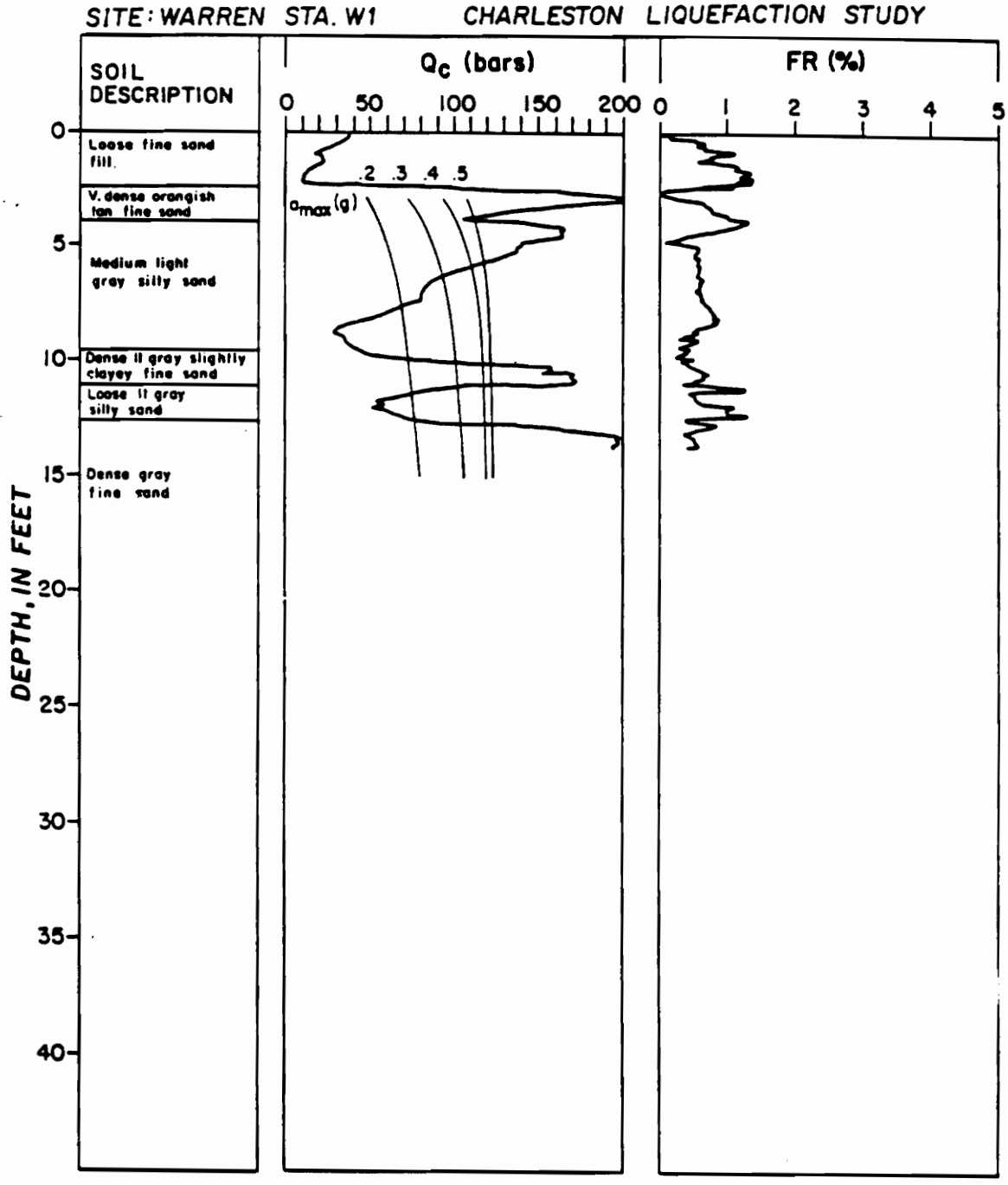
SITE: WARREN STA. W1
CHARLESTON LIQUEFACTION STUDY
SOIL DESCRIPTION
Loose fine sand fill.
V. dense orangish tan fine sand
Medium light gray silty sand
Dense ll gray slightly clayey fine sand
Loose ll gray silty sand
Dense gray fine sand
Qc (bars)
0 50 100 150 200
FR (%)
0 1 2 3 4 5
amax (g)
.2 .3 .4 .5
DEPTH, IN FEET
0 5 10 15 20 25 30 35 40

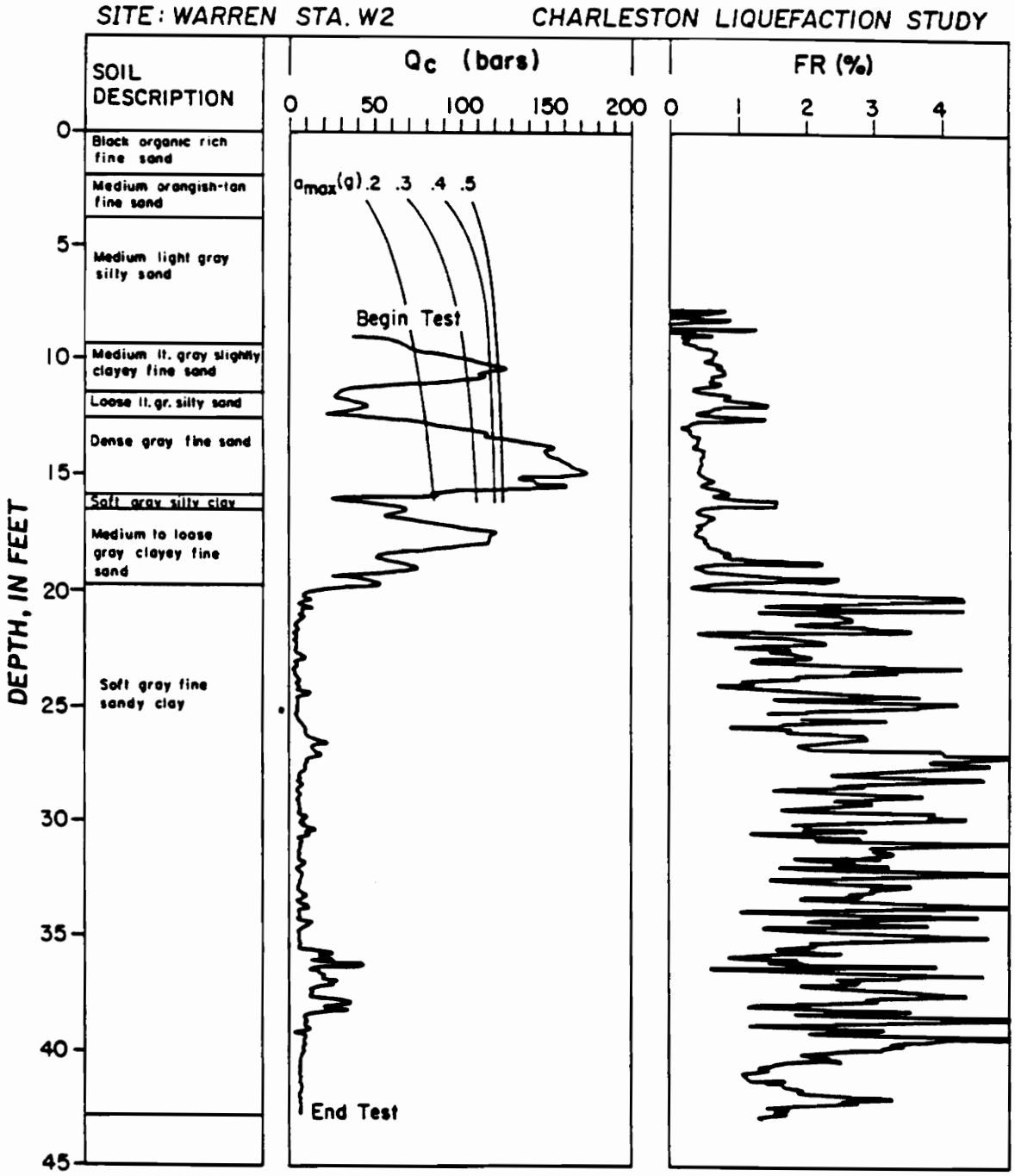
SITE: WARREN STA. W2
CHARLESTON LIQUEFACTION STUDY
SOIL DESCRIPTION
Qc (bars)
FR (%)
0 50 100 150 200
0 1 2 3 4
Black organic rich fine sand
Medium orangish-tan fine sand
Medium light gray silty sand
Medium lt. gray slightly clayey fine sand
Loose lt. gr. silty sand
Dense gray fine sand
Soft gray silty clay
Medium to loose gray clayey fine sand
Soft gray fine sandy clay
amax(g) .2 .3 .4 .5
Begin Test
End Test
DEPTH, IN FEET
0
5
10
15
20
25
30
35
40
45

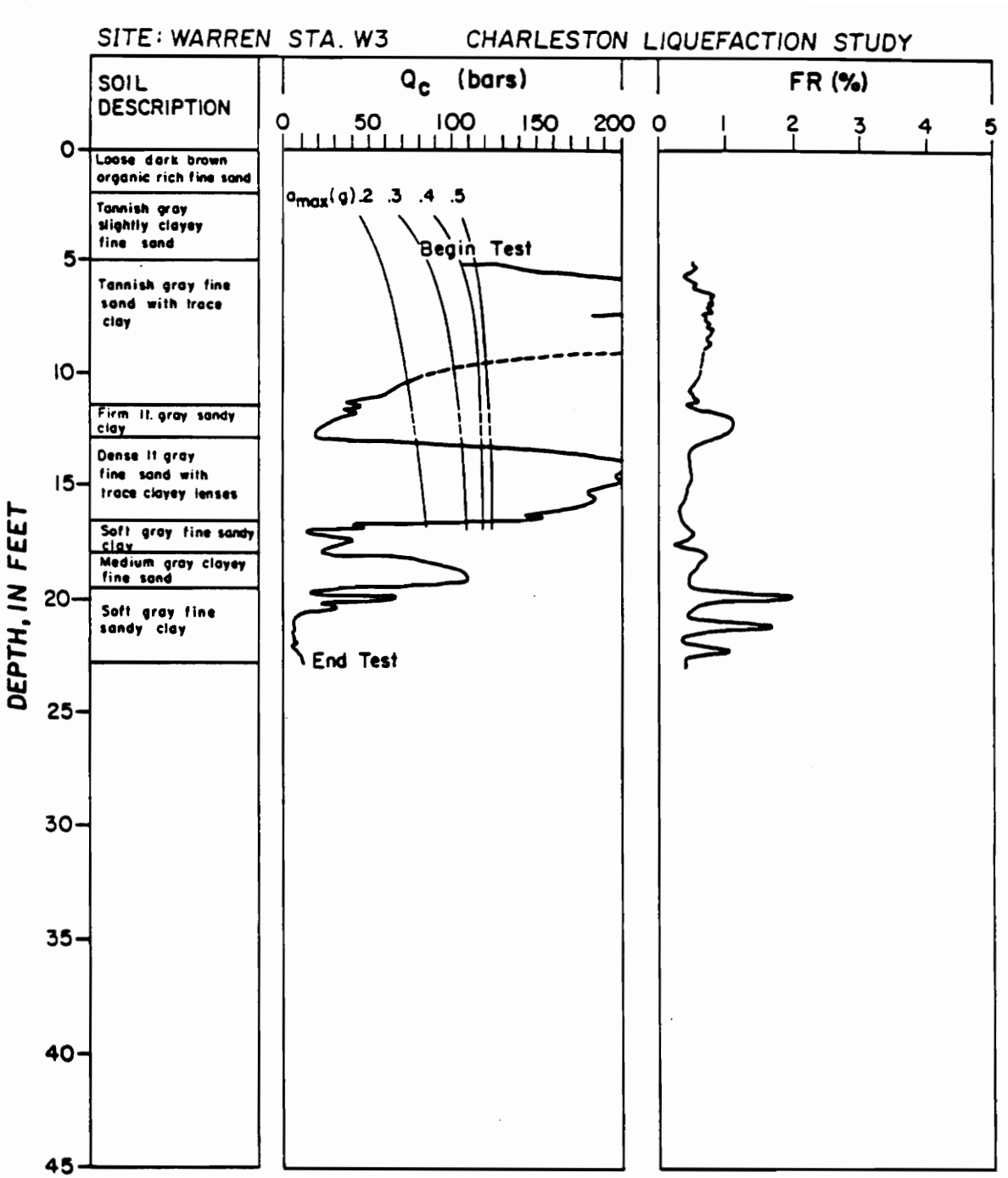
SITE: WARREN STA. W3
CHARLESTON LIQUEFACTION STUDY
SOIL DESCRIPTION
Q_c (bars)
FR (%)
0 50 100 150 200
0 1 2 3 4 5
a_{max}(g) .2 .3 .4 .5
Begin Test
End Test
DEPTH, IN FEET
0
5
10
15
20
25
30
35
40
45
Loose dark brown organic rich fine sand
Tannish gray slightly clayey fine sand
Tannish gray fine sand with trace clay
Firm lt. gray sandy clay
Dense lt gray fine sand with trace clayey lenses
Soft gray fine sandy clay
Medium gray clayey fine sand
Soft gray fine sandy clay

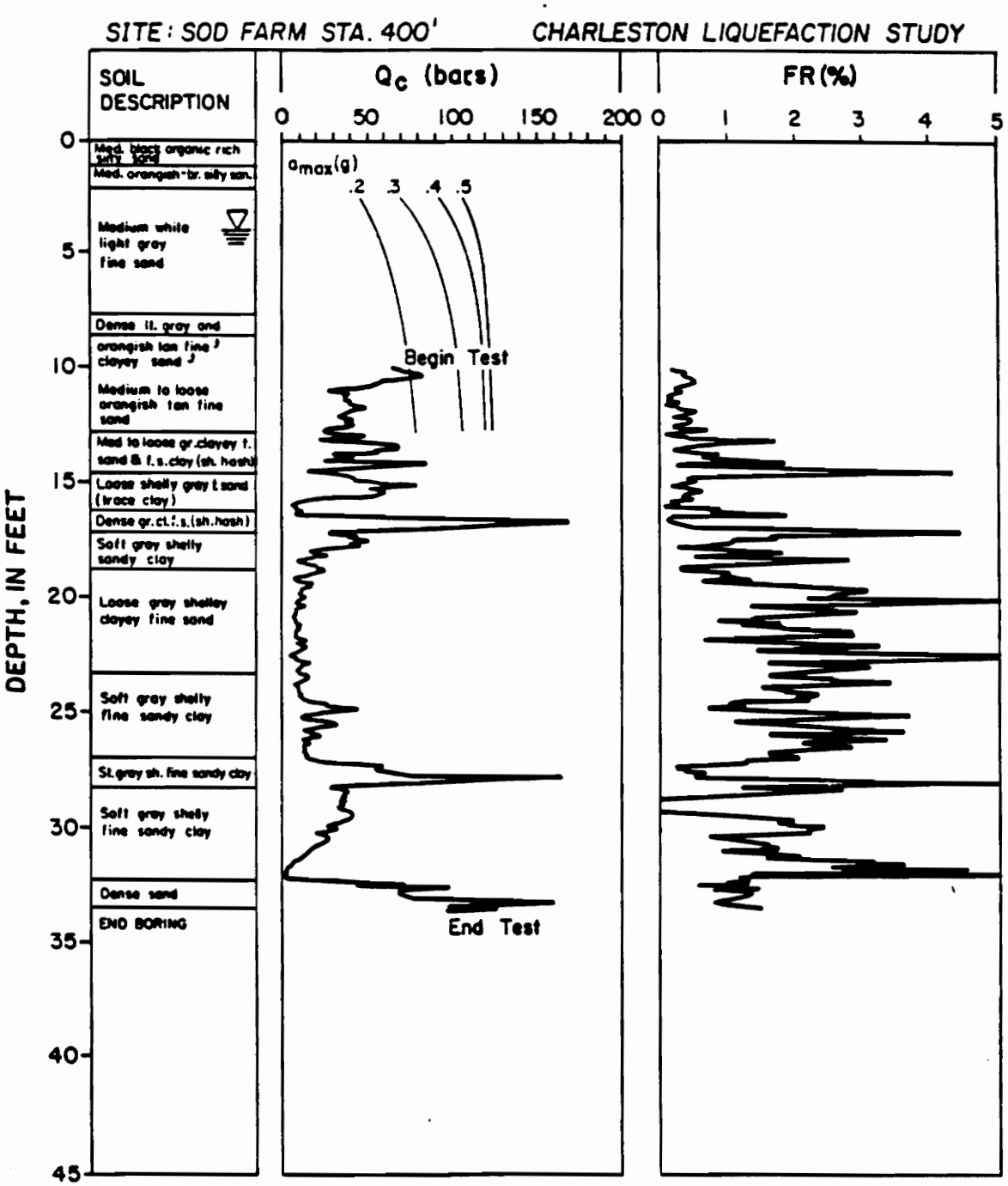
SITE: SOD FARM STA. 400'
CHARLESTON LIQUEFACTION STUDY
SOIL DESCRIPTION
Qc (bars)
FR(%)
DEPTH, IN FEET
amax(g)
.2 .3 .4 .5
Begin Test
End Test
Med. black organic rich silty sand
Med. orangish-br. silty san.
Medium white light gray fine sand
Dense lt. gray and orangish tan fine clayey sand
Medium to loose orangish tan fine sand
Med to loose gr.clayey f. sand & f.s.clay (sh. hash)
Loose shelly gray f sand (trace clay)
Dense gr.cl.f.s.(sh.hash)
Soft gray shelly sandy clay
Loose gray shelley clayey fine sand
Soft gray shelly fine sandy clay
St.gray sh. fine sandy clay
Soft gray shelly fine sandy clay
Dense sand
END BORING

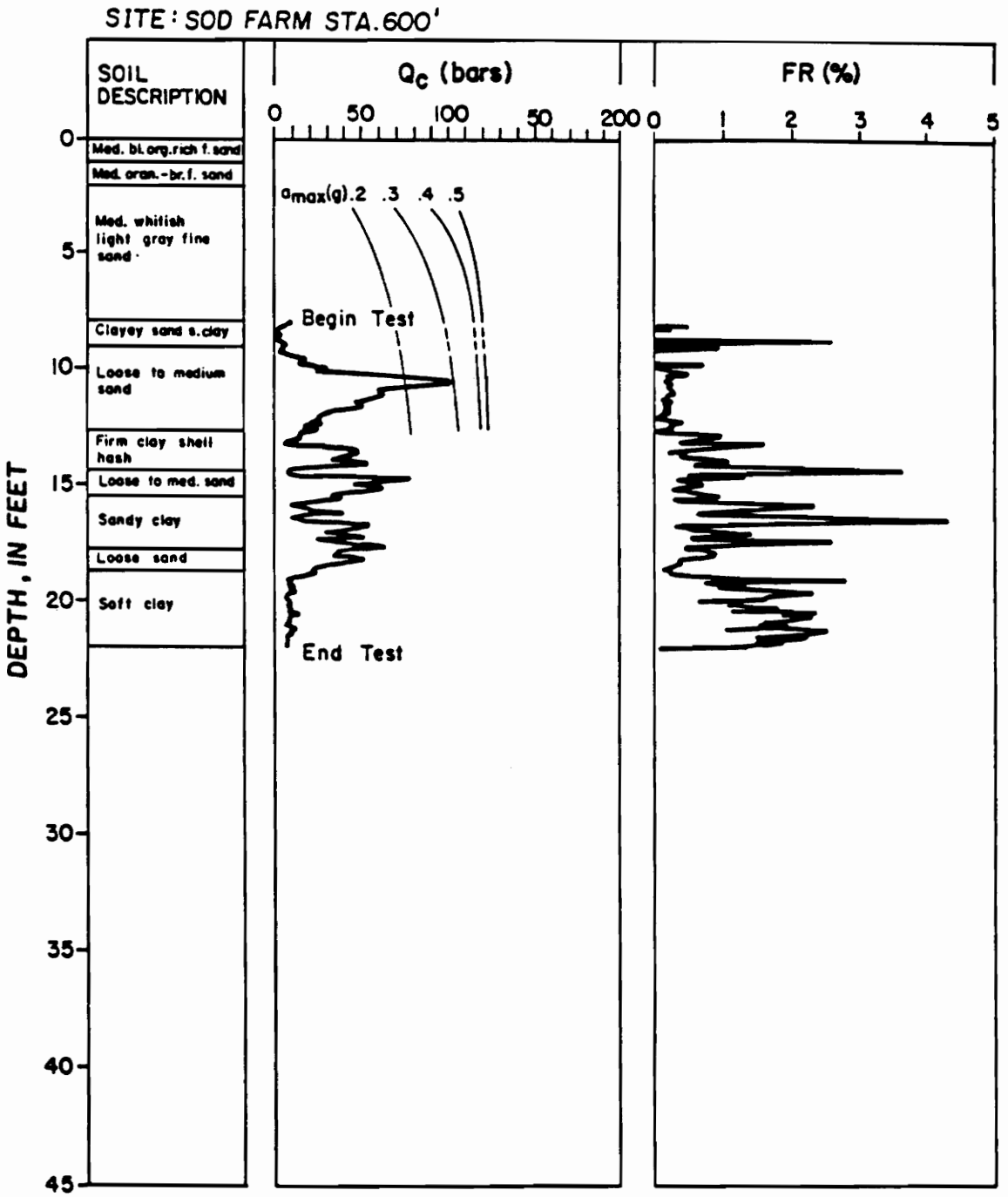
SITE: SOD FARM STA. 600'
SOIL DESCRIPTION
Qc (bars)
FR (%)
0
50
100
50
200
0
1
2
3
4
5
Med. bl. org. rich f. sand
Med. oran.-br. f. sand
Med. whitish light gray fine sand
Clayey sand & clay
Loose to medium sand
Firm clay shell hash
Loose to med. sand
Sandy clay
Loose sand
Soft clay
amax(g) .2 .3 .4 .5
Begin Test
End Test
DEPTH, IN FEET
0
5
10
15
20
25
30
35
40
45

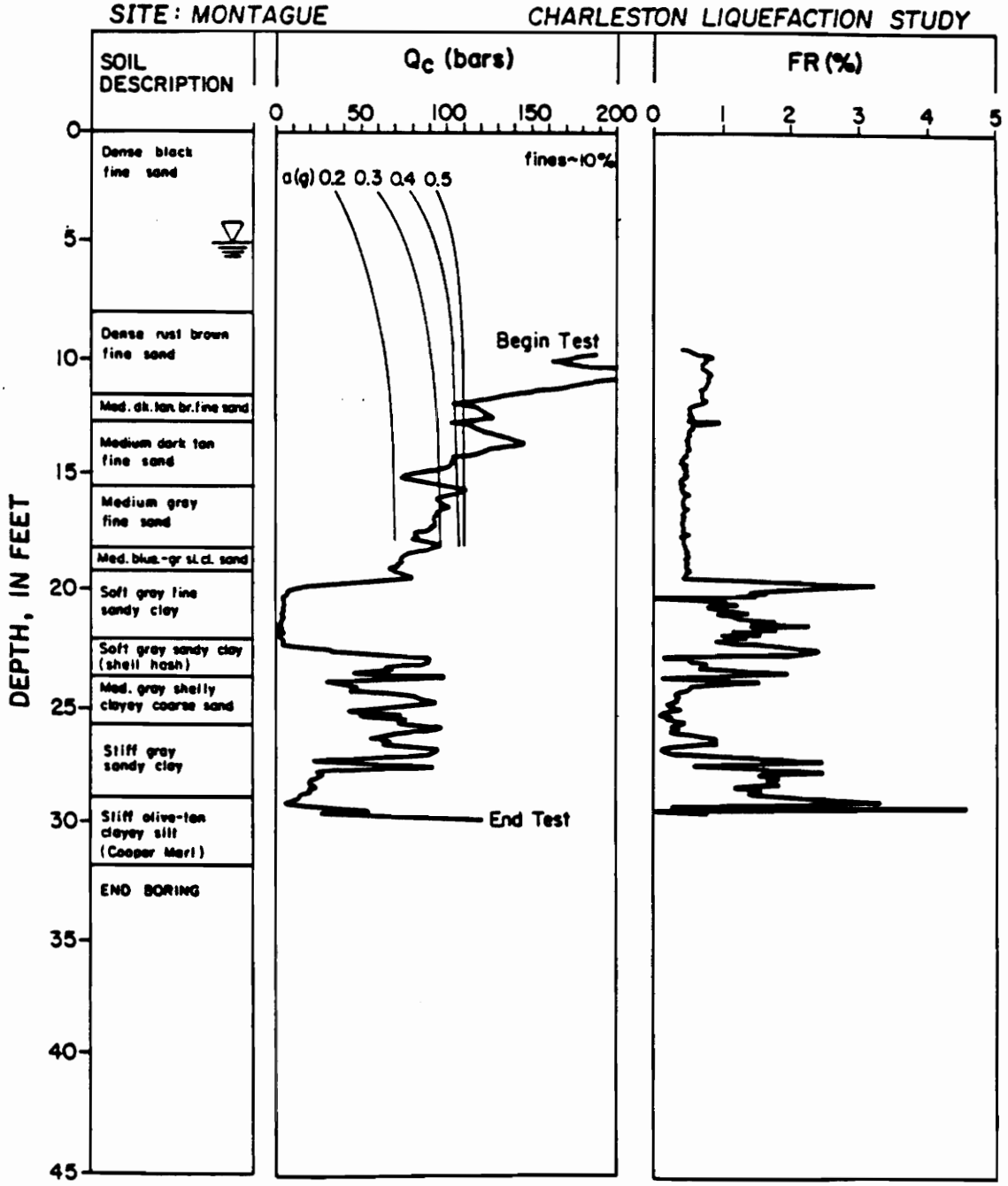
SITE: MONTAGUE
CHARLESTON LIQUEFACTION STUDY
SOIL DESCRIPTION
Qc (bars)
FR (%)
0 50 100 150 200
0 1 2 3 4 5
fines~10%
a(g) 0.2 0.3 0.4 0.5
Begin Test
End Test
DEPTH, IN FEET
0
5
10
15
20
25
30
35
40
45
Dense black fine sand
Dense rust brown fine sand
Med. dk. tan br. fine sand
Medium dark tan fine sand
Medium grey fine sand
Med. blue-gr sl. cl. sand
Soft grey fine sandy clay
Soft grey sandy clay (shell hash)
Med. grey shelly clayey coarse sand
Stiff grey sandy clay
Stiff olive-tan clayey silt (Cooper Marl)
END BORING

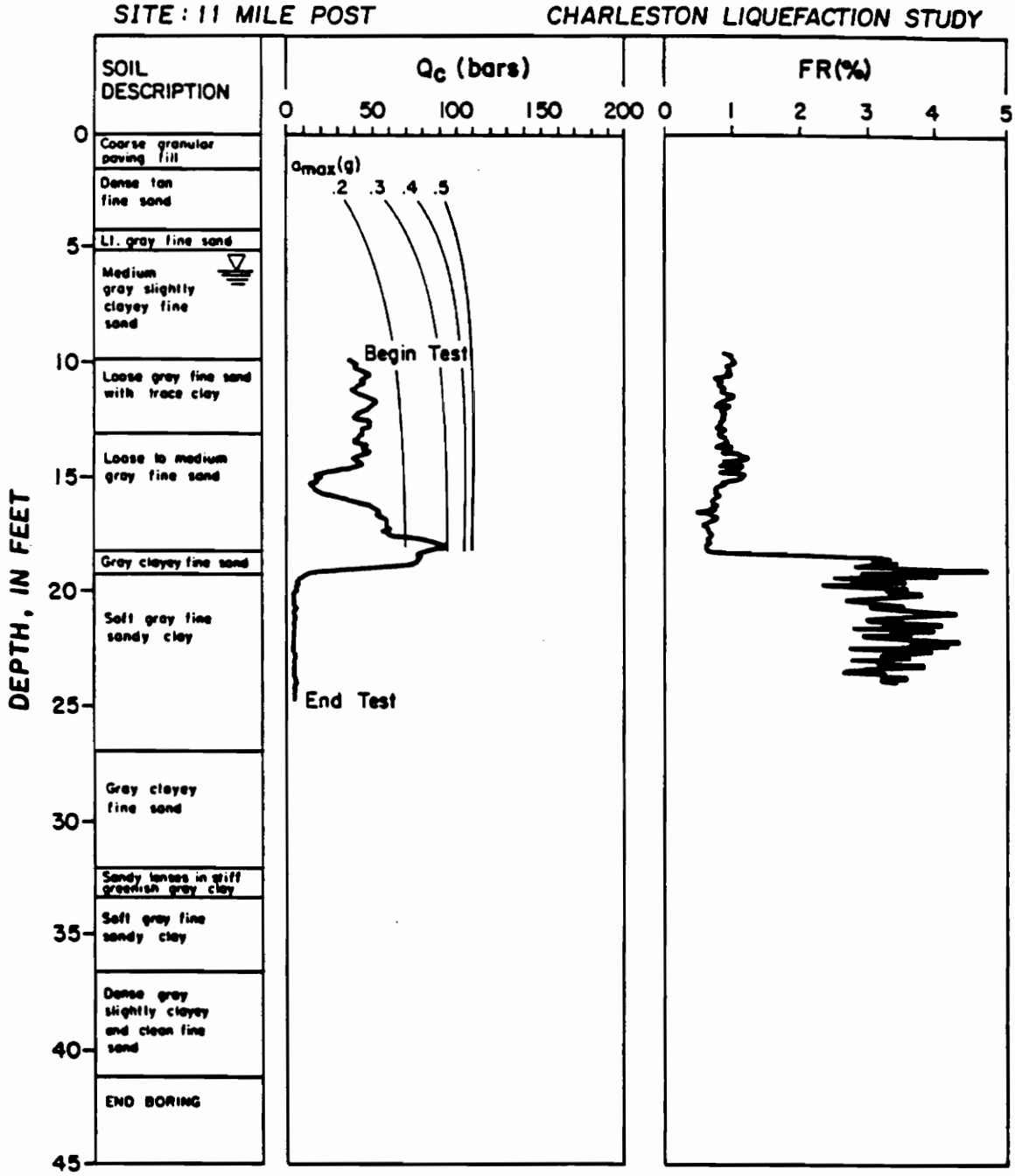
SITE : 11 MILE POST
CHARLESTON LIQUEFACTION STUDY
SOIL DESCRIPTION
Qc (bars)
FR(%)
0 50 100 150 200
0 1 2 3 4 5
amax(g)
.2 .3 .4 .5
Begin Test
End Test
DEPTH, IN FEET
0
5
10
15
20
25
30
35
40
45
Coarse granular paving fill
Dense tan fine sand
Lt. gray fine sand
Medium gray slightly clayey fine sand
Loose gray fine sand with trace clay
Loose to medium gray fine sand
Gray clayey fine sand
Soft gray fine sandy clay
Gray clayey fine sand
Sandy lenses in stiff greenish gray clay
Soft gray fine sandy clay
Dense gray slightly clayey and clean fine sand
END BORING

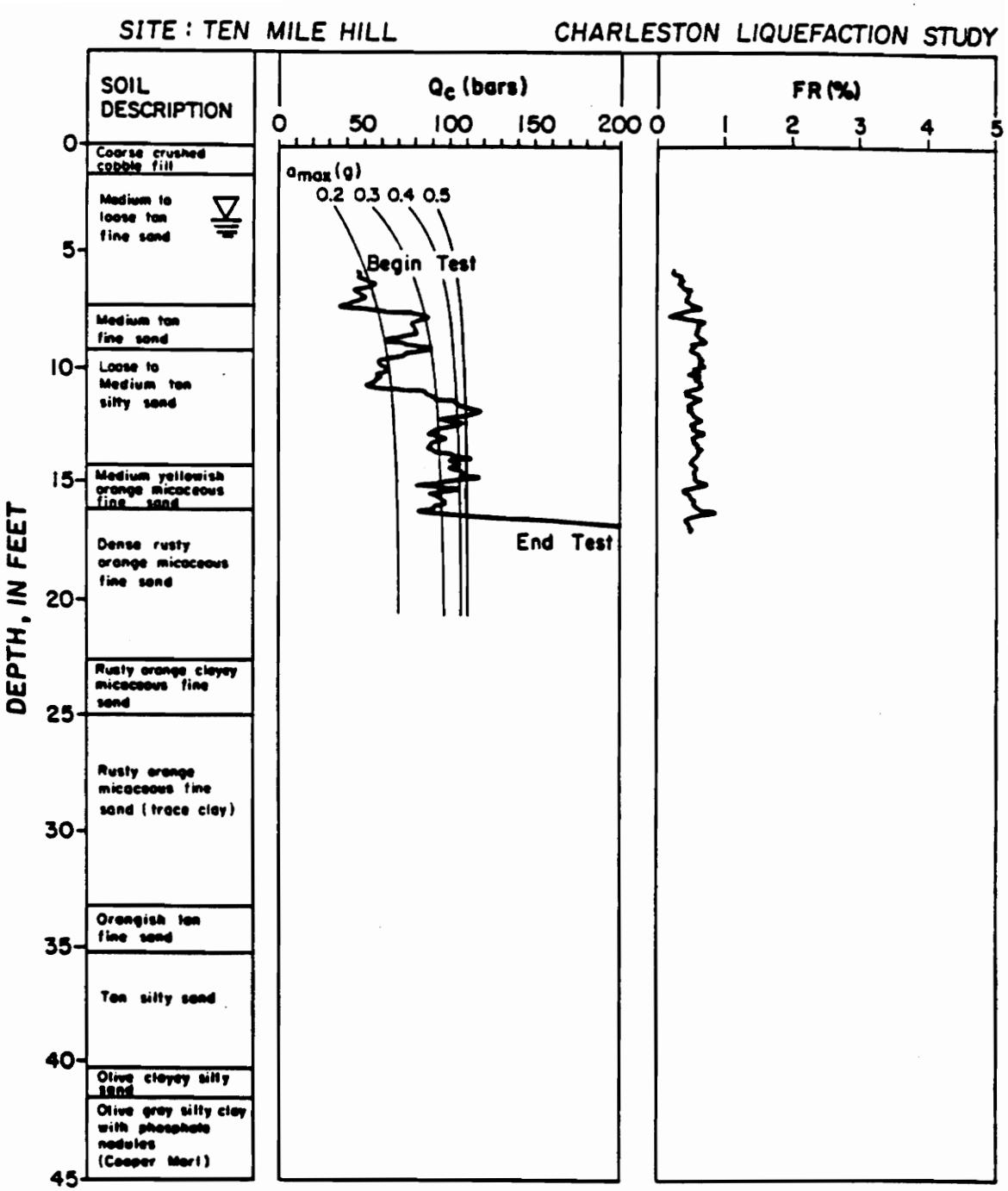
SITE : TEN MILE HILL
CHARLESTON LIQUEFACTION STUDY
SOIL DESCRIPTION
Q_c (bars)
0 50 100 150 200
FR (%)
0 1 2 3 4 5
a_{max} (g)
0.2 0.3 0.4 0.5
Begin Test
End Test
DEPTH, IN FEET
0
5
10
15
20
25
30
35
40
45
Coarse crushed cobble fill
Medium to loose tan fine sand
Medium tan fine sand
Loose to Medium tan silty sand
Medium yellowish orange micaceous fine sand
Dense rusty orange micaceous fine sand
Rusty orange clayey micaceous fine sand
Rusty orange micaceous fine sand (trace clay)
Orangish tan fine sand
Tan silty sand
Olive clayey silty sand
Olive grey silty clay with phosphate nodules (Cooper Marl)

References

1. ASTM, "American Society for Testing and Materials, Standard Method for Deep Quasi-Static, Cone and Friction-Cone Penetration Tests of Soil" , Designation: D3441, 1979

2. Amick, D. and Talwani, P., "Earthquake Recurrence Rates and Probability Estimates for the Occurrence of Significant Seismic Activity in the Charleston Area: the Next 100 Years", *Proceedings of the Third U.S. National Conference on Earthquake Engineering*, Vol. 1, EERI, Aug., 1986, pp. 55-64.

3. Baldi, G., Bellotti, R., Ghionna, V., Jamiolkowski, M. and Pasqualine, E., "Penetration Resistance and Liquefaction of Sands", *Proceedings of the Eleventh International Conference on Soil Mechanics and Foundation Engineering*, Vol. 4, 1985, pp. 1891-1896.

4. Bollinger, G.A., "Reinterpretation of the Intensity Data for the 1886 Charleston, South Carolina, Earthquake", in Rankin, D.W., ed., *Studies related to the Charleston, South Carolina, Earthquake of 1886*, A preliminary report: U.S. Geol. Survey "Professional Paper 1028", 1977, pp. 17-32.

5. Bollinger, G.A., "Speculations on the Nature of Seismicity at Charlston, South Carolina," U.S. Geological Survey *Professional Paper 1313*, pp. T1-T11, 1983.

6. Campbell, K.E., "An Empirical Estimate of Near-Source Ground Motion for a Major $m_b = 6.8$, Earthquake in the Eastern United States", *Bulletin of the Seismological Society of America*, Vol. 76, No. 1, Feb. 76.

7. Castro, G. and Poulos, S.J., "Factors Affecting Liquefaction and Cyclic Mobility", *Journal of the Geotechnical Division*, ASCE, Vol. 103, No. GT6, June, 1977, pp. 501-516.

8. Clough, Wayne, G., and Chameau, Jean-Lou, "Seismic Response of San Francisco Waterfront Fills", *Journal of the Geotech. Eng. Div.*, ASCE, Vol. 109, No. 4, Apr. 1983, pp. 491-506.

9. Cox, J.M., "Paleolseismological Studies in the Charleston, S.C. Area", Thesis presented to the University of South Carolina, Columbia, 1984.

10. Cullen, C.J., "Engineering Tests on Sands Associated with Charleston, S.C. Seismic Events",Thesis presented to Virginia Polytechnic Institute and State University in fulfillment of the requirements for the degree of Master of Engineering, 1985.

11. Douglas, B.J., Olsen, R.S. and Martin, G.R., "Evaluation of the Cone Penetrometer Test for SPT-Liquefaction Assessment", In-situ Testing to Emuluate Liquefaction Susceptibility, Preprint 81-544, ASCE National Convention, St. Louis, Missouri, 1981.

12. Dutton, C.E., "The Charleston Earthquake of August 31, 1886", *U.S. Geological Survey Annual Report 1887-1888*, pp. 203-528.

13. Finn, W.D., Bransby, P.L. and Pickering, D.J., "Effect of Strain History on the Liquefaction of Sand", *Journal of the Soil Mechanics and Foundations Division*, ASCE, Vol. 96, No. SM6, Proc. Paper 7670, Nov., 1970, pp.1917-1934.

14. Gelinas, R.L., "Mineral Alterations as a Guide to the Age of Sediments Vented by Prehistoric Earthquakes in the Vicinity of Charleston, S.C.", Thesis presented to the University of North Carolina in partial fulfillment of the requirements for the degree of Master of Science, 1986.

15. Hardman, S.L. and Youd, T.L., *State-of-the-Art for Assessing Earthquake Hazards in the United States*; Report 22: "Mapping the Extent and Thickness of Liquefiable Soil Layers at Engineering Sites", U.S.Army Engineer Waterways Experiment Station, Vicksburg, MI, Feb., 1987.

16. Ishihara, K., "Stability of Natural Deposits During Earthquakes", *Proceedings of the Eleventh International Conference on Soil Mechanics and Foundation Engineering*, San Francisco, Vol.1, 1985, pp. 321-376.

17. Johnson, W.J. and Bazan-Zurita, E., "Adequacy of Existing Building Codes for Charleston, South Carolina in Light of Recent Discoveries of Seismic Hazard", *Third U.S. National Conference on Earthquake Engineering, Charleston, South Carolina*, Vol. 3, 1986.

18. Krinitzsky, E.L. and Chang, F.K., *State-of-the-Art for Assessing Earthquake Hazards in the United States*; Report 25: "Parameters for Specifying Intensity-Related Earthquake Motions", U.S.Army Engineer Waterways Experiment Station, Vicksburg, MI, Sept., 1987.

19. Ladd, R.S., "Specimen Preparation and Cyclic Stability of Sands", *Journal of the Geotechnical Engineering Division*, Vol. 103, No. GT6, June, 1977.

20. Marcuson III, W.F. and Bieganousky, W.A., "Laboratory Standard Penetration Tests on Fine Sands", *Journal of the Geotechnical Engineering Division*, Vol. 103, No. GT6, June, 1977.

21. McCartan, L., Lemon, E.M., Jr., and Weems, R.E., Geologic map of the area between Charleston and Orangeburg, South Carolina, U.S. Geol. Survey, Misc. Investigation Series, Map I-1472.

22. National Research Council, "Liquefaction of Soils During Earthquakes", Committee on Earthquake Engineering, National Academy of Sciences, 2101 Constitution Ave., N.W., Washingtion, D.C., 20418, March 28-30, 1985, p. 188.

23. Nuttli, O.W., Bollinger, G.A., Herrmann, R.B., *The 1886 Charleston, South Carolina, Earthquake-A 1986 Perspective*, U.S. Geol. Survey *Circular 985*, 1986.

24. Nuttli, O.W., Herrmann, R.B., Jost, M.L. and Bollinger, G.A., "Numerical Models of the Rupture Mechanics and Far Field Ground Motions of the 1886 South Carolina Earthquake", .U.S. Geol. Survey *Bulletin 1586*, in revision, 1988.

25. Obermeier, S.F., unpublished map, 1987.

26. Obermeier, S.F., personal communication, 1987.

27. Obermeier, S.F., personal communication, 1988.

28. Obermeier, S.F., Gohn, G.S., Weems, R.S., Gelinas, R.L. and Rubin, M., "Geologic Evidence for Recurrent Moderate to Large Earthquakes Near Charleston, South Carolina", *Science*, Vol. 277, January, 1985, pp.408- 411.

29. Obermeier, S.F., Jacobson, R.B., Powars, D.S.. Weems, R.E., Hallbick, D.C., Gohn, G.S. and Markewich, H.W., "Holocene and Late Pleistocene Earthquake-Induced Sand Blows in Coastal South Carolina", *Proceedings of the Third U.S. National Earthquake Engineering Conference*, 1986, pp.197-208.

30. Obermeier, S.F., Weems, R.E., Jacobson, R.B., "Earthquake-Induced Liquefaction Features in the Coastal South Carolina Region", U.S. Geol. Survey *Open-File Report 87-504*, Jan., 1987.

31. Peck, R.B., "Liquefaction Potential: Science vs. Practice", *Journal of the Geotechnical Engineering Division*, ASCE, Vol. 105, No. GT3, March, 1979, pp. 393-398.

32. Peters, K.E. and Herrmann, R.B., *First-Hand Observations of the Charleston Earthquake of August 31, 1886, and other Earthquake Materials* , Bulletin 41, South Carolina Geological Survey, 1986.

33. Rizzo, P.C., O'Hara, F.F., and Zullo, E.G., "Ground Motion Amplification Studies for Sites in the Charleston Area",*Third U.S. National Conference on Earthquake Engineering, Charleston, South Carolina*, Vol. 1, 1986.

34. Robertson, P.K. and Campanella, R.G., *Guidelines For Use & Interpretation of the Electronic Cone*, Hogentogler & Company, Inc., Third Edition, Gaithersburg, MD, Nov., 1986.

35. Robertson, P.K. and Campanella, R.G., *Liquefaction Potential of Sands Using the CPT*, *Journal of Geotechnical Engineering*, ASCE, Vol. III, No. GT3, 1985, pp. 384-403.

36. Robertson, P.K., Campanella R.G. and Wightman, A., "SPT-CPT Correlations", *Journal of Geotechnical Engineering*, ASCE, Vol. 109, No. GE11, 1983, pp. 1449-1459.

37. Robinson, A. and Talwani, P., "Building Damage at Charleston, South Carolina, Associated with the 1886 Earthquake", *Bulletin of the Seismological Society of America*, Vol. 73, No. 2, April, 1983, pp. 633-652.

38. Seed, H.B. and De Alba, P., "Use of SPT and CPT Tests for Evaluating the Liquefaction Resistance of Sands", *Proceedings of In-Situ'86, Geotechnical Special Publication No. 6*, Use of In-Situ Tests in Geotechnical Engineering, June, 1986, pp. 281-302.

39. Seed, H.B. and Idriss, I.M., "Simplified Procedure for Evaluating Soil Liquefaction Potential", *Journal of the Soil Mechanics and Foundations Division*,ASCE, Vol. 97, No. SM9, Sept., 1971, pp. 1249-1277.

40. Seed, H.B. and Idriss, I.M., *Ground Motions and Soil Liquefaction During Earthquakes*, EERI Monograph Series, Vol. 5, Dec., 1982.

41. Seed, H.B., Idriss, I.M. and Arango, I., "Evaluation of Liquefaction Potential Using Field Performance Data", *Journal of the Geotechnical Engineering Division*, ASCE, Vol. 109, No. 3, March, 1983. pp. 458-482.

42. Sieh, K., "Prehistoric Large Earthquakes produced by Slip on the San Andreas Fault Near Pallett Creek, California", *Journal of Geophysical Research*,Vol. 83, 1978, pp.3907-3939.

43. Sims, J.D., "Determining Earthquake Recurrence Intervals from Deformational Structures in Young Lacustrine Sediments", *Tectonophysics*, Vol. 29, pp. 141-152, 1975.

44. Stockton, R.P., *The Great Shock*, Southern Historical Press, Inc., Easley, S.C., 1986.

45. Sweeney, B. and Clough G.W., "Portable Mini-Cone System for Field Liquefaction Studies", *Proceedings of the Third U.S. National Conference on Earthquake Engineering*, Vol. 1, EERI, Aug., 1986, pp. 659-670.

46. Talwani, P. and Cox, J., "Paleoseismic Evidence for Recurrence of Earthquakes near Charleston, South Carolina", *Science*, Vol. 228(4711), pp. 379-381, 1985.

47. *The News and Courier.*, Charleston, S.C., Sept. 3, 1886.

48. Thorson, R.M., Clayton, W.S., Seeber, L., "Geologic Evidence for a Large Prehistoric Earthquake in Eastern Connecticut", *Geology*, Vol. 14, June, 1986, pp. 463-467.

49. Tinsley, J.C., Youd, T.L., Perkins, D.M., Chen, A.T.F., "Evaluating Liquefaction Potential", Evaluating Earthquake Hazards in the Los Angeles Region - An Earth-Science Perspective, U.S. Geol. Survey *Professional Paper 1360*, 1985, pp. 263-315.

50. Vaid, Y.P., Chern, J.C., Tumi, H., "Confining Pressure, Grain Angularity, and Liquefaction", *Journal of Geotechnical Engineering*, ASCE, Vol. 111, No. 10, Oct. 1985.

51. Vestry of St. Michael's Church, *A Guide To St. Michael's Church, Charleston*, Nelsons' Southern Printing Co., Charleston, S.C., 1979.

52. Weems, R.E., Obermeier, S.F., Pavich, M.J., Gohn, G.S. Rubin, M., Phipps, R.L., and Jacobson, R.B., "Evidence for Three Moderate to Large Prehistoric Holocene Earthquakes Near Charleston, S.C.", *Proceedings of the Third U.S. National Conference on Earthquake Engineering*, Vol. 1, EERI, Aug., 1986, pp. 3-13.

53. Youd, T.L., "Recurrence of Liquefaction of the Same Site", *Proceedings on the Eighth World Conference on Earthquake Engineering*, Vol. 3, pp. 231-238, 1984.

54. Youd, T.L. and Bennett, M.J., "Liquefaction Sites, Imperial Valley, California", *Journal of the Geotechnical Engineering Division*, ASCE, Vol. 109, No. 3, March, 1983, pp. 440-458.

55. Youd, T.L. and Perkins, D.M., "Mapping Liquefaction-Induced Ground Failure Potential", *Journal of the Geotechnical Engineering Division*, Vol. 104, No. GT4, pp. 433-446, April, 1978.

Vita

Stephen Eugene Dickenson was born July 31, 1962 in Salem, New Jersey and quickly persuaded his parents to move back to their native west coast. He grew up in the east bay and south peninsula regions of the San Francisco Bay area, with a brief stint in Houston, Texas. Extensive wanderings throughout coastal and mountainous northern California have instilled a reverence for wilderness and zealous passion for hiking, kayaking and fishing. After graduating from Homestead High School, Cupertino in 1980, and spending two years at De Anza Community College he transferred to the University of California at Berkeley where he received his B.A. degree in Geology in 1985. Following graduation he was employed with the U.S. Geological Survey for 14 months, the first four months as a Geologist in the Branch of Engineering Geology and Tectonics in Menlo Park, California. The remainder of that time he worked in the Geotechnical Engineering laboratory for the Branch of Atlantic Marine Geology in Woods Hole, Massachussets. During his residence on Cape Cod he succombed to the charming wiles of, and was married to Julia Marie Andersen in September, 1986. He then began graduate studies at Virginia Polytechnical Institute and State University to persue an M.S. degree in Civil Engineering with a concentration in Geotechnical Engineering.

Stephen Dickenson